Cranfield Institute of Technology

School of Mechanical Engineering

Department of Applied Energy

Ph.D Thesis

Academic Year 1991-1992

Hilal Ali Zaher Al-Hinai

Natural Cooling Techniques For Buildings in Hot Climates

Supervisor: Dr W.J. Batty

September 1992

The many thousands of miles I travelled in Oman, in carrying out part of the research for this work, have inflamed in me a love and admiration for this country. My admiration is especially with the ingenuity of its vernacular architecture, from which I have learned a lot about energy efficient building design. And it is to this country I dedicate this work.

To my Country

The Sultanate of Oman

Abstract

Modern development in many Third World countries in the hot regions of the world, have been accompanied by the construction of highly energy-wasteful buildings. The interiors of these buildings have to be mechanically air-conditioned in order to achieve thermal-comfort conditions. The consequence of this, has been the rapid increase in electricity-generating plant capacity to match demand (of which, for example at present in Oman, more than 70% nationally is used for air-conditioning modern, energy-inefficient buildings).

The aim of this work was to find the most suitable way of stabilising or even reducing the electricity demand in a country like Oman. The first step taken to achieve this aim, was to study and draw out lessons from the vernacular architecture of the different climatic regions in Oman. This has been followed by a literature survey that looks at passive and active natural cooling techniques for buildings in hot climates. Mathematical models were then developed to analyze and compare those passive techniques that are most suitable for an environment like that of Oman. Different ways of reducing the heat gain through the roof were investigated and compared. These include the addition of insulation, shading, air-cooling of the roof when the ambient air temperature is lower than that of the roof, and roof ponds. Roof ponds were found to be the most effective of those techniques analyzed. An improved design of the roof pond (the Water Diode roof pond) that eliminates the need for covering the roof pond during the day and uncovering it at night, was suggested and analyzed. The analysis showed promising results.

Mathematical models were also developed to analyze and compare different ways of reducing the heat gain through the walls. These included the use of closed cavities, naturally ventilated cavities, the addition of insulation, and the effect of using brick as compared to concrete block. The analysis suggested that the combination of a Water Diode roof pond and insulated brick wall construction will reduce the heat gain through the envelope of a single room by more than 90%, when compared to a room with un-insulated roof and single-leaf concrete block walls.

An empirical validation of the mathematical models was conducted. The results showed a good agreement between the actual and predicted values. An economical analysis of the commonly used roof and wall constructions in Oman, was also conducted. This compared the life-cycle cost of nine different construction techniques, with eight different air-conditioning schedules. The result of this analysis showed a clear advantage of using roof insulation, reflective double glazing, and insulated walls with brick outer-leaf and concrete block inner-leaf.

Acknowledgements

I would like to take this opportunity to express my thanks to my supervisor Dr. W.J. Batty for his invaluable help and guidance throughout this research work. Thanks are also due to Prof. S.D. Probert, and all the staff in the Applied Energy group at CIT.

I would like also to express my gratitude to the Omani government, who provided me with the financial support to carry out this research work, and to the many individuals who helped me in this research work. Especial thanks are due to my parents, brothers and sisters who have supported and encouraged me throughout my period of study. Sincere thanks are also due to all my friends in Cranfeild, whose support and encouragement provided me with a big boost in reaching my aims. Especially mentioned are Karam Fayed, Mahmood Tahat, Jala Akber and Khamees Al-Balushi.

Many thanks for the great help I received from the following organisations in the Sultanate of Oman:

Sultan Qaboos University.
Department of Meteorology - Ministry of Communications.
Department of Projects - Ministry of Housing.
The Development Council.
Al-Hinai Building establishment.
Oman Engineering Consulting Office.
Bisan Engineering Consulting Office.
Al-Hilal Contracting Company.
Al-Salah Contracting Company.
Mutrah Insofoam.
Photo House.

Finally, special appreciation is due to my wife and son (Khalid), who put up with my many moods during the period of this study. They helped me in moments of despair and gloom, and their support was a constant source of encouragement.

Contents

Chapter 3

Natural-Cooling Techniques for Residential Buildings in Hot Climates - An Over view

Chapter 4

Mathematical Modelling of Heat Transfer Through Different Roof Constructions

Chapter 5

The Water Diode Roof Pond

Chapter 6

Mathematical Modelling of Heat Transfer Through Different Wall Constructions

Chapter 7

Empirical Validation of The Mathematical Models

Chapter 8

Economic Analysis of Commonly Used Wall and Roof Constructions

Chapter 9

Conclusions and Recommendations

Appendices

List of Figures

List of Tables

Notations

A	cross-sectional area (m^2)
A_i	Anisotropy index
A_{Du}	The surface area of the body (m^2).
a	Constant.
b	Constant
C_s	The cloud-cover correction factor
C_p	Specific heat capacity ($Jkg^{-1}K^{-1}$)
D_h	Hydraulic diameter.
d	Water layer depth (m)
day	Day of the year (1-365).
f	Modulating factor
Gr	Grashof number
G_{sc}	Solar constant (= 1367 Wm^{-2})
g	Acceleration due to gravity (m^2s^{-1})
H	Monthly averaged daily global radiation ($KJm^{-2}day^{-1}$)
h	The convective heat-transfer coefficient ($Wm^{-2}K^{-1}$), solar time, height of water column (m).
$\bar{h}$	The average heat transfer coefficient.
h_m	Mass transfer coefficient ($kgm^{-2}s^{-1}$).
h_{fg}	Latent heat of evaporation of water (JK^{-1}).
I	Total hourly solar radiation falling on a horizontal surface (Wm^{-2}).
I_b	The hourly direct solar radiation on a horizontal surface (Wm^2).
I_d	The hourly diffuse solar radiation on a horizontal surface (Wm^2).
I_{cl}	A factor indicating the clothing resistance with respect to the rate of thermal energy loss from the human body; I_{cl} =0 for a nude person; I_{cl} =0.5 Cl_o for a lightly clothed person; I_{cl} =1.0 Cl_o for a medium-clothed person, i.e. wearing a suit and normal undergarments; I_{cl} =1.5 for a heavily clothed person.

$\bar{K}_T$ The monthly averaged clearness index.

k Thermal conductivity ($Wm^{-1}K^{-1}$).

K(H) A factor related to the time of the day; it gives a representation of the effect of ground warming on the effective temperature of the sky.

L length (m)

L_c Characteristic length, analogous to the hydraulic diameter (m)

L(H) A factor related to the time of the day: it provides a representation of the effect of the altitude thickness of the atmospheric boundary layer on the effective temperature of the sky.

l The distance between two nodes.

M The metabolic rate (W or cal hr^{-1} as stated)

m Mass flow rate (Kgs^{-1})

m_v Mass transfer of vapour ($Kgm^{-2}s^{-1}$)

Nu Nusselt number

n Refractive index.

n/10 The ratio of the area of opaque-sky cover area to the total area of clear-sky

P_d Pressure difference.

P_t Total pressure (Nm^{-2}).

p Partial pressure (Nm^{-2})

Pr Prandtl number

Q_{conv} Convective heat gain rate (W)

Q_{net} The net rate of heat loss from an exposed horizontal dry surface (Wm^{-2})

Q_{rad} The radiative rate of heat loss from an exposed horizontal dry surface (Wm^{-2})

Ra Rayleigh number.

R_b Beam radiation ratio

Re Reynold number

r The ratio of the total radiation for the hour to that of the whole day.

r_{pa} The reflection of the parallel component of beam radiation on the water surface.

r_{pe} The reflection of the perpendicular component of beam radiation on the water surface.

s Space between the two leaves (m)

T Temperature (K)

T_{amb} The mean monthly outdoor temperature (K)

T_{dp} Dew-point temperature (K)

T_n The natural temperature, as defined by Humphreys[2-2] (K)

T_{sky} The effective temperature of the sky (K)

ΔT Temperature difference (K)

t Temperature (°C)

t_{dbi} The initial dry-bulb temperature (°C)

t_{dbs} The dry-bulb temperature of supply air (°C)

t_{wb} The wet-bulb temperature of the air (°C)

V Velocity (ms^{-1})

W Humidity ratio.

WD Wind direction (deg.)

Greek

α Absorptance

β Coefficient of thermal expansion (k^{-1})

γ Azimuth angle (deg.)

δ Declination angle of the sun (deg.)

ϵ Emissivity

μ Dynamic viscosity ($Kgm^{-1}s^{-1}$)

π Constant ratio

ν Kinematic viscosity (m^2s^{-1})

θ Angle of refraction (deg.)

σ Stefan-Boltzmann constant (= $5.67x10^{-8}Wm^{-2}K^{-4}$)

ρ Reflectance, Density (Kgm^{-3})

τ Transmittance

ϕ The relative humidity, $0 \leq \phi \leq 1$, Latitude of the location (deg.)

ω Hourly angle of the sun (deg.)

Subscripts

a Air.

acv Air in cavity.

ai Room air.

ao Ambient air.

b Beam radiation, buoyancy.

c Ceiling, Concrete.

c1 Screed.

c2 Reinforced concrete slab.

cvi Outer surface of cavity.

cvo Inner surface of cavity.

conv Convective

dp Dew point.

evap Evaporative.

f Floor.

g Gas or dry air.

i Inside, inner surface, inlet.

net The net long-wave radiation heat exchange

o Outside, outer surface, outlet.

p Parallel

r Roof.

s Insulation, sun rise / sun set.

sa Saturation at air temperature.

sat saturated air.

sw Saturation at water temperature.

T1 At the temperature of node 1.

T4 At the temperature of node 4.

t Total

v Vapour.

vs Vertical surface.

w Water, wall.

Abbreviations

ACH Air changes per hour.

ARI Air-conditioning and Refrigeration Institute.

B A room with single leaf brick walls.

BNB A room with brick inner leaf; closed cavity; and brick outer leaf walls.

BSB A room with brick inner leaf; insulation; and brick outer leaf walls.

BVB A room with brick inner leaf; ventilated cavity; and brick outer leaf walls.

H A room with single leaf concrete block walls.

HNB A room with concrete block inner leaf; closed cavity; and brick outer leaf walls

HNH A room with closed cavity concrete block walls.

HSB A room with concrete block inner leaf; insulation; and brick outer leaf walls.

HVB A room with concrete block inner leaf; ventilated cavity; and brick outer leaf walls.

HVH A room with ventilated cavity concrete block walls.

HSH A room with insulated concrete block walls.

GLOSSARY

Areesh: A room, the envelope of which is made from palm-frond stems. Such a construction allows high rates of ventilation while maintaining privacy and security; see Fig.(3.6).

Cl_o: An expression describing the thermal insulation of clothing, measured from the skin to the outer surface of the clothes, but excluding the external convective surface resistance. 1 Cl_o =0.155 m^2 Wk^{-1}, and this represents approximately the thermal resistance of a lounge suit with normal underwear.

Dahreez: A shaded space adjoining a courtyard and used as the living area in a courtyard house. It is cooled at night by the cold air collecting into the courtyard, and it stays cool all day since it is protected from direct solar insulation; see fig.(3.3).

Earth berming: A mound of earth abutting a house wall it helps stabilise the temperature inside the house.

Malkaaf: A structure designed to capture the wind or breeze and guide it through an air gap in the wall to air vents in the rooms below. They also work as suction devices when the wind is coming from the opposite direction; see Fig.(3.10).

Mean radiant temperature: The uniform temperature of surrounding surfaces which will result in the same rate of heat exchange by radiation from or to a person as occurs in the actual environment.

Mebit: A lightweight room on the roof enclosed on all 3 sides by lattice woodwork which allows air through but sharply reduces the amount of solar insolation falling on the roof. Mebits are frequently used as sleeping areas in summer.

Rowshin: Wooden balconies by lattice woodwork, so as to allow a high rate of ventilation while maintaining privacy; see Fig.(3.5).

Chapter (1)

Introduction

Chapter (1)
Introduction

1.1 The Problem

In most developing countries in the hot regions of the world during the last 50 years there have been many buildings constructed that are highly energy-wasteful. The interiors of these buildings have to be mechanically air-conditioned in order to achieve thermal-comfort conditions. Consequently, vast financial expenditures have and are being spent upon the installation and operation of the electricity-generating plants needed to supply the maximum power demand during summer.

The Sultanate of Oman, is one of these countries. The rapid and widespread construction of energy inefficient buildings in Oman, has caused a huge rise in electricity demand with a characteristic, and increasing, summer-peak load - see Figure (1.1). The air-conditioning of buildings accounts for at least 70% of the nation's annual electricity-consumption. The growth in electricity-generation capacity needed to supply the summer-peak load, has been achieved at a considerable cost to the nation. Unfortunately, the high annual rate of increase in the electricity demand is likely to continue because of the present pattern of population growth (estimated at ~3.5% per annum) and the simultaneous increase in energy consumption per capita. This is especially true for the comparatively under-developed Northern regions of Oman, where about two thirds of the population live, but their power consumption per capita represent less than 10% of the consumption per capita in the Muscat region - see Figure (1.2). Thus even a relatively small rise in electric-power consumption per capita in the Northern regions, due to changes in living standards, will cause a sharp rise in the national electric power consumption.

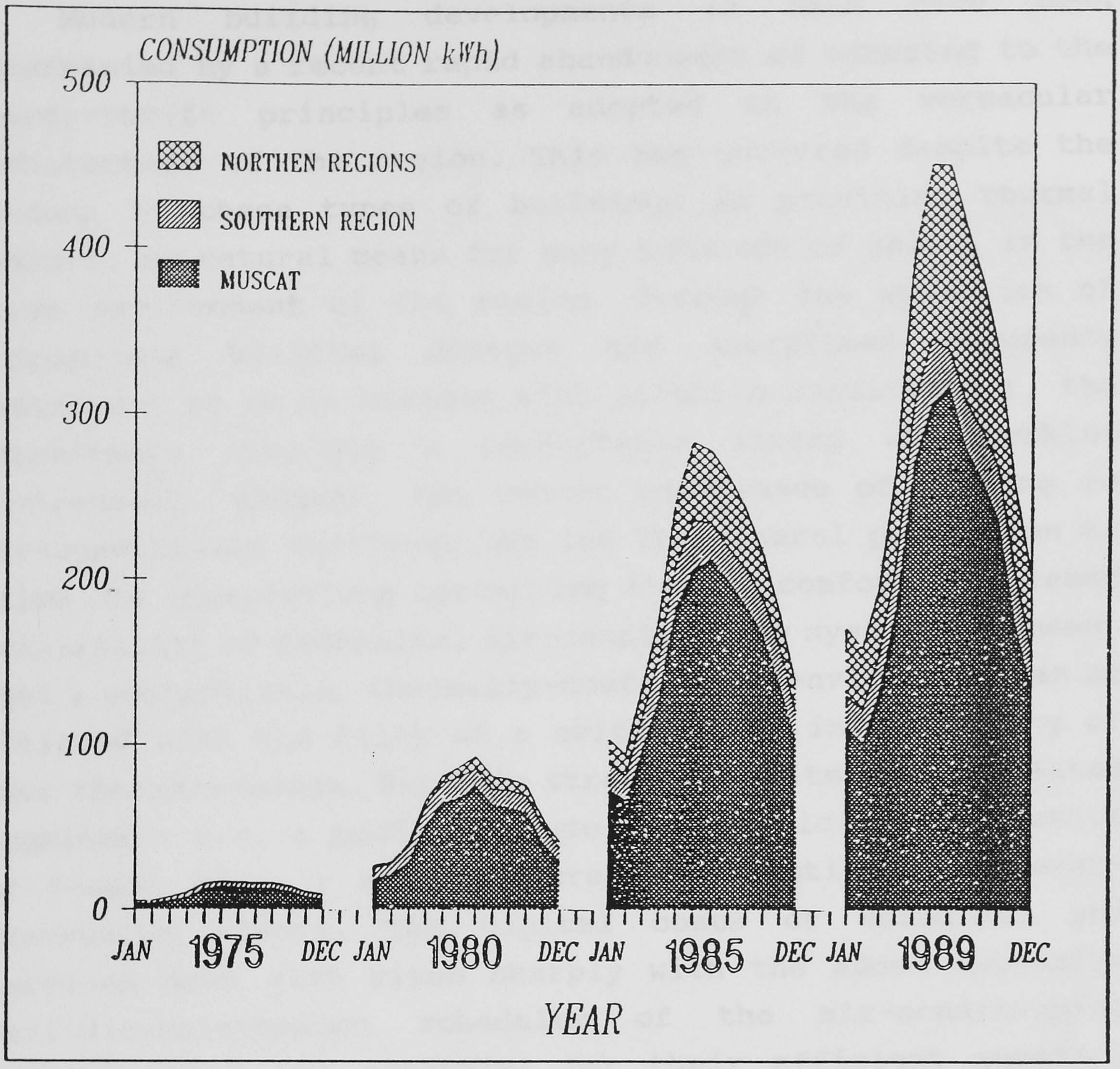

Figure 1.1: Changes in the annual variations of electric-power consumptions in Oman, during the period from 1975 to 1989.

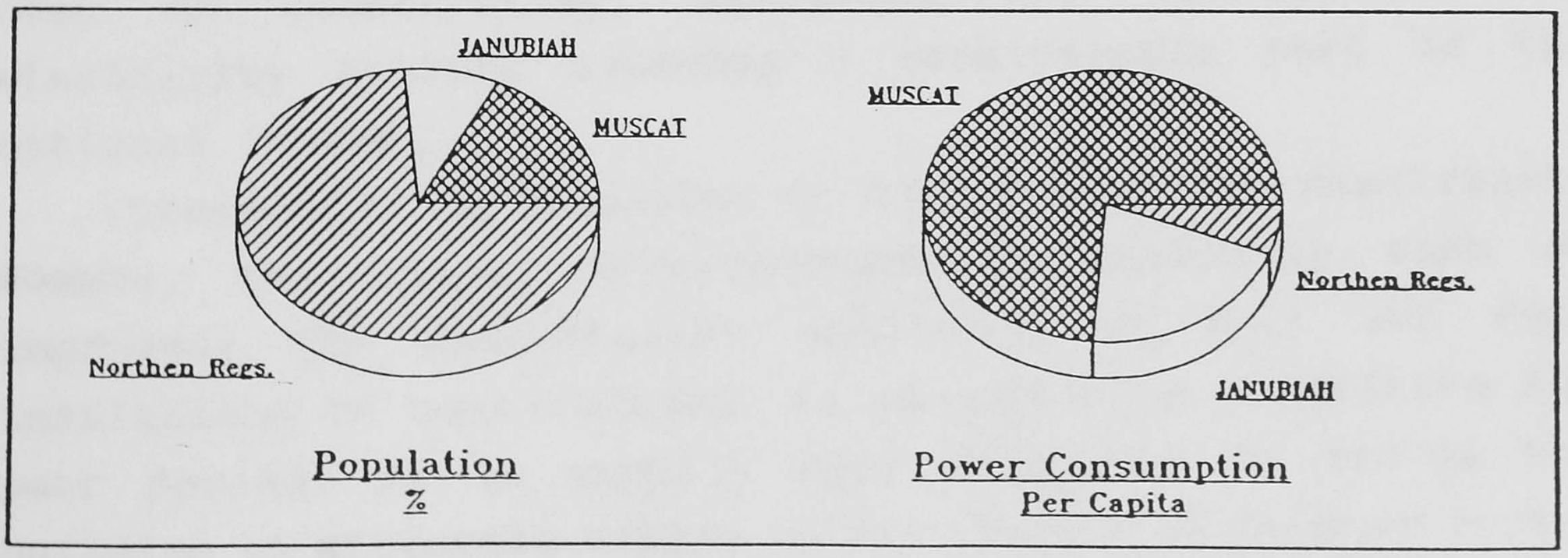

Figure 1.2: A comparison between the population distribution and the electric-power consumption per capita, for the three regions in Oman.

Modern building developments in Oman have been accompanied by a recent rapid abandonment of adhering to the energy-thrift principles as adopted in the vernacular architecture of the region. This has occurred despite the success of these types of buildings in providing thermal comfort, by natural means for many hundreds of years, in the harsh environment of the region. Through the selection of appropriate building designs and associated occupancy patterns (to be in harmony with climatic conditions), the inhabitants attained a comfortable living and working environment. However, the recent experience of working in air-conditioned buildings has led the general population to raise its expectations concerning thermal comfort. The ready availability of mechanical air-conditioning systems has meant that a controllable, thermally-comfortable environment can be achieved with the flick of a switch, even in a building of poor thermal-design. But this strategy has its own associated problems - e.g. a profligate use of electricity (and hence of fossil fuels) and so increased pollution from power-generating plants. The capital costs of buildings and services have also risen sharply with the added expensive periodic-maintenance schedules of the air-conditioning systems which are essential for their efficient running. There are other drawbacks, such as the increased noise associated with some mechanical air-conditioning systems. The cost of constructing, operating and maintaining the electricity network consumes a considerable part of the national income.

Therefore, to stabilise or even reduce the electricity demand, the energy effectiveness of buildings must be improved. The afterthought additions of wall and roof insulations to constructions is an expensive substitute for poor design. It is usually more effective to design the building to attenuate within it the effects of changes in the weather, i.e. taking advantage of the beneficial, and isolating the undesirable, elements of the micro-climate. As

a consequence of these factors, the following research objectives and methodologies were developed.

1.2 Research Objectives and Methodology

The aim of this research work is to study the Natural Cooling Techniques For Buildings, and to develop an optimised cooling strategy that is suitable to an environment like that of Oman, and is readily acceptable to the people. To achieve this objective, the following were carried out:

- A study of the vernacular architecture of Oman was conducted. This has been presented in **Chapter 2.**
- In **chapter 3**, an over-view of the natural cooling techniques for buildings in hot climates is presented. This includes both passive and active solar cooling techniques.
- Mathematical models were then developed to compare the thermal performance of the most appropriate passive cooling techniques. The mathematical models for different passive roof cooling techniques have been presented in **chapter 4.**
- The simulation results of chapter 4, have led to the development of the Water Diode roof pond, described in **chapter 5.**
- Single-room models comparing the thermal performance of different wall constructions, and the combination of different roof and wall constructions are presented in **chapter 6.**
- Empirical data was collected in order to validate the mathematical models. The results of this validation exercise are presented in **chapter 7.**
- An economical analysis of the appropriate developed constructions, compared with standard constructions, is presented in **chapter 8.**
- The conclusions and recommendations are presented in **chapter 9.**

Chapter (2)

Vernacular Architecture of Oman : Features Which Enhance Thermal Comfort Achieved Within Buildings

Chapter (2)

Vernacular Architecture of Oman : Features Which Enhance Thermal Comfort Achieved Within Buildings

2.1 Oman and its Climate

The Sultanate of Oman lies at the south-eastern corner of the Arabian Peninsula, stretching between latitudes 16 and 26 °N. It is part of the arid belt in the northern hemisphere, and is a region subjected to severe climatic variations. The maximum temperature recorded in the capital, Muscat, is 49.5 °C and the humidity varies from very high (>95 %) along the coast to very low (<10 %) in the interior desert region.

The population, estimated at about two million, is distributed mainly on, and around, the two mountain ranges in the north and south of the country. This is principally because the rain falling on the mountains provides the water resource needed for sustaining farming and life. Much of this water passes along several, winding valleys, which can experience flash flooding. These create, fertile plots of land on which some settlements have developed. However most settlements occur on the fertile plains between the mountain ranges and the coast; there, the fresh-water table is close to the ground's upper surface. This facilitates the cultivation of land close to the sea and the establishment of settlements for fishermen, farmers and traders.

The inland settlements, based mainly on agriculture with small-scale service industries, are located along the valleys in and around the mountain ranges. In the past, the desert was inhabited mainly by nomads. The few oases that exist around the edge of the desert, derive their water supplies from the mountain ranges through man-made underground channels, called "Falajs".

Due to the strategic location of Oman, historically, Omanies commanded the shipping routes between East Africa, the Arabian Peninsula, Persia, India and China. As a result, they tended to be travellers, and their contacts with other cultures must have influenced the Omani vernacular architecture.

In Oman, the climate varies from bitterly cold on the high mountains, to being hot and humid along the northern coast, to warm and tropical in the south, to hot and arid in the desert. Thus the vernacular architectures in these different regions developed to take account of each particular set of climatic conditions applying locally. The different civilisations which evolved have enriched this diversity of architecture and made it a valuable resource of examples of what can be achieved.

Unfortunately, our detailed understanding of those vernacular architectural features introduced to compensate for the adverse climatic conditions is now being ignored and so in danger of being forgotten through not being employed regularly. This has prompted the present survey, which reviews how thermal comfort was achieved via the vernacular architecture of Oman.

2.2 Why Study Vernacular Architecture ?

During thousands of years, the inhabitants of each region of the world have evolved methodologies and systems for ameliorating the effects of the extremes of their local climate. For each region, these can be observed in the forms of clothing worn, the diurnal-nocturnal work patterns and the construction of, and activities undertaken within, buildings.

In Oman, mass modernisation began in 1970. The subsequent rapid developments were paid for largely from oil revenues. Thus, within two decades, Oman has been transformed technologically from a country still living in the Middle Ages to one partly living as the developed nations of the pate 2oth century. As a direct consequence of the availability of electricity, the widespread introduction and use of mechanically air-conditioned, concrete-block buildings has ensued. Generally, these constructions are highly energy-inefficient. Too often, unfortunately, the traditional vernacular building designs have been abandoned. The main reasons for this are:

- The foreign building designers and labour brought in to help develop the country are experienced in the construction of concrete-block buildings, but have little concern for, or knowledge of, the region's climate, local vernacular architecture or indigenous-building materials and methods of construction.
- Compared with the local traditional houses, concrete-block buildings tend to be more hygienic, are easier to keep clean, require less maintenance and tend to have longer lives.

The main priority of a vernacular building in a severe climate like that encountered in Oman, was to provide a shelter, which was thermally comfortable despite the absence of purchased energy supplies. Thus the building's design,

orientation and constructional materials were chosen to achieve an acceptable thermal performance for the building [1-3].

By studying the vernacular architecture of each region, a large information and experience resource (evolved over the centuries) can be tapped. One can then discern how the choice of materials and the designs of buildings have evolved, in response to the local climates, in order to try to ensure the achievement of thermal comfort within the building by natural means. However it would be unrealistic to reject totally the benefits which modern technology can offer to help us ensure a better artificial environment within buildings. Nevertheless, instead of relying wholly upon mechanical means and the use of fuel or electricity to achieve an acceptable behaviour of the building, its designer should direct his/her efforts to build in features which result in automatic natural climatic-control of the internal environment, and which may be supplemented, if necessary, by artificial means.

Building designers and planners in Oman should be aware that the availability of cheap (i.e. highly-subsidised) electricity is based on the present generous supplies of oil. But this non-renewable national resource will be economically exhausted within forty years in Oman. This is far shorter than the life of each modern building. Also it has been recognised that the national electricity grids in Iraq and Kuwait were disrupted very quickly during the Gulf War of 1990/1991. These factors should encourage the people in the region to learn from the lessons of vernacular architecture, so that new buildings will remain habitable and reasonably comfortable for extended periods, even in the event of an electricity-supply failure.

For this study, the country was divided into four climatic regions, namely:- the Coastal, Mountainous, Desert, and Southern Regions - see Figure 2.1. Variations in the vernacular architecture of these climatic regions have been assessed.

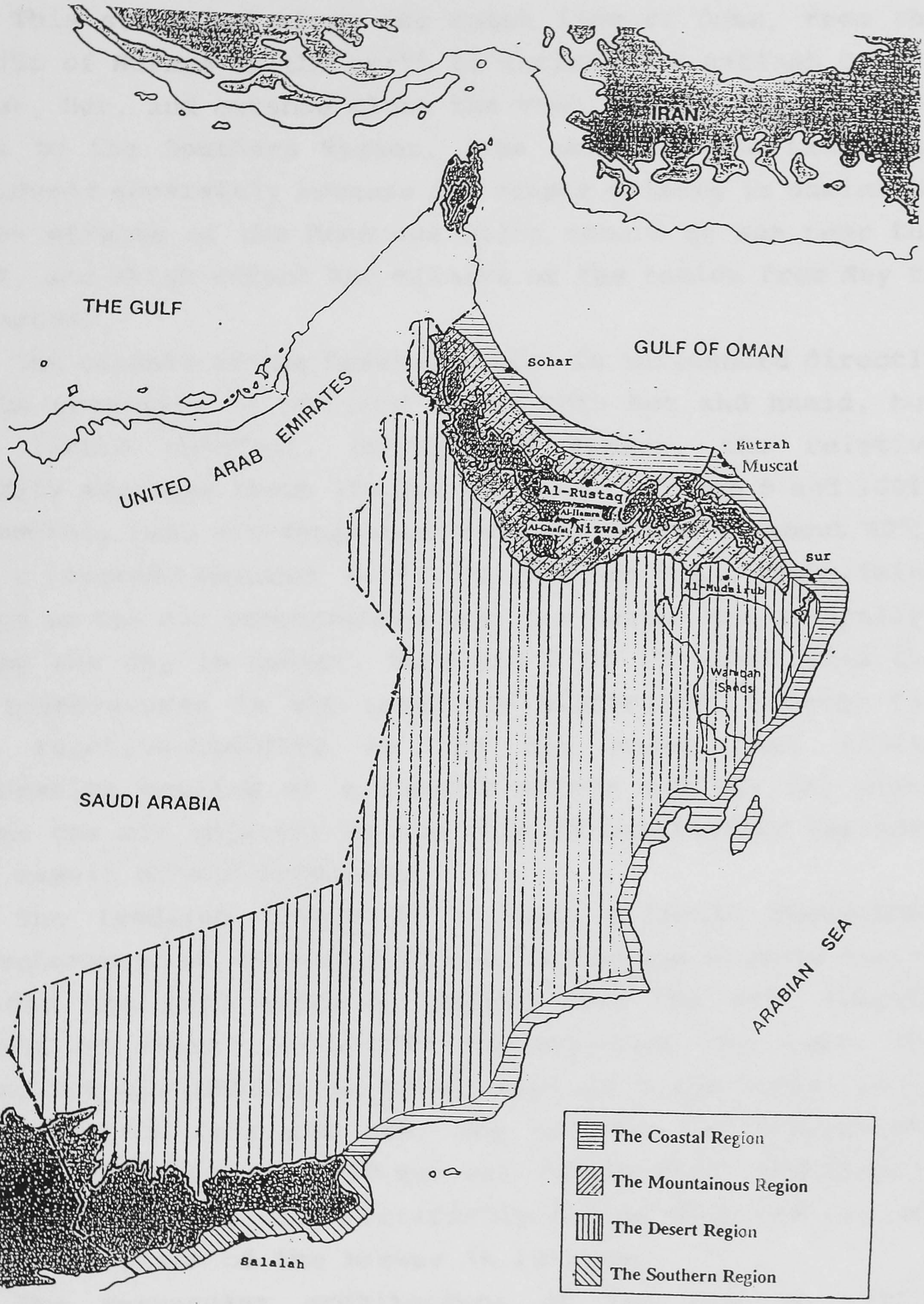

Figure 2.1: A map of the Sultanate of Oman showing the four climatic regions described.

2.3 The Coastal Region

This stretches along the coast line of Oman, from the Straits of Hurmuz in the north to include the Batinah Coast, Muscat, Sur, and extends along the vast, mainly uninhabited, coast to the Southern Region. (The coast of the latter is considered separately because its summer climate is dominated by the effects of the Monsoons which occurs at sea near the coast, and which affect the climate of the region from May to September).

The climate of the Coastal Region is influenced directly by its proximity to the sea: it is both hot and humid, but with little rainfall. During the summer, the relative humidity averages about 75% but can range between 5 and 100%. The monthly mean air-temperature during summer is about 33°C, with a recorded maximum of 49.5°C. The sea has a stabilising effect on the air temperatures near the beach, and generally, during the day in summer, they are 2 to 3°C lower than the air temperatures in the immediate hinterland. However the high relative-humidity of the air means that little evaporative cooling of a human's skin's surface can ensue unless the air adjacent to the skin is continually replaced as a result of air movements.

The land/sea breeze is a local climatic phenomenon characteristic of coastal regions. It happens because during the day the land heats up faster than the sea, thereby causing an upward convective current over the land. The rising hot air results in cooler air, at a low level, being drawn in from over the sea. The greater the temperature difference between the land and sea, the stronger the breeze. At night, the land cools relatively faster than the sea and so the direction of the breeze is reversed.

The vernacular architecture of the coastal region evolved to benefit from this phenomenon. Because air movement is an important aid to achieving thermal comfort in this high-humidity region, houses were designed to harness this

breeze and guide it into the inhabited spaces, thereby cooling the occupants. To achieve this, houses were built facing the sea, with many openings in the sea-facing walls. The coastline in this region runs almost north to south and so in order to face the sea, most houses were built on approximately north-south axes. At the latitudes of Oman (16→26°N), the east and west walls receive more solar radiation daily during summer than do the south and north walls - see Figure 2.2. To overcome this, most houses incorporate shading devices on their east walls, and their west walls have relatively few openings.

Along the coast, slight differences in the prevailing climatic conditions occur. Also, the local availability of materials, and the social and economic environments, influenced the vernacular architecture of these different coastal regions. Consequently, the coastal region has been divided into three sub-regions namely the Batinah Coast, Muscat Region, and Sur.

2.3.1 The Batinah Coast

This crescent-shaped plane, stretches from the frontier with the United Arab Emirates in the north to the Muscat Region in the south. Surrounded by the Western Hajar mountain range and the sea, the plane extends 30 km at its widest and slopes gently towards the sea. Near the coast, the fresh-water table, fed by the rain falling on the mountain range, is close to the surface. This has facilitated the cultivation there of an almost uninterrupted narrow strip of land. With agriculture, fishing and sea-trade, many settlements grew

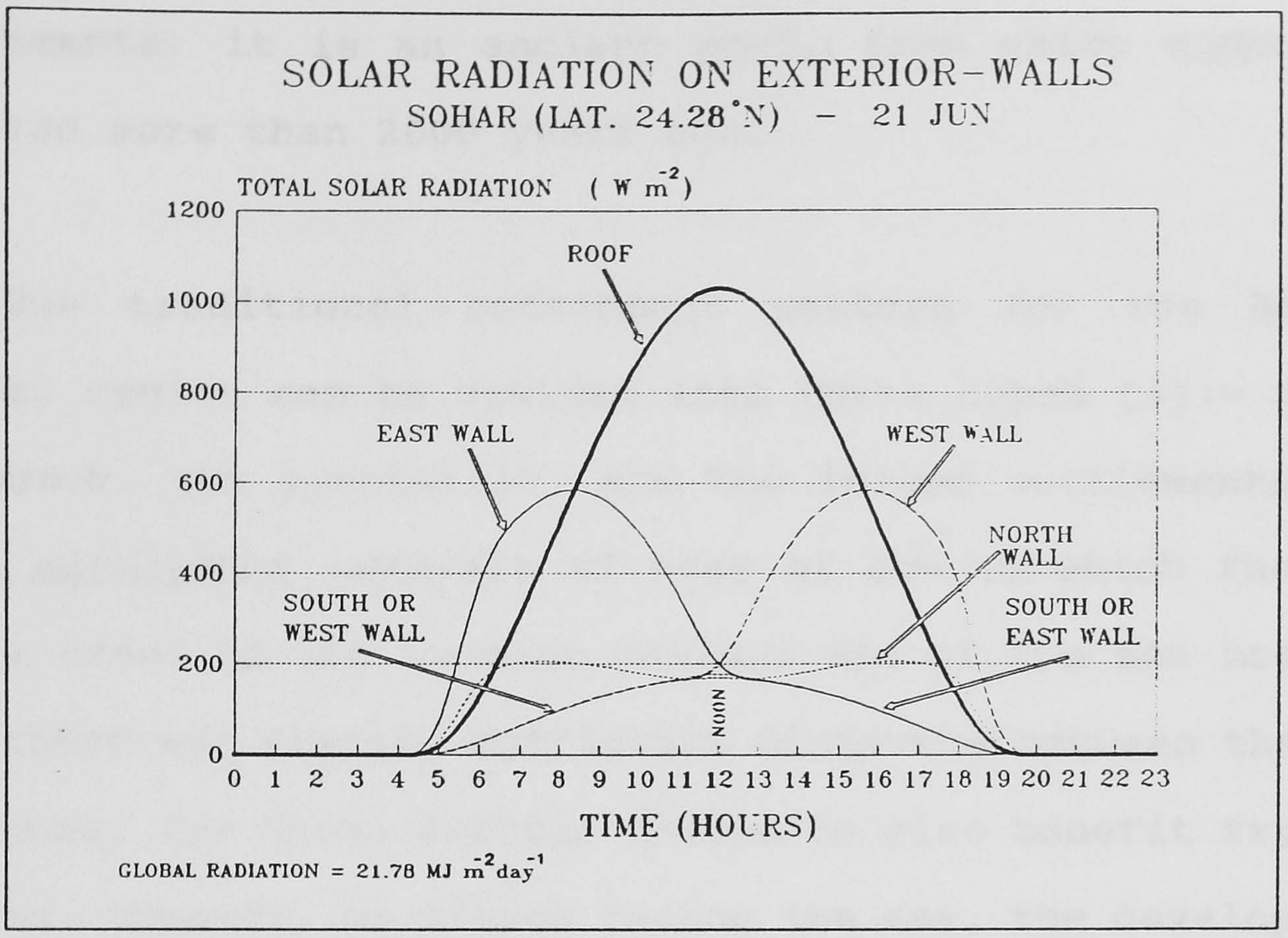

Figure 2.2: The estimated solar insolation falling on the exterior walls of a building in Sohar (Latitude 24.28 ^{0}N) on (a) the 21st of June and (b) the 21st of December.

along this coast. Sohar is the most famous of these settlements: it is an ancient port, from which copper was exported more than 2000 years ago.

The traditional settlement pattern for the Batinah Coastal region can be divided into three types [4]:- namely the beach, the plantation, and the inland settlements. The beach settlement consists of rows of houses which face the sea in order to try to make maximum use of the sea breezes. Also there are usually sufficient distances between the rows of houses, for those further inland to also benefit from the breezes. However, on slopes facing the sea, the developments are more congested. A central nucleus of buildings is usually found between the beach houses and the plantation strip. This often contains a central mosque, a large fort and a market place. Also the houses of the wealthy merchants and the plantation owners tend to be located here. Scattered within the plantation strip, are the summer houses of the plantation owners and workers. These are occupied only during summer when harvesting occurs and are located where the densely-packed palm trees provided a cool, pleasant and shaded environment. Inland from the plantation strip, but not far from it, are scattered groups of temporary summer houses. These are occupied by herdsmen, who come to the towns for the harvesting of dates.

Vernacular houses along the Batinah Coast were generally of relatively low mass, being constructed of low-density

materials, and have many openings in their sea-facing walls - see Figure 2.3(a-f). Such houses do not store significant amounts of heat in their structures, because relatively little is absorbed during the day and so only a small amount is emitted to the inner space at night. This is especially advantageous because the night-time breeze is not as effective for cooling as the day-time breeze. The reason for this is that the beach slopes downward towards the sea, and so the land breezes passing over the palm-tree plantation, tend to be weak at the level of the beach houses.

Until about 1975, the palm-frond house, the "Areesh", was the dominant man-made feature of the Batinah Coast [5]. Built almost entirely from palm trees, i.e. indigenous, readily-available materials, it was cheap and easy to construct and thermally comfortable. It was the recommended dwelling for the hot humid climatic conditions of the region. Unfortunately, such palm-frond houses can only rarely be found nowadays. The main reason for their rapid decline in popularity is that, it is considered unsafe to supply them with electricity. They are also unsuitable for mechanical air-conditioning. They incur other disadvantages such as they (i) can easily catch fire, (ii) provide little protection against rain floods resulting from rainfall, (iii) have a relatively short life span and (iv) only provide little privacy and security. Unfortunately however, with their disappearance, knowledge of their constructions and an appreciation of their advantages are gradually being

Figure 2.3(a): The use of palm-frond panels and shading-devices on the sea-facing wall of a vernacular house in Sohar.

Figure 2.3(b): A vernacular house, in Sohar, with large openings through the sea-facing wall.

Figure 2.3(c): A one-roomed building constructed from palm-frond panels, on the beach at Sohar.

Figure 2.3(d): A heavy-structure vernacular house in Sohar. Many, large windows, are found in the walls of the sea-facing side of such houses.

Figure 2.3(e): A vernacular house in Sohar. The house is designed to encourage air-movement and reduce solar gains, while maintaining privacy and security.

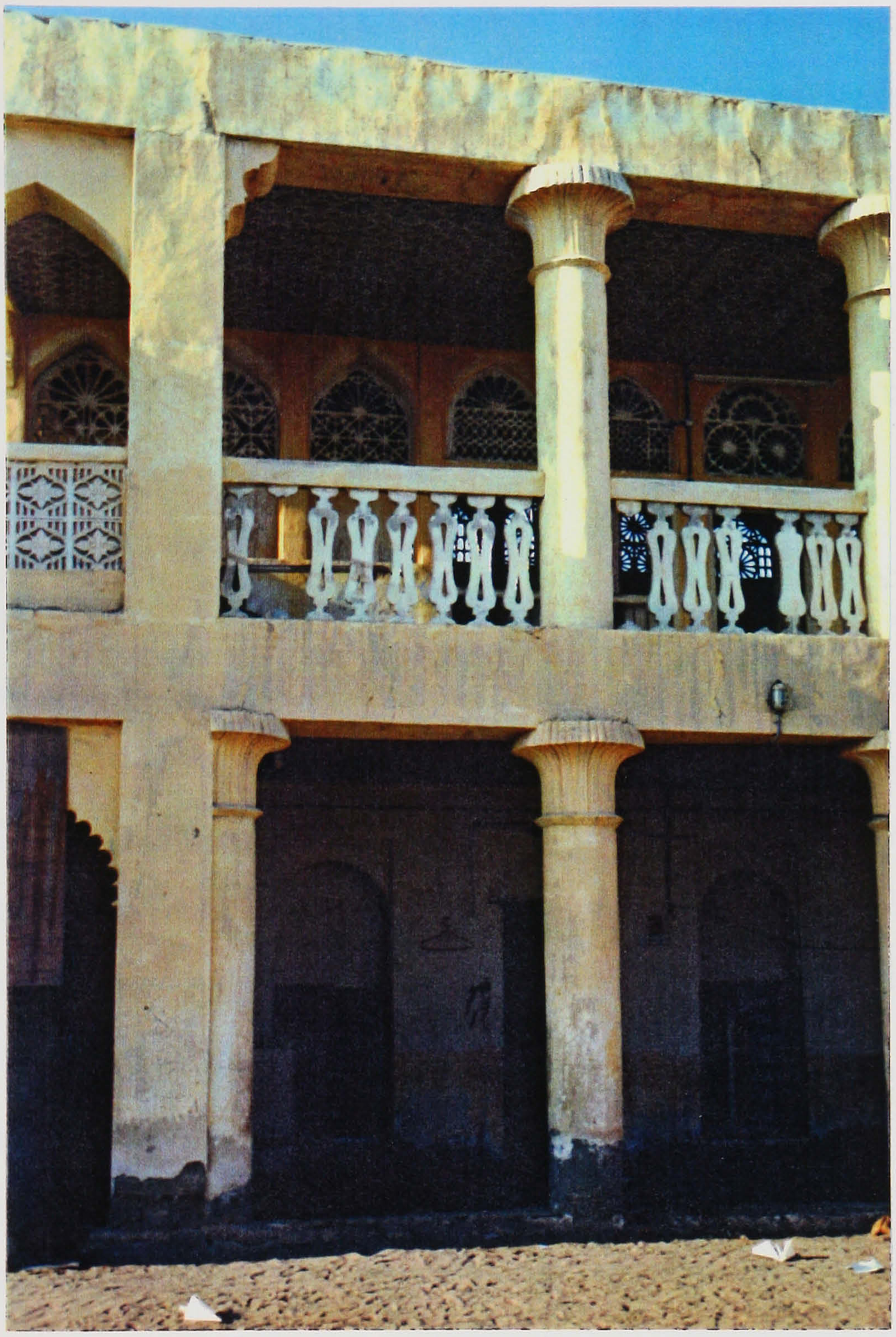

Figure 2.3(f): The front side of the house in 2.3(e). This is the side facing towards the sea.

forgotten. Although it is acknowledged that the "Areesh" is not a suitable construction for most modern habitations, nevertheless there are beneficial design lessons to be learned (which can be applied toady) from the success of such structures concerning the achievement of thermally-comfortable environments within buildings, and some appropriate applications still exist (e.g. for housing animals).

The vernacular houses of the Batinah Coast can be divided into three types:

(i) The Summer-Winter Convertible:

This simple structure, consisted of rooms made from palm fronds. The stems of the palm fronds were made into panels with which the walls and roofs were constructed. These air-leaky panels facilitate ventilation, while maintaining some privacy and security. When winter approaches, another layer of panels would be added to impede air infiltration.

(ii) The Two-Tier House:

In this type of house, the rooms facing the sea were intended primarily for summer use, whereas the others were intended for winter occupation. The rooms were often built around a large courtyard, which helped induce air flows through the summer rooms. The summer part of the house was sometimes made from palm-frond panels, or had several large windows in its outer walls. The winter part was constructed from either mud-brick walls or palm-frond panels overlaid with mud plaster and contained only a few openings.

(iii) Mud-Brick or Stone Buildings:

These were used for fortified houses, shops and generally where achieving security was paramount. They also occur in settlements further inland from the coast, i.e. where the humidity is lower.

2.3.2 The Muscat Region

This narrow coastal strip includes both the old towns of Muscat and Mutrah. These are located on land where the mountains meet the sea, and adjacent to excellent harbours. The mountains provided protection against attacks from inland as well as locations for high look-out posts and gun emplacements to fend off attacks from the sea. The neighbouring presence of the large thermal mass of the mountains, so close to residential areas, also helps to stabilise the temperature of the surrounding air, which is generally a few degrees higher than for the other coastal areas of Oman. This results in a lower relative humidity; the mean relative-humidity during the summer months being less than 60%.

The presence of the mountains also affects the daily cycle of land⇄sea breezes. Because of their higher thermal capacity and thermal conductivity, the mountains heat up at a lower rate than the land generally, and this delays the onset of the sea breeze. Similarly the land breeze is delayed by a few hours in the evening.

The topography of Muscat is an enclave of land

surrounded by high mountains and open on one side to the sea. It functioned largely as a seat of political power, and this is reflected in its vernacular architecture. Historically, the settlement pattern of Muscat can be divided into three groups, according to the social positions of the inhabitants. These are :- (i) the ruling-family and influential-class district; (ii) the middle-class houses; and (iii) the low-income settlements. The first is a walled area located at the mouth of the enclave, where the sea breeze is most effective. Security and prestige were a dominant feature of these buildings. For achieving thermal comfort in this high temperature, high solar-intensity region, the houses must have sufficient thermal inertia to remain cool until around mid-day, when the sea breeze starts to be effective. The courtyard house was of a design suitable for this purpose [6], both in terms of thermal comfort and security, especially because the local humidity is not as high as for other coastal regions of Oman. Houses in this district were of a two or three-storey courtyard design, in which the ground storey had few windows but many high-level air-vents. The upper storeys had many more windows, above each of which there was also a high-level air-vent. These high-level air-vents permitted hot air to escape from the room to the ambient environment and hence to be replaced by relatively cool air from the courtyard. At night, the courtyard loses heat by radiation to the sky, while being protected from the warming effect of the wind by the surrounding rooms.

Relatively cool air thus tends to become stratified at night in the courtyard, from which it seeps into the surrounding rooms. The hot air in the rooms is thereby convected out through the high-level air vents and replaced by this denser cool air, thus cooling the structure of the rooms. The relatively-cool heavy-structure of the building and the cool air in the courtyard as well as that trapped in the surrounding rooms, continues to provide cooling until about mid-day when the Sun shines directly down onto the courtyard. By this time, the sea breeze starts to be effective and opening the windows in the upper storeys (at which height the wind speeds tend to be higher than nearer the ground) facilitates relatively cool air entering the building.

The middle-class houses were clustered in the centre of the town and were mainly of single-storey courtyard design, with some rooms having many windows and others with hardly any. The majority of such houses each had a semi-open shaded space, the "Dahreez", separating the bedrooms from the courtyard. This remains relatively cool, even when the Sun shines directly on the courtyard and so it was often used as the family's main living area.

Low-income settlements were usually found in groups near the mountain. These were mostly palm-frond houses, the thermal-comfort advantages of which have been discussed earlier. The local eddies caused by the daily cyclic temperature variations provide a source of cooling air. During the day, the air rises up the face of slope due to

surface warming. In the evening the slope's surface cools relatively rapidly, thus reducing the temperature of the air adjacent to it, and so a downward breeze of cool air ensues.

The town of Mutrah has a much more open lay-out than that of Muscat: it was built on a strip of land (of < 500m width) between the sea and the mountain and stretches around the harbour. Generally the humidity in this area is slightly higher than that of Muscat and the air temperature is somewhat lower.

The vernacular architecture of Mutrah indicates the historical social mix of the town, where a large number of Hyderabdi (or Luwatiya) merchants settled. Their walled residential quarter is still a prominent feature. Because of their need for security and privacy in a densely-populated land plot, they had to find other means for achieving thermal comfort in this hot humid region. The houses were mostly two-storey buildings with the ground floor raised 2 to 3 m above ground level in order to prevent flooding by the sea, which would otherwise occur occasionally. The ground-storey walls incorporated many tall windows, and because of their raised level, they maintained privacy and security and utilised the slightly higher (than at ground level) air-speeds of the local breezes. Cantilevered wooden-balconies are a predominant feature of these houses, which are only rarely found elsewhere in Oman. These balconies stretch, at first-floor level, along the wall facing the sea, and are covered by sloping roofs - see Figure 2.4(a). The walls, from which

Figure 2.4(a): Example of the houses on the beach at Mutrah.

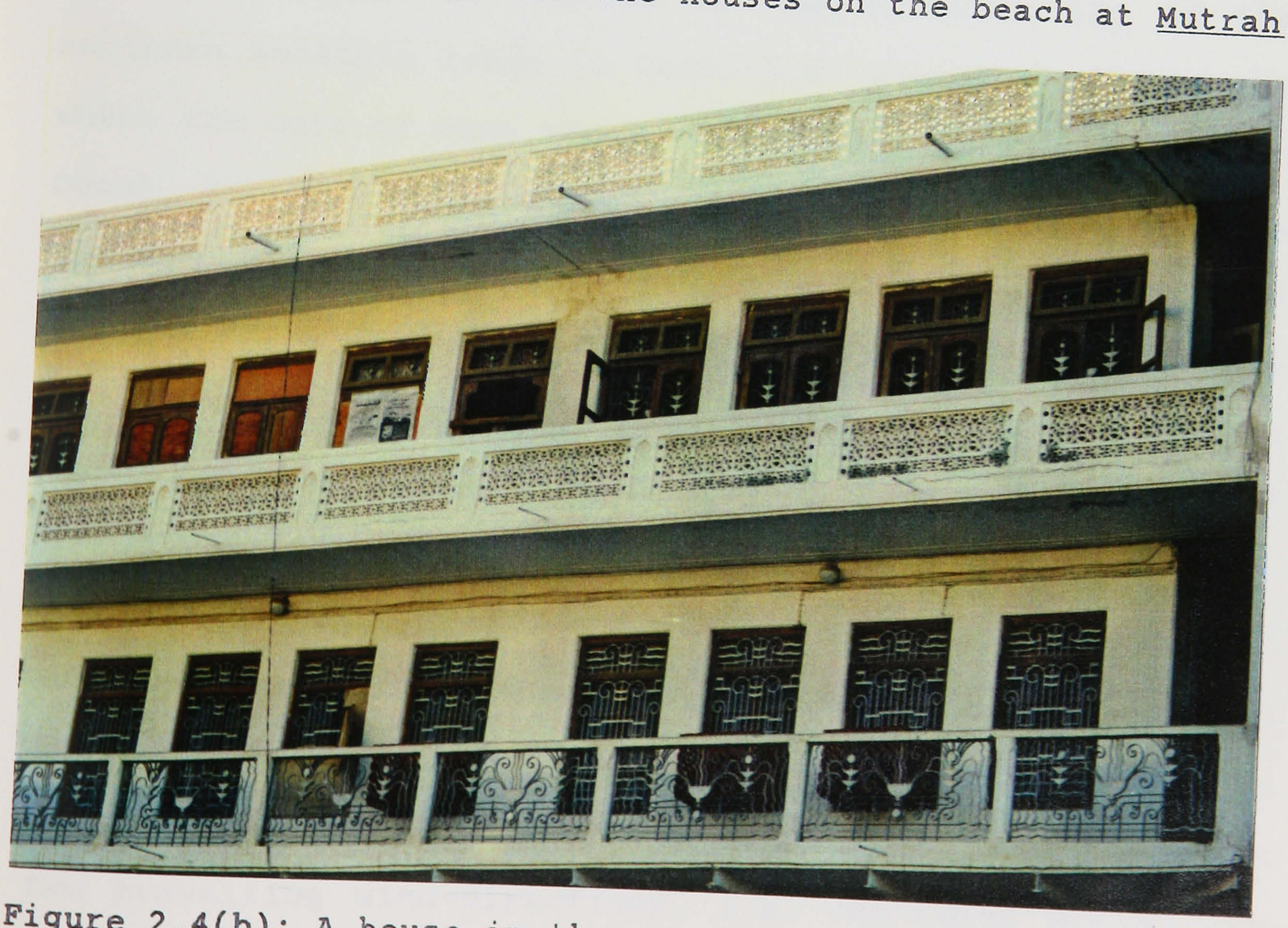

Figure 2.4(b): A house in the centre of Mutrah.

these protrude, mostly consist of glazed doors and tall windows. The balconies often functioned as extensions to the living spaces and provided places where the occupants could sit or sleep, simultaneously providing shading for lower openings in buildings.

Inland from the beach, the need for high ventilation-rates is exemplified by the number and size of openings in buildings - see Figure 2.4(b). The palm-frond house was also popular in Mutrah.

2.3.3 Sur

This region is located at the southern tip of the northern mountain range in Oman, i.e. almost at the corner where the Gulf of Oman meets the Arabian sea and the Indian Ocean. Sur is a major town in Oman, and was a busy port on the shipping routes between the north and south of Oman and between the East African coast and the Arabian Gulf, Persia and India. Relative to the other towns in Oman, Sur is densely populated and this shows in the settlement pattern of the area.

Its climatic conditions differ slightly from those of the other coastal regions due to its more open location and its proximity to the desert (i.e. Waheeba Sands in particular). The wind speed is generally higher and there are two prevailing wind-directions, i.e. northerly during the winter months and south-westerly during the summer months.

The climate during the latter is hot and humid, and thus air movements are desirable for maintaining thermal comfort. However the winter months are relatively cold and windy, and thus during this season, it is desirable to restrict air flows into the building. To satisfy these conflicting demands, especially because the wooden windows employed tend not to be air-tight, even when firmly shut, different-purpose rooms were built, i.e. primarily for either summer or winter habitation. The summer rooms have many windows facing the sea and are usually on the first storey in a two-storey building - see Figure 2.5(a). The winter rooms are usually at ground-storey level and have hardly any windows - see Figure 2.5(b). The rooms, in almost all of the vernacular houses of Sur, were built along two or three sides of the walled perimeter of each building plot, leaving a large central courtyard. This provided privacy, but it also ensured that an adequate cooling-air flow to the summer rooms ensued. In the densely-populated part of Sur, called " Sur-Al-Sahil ", the settlement pattern is very irregular; there are spaces and narrow lanes separating the houses. These irregularities could have been part of a deliberate design-policy intended to utilise the air flows through gaps between already existing houses.

An interesting feature of the vernacular houses of Sur is the design of windows, which could provide good control of the air flows into the associated room. The windows were divided into many small sections, each of which could be

Figure 2.5(a): The summer-rooms in a walled-perimeter house in Sur.

Figure 2.5(b): The inside of a winter room in the house shown in 2.5(a). The absence of windows is clearly noticeable.

Figure 2.5(c): Windows with louvres, in a house in Sur, where each slat could be opened or closed independently.

opened or closed independently. Some of the houses had windows with louvres, where each of the vanes could be opened or closed independently - see Figure 2.5(c). Many had wooden lattice work, especially those at ground level. These lattices maintained privacy while allowing air flows through them. These elaborate windows were devised in response to the windy conditions prevailing in the region.

The walls of the vernacular houses of Sur were built mostly from soft limestone, which needed regular maintenance but is readily available locally. During the cold season, such high-density walls transmit heat (absorbed during the day) into the inner space <u>at night</u>, thus maintaining (as desired) a higher than ambient air temperature inside the closed winter rooms.

2.4 <u>The Mountainous Region</u>

This includes the towns in and around the northern mountain range, extends from the northern borders with the United Arab Emirates to the north-eastern corner of Oman and runs approximately in line with the coast. It separates the coastal region from the desert area. The highest peak, 3,075 metres above the sea level, lies to the south east at "Jabal Al-Akhdar" (i.e. the Green Mountain).

The rainfall on the mountain occurs intensely (and for only a short period each year), and so during this time it <u>pours</u> into valleys, thereby causing flash floods. These, with

the rich soil they carry, have created fertile plots of land alongside the winding routes of the valleys. Thus almost all the major settlements in this region are located on the flanks of these valleys.

The climate of the region is influenced significantly by the impressive mountain range. With its high thermal capacity, it moderates the diurnal and annual local ambient-temperature fluctuations. Nevertheless, the resulting temperature variations generally exceed those experienced on the coast, but they are less than those for the desert. Also, because of the higher altitude, the average temperature is generally lower. However, the solar intensity exceeds that on the coast, partly due to the lower moisture content of the air. The prevailing wind direction is northerly during the winter months, and south-westerly in summer. The northerly wind, called the "Alwi", is too cold for the local population in this hot region, and the south-westerly summer wind, called the "Samum", coming from the Empty Quarter Desert is too hot and dry. There is also a local thermally-induced slope/valley breeze, which is a daily occurring phenomenon, in these mountainous regions.

There are slight climatic differences between the sea-facing and the desert-facing sides of the mountains, e.g. the humidity is somewhat higher on the sea-facing side. Also, there, the towns lie to the east of the mountain range, and being located in valleys near the base of the mountains, they tend to be shaded from the effect of the Sun during the late

hours of the day. But most importantly, these towns are sheltered from the hot dry south-westerly wind blowing from the desert. Together with other social and economic factors, these climatic variations have created differences in the settlement patterns across the region, but generally the vernacular-house forms tend to be similar.

Settlements in this region occur where there is fertile land and an adequate supply of fresh-water to irrigate it. Generally houses were built on raised plots (which are not suitable for agriculture) and so do not get flooded. Palm trees cover more than 80% of the cultivated land. Groups of houses are found either within the cultivated area or beside it. There are two clear effects of the climate on the vernacular architecture of this region, and on human responses to the climate. The first is the clustering of houses, which is particularly apparent on the desert-facing side of the region. Houses here are two or three-storeys high, and densely packed together : they share two or three common walls, and/or are separated by narrow twisting lanes. The clusters of houses are generally located on the lee-ward side of the palm-tree plantation, i.e. with regard to the direction of the hot summer wind. The plantation thereby helps to condition the air stream, via the process of transpiration of the trees, so cooling and increasing its moisture content before it reaches the houses. Clustering protects the houses from the high-intensity insolation and the penetration of unwanted hot or cold winds. The narrow

lanes, which remain shaded until almost mid-day, provide a source of relatively-cool air: being connected to the palm-tree gardens, they serve to channel relatively-cool air from the gardens to the houses.

The walls of these houses are constructed from bricks of baked mud, which has a low thermal conductivity ($\approx 0.4\ Wm^{-1}K^{-1}$) but a high thermal-storage capacity. These thick walls help attenuate solar gains and nocturnal heat losses and so stabilise the temperatures within the houses, despite the large diurnal-nocturnal temperature fluctuations to which they are exposed. Another feature of these houses is the high ceilings, which facilitates air stratification, so that the inhabitant's immediate environment is relatively cool air.

Several activities, intended to reduce the impact of the harsh climate, were practised. Spraying water on floors and on the surfaces of the narrow lanes was a daily task for many of the inhabitants of this region: it was carried out once in the morning and once in the afternoon. This reduced the temperature of the local environment by evaporative cooling. Another evaporative-cooling measure (used mainly for the provision of cold drinking-water), was the hanging of slightly-porous water-jars within the window apertures. Ventilation air entering the building through the windows passed over the wet external surfaces of these water jars, which were thereby cooled by the induced evaporation of the water from their external surfaces: simultaneously the air passing over their external surfaces was humidified and

slightly cooled. In most parts of Oman, this use of porous water jars was the main method of cooling water for drinking, before the recent arrival of the electric refrigerator.

Another human response to the weather was the local migration in summer from the clustered houses to the plantation. Date growing was the main source of income for the inhabitants of this region, and so most of the population used to move in summer to the plantation area, where it was cooler, in order to carry out the harvesting. Houses in the plantation tended to be built in the occupant's own palm-tree garden, and so they were relatively scattered. They were also shaded by the tall palm trees, surrounded by watered land where evaporative cooling ensued, and their walls had many large openings. So generally, these summer houses provided a much more pleasant environment, at least from a thermal comfort point of view, than the clustered houses.

A third human response, in order to try to achieve thermal comfort, especially for those staying in one of the clustered houses, was to spend the evening hours, and to sleep at night, on the roof. This is because during the evening, and especially at night, the ambient air is cooler than that "indoors", and also thermal comfort is enhanced by radiative heat loss to the relatively-cold clear night-sky.

The general orientation of the traditional house in this region is south facing. Because of the solar azimuth angles, this orientation is best for reducing solar gains in summer, at the low latitude of the region - see Figure 2.6. In most

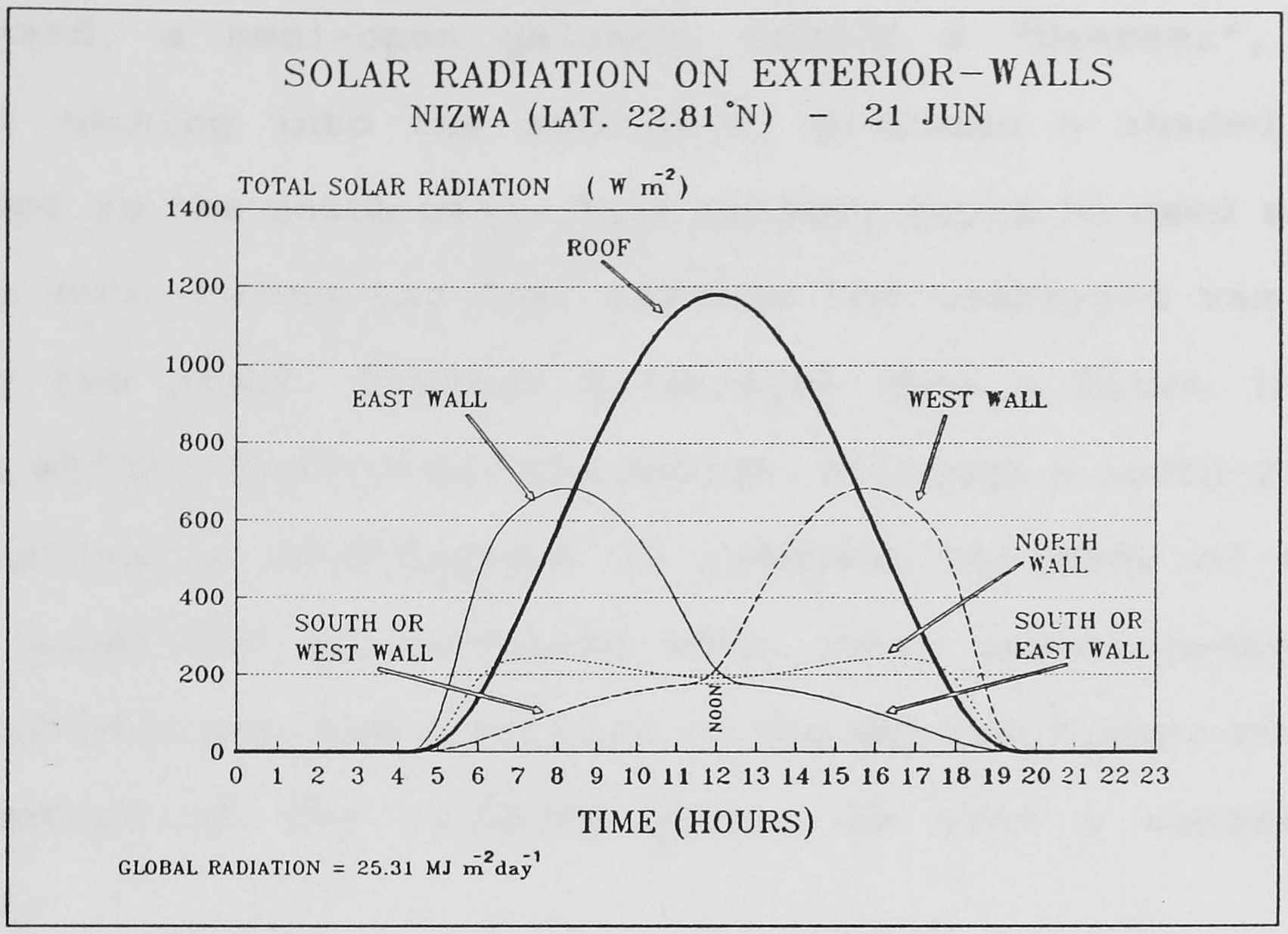

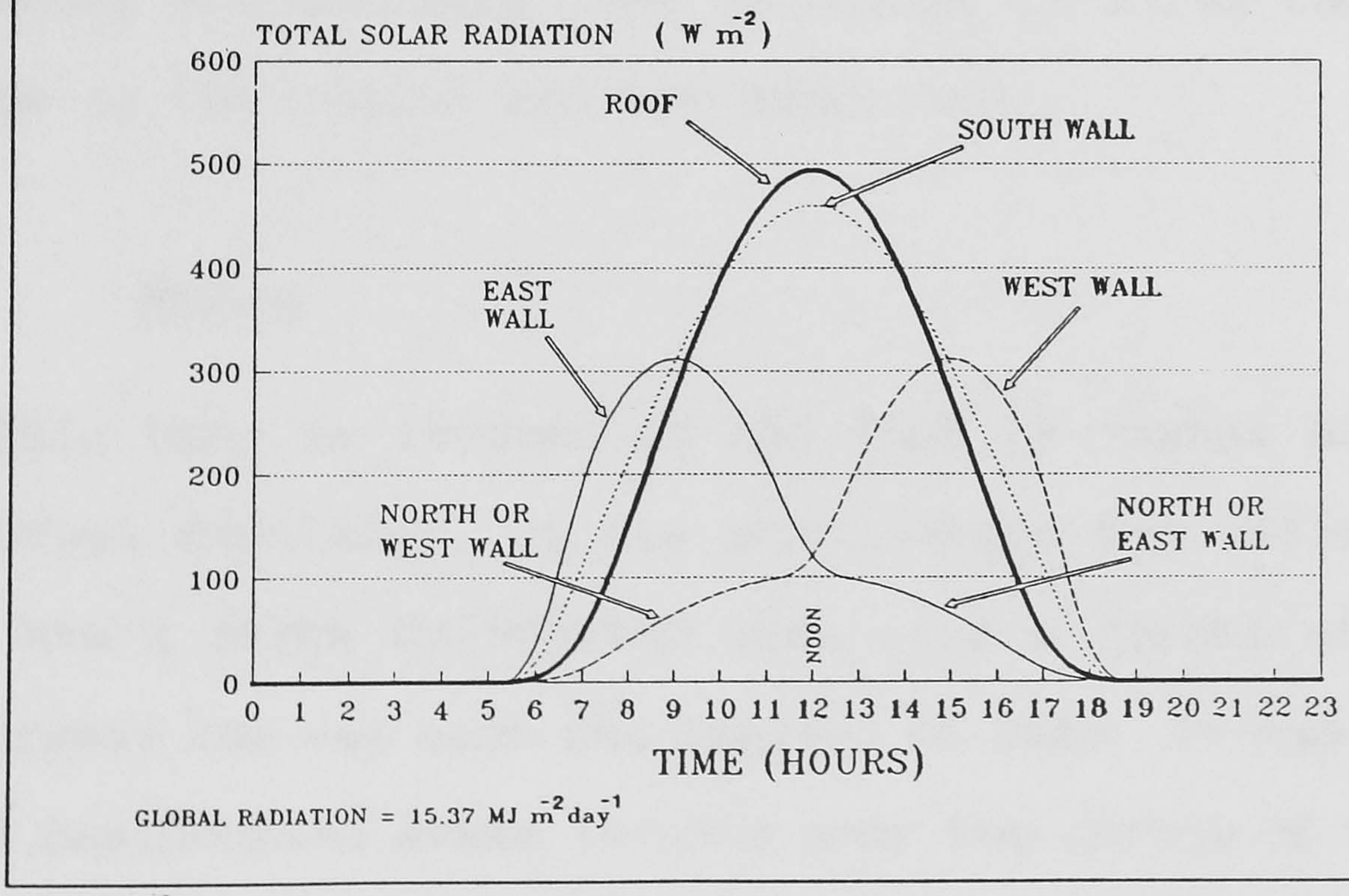

Figure 2.6: The estimated solar insolation falling on the exterior walls of a building in Nizwa (Latitude 22.81 ^{0}N) on (a) the 21st of June and (b) the 21st of December.

big houses which have a perimeter wall enclosing an external courtyard, a semi-open gallery, namely a "Dahreez", with arches opening into the courtyard, provides a shaded area adjacent to the south wall. This gallery could be used as the living zone during the day, whereas the courtyard was used during the night. Figures 2.7(a)&(b) show a house in Al-Ghafat which illustrates this design. Although a south-facing orientation is advantageous in reducing the rate of solar gain, sometimes it conflicts with other requirements and restrictions (eg. the direction of the welcome breeze and the orientation of the building plot), so then a compromise ensued.

To illustrate some of these points, as well as to appreciate the effects of the topography and climate on the indigenous architecture, the buildings in three towns and a village in the region are now described.

2.4.1 Nizwa

This town is located at the foot of "Jabal Al-Akhdar" (the Green Mountain), at the point where two valleys meet. Nizwa has a large cultivated area (i.e a forest of ~25,000 palm trees) and was once the capital of Oman. It has densely-packed residential areas located near the centre of town, and to the east of the cultivated land [7]. The houses in these areas are clustered, two or three storeys high, and separated by narrow twisting lanes leading to the plantation - see Figure 2.8(a). Courtyards are rare in these houses, so are

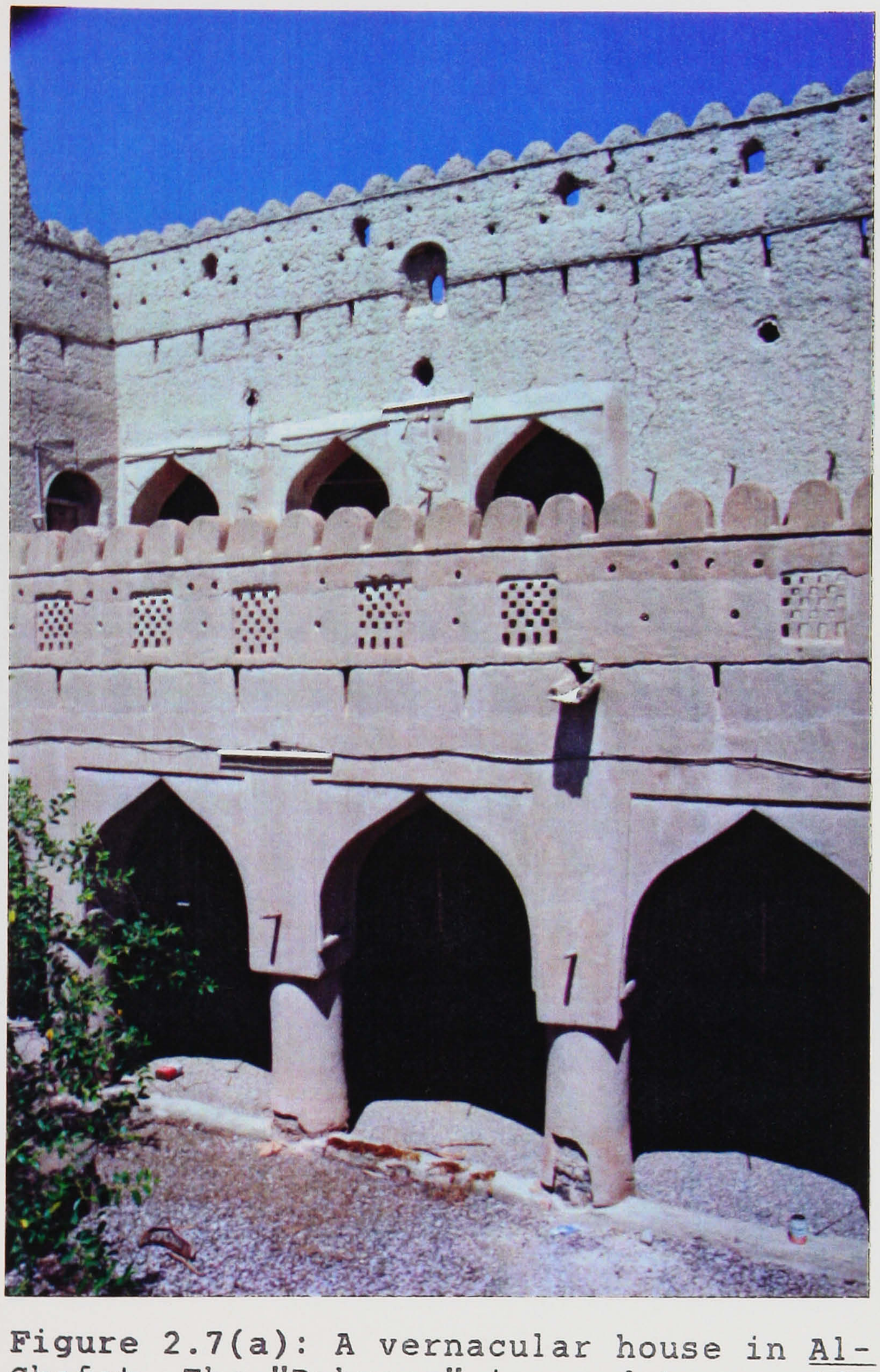

Figure 2.7(a): A vernacular house in Al-Ghafat. The "Dahreez" is used to provide shading and a shaded semi-open space along the southern wall of the building in both the ground and first stories.

Figure 2.7(b): The inside of the "Dahreez" in the first story of the building in 2.7(a).

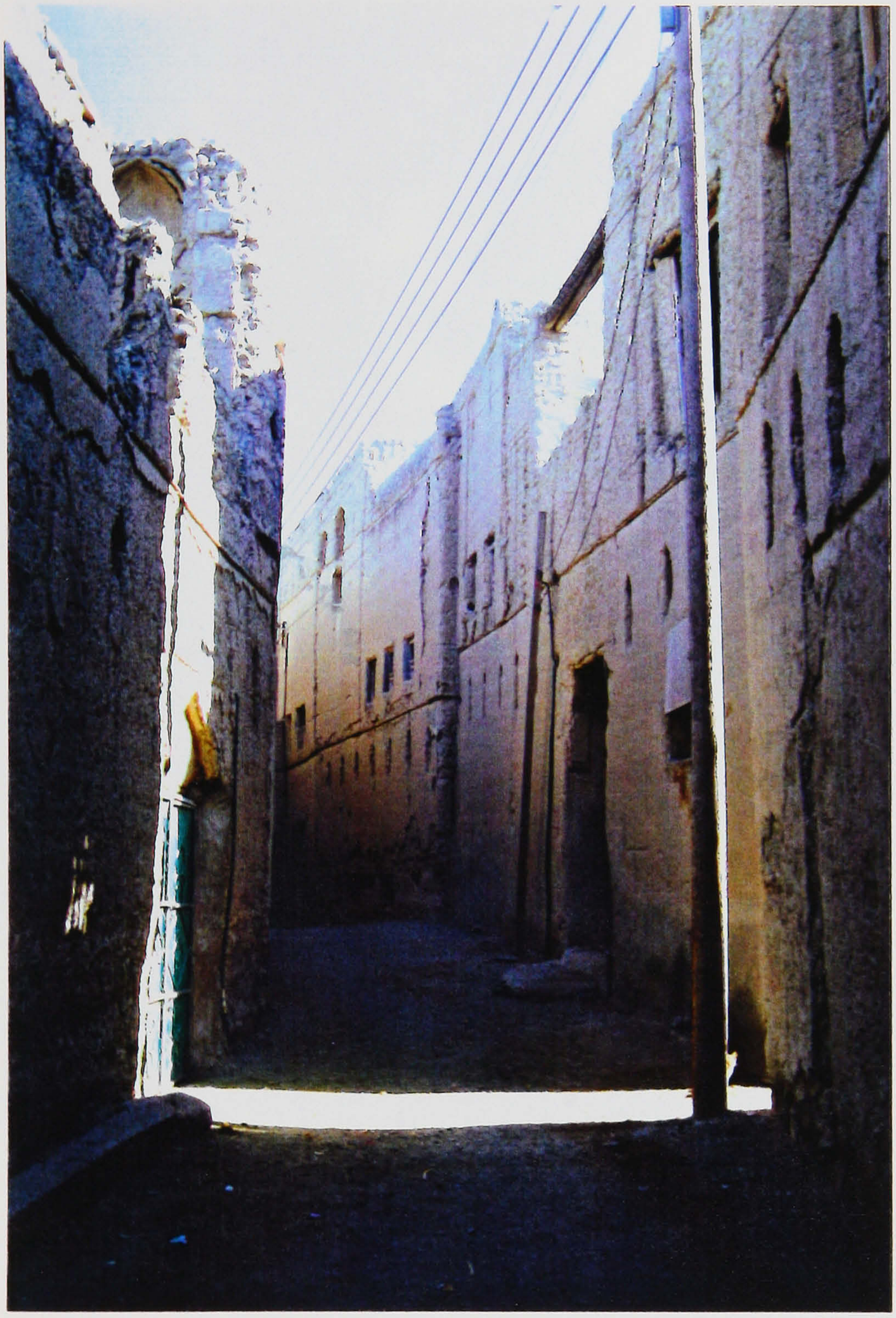

Figure 2.8(a): An alley way in the old town of Nizwa.

Figure 2.8(b): A typical summer house in Nizwa.

windows in the ground-storey walls. The mud-brick walls are about 500mm thick, and high-level air vents are found in all the walls of all the storeys. During winter, these were often blocked with pieces of cloth. The roofs of these houses have slightly-raised perimeter walls, so providing some privacy when the roof is used for sleeping. The summer houses - see Figure 2.8(b) - are scattered all over the plantation.

The mountain range lies to the east of the town, and so the daily, thermally-induced, slope/valley breeze has a predominantly east-west direction. This is approximately the direction of the narrow lanes onto which the windows open. The hot, dry air passing through the plantation is cooled and gains moisture before reaching the houses. Also the plantation, with its tall palm trees, shields the clusters of houses from the direct effect of the hot south-westerly summer wind.

2.4.2 Al-Rustaq

This town is located at the foot of Jabal Al-Akhdar, but on the sea-facing side of the mountain range. Al-Rustaq controlled the quickest route connecting the Batinah Plain with the interior of Oman. Its vernacular architecture exhibits many similarities to that of Nizwa, but the sizes of the clusters tend to be smaller, and these are well scattered in the plantation area. Also the density of houses within a cluster is less than that in Nizwa, and many houses stand alone - see Figure 2.9. Generally, the houses here have more

Figure 2.9: Vernacular houses in Al-Rustaq.

windows and larger openings in the upper-storey walls than those in Nizwa. This scattering and increased separation between houses could be attributed partly to the climatic conditions experienced, i.e. the humidity is higher, the solar intensity is lower and the high mountain provides a shading and protecting effects from (i) the direct solar radiation during the late afternoon and (ii) the prevailing south-westerly and northerly winds.

Because the houses are scattered over the plantation area and most people prefer to live near their gardens, summer houses like those of Nizwa are not found in Al-Rustaq.

2.4.3 Al-Hamra

This town is renowned for its beautiful vernacular architecture : the relatively small settlement incorporates the previously-mentioned passive-solar design features, for achieving thermal comfort. Also located at the foot of Jabal Al-Akhdar, on the desert-facing side, the settlement forms a strip, with approximately an east-west axis, on a slope facing a palm-tree plantation. Behind it (on the north side), the mountain range rises sharply. The houses, which have a south-facing orientation (i.e. with an approximately east-west axis), are designed in rows and separated from each other by narrow lanes. The big houses tend to be near the bottom of the slope, i.e. adjacent to the plantation and close to the water-supply channel (the "Falaj"), which

separates the plantation from the residential area. The house form is similar to that for the rest of the region, i.e. constructed from thick mud-brick walls, with hardly any windows for the ground storey. However clustering is not common in Al-Hamra.

The south-facing orientation of the houses combines the advantages of reducing summer solar gains and harnessing the slope/valley breeze. During the day, the up-slope breeze draws cool air from the plantation through the rows of houses.

Houses in Al-Hamra are of a slightly different character from other houses in the region. One of their distinct features is the two-level window : a typical window stretches downward to near floor level, but there is a smaller window above it, and a high-level air vent near the ceiling - see Figures 2.10(a to d). These windows provide larger apertures as well as better control when required, both with respect to air movements and privacy. The ground storey, especially in big houses, was used mainly for storage, cooking, washing and for housing animals. The main living area is on the first storey, and is surrounded, on two or three sides, by bedrooms. The upper storeys have many windows, especially in the south-facing wall, in order to capture the cool breeze coming from the plantation.

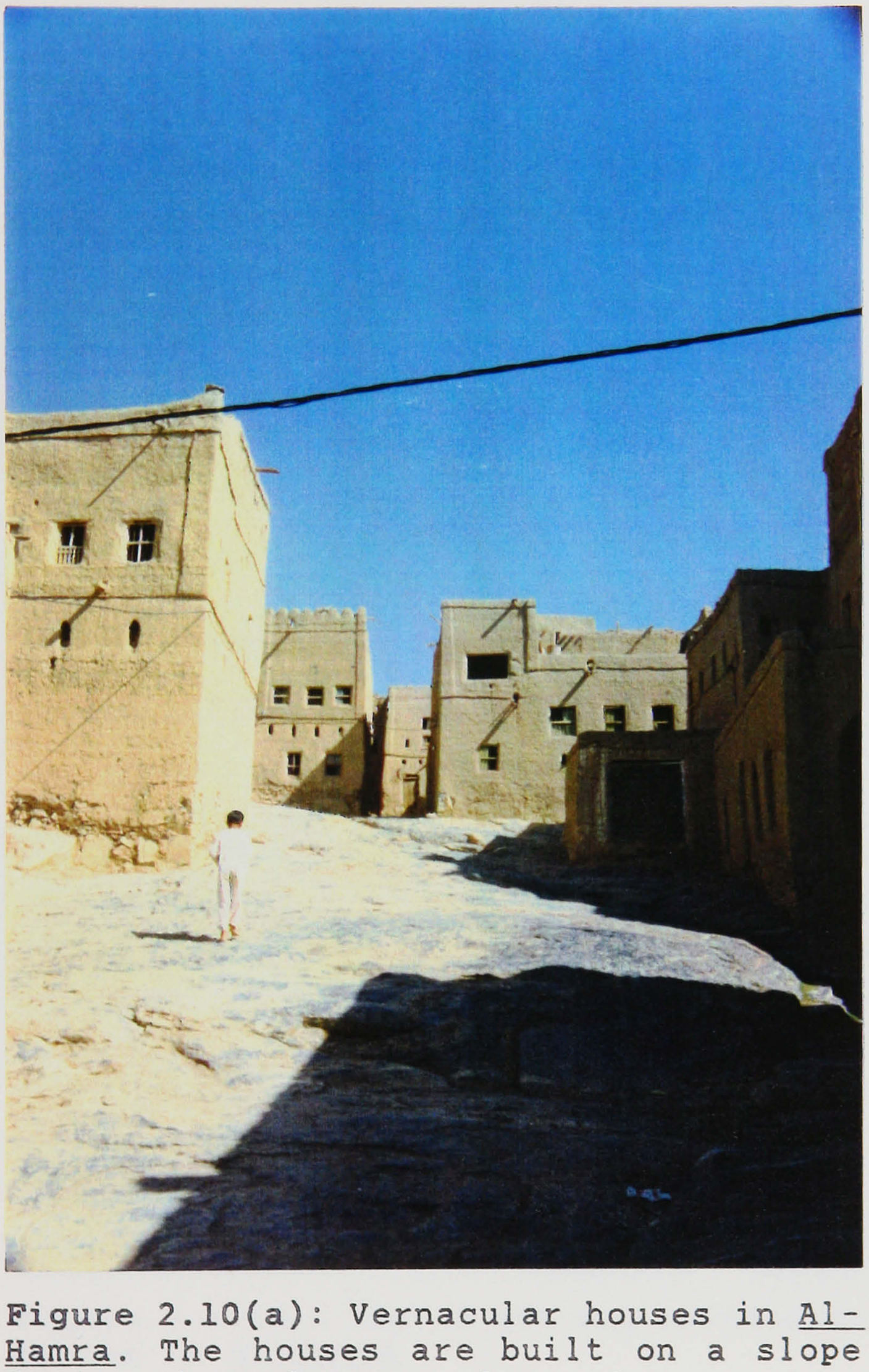

Figure 2.10(a): Vernacular houses in Al-Hamra. The houses are built on a slope facing the palm-tree plantation.

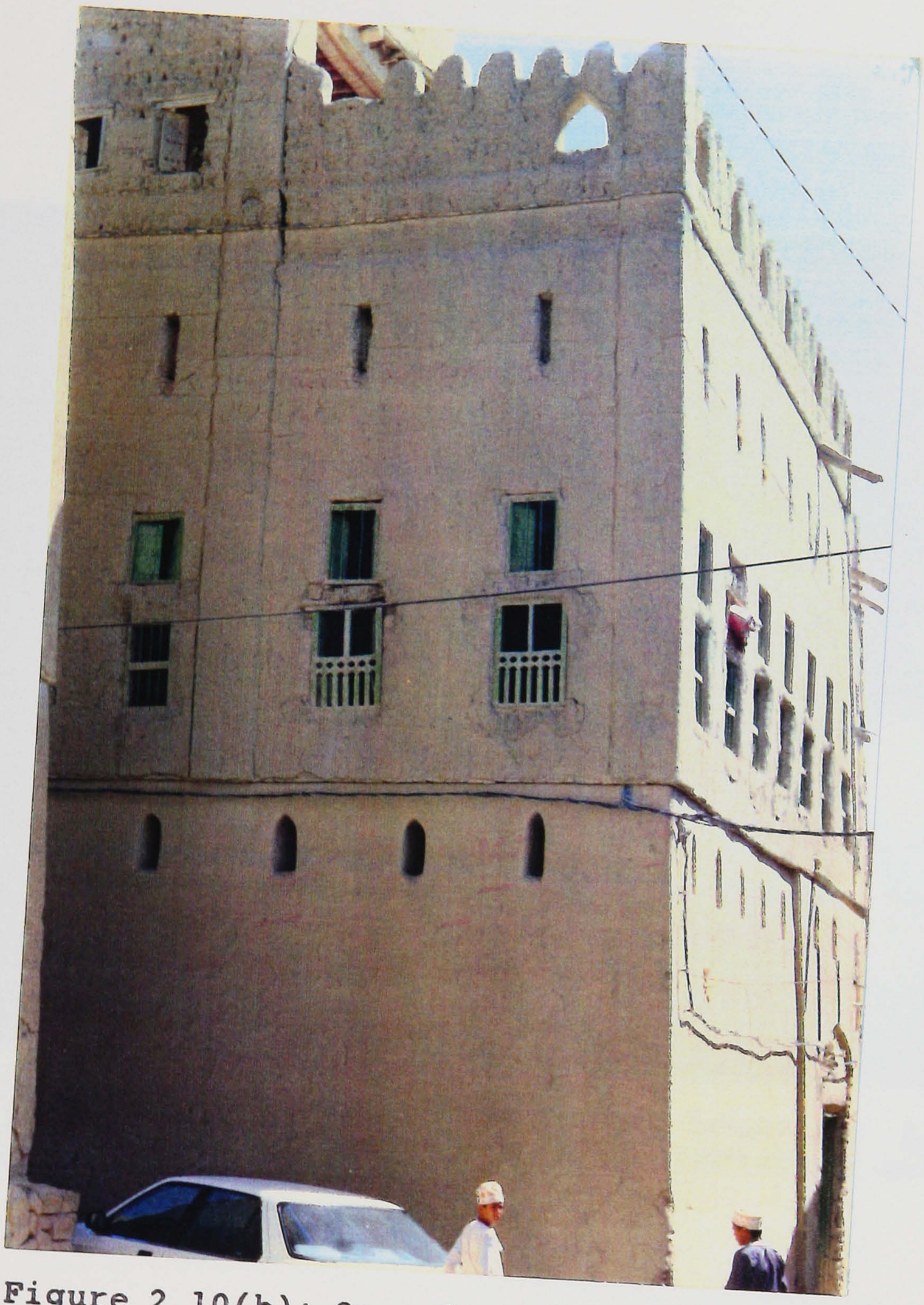

Figure 2.10(b): One of the big vernacular houses in Al-Hamra.

Figure 2.10(c): The living-room of a house in Al-Hamra. Relatively cool air from the palm-tree plantation enters the house through the double-windows.

Figure 2.10(d): One of the bedrooms in the house in 10(c). The double-window, high-level air vent and the high ceiling are important features in maintaining thermal comfort.

2.4.4 Al-Missfah

This is a small village, high on the mountain, just above Al-Hamra. At such a high altitude, the weather is not particularly hot, even in mid-summer. Although the houses exhibit some of the features mentioned earlier for enhancing the thermal comfort in summer, the indigenous houses of Al-Missfah tend to cater more for thermal comfort during the relatively cold winter months. Windows, and other apertures, even high-level air vents, are rare for the ground storey. Also, the number of windows for an upper storey is usually less than that for a house near the valley floor.

The walls were constructed from stone and gypsum plaster, mainly due to the ready availability of stone. Being denser and with fewer pores per unit volume, stone is a better conductor of solar-heat gain than baked-mud bricks. The houses were built on a south-facing slope above "terraced" palm-tree gardens. The south-facing orientation of the building is preferred for both summer and winter occupation.

2.5 The Desert Region

This designation refers to the towns in or close to the desert. The climate of this region is influenced by its proximity to the desert; being hot and dry in summer, yet cold in winter. Nevertheless, the presence of buildings and vegetation in each towns produces a micro climate which differs significantly from that of the barren desert : the air temperature during the day being lower and the moisture content of the air higher. However, compared with the other regions of Oman, the climate here is hotter and drier, with large nocturnal-diurnal as well as summer-winter temperature swings.

The vernacular architecture of this region attempts, with a reasonable measure of success, to use the available natural means for attenuating and/or isolating the distressing effects of the climate. There are two main processes available for natural cooling:- the first is radiative heat exchange with the cold clear-sky at night; and the second is evaporative cooling. The undesirable climatic processes are solar gain and the hot, dry and sometimes dusty air blowing from the desert.

The 'internal' courtyard house (as distinct from the external courtyard which is formed by the encompassing perimeter wall, but which is not an integral part of the building) is common in this region, especially for big houses. The courtyard is often surrounded by a semi-open gallery, i.e. the "dahreez", into which the rooms of the

house open. The windows in these rooms also open into the dahreez : only small high-level air vents open directly to the outside. The walls are thick, constructed from either mud brick, or stone and fired clay, the latter being stronger and requiring less maintenance.

It is clear that this house form tries to isolate the internal spaces of the building from the harsh effects of the ambient environment, whether it be with respect to solar gain or hot dusty air. This is the main reason for the absence of windows in the external walls.

However, after sunset, the air and surface temperatures drop considerably due to thermal radiation occurring to the clear night-sky. This radiation loss allows surfaces to cool significantly, i.e. to below the ambient-air temperature. The achieved cooling is enhanced when the surface is protected from the warming effect of the wind. This ensues in a courtyard protected by the building surrounding it. In the early part of the evening, the air in the courtyard, being warmed by the surrounding surfaces which have absorbed heat during the day, becomes warmer than the ambient air. The warm air in the courtyard thus rises, drawing in the cooler ambient air, and causing a convection current which gradually cools the courtyard and the surrounding structure. The high-level air vents in the external walls also facilitate the convective cooling of the rooms. When the courtyard and surrounding rooms attain the temperature of the ambient air, i.e. a few hours after midnight, convection stops. However

the courtyard keeps on losing heat by long-wave radiation to the night sky, further cooling the air in the courtyard which tends to stratify and seeps into the surrounding rooms. The relatively-hot air in the rooms thus convects to the outside through the high-level air vents. This in turn cools the heavy structure of the building, which acts as a storage medium for the "coolth" which will help to prolong the maintenance of thermal comfort during the subsequent day.

This house form can be seen (Figure 2.11) in the town of Al-Mudairub, which is not far from the Waheebah-Sand desert. Many towns in the eastern region of Oman are located at the north-eastern edge of this relatively-small desert. To its north lies the northern mountain range, and to its south is the sea. The difference in temperature between the mountains and the sea causes a daily night-time breeze through the desert, known locally as the "Koos", which comes from the sea to the south.(The sea is also to the east of this desert, but here high ground separates the two). This breeze starts early in the evening, when the desert cools down, and continues until sunrise. The reverse process, that should occur during the day, is interrupted by the rising hot air due to the desert's surface warming. In some of these towns, especially those which are partly in the desert, people welcome this breeze, which gives relief from the hot dry dusty environment, and so spend the late afternoons and evenings in open spaces outside their houses. They also used to sleep outside, on the sand dunes at the outskirts of the town.

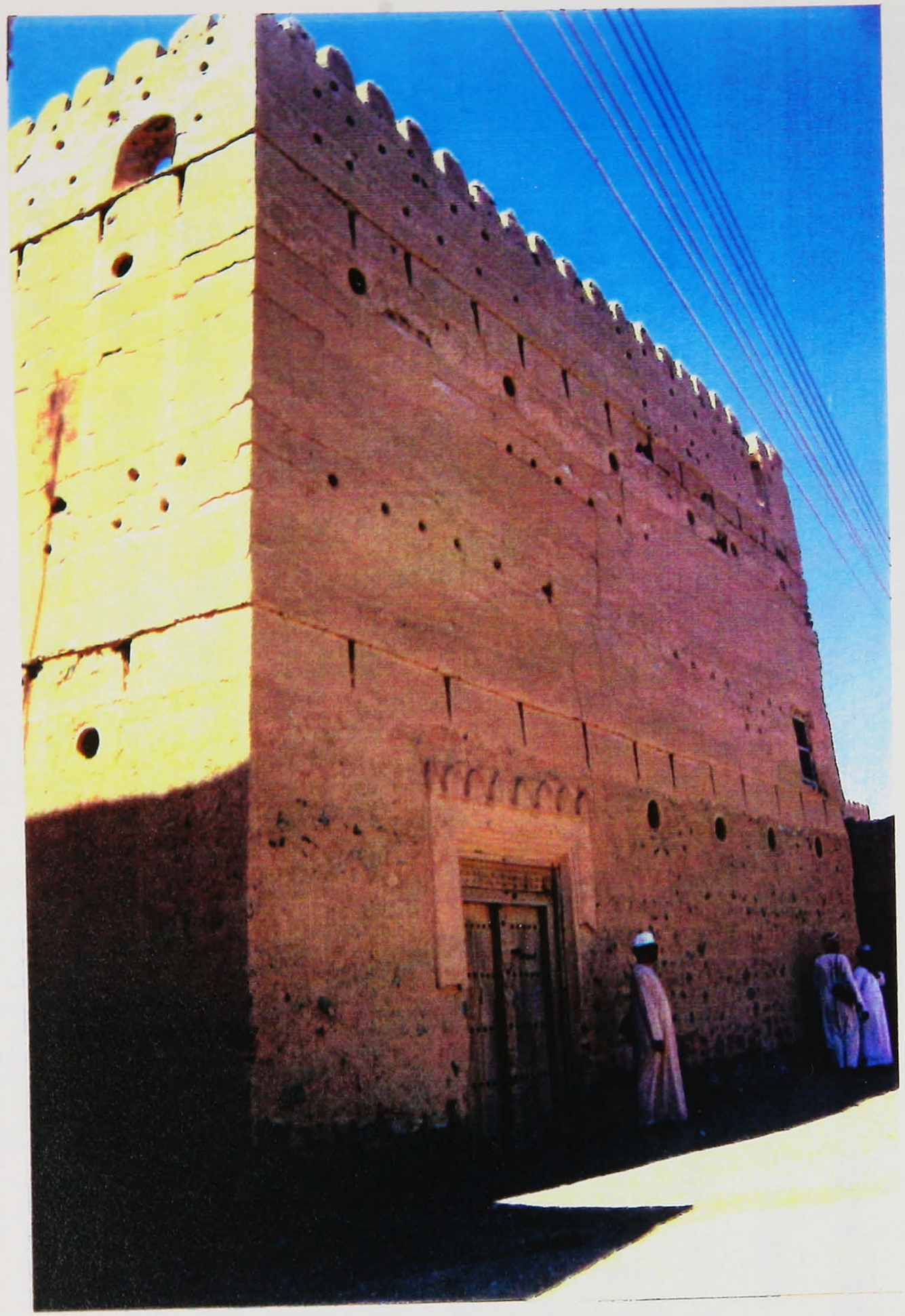

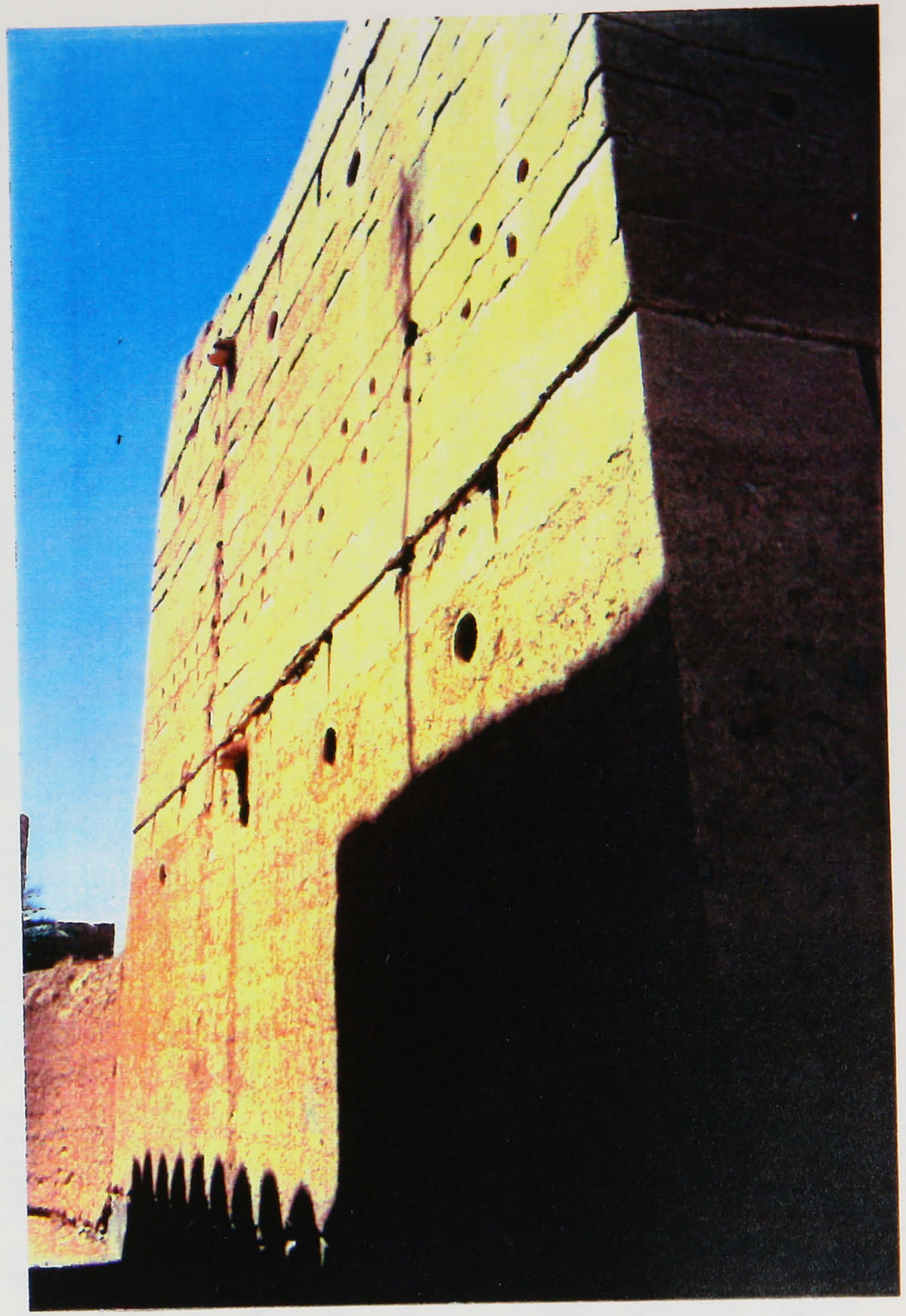

Figures 2.11(a&b): The outside of vernacular houses in Al-Mudairub: note the absence of windows.

2.6 The Southern Region

This is also dominated by a mountain range, the" Jabal Al-Qara",which stretches almost from east to west close to latitude 17°N. It separates the coastal plain (which is 8 km at its widest) from the desert. Most towns in this region occur along the almost south-facing coast. Salalah is the biggest, consisting of groups of settlements parallel with the coast. There is a narrow band of plantation (consisting mainly of coconut palm trees) separating the beach settlements from the inland settlements. In the past, the beach settlements were inhabited by fishermen and the servants working in the palace of the Sultan, which is also located along the beach [8].

The region is considered to be part of the warm humid tropical belt and, unlike the northern regions of Oman, it remains green for most of the year. This is due to the indirect effect of the Monsoon winds which pass near the coast. The winds cause the air to become saturated, so forming a mist and low-level clouds, and the moisture subsequently falling as drizzle on the mountain. During this season (known locally as "Al-Khareef"), which starts in June and ends in September, the mean monthly humidity exceeds 85%. Because of the thick clouds and high humidity, the global solar radiation on the horizontal-ground surface drops sharply from around 23.4 $MJm^{-2}day^{-1}$ just before the start of the season, to as low as 3.6 $MJm^{-2}day^{-1}$. (The Sun passes vertically above Salalah during the first week of May and the

second week of August). Because of the drop in solar radiation, the mean-monthly air temperature drops from about 30 °C in May to less than 25 °C in August. So the primary source of discomfort during this season is the very high humidity.

Generally there are two prevailing wind directions in the region, southerly from March to October and northerly during the winter months. From a thermal-comfort point-of-view, the northerly wind in winter is disliked, because it is relatively cold, dry, dusty and often strong. On the other hand, the southerly wind brings welcome relief from the high humidity in summer. There are also the superimposed diurnal-nocturnal cyclic land⇄sea breezes : southerly during the day and northerly at night. But, due to the relatively low insolation-intensity during the humid season, the effect of this breeze is not prominent. Also the interaction between the prevailing wind in summer and this breeze system strengthens the day-time breeze, and renders ineffective the northerly night-time breeze.

The vernacular architecture of the region has made use of the prevailing climatic conditions for achieving thermal comfort. In the old town of Salalah, the settlements occur in groups parallel with the coast. Houses in these groups also face south, i.e. towards the coast. This orientation is advantageous in terms of reducing the solar gain in summer, increasing the solar gain in winter (see Figure 2.12), and harnessing the summer breeze.

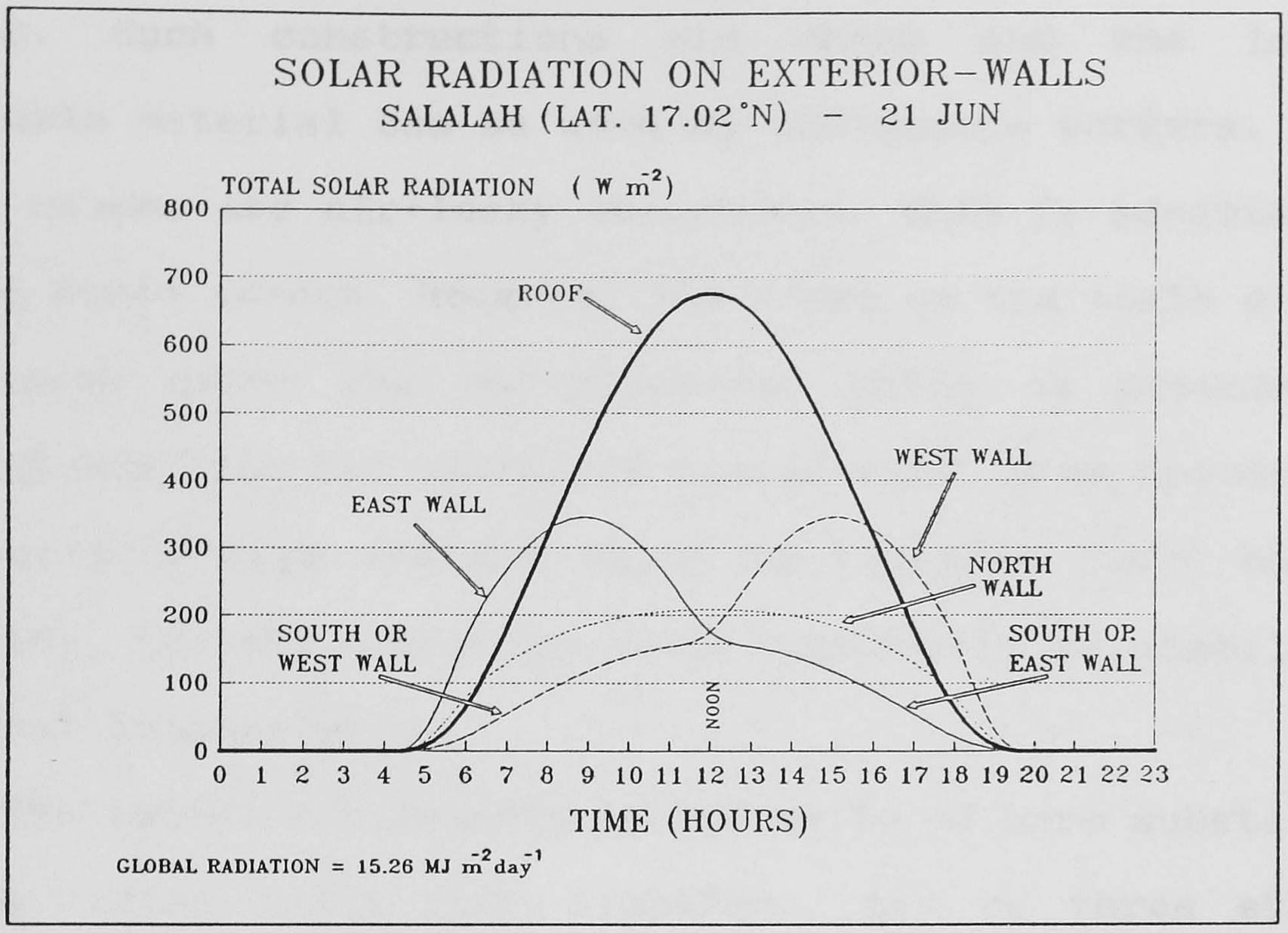

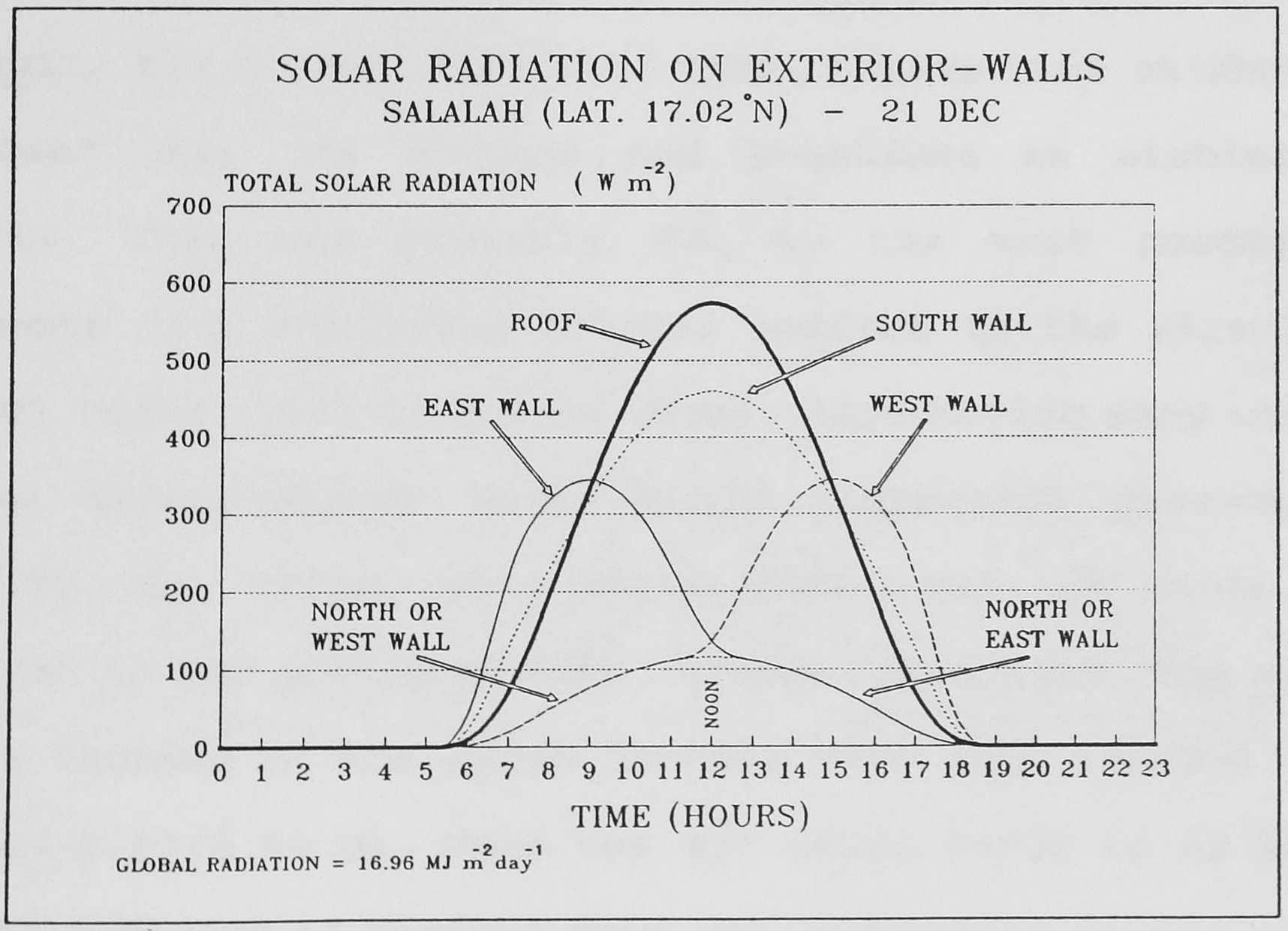

Figure 2.12: The estimated solar insolation falling on the exterior walls of a building in Salalah (Latitude 17.01 ^{0}N) on (a) the 21st of June and (b) the 21st of December.

The beach settlement consisted mainly of palm-frond houses. Such constructions are cheap and the locally available material can be used by indigenous workers. Palm-frond houses are air-leaky structures: this is advantageous in the humid season. However, the rooms on the north side of the house often had mud-plastered walls to protect the inhabitants from the northerly winter-wind. Some houses also had mud-plastered western walls to increase their thermal capacity, thereby enhancing their capability of stabilizing internal temperatures.

The inland settlements tended to be of more substantial houses, often built from limestone, two or three storeys high, with their long southerly-facades facing the sea. Generally the ground storeys of these houses were uninhabited and used only for storage and sometimes as stables for animals. This was probably due to the much needed air movements (for achieving thermal comfort in the warm humid season) being least at ground level. Also having many windows in the ground-storey walls would compromise privacy and security. So, often, only small high-level air vents were employed in the ground storey. On the other hand, the south-facing facades of the upper storeys have many windows - see Figures 2.13(a to d). Here the air speed tends to be higher and the presence of windows does not compromise significantly the privacy or security achieved. Windows were built typically into the east and west facades but not into the north wall of each house, which contains only high-level air

Figures 2.13(a-d): Examples of the vernacular architecture of the Southern Region of Oman.

vents. This absence of northerly windows protected the inhabitants against the unwelcome northerly winds in winter. Houses were generally built well apart from each other, so as not to be in the wind "shadow" of neighbouring houses, thus allowing the wind to reach all the houses, especially at the levels of the upper storeys. Many of these houses incorporated a low perimeter-wall enclosing a courtyard on the south side to prevent other houses being built in close proximity and which would thereby obstruct the sea breezes - see Figure 2.13(c).

The rooms in these houses were built around a large stair-well, which also acts as a small internal courtyard, thereby providing some lighting as well as facilitating ventilation. There were often windows opening onto this courtyard to encourage air movements through the rooms.

In winter, the thick limestone walls store and transmit some of the solar energy, falling on them during the day, in order to heat the internal spaces, especially at night and in the early morning hours. This desirable behaviour is due to the long thermal-signal time lag (≈18 hours) produced by the thick limestone walls.

2.7 Conclusions and Discussion

This review of the vernacular architecture of Oman shows that the building forms adopted in different regions relate specifically to the provision of thermal comfort by taking due regard of their characteristic regional topographies and climates. In the coastal region, vernacular buildings utilised the sea breezes for achieving thermal comfort. These rows of buildings face the sea and have many large apertures in the sea-facing walls. The houses are separated by sufficient distances so as to allow the breeze to reach all of them. Often shading devices were incorporated for east-facing walls to reduce the solar gain; low-density indigenous materials, e.g. palm-fronds, were used in the construction to reduce the heat storage in the fabric of the buildings.

In the mountainous region, the vernacular architecture relied on the effect of vegetation to modify the micro-climate. Buildings were located, in groups or clusters, either within the palm-tree gardens, or to their lee-ward side with respect to the prevailing wind direction in summer. Some towns were built on slopes, facing the palm-tree gardens, thus utilising the slope ⇄ valley breezes. Thick, mud-brick walls, were used to moderate the large nocturnal-diurnal temperature swings, thereby keeping the inner spaces relatively cool during the day. Simultaneously, the use of high, well-insulated ceilings, and high-level air vents tended to make the associated rooms more comfortable. The general orientation of vernacular houses in this region is south-facing, which is

desirable for reducing solar gains in summer yet increasing them in winter.

In settlements in the desert region, a courtyards was used as a modifier of each building's micro-climate. Radiative cooling to the sky at night reduces the temperature of the courtyard to below that of the ambient air. The rooms of such a building open onto a semi-open gallery surrounding a central courtyard. Very few windows were employed in the outside wall. The vernacular buildings were often built from stone and gypsum; the heavy structure acting as a temperature stabiliser.

While vernacular buildings may not achieve the consistent and tight control available by means of mechanical air-conditioning systems, they can provide comfort conditions for most of the year without requiring the on-going expenditure of any fossil fuels.

It will be an exciting challenge for modern building designers to once again adopt some of these vernacular energy-thrift architectural features. This could be beneficial for commercial as well as domestic buildings and does not preclude the use of modern materials. Even where mechanical air-conditioning is still considered desirable, the energy consumption rates for cooling could be drastically reduced by the implementation of vernacular energy-thrift principles !

2.8 References :

1) A.A.M. Sayigh, Passive and Active Buildings in the Arabian Gulf Area, Proceedings Of The Third International Passive And Low-Energy Architecture Conference, Mexico City, Mexico, PP 384 - 395, 1984.

2) M.N. Bahadori, Natural Cooling in Hot Arid Regions, Solar Energy Applications in Buildings, Edited by A.A.M. Sayigh, Academic Press Inc., New York, PP 195 - 225, 1979.

3) A.V. Alp, Vernacular Climate Control in Desert Architecture, In Energy And Buildings For Temperate Climates, Edited By E. Fernandes and S. Yannas, Pergamon Press, Oxford, PP 67 - 80, 1989.

4) P.M. Costa, The Batinah And Its Built Environment, The Journal Of Oman Studies, Vol 8, Part 2, PP 109 - 116, Ministry Of National Heritage And Culture, Sultanate Of Oman, 1985.

5) P.M. Costa, The Palm-Frond House Of The Batinah, The Journal Of Oman Studies, Vol 8, Part 2, PP 117 - 120, Ministry Of National Heritage And Culture, Sultanate Of Oman, 1985.

6) C.L. Hinrichs, The Courtyard House Form: A Traditional Dwelling In The Mediterranean Region, In Energy And Buildings For Temperate Climates, Edited By E. Fernandes and S. Yannas, Pergamon Press, Oxford, PP 53 - 60, 1989.

7) P.M. Costa, Notes On Settlement Patterns In Traditional Oman, The Journal Of Oman Studies, Vol 6, Part 2, PP 247 - 305 , Ministry Of National Heritage And Culture, Sultanate Of Oman, 1983 .

8) P.M. Costa and S. Kite, The Architecture Of Salalah And The Dhofar Litteral, The Journal Of Oman Studies, Vol 7, PP 131 - 153, Ministry Of National Heritage And Culture, Sultanate Of Oman, 1984 .

Chapter (3)

Natural-Cooling Techniques for Residential Buildings in Hot Climates - An Over View

Chapter (3)

Natural-Cooling Techniques for Residential Buildings in Hot Climates - An Over View

3.1 Introduction

The natural cooling of the interiors of buildings has received rapidly increasing attention during the past two decades. This is due mainly to the success achieved in the solar ***heating*** of buildings and also due to the threats arising from increasing unit fuel prices. Solar ***cooling*** is a correct description only when applied to active systems (eg. solar refrigerators). Most natural-cooling systems rely on reducing the rates of solar-heat gains and utilising natural heat sinks like the 'sky' or upper atmosphere (via radiative cooling at night), the cooler ambient air then available (via convective cooling), the sub-surface ground (via conductive cooling) and the latent-heat loss via water evaporation. Active solar-cooling systems possess the major advantage that the maximum solar power is available when the refrigeration demand is greatest. Under such circumstances, theoretically, the need for energy storage is then minimised. Radiative cooling to the sky at night (at effectively -40°C), on the other hand, requires a means for storing this 'coolth' until it is needed.

Natural-cooling techniques for buildings can be classified into three groups: (i) passive, (ii) hybrid and (iii) active. Passive cooling generally requires the ejection of heat from buildings by natural means, which do not dissipate non-renewable energy. However, the use of fans or pumps, which require small amounts of electrical power, can enhance significantly the rates of convective and/or evaporative cooling. When such fans or pumps are employed

with passive cooling, the system is termed hybrid. In active solar cooling, the insolation collectors provide an energy source for the cooling system, which otherwise would require the dissipation of non-renewable energy sources.

Before the advent of mechanical refrigeration, ingenious use was made of the many means of cooling (e.g. damp cloths hung in draughts created by the connective stack effect in buildings). So dwellings and life styles were developed to make best possible use of these sources of cooling. The introduction of mechanical refrigeration permitted not only the ability to increase the likelihood of achieving complete thermal comfort for more extended periods, but also a great deal of flexibility in building design, and simultaneously led to changes in life style and work habits. However, increasingly, the use of a 'higher technology' resulted in natural-cooling techniques being ignored. Now with the growing realisation of the rapid depletion of non-renewable energy sources and of the adverse environmental impacts of fossil-fuel dissipating processes, it is accepted that it is foolish to continue consuming vast amounts of non-renewable fuels for the air-conditioning of buildings, when our ancestors achieved thermal comfort by natural means.

In trying to benefit from the experience of the past, many researchers, mainly architects, have reappraised the vernacular architecture of various regions of the world. The literature is full of descriptive reviews in this field, but unfortunately surprisingly little as yet of pertinent benefit to society has been incorporated as standard wise practice in modern building designs.

3.2 Thermal Comfort

The aim of cooling a building in a hot climate is to provide an artificial environment which is comfortable thermally. The human body generates heat at a rate depending on its activity level (i.e. metabolic rate: if the rate of

associated loss of heat to the environment is less than what the body needs to achieve by convection and radiation, then perspiration occurs, and this indicates that the body is in a state of thermal discomfort).

Some of the theoretical tools developed for assessing whether thermal-comfort conditions will be achieved in a proposed design are too complex for the average architect to use with confidence. Therefore simplified comfort-zone charts have been developed, but because these charts have been produced primarily by institutes located mainly in cold or temperate climates, and what is regarded as comfortable is dependent somewhat on the long-term history of prevailing conditions previously encountered, architects in other regions should not rely solely upon the recommendations in these charts. Most have been derived for persons wearing clothing typically with Cl_o value (I_{cl}) of unity, whereas people in hot climates generally employ far lighter clothing (i.e. $I_{cl} \leq 0.5$). These criteria are based on the requirements of those working in office buildings. There, air speeds of 0.5 ms^{-1} are generally not acceptable because papers can then be blown around, but air speeds as high as 1.5 ms^{-1} can be tolerated in residential buildings. However, the part of the body which is exposed to the draught can dictate whether or not discomfort is felt: for example, a draught of 0.5 ms^{-1} is regarded as uncomfortable on the ankles, whereas a 1.5 ms^{-1} draught on the face would be acceptable. As Figure (3.1) shows, there is a difference of about 5^0C in the air temperature required for comfort between the situation in which light clothing is worn in a 1.5 ms^{-1} draught and that for medium clothing and a 0.2 ms^{-1} air speed, both in 50 % relative humidity environments [1].

Acclimatization to the surrounding environment is something which has usually been considered as marginal in thermal-comfort analyses. However, as can be illustrated by the expression developed by Humphreys [2] for the neutral temperature, T_n (i.e. the temperature at which the majority

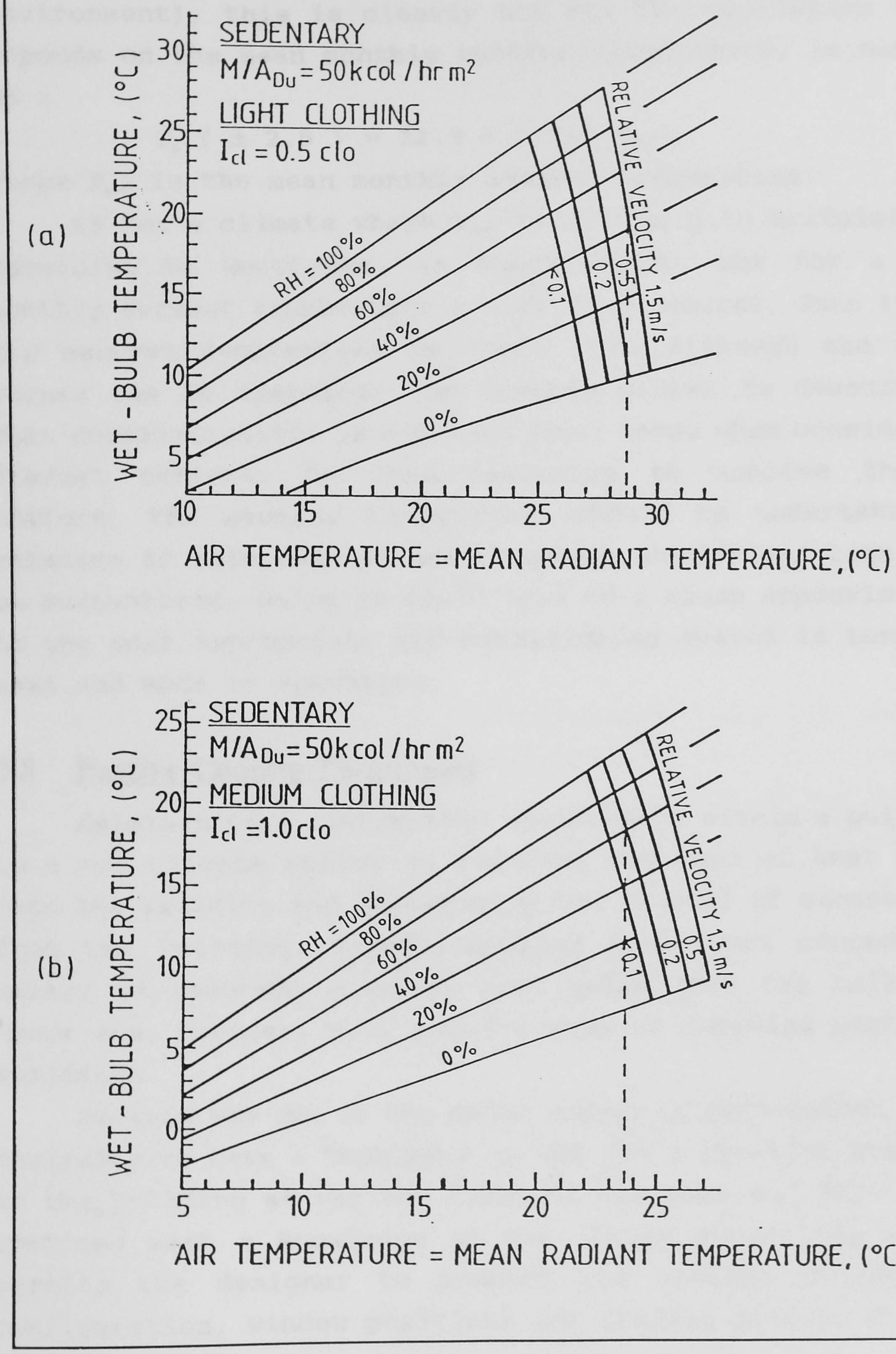

Figure 3.1: The effects of clothing and air speed on the air temperature required for thermal comfort.

of people feel comfortable, when exposed to that environment), this is clearly not so. The expression which depends on the mean monthly outdoor temperature, is defined as :

$$T_n \ (\pm 2.5) = 11.9 + 0.534 \ T_{amb}$$

where T_{amb} is the mean monthly ambient temperature.

So for a climate where $T_{amb} \approx 15.5°C$ (e.g.in Britain), T_n, according to Humphreys, is about 20.2°C, but for a mean monthly outdoor temperature of 36°C (e.g. Muscat, June 1988), the neutral temperature is about 31°C. Although the exact values can be disputed, the example serves to demonstrate that acclimatization is not a marginal issue when considering thermal comfort. So when designing to achieve thermal comfort, the neutral temperature should be undertaken in relation to mean ambient environmental conditions likely to be encountered. Doing so would lead to a close approximation to the most appropriate air-conditioning system in terms of cost and mode of operation.

3.3 Passive-Cooling Techniques

Maintaining a comfortable environment within a building in a hot climate relies on reducing the rate of heat gains into the building and encouraging the removal of excess heat from the building. Passive-cooling techniques concentrate mainly on reducing unwanted heat gains into the building. There are, however, many passive ways of removing heat from buildings.

Because the sun is the major source of heat gains, it is desirable to have a knowledge of the sun's position relative to the building at various times of the year and day. This, combined with a knowledge of the likely prevailing winds, permits the designer to predict the optimal orientation configuration, window positions and shading devices for the building.

The **shape** of the building plays an important role in

controlling the rate of heat gains. the aim is to expose the least surface area to direct insolation and the ambient air. Hemispherical shapes have the least surface area to volume ratio. But construction difficulties, high costs of construction and constraints on the inner space have made this a design option only rarely adopted for large buildings. The domed roof of a single-room dwelling is the nearest to the hemispherical shape that has featured in some vernacular architectures. But domed roofs have probably been incorporated for the other thermal advantages they possess, for example the radiation propagated from the roof, which is the building's surface most exposed to the sum, onto the inhabitants, tends to be reduced. An opening at the crown of the dome permits the escape of heated air, thus causing buoyancy-induced ventilation. Also, if there is a wind blowing, from any direction, it will induce a suction at the crown so increasing the ventilation rate from the room below - see Figure (3.2).

Cubical-shaped buildings have relatively low surface area to volume ratios, but although they can, as a result, inhibit solar gains through the envelope, they do not tend to encourage natural ventilation through the enclosed space. Modern designers of buildings for cold temperate climates tend to favour rectangular shapes with relatively large south-facing walls (compared with east- and west-facing walls in the northern hemisphere) and north-facing walls in the southern hemisphere. These increase the rates of solar gain. Such shapes can also be beneficial for the purpose of cooling in hot climates. During summer for low latitudes, the south-facing wall receives *less* solar radiation per unit area than the east- or west-facing walls [3]. In general, the shape and orientation of a building should be dictated by the local climate and latitude. In hot climates, the design should be an optimum that often leads to a compromise between reducing solar gains and taking advantage of any cool summer breezes available.

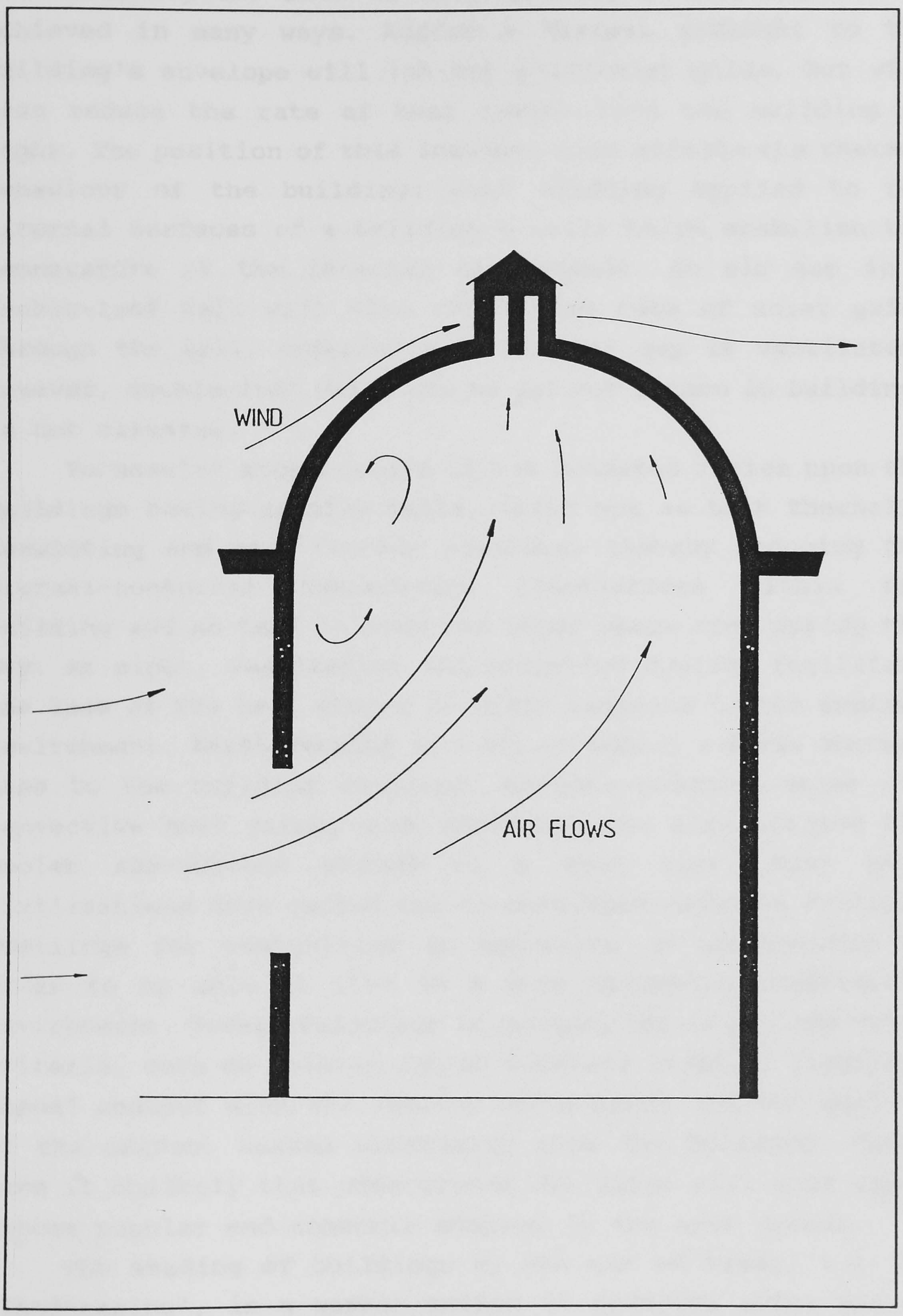

Figure 3.2: Air currents in a room and around its domed roof with a cupola vent at its azimuth.

Reducing the rate of heat gain by a building can be achieved in many ways. Adding a **thermal insulant** to the building's envelope will inhibit solar-heat gains, but will also reduce the rate of heat losses from the building at night. The position of this insulant also affects the thermal behaviour of the building: such cladding applied to the external surfaces of a building's walls helps stabilise the temperature of the internal environment. An air gap in a double-leaf wall will also reduce the rate of solar gains through the wall, especially if the air gap is ventilated. However, double-leaf walls are as yet not common in buildings in hot climates.

Vernacular architecture in hot climates relies upon the buildings having **massive walls**, which act as both thermally insulating and heat-storage elements, thereby reducing the diurnal-nocturnal temperature fluctuations within the building and so tend to keep the inner space cool during the day. At night, ventilation and radiative cooling facilitate the loss of the heat stored in these elements to the ambient environment. **Earth berming** is a way of adding a large thermal mass to the building envelope. Besides reducing solar and convective heat gains, such buildings can also utilise the cooler sub-surface ground as a heat sink. Many past civilisations have carved out or developed caves as suitable dwellings for communities in mountains or underground in order to be able to live in a more thermally comfortable environment. Modern buildings in general try to satisfy other criteria, such as maintaining an adequate level of lighting, visual contact with the ambient environment and the quality of the outdoor scenes observable from the building. These make it unlikely that underground dwellings will once again become popular and commonly adopted in the next decade.

The **shading** of buildings by the use of trees, i.e. by 'landscaping', is a common method of reducing solar gains, especially in regions where water availability is not a problem. Even in deserts, a Bedouin tribesman will tend to

put up his tent under a palm or other tree. The trees also provide a pleasant outlook for the occupants of the buildings. Trees evaporatively condition the surrounding air, and where watering of the tree is necessary, as in hot arid countries, the shaded, wet ground becomes cool as well. The shaded region becomes an extension of the living space, and before the advent of mechanical air-conditioning, people often spent the hot hours of the day beneath such trees. However, as shading devices, they do not usually feature in modern architecture, because a full-size tree takes years to grow, while the designer must satisfy comfort conditions as soon as the building is ready for habitation.

In the vernacular architecture of most hot regions of the world, reducing heat gains has been achieved by the **clustering** of houses, i.e.the use of common walls and narrow streets. Such clustering was also a mean of obtaining improved security and defence, but since this requirement has disappeared, people now usually prefer to live in detached houses with as much space between them and their neighbours as can be afforded. Thus clustering has become a less-attractive option for achieving thermal comfort, especially in the uncrowded parts of the world.

In the regions where clustering of houses was commonplace, **courtyards** were a common feature. These provided a private, shaded, open-air environment for most of the day. Although courtyards are a feature of many Islamic houses, courtyards have featured in the architecture of several ancient civilisations, thousands of years before Islam. At night, an open courtyard loses heat by radiation to the sky, while being protected from the warming effect of night winds. Relatively cool air stratifies in the courtyard, and seeps into the surrounding rooms, thereby cooling them. During the following day, the air of the courtyard, which is shaded by its four walls, and the surrounding rooms, heats up slowly but remains cool until late in the day, when the sun shines directly into the courtyard. In some courtyards, trees are

planted to provide shade even then and to condition the air in the local environment. The 'dahreez' or veranda is the shaded side of the courtyard: it is the place where the family tends to spend significant periods - see Figure (3.3).

External courtyards, which are more common in unclustered houses, consist of parts of the building plot whose enclosure is completed by walls. This type of courtyard is not incorporated into the house, but usually left as a garden space. When planted with trees or shrubs, these serve to condition the air around the house - see Figure (3.4).

An **atrium** is a type of courtyard, but with a transparent roof: it is incorporated mainly in houses where the courtyard would otherwise require heating during winter. For similar purposes, conservatories of glass are incorporated in the northern hemisphere on south-facing walls of buildings: they help in harnessing solar energy and provide day lighting. Both atria and conservatories can also help increase natural ventilation in deep-plan buildings, as a result of the stack effect occurring due to the ensuant natural buoyancy.

Reducing solar gains can also be achieved by shading (e.g. using trees) the various elements of the building envelope. Shading of the walls can also be achieved by having extended roofs (e.g. wide eaves), balconies and fixed or moveable shading devices. The roof, which is the building element most exposed to the sun, is the major source of solar-heat gain, especially in single-storey buildings. So shading of roofs can have large effects in reducing the cooling loads. In some old buildings in Jeddah, Saudi Arabia, shading of the roofs was achieved by constructing lightweight rooms or 'mabits' on the roof [4]. These were made of lattice woodwork with 50% voids, and were used actively by the families in the evenings and for sleeping at night. Among the different approaches to achieving the passive cooling of roofs are shading by plants as well as the uses of moveable canvas tarpaulins, roof gardens and inverted earthen pots on the roof [5]. Shading the roof by the use of a vegetable

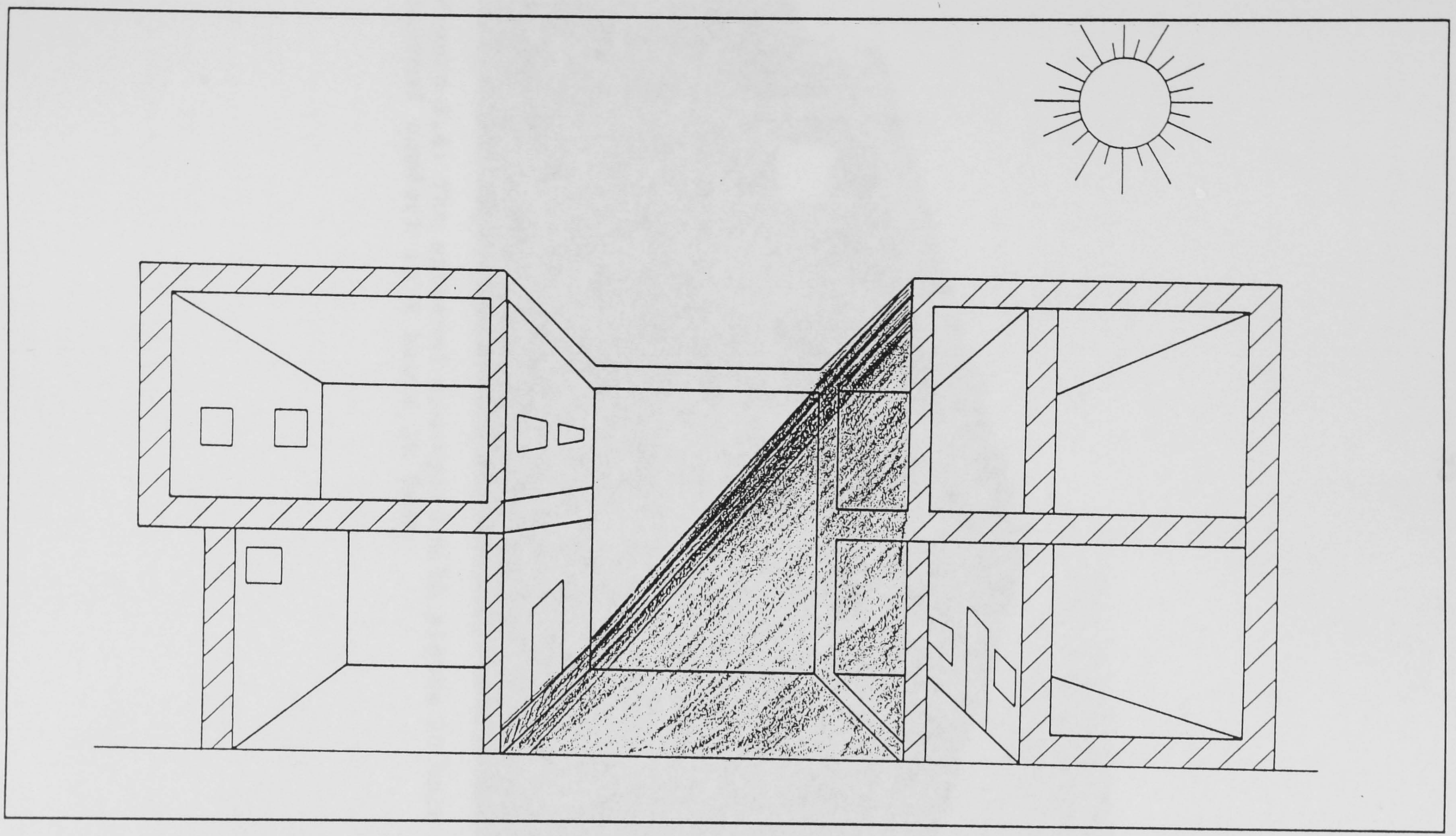

Figure 3.3: A cross-section of a courtyard-house showing how the Dahreez the shade and the relatively cool air that accumulates in the courtyard.

Figure 3.4: The external courtyard with plants to help achieve thermal comfort in a house in Oman.

pergola or covering the roof with a film of water were found to be the wise choices [5]. **Roof lawns** have also been used to reduce the rate of solar-heat gain through a roof as well as to help maintain comfortable conditions in the house [6]. Unlike a thin layer of concrete, which can transfer about 50% of the solar energy incident on it, a similar thickness of soil in which grass is grown,will only transfer about 5% of the solar energy. Also, the latter will create a more pleasant environment in which to spend the late afternoon and early evenings hours.

The Haj terminal of Jeddah Airport, Saudi Arabia, in external appearance is composed of large tent-like structures which shade the buildings and waiting areas beneath them. It is a modern example of how shading can be used to reduce solar-heat gains. Each of these structures has an opening at its top which encourages ventilation of the zone beneath them.

Windows are paths for major heat gains to, and losses from, buildings. However, vernacular architecture in hot regions has rarely incorporated glass in windows. Glass has the characteristic of transmitting short-wave solar radiation and preventing the escape of long-wave heat radiation emitted in the room. Traditional windows, mostly made of wood and usually with an outer louvred layer, can permit light and air transmission while preventing sunshine from directly entering the room. With the incorporation of mechanical air-conditioning, such traditional windows have disappeared from modern buildings. People now prefer glass windows, because they exclude noise, drafts and airborne dust, but proper care should be taken in their thermal design. The choice of a suitable quarter-wavelength thick film, bonded between (and so protected by) two sheets of glass in order to achieve highly reflective windows, or the adoption of double glazing can reduce the cooling load encountered.

The distribution of windows in the building envelope should also be carefully considered. In the northern hemisphere, for latitudes up to 40°N, south-facing windows will introduce ***less*** solar-heat gains into the building during summer than those of a similar size facing east or west. This is due to the fact that for such locations more solar radiation per unit area falls during the summer months on either the east or west walls than that on a south wall.

However, windows can also act as natural-ventilation facilitators in buildings which are not mechanically air-conditioned: the ventilation will in general be greater if the window area is larger and by positioning the windows to facilitate the passage through the building of the prevailing wind. This often tends to conflict with the requirement for the reduction of solar-heat gains, so the designer must optimise the design, and provide shading in order to reduce the solar-heat gains. **External shading devices**, which can be fixed or moveable, tend to be more effective in reducing heat gains than mid-pane or internal ones. Moveable external shading devices can be part of the window structure, and operated by the occupant in the same way as opening or closing windows. Louvred non-transparent outer panes have the advantage of reducing solar gains, while maintaining ventilation and security. It is recommended that fixed external shading devices should always be incorporated as a part of the initial design of the building envelope, and not as an afterthought!

A **naturally ventilated air gap**, 5.0 cm wide in the eastern and western walls, can considerably reduce the solar-heat gains [7]. Such walls could be used in conjunction with an air-cored concrete-slab ceiling connecting the east-and west-facing walls. Then the lower-temperature air from the shaded side of the building could be drawn by natural-buoyancy forces or a fan through the ceiling and walls. In the morning, the sun shines on the eastern wall and the building shades a large area of the ground near its western

side. The air, the ground and other surfaces in that shade, which have cooled during the night, stay relatively cool until the sun shines directly on them. So the relatively cold air from there could be drawn through the building structure to cool the ceiling and the eastern wall. In the afternoon the sun shines on the west wall, and the eastern side of the building will be in the shade, and the process is reversed so that some (but far less) air cooling of the west wall ensues. If the outer layer of the western wall has a sufficient thermal-storage capacity that leads to air movements at night (in a similar way to a solar chimney), the cooler ambient air at night could be used to cool the building structure. Conversely, the outer layer of the eastern wall should have a short response time and thermal-storage capacity, so that solar gain can be effective in promoting a buoyancy-driven flow even in the early morning. During the afternoon, thermal balancing will cause such air motions to cease.

Additional cooling by the buoyancy-driven air can be achieved by making it pass over wetted surfaces or a water pool (thereby inducing vaporisation with the loss of latent heat from the surface) before it enters the air gap in the building structure. Because the air does not enter the rooms, of the inhabited building, no discomfort would arise as a result of the increase in the humidity ratio.

3.3.1 Ventilation

This does not necessarily contribute to achieving thermal comfort by removing excess heat from the building. It could do so by increasing the speed of the air passing over a human's skin and thereby increasing the evaporation rate of perspiration to cool the body. Ceiling fans are found to extend the upper limit of thermal comfort by American Society of Heating, Refrigeration and Air-Conditioning Engineers (ASHRAE), from 26 to 29°C at a relative humidity of 50% [8].

In passive systems, ventilation plays a major role in achieving thermal comfort, especially in hot humid regions. Traditional houses have been designed to take advantage of the prevailing winds or breezes. In coastal regions, houses usually face the sea to take advantage of the sea-to-land breezes which occur during the day. The narrow streets, perpendicular to the coast, tend to channel the cool air coming from the sea and so increase its speed. Buildings have wooden balconies, called 'rowshin' (see Figure 3.5) which project into the narrow streets, thereby acting in a way analogous to a heat-exchanger fin, and so cool the occupants who sleep or sit in these cantilevered zones. These were a common feature of many coastal areas in hot climates. The lattice wooden structure of the rowshin promotes ventilation whilst inhibiting solar gains and also provides privacy for the occupants. Similarly, the 'areesh' (see Figure 3.6), which is a low-cost summer house made of palm-tree leaves, used to be a common feature of many coastal areas around the Arabian Peninsular. These rooms are very air-leaky structures, which can provide a thermally comfortable environment while maintaining privacy.

In hot humid regions where there is a high rain fall, the roof is the main component that provides protection from solar insolation and rain. The walls provide privacy and security, but tend to impede the air flows desirable for achieving thermal comfort.

In general, designers of vernacular architecture took advantage of the local microclimate, which is influenced by the morphology, such as hill slopes, valleys and plains and thermal properties of local materials. The sea-to-land breezes near the coast (see Figure 3.7) [8] are a phenomenon occurring daily which, if taken advantage of in the designed system, can improve the thermal comfort achieved. Methods of harnessing these relatively cool breezes and guiding them through a building have been developed even for multistorey

Figure 3.5: A Rowshin fitted to a house in Oman.

Figure 3.6: An Areesh, used in the summer by Bedwins in Oman.

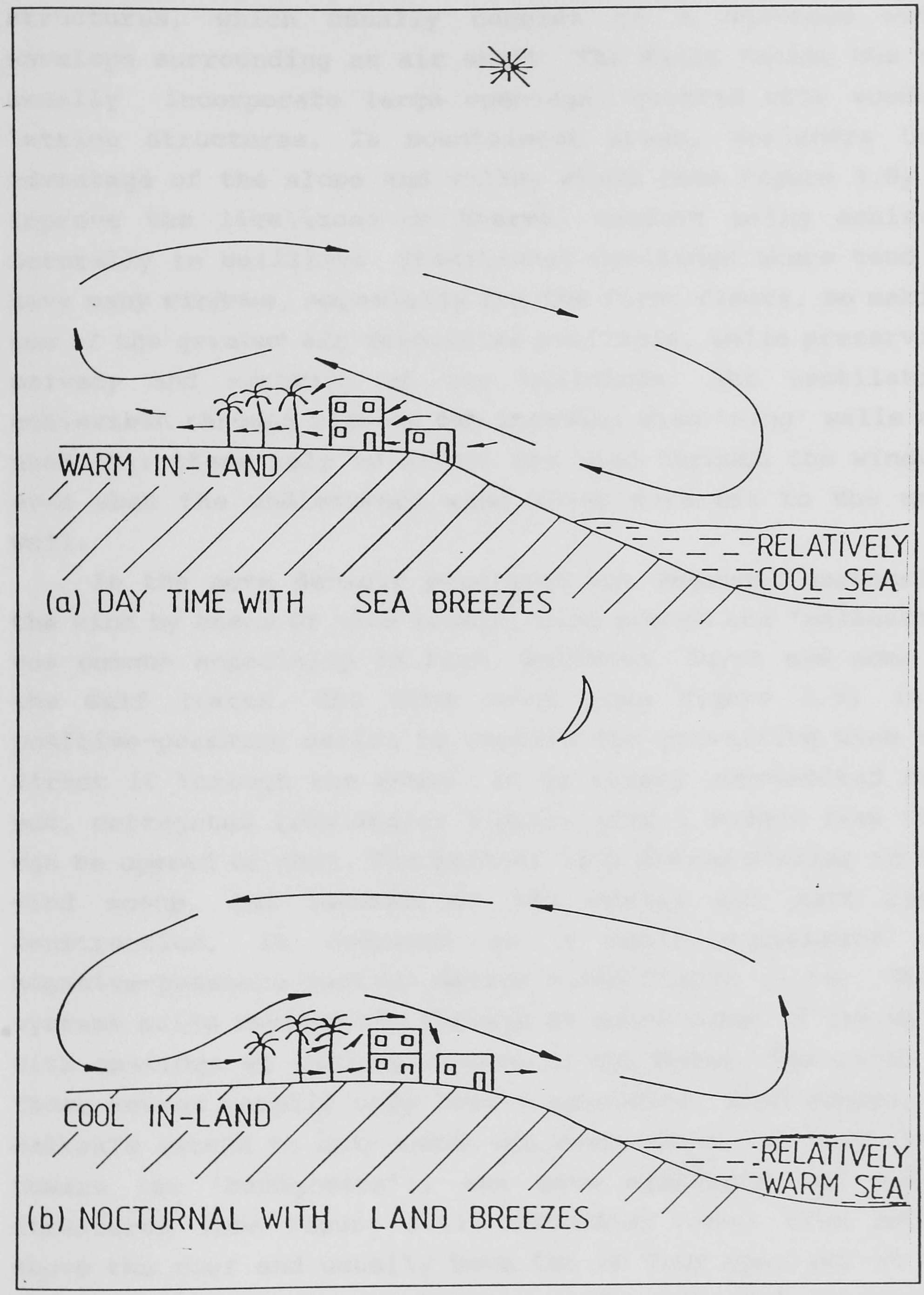

Figure 3.7: The daily cycle of the thermally-induced land/sea breezes, caused by the variation in land and water surface temperatures.

structures, which usually consist of a one-room width envelope surrounding an air shaft. The walls facing the sea usually incorporate large openings, covered with wooden-lattice structures. In mountainous areas, designers took advantage of the slope and valley winds (see Figure 3.8) to improve the likelihood of thermal comfort being achieved naturally in buildings. Traditional dwellings there tend to have many windows, especially for the first floors, so making use of the greater air velocities available, while preserving privacy and security of the buildings. The ventilation achievable through windows can increase when 'wing' walls are used [9]: these help to direct the wind through the window, even when the undisturbed wind moves parallel to the main wall.

In the more densely populated hot regions, harnessing the wind by means of wind towers, wind scoops and 'malkaafs', was common especially in Iran, Pakistan, Egypt and some of the Gulf States. The wind scoop (see Figure 3.9) is a positive-pressure device to capture the prevailing wind and direct it through the house. It is simply constructed from mud, corrugated iron and/or timber, with a wooden flap that can be opened or shut. The malkaaf is a device similar to the wind scoop, but because of its design and more rigid construction, it operates as a positive-pressure and negative-pressure suction device - see Figure (3.10). These systems guide ambient air through an outer layer of the wall, with openings at various levels in the house. The rooms in these houses usually open onto a courtyard. Wind scoops and malkaafs extend to only about one metre above the roof. Wind towers (or 'baddgreers'), are more elaborate and taller structures (see Figure 3.11) extending about five metres above the roof and usually have two or four openings at the top in order to try to capture winds from any direction. Because of their heavy structures, they can also act as solar chimneys in the absence of wind. Wind towers can also incorporate evaporative cooling, by making the air pass

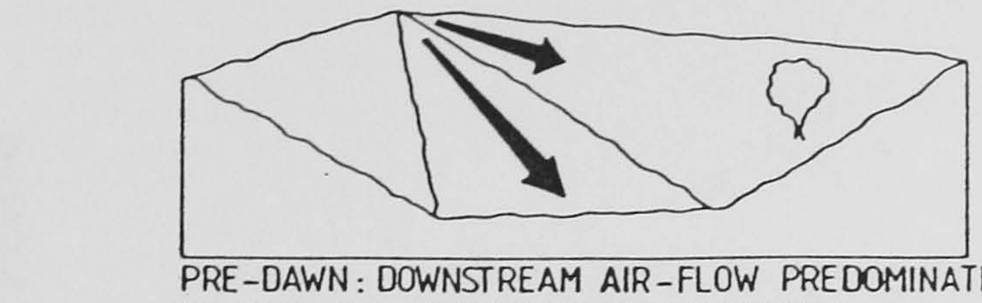

PRE-DAWN: DOWNSTREAM AIR-FLOW PREDOMINATES AS COOL AIR WASHES DOWN THE VALLEY.

MORNING: BREEZE RISES UP FACE OF SLOPE DUE TO SURFACE WARMING.

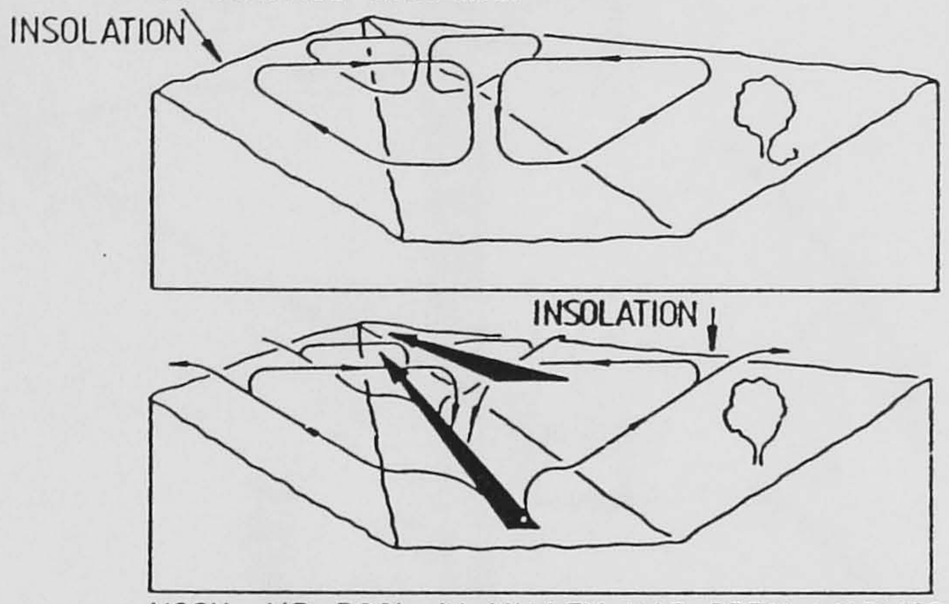

NOON: AIR POOL IN VALLEY HAS BEEN WARMED AND CREATES UP-VALLEY BREEZE.

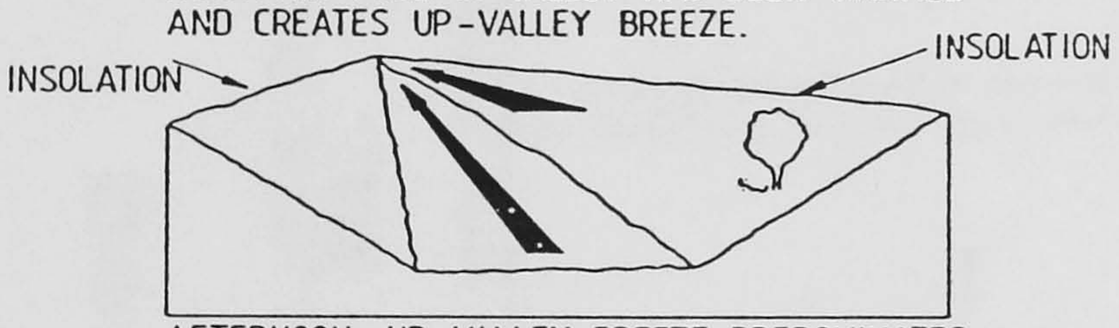

AFTERNOON: UP-VALLEY BREEZE PREDOMINATES AS SURFACES REACH MAXIMUM TEMPERATURE.

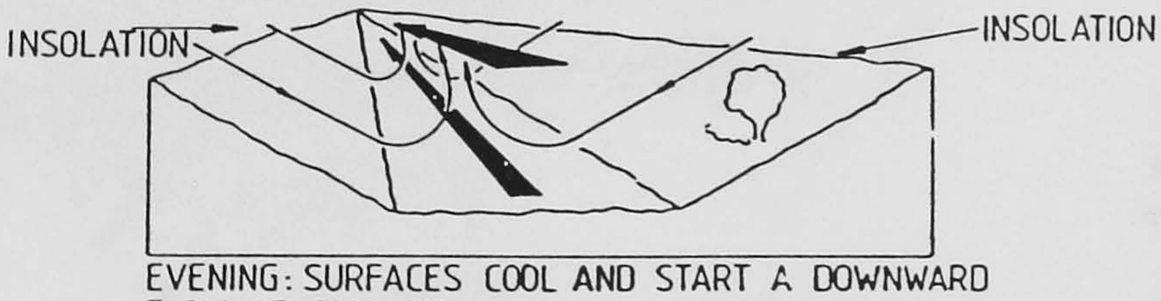

EVENING: SURFACES COOL AND START A DOWNWARD FLOW OF COOL AIR.

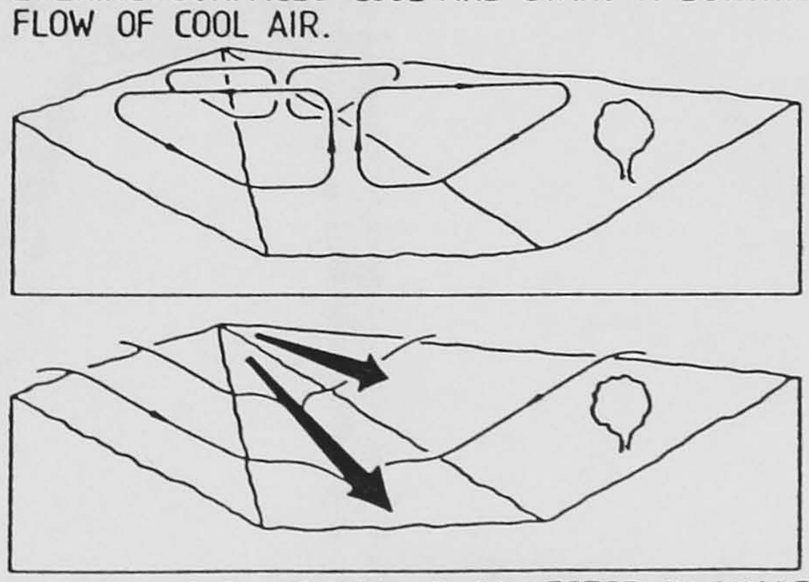

MIDNIGHT: COOL HEAVY AIR COLLECTED IN VALLEY BEGINS TO FLOW DOWN STREAM.

Figure 3.8: The thermally-induced air movements in a valley.

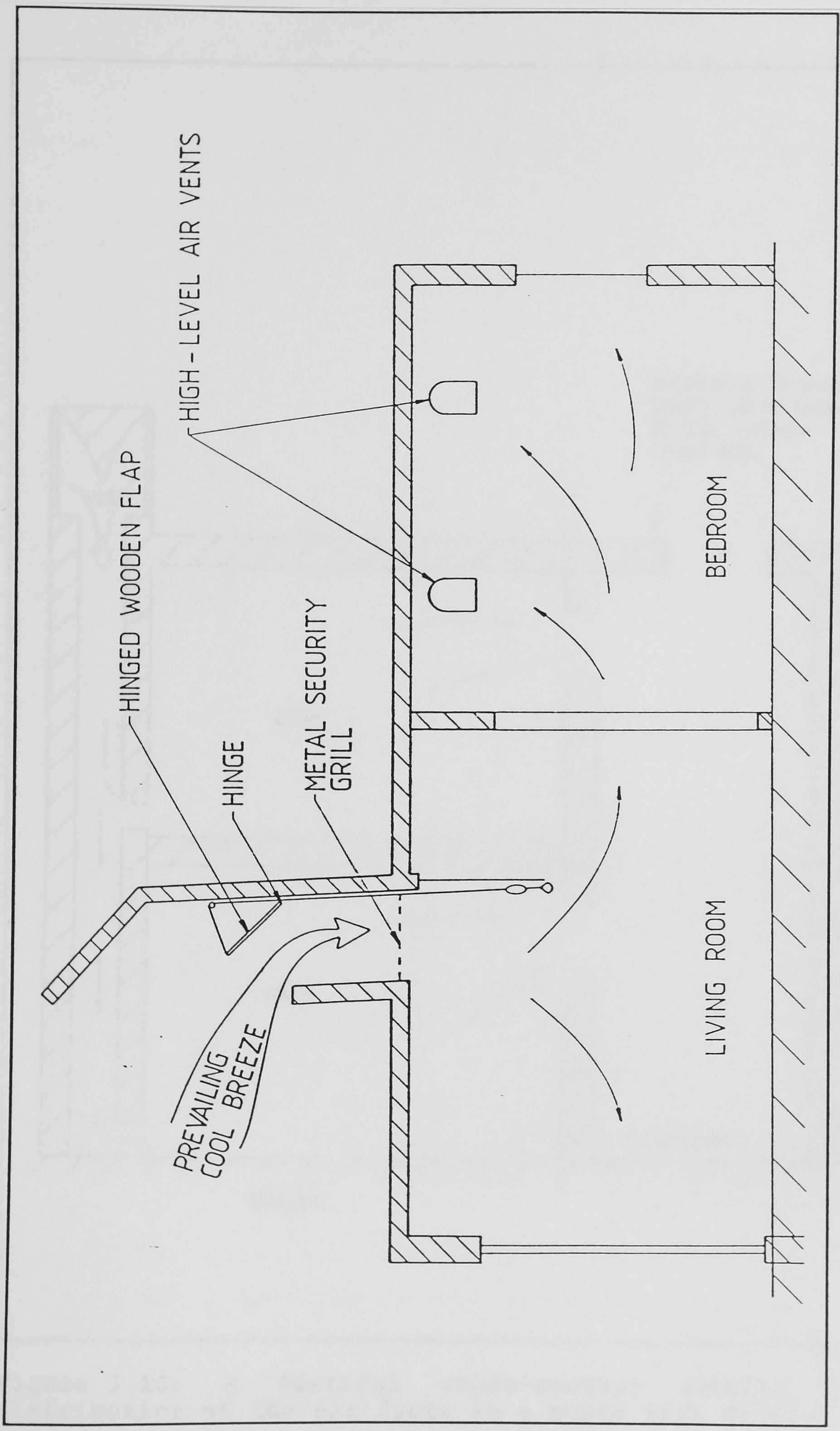

Figure 3.9: A vertical cross-section of a house fitted with a wind scoop.

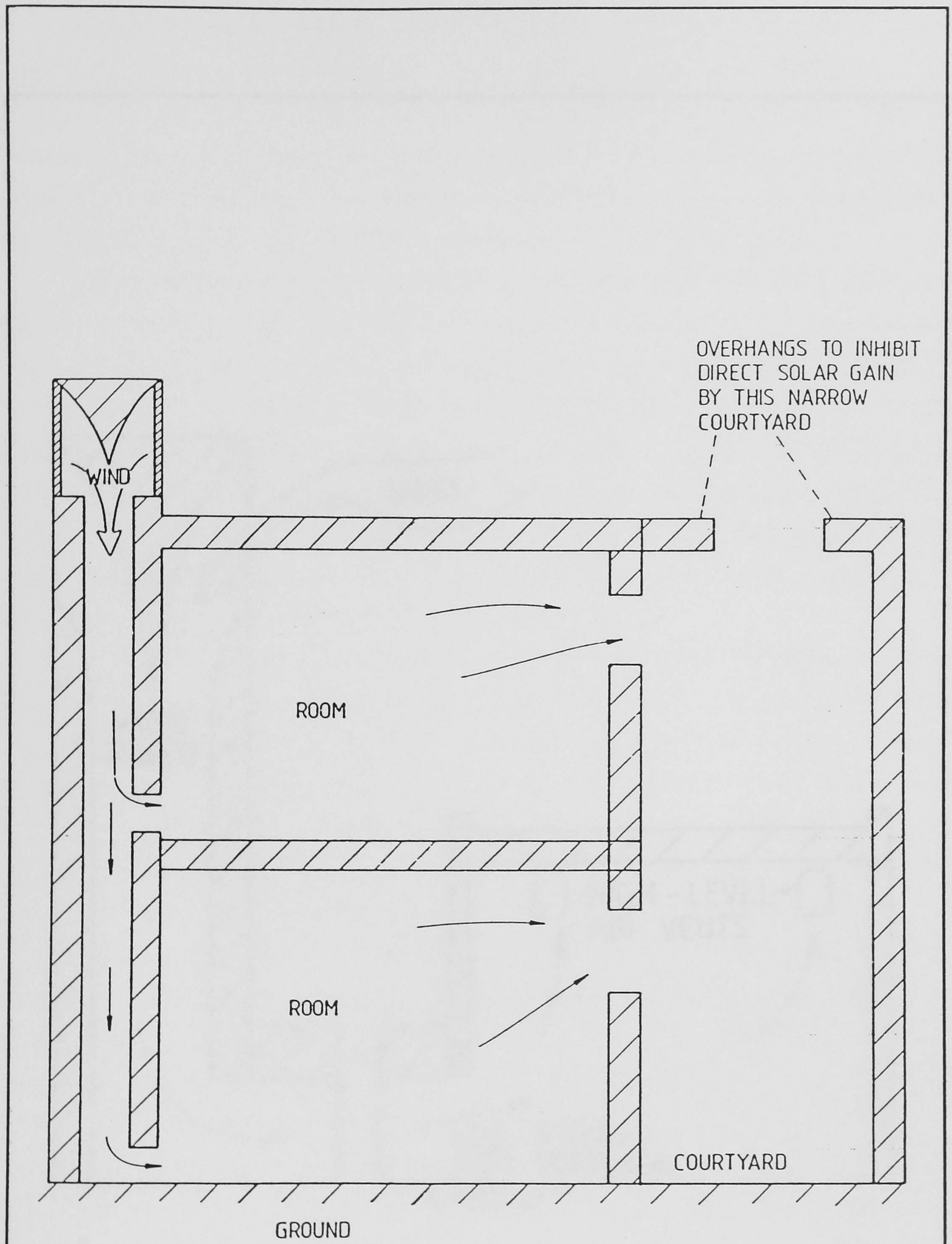

Figure 3.10: A vertical cross-section showing the distribution of the air ducts in a house with Malkaaf.

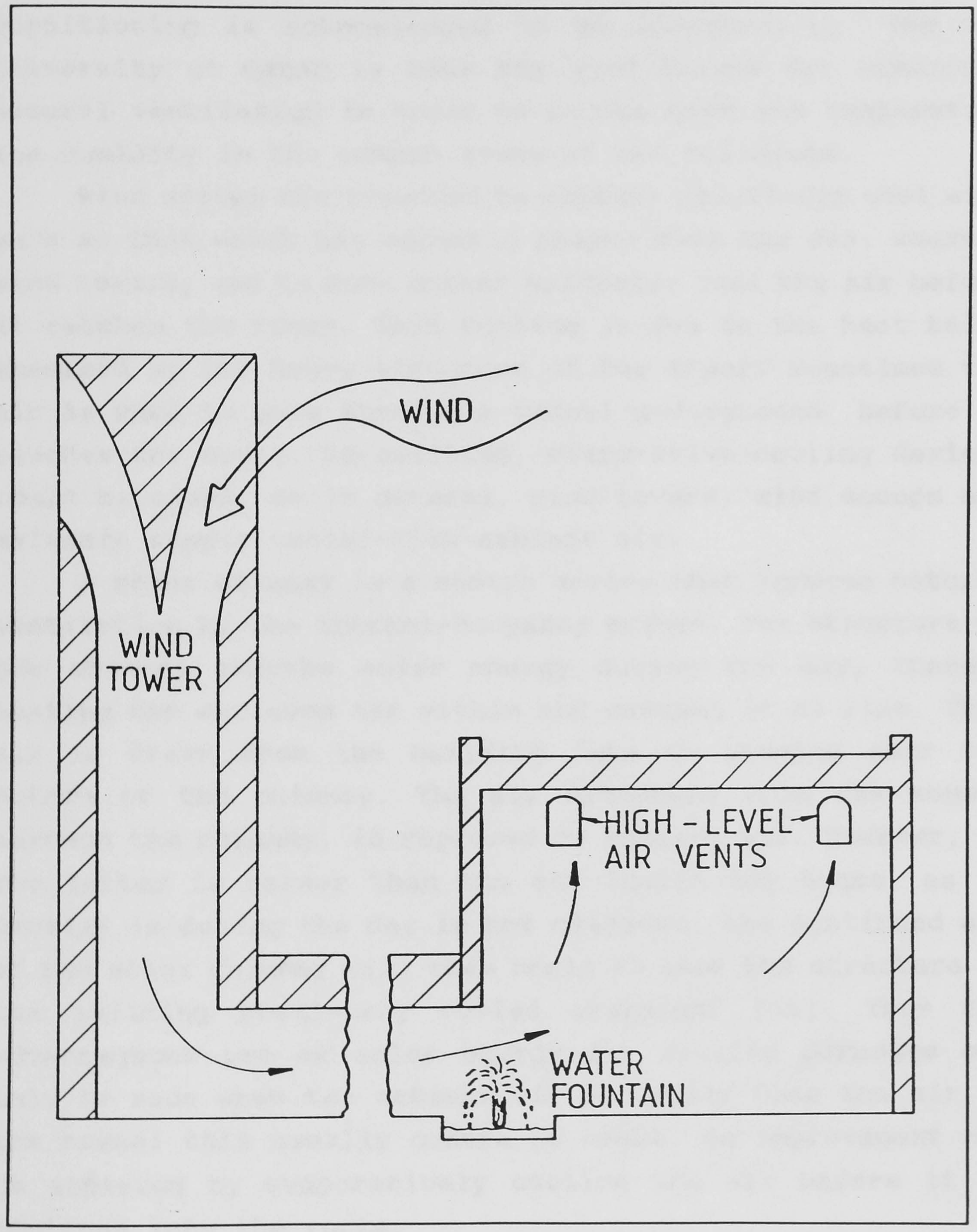

Figure 3.11: A vertical cross-section of a connected to a wind tower.

through or across wetted surfaces or water fountains [10].

Wind scoops, malkaafs and wind towers are still being used in new buildings, in places where modern air-conditioning is acknowledged to be uneconomical. The new university of Qatar in Doha has wind towers for achieving natural ventilation in order to reduce both the temperature and humidity in the common areas of the buildings.

Wind scoops are intended to capture relatively cool air, such as that which has recently passed over the sea, whereas wind towers, and to some extent malkaafs, cool the air before it reaches the rooms. This cooling is due to the heat being absorbed by the heavy structure of the tower. Sometimes the air is made to pass through a tunnel underground, before it reaches the house. In addition, evaporative-cooling devices could be added. So in general, wind towers, wind scoops and malkaafs supply cooler-than-ambient air.

A **solar chimney** is a modern device that induces natural ventilation by the thermal-buoyancy effect. The structure of the chimney absorbs solar energy during the day, thereby heating the enclosed air within and causing it to rise. Thus air is drawn from the building into an opening near the bottom of the chimney. The air exhausted from the house, through the chimney, is replaced by ambient air. However, if the latter is warmer than the air inside the house, as it usually is during the day in hot climates, the continued use of the solar chimney will then begin to heat the structure of the building previously cooled overnight [11]. Thus the advantageous use of solar energy for cooling purposes can only be made when the ambient air is cooler than the air in the house: this usually occurs at night. An improvement can be achieved by evaporatively cooling the air before it is admitted into the rooms.

To sum up, solar chimneys, having relatively low construction costs, can move air without the need for the expenditure of conventional forms of energy, and can help achieve comfort by cooling the building structure at night.

They can also improve the comfort of the inhabitants during the day if they are combined with an evaporative-cooling device.

Trombe-Michell walls operate according to a principle similar to that of the solar chimney. Each has an outer glass layer with an air gap between it and the wall. The (short-wave) solar energy emanating from the sun (at $\approx 6 \times 10^3$ K) is readily propagated through the glass, thereby heating the wall, but the long-wave thermal radiation emitted by the wall (at near room temperature) cannot escape through the glass. Thus the air between is heated and will rise, due to the buoyancy forces generated. In winter, the heated air can be admitted into the room. In summer, the hot air is vented to the environment outside, and compensatory cooler ambient air sucked into the room via an opening in the opposite wall. The air circulation thus caused is usually sufficient for thermally comfortable conditions to be achieved during summer in cold and temperature climates, but if the ambient air is too hot for comfort, it will cause a rise in the indoor temperature.

3.3.2 Radiative cooling

Solar radiation that reaches the Earth is in the waveband from 0.3-3.0 μm. The Earth's surfaces that are warmed by solar radiation emit heat at longer wavelengths, mainly in the range 8-13 μm. Fortunately, the Earth's atmosphere is relatively transparent to heat in this wavelength range, called the atmospheric window, through which heat from the Earth's surface is emitted to the cooler sky. The transparency of this 'window' is, however, reduced by an increase in the amount of water vapour and dust in the atmosphere. The temperature of outer space should be about absolute zero because all radiation would be absorbed and none returned, but in practice, even for a clear sky with no

clouds present, the effective temperature is approximately -45°C. In general the effective temperature of the sky, T_{sky} (in K) [12] is:

$$T_{sky} = \varepsilon_{at}^{0.25} T_a$$

where ϵ_{at} is the average emissivity of the atmosphere and T_a is the absolute temperature of the air at ground level.

Several models have been used to predict the average emissivity of the atmosphere with turbidity and in particular with water-vapour concentration. The average emissivity, ϵ_{at}, of the atmosphere is almost a linear function of the dew point, t_{dp},[13], and for $-28°C < t_{dp} < 15.6°C$:

$$\varepsilon_{at} = 0.74 + 0.006\, t_{dp}$$

The dew point can be computed from the ambient air temperature, t_a, (°C) and the relative humidity (ϕ) by the expression suggested by Murray [14]:

$$t_{dp} = \frac{237.3\left[\frac{\ln\phi + \mathbf{a}\, t_a}{t_a + 237.3}\right]}{\mathbf{a} - \ln\phi + \frac{\mathbf{a}\, t_a}{t_a + 237.3}}$$

where **a** is a constant = 17.27 and $0 \le \phi \le 1$

Another model for representing the sky temperature has presented [15], as :

$$T_{sky} = [T_a + K(H) + L(H)\,(t_{dp} - t_a)]\,\varepsilon_{at}^{0.25}$$

K and L are regression parameters related to the time of the day and depend on the tri-hourly index H (H=4 at sunrise, and thus H=5 3 hours after sunrise, etc., see Table 3.1). K(H) and L(H) express the radiative influences of the ground temperature and the altitude thickness of the atmospheric boundary layer, respectively, upon the effective temperature of the sky.

Table 3.1: The relationship between the Hourly Index, **H**, and the regression parameters **K(H)** and **L(H)**.

H	**1**	**2**	**3**	**4**	**5**	**6**	**7**	**8**
K(H)	6.45	7.18	7.65	3.86	0.18	2.90	4.85	5.65
L(H)	0.435	0.620	0.616	0.399	0.276	0.290	0.211	0.364

The net rate of heat loss, $\dot{q}$, from a horizontal flat roof to a clear sky by radiation is found from the Stefan-Boltzmann equation

$$\dot{q} = \sigma \varepsilon_r (T_r^4 - T_{sky}^4)$$

When the sky is partly covered with clouds, its effective radiative temperature rises until, with complete coverage by relatively low clouds, it becomes virtually the same as the air temperature. A cloud-cover correction factor, $\mathbf{C_s}$, has been defined [13], as the ratio of the atmospheric radiation with n/10 opaque-sky cover area to the clear-sky atmospheric radiation under the same ground-temperature conditions. The cloud-cover correction factor developed from data obtained when the cloud cover was at low altitude is :

$$C_s = 1 + 0.022n - 0.0035n^3 + 0.00028n^3$$

Higher-level clouds are colder and so thy have less effect than comparable low-level clouds.

The equation for the radiative rate of heat loss, $\dot{q}_{rad}$, from a horizontal roof can thus be modified to :

$$\dot{q}_{rad} = \sigma \varepsilon_r (T_r^4 - C_s T_{sky}^4)$$

Convective intrusion is a term used to express the total warming effect of both buoyancy and wind-driven convective heat transfers from the air to a surface being cooled by radiative heat loss to the night sky. During the day the roof temperature is higher than that of ambient air and so the

roof loses heat to the air, but, during the early morning hours, the roof is at a lower temperature than the air, due to radiative heat losses to the sky, and so the roof gains heat by convection from the air. So this convective intrusion must be minimised if the radiatively cooled surface is to have a lower temperature than that of the surrounding air. To do so, the surface to be cooled should be covered with a layer transparent to long-wave thermal radiation (i.e. in the waveband from 8 to 13 μm). This reduces the convective heat exchange with the air, while allowing the surface to lose heat to the night sky. Polyethylene sheets are about 70% transparent to long-wave heat radiation,and so thy are most commonly used for minimising convective intrusion. The convective heat-transfer coefficient, h_c, depends mainly on wind speed, but is also influenced by turbulence-causing obstructions. For a roof with no protrusions

$$h_c = 5.7 + 3.8\,V$$

where V is the wind speed. So the net cooling rate from an exposed horizontal dry roof can be expressed as :

$$\dot{q}_{net} = \sigma\,\varepsilon_r\,(T_r^4 - C_s\,T_{sky}^4) + h_c\,(T_r - T_a)$$

Selective-cooling surfaces have been used to enhance the long-wave heat radiation loss to the sky, and simultaneously reflect short-wave solar radiation. As such they, are highly reflective to short-wave (0.3-3 μm) solar radiation and highly emissive for long-wave radiation, particularly in the wavelength band between 8 and 13 μm. White paint is a good example of a selective surface; its absorptivity for solar radiation can be as low as 0.20, while its emissivity for long-wave radiation is between 0.9 and 0.96. The most appropriate surface for buildings in hot climates is often white plaster, which has a solar absorptivity as low as 0.08 and a long-wave emissivity exceeding 0.90. However, as the selective surface cools to the dew-point temperature, moisture starts to condense on it and the emissivity of water then tend to dominate. When dust combines with this condensed

water, it will stick to the surface, and so significantly affect its heat-transfer performance. This makes the more commonly available materials, such as white plaster and white paint, often the most cost-effective design solutions. However, even these surfaces need to be maintained clean to remain highly effective.

Radiative-cooling applications

The use of a building's roof, both as a nocturnal radiator and as the cold store, is often a cost-effective solution. During the night the roof is exposed to the night sky, losing heat by long-wave radiation and also by convection. During the day, the roof should be externally insulated in order to minimise the heat gains from solar radiation and the ambient air. The roof can then absorb heat from the room below. Ceiling fans can then assist in achieving thermal comfort within the building, especially during the late afternoon.

However, as yet there are no simple and inexpensive movable roof insulation systems readily available commercially. So, alternatively, the 'coolth' generated during the night could be transferred to the building fabric or a cold store. The transfer medium could be air, water or other liquids. In a system that uses air as a heat-transfer medium, a metallic roof, painted white is placed over the roof proper with a horizontal air gap of vertical width 5-10cm. During the night, ambient air is drawn through the gap, and then used to cool either the building fabric or a storage medium, such as a rock-bed store. The air drawn through the gap, in practice, can be cooled by up to about two-thirds of the temperature difference between the metallic roof and the ambient air, depending on the air flow rate[16].

The Iranians have produced ice using the concept of radiative cooling for several centuries. However, radiative cooling to provide thermal comfort in dwellings was pioneered by Yanigamachi in tokyo approximately 25 years ago [12]. In

this system, heat is rejected, by radiation to the sky, from tubes in contact with a sheet metal roof through which water is circulated. The cooled water is stored in a tank to act as a heat sink for the next day. A system combining radiative and evaporative cooling was developed by Harold Hey in the mid-1960s: the"sky therm", or"roof pond" as it is now most commonly known (see Figure 3.12), consists mainly of a water pond in direct contact with the roof and covering the whole area of the roof. The thickness of the water layer is 3±1 cm, the water being contained in polyethylene bags. The pond is covered by a thermally insulating layer during the day in order to reduce heat gains to the pond. During the night, the pond is uncovered, so that it can lose heat by long-wave radiation to the sky and by convection to the now cooler ambient air. The roof containing the water-filled polyethylene bags could also be flooded when evaporative cooling is required. Hey claims that the sky therm system, when properly designed, can achieve thermal comfort in single-story buildings in most climatic zones [17], but the assistance of a small fan may be necessary in humid regions. The main obstacles to the widespread use of roof-pond systems are the provision and operation of the movable insulation required for effective operation. Also the roof should be capable of supporting an extra 200-400 kg per m^2 area of water, and it should be 100% waterproof. However, in arid regions, where water is scarce the loss of water by evaporation will add significantly to the operational costs.

The cooling capabilities of several roof ponds, with a variety of modifications, have been investigated. These include shading the pond with floating table-tennis balls; the provision of floating insulation which is flooded during the night by pumping water over it; and the provision of sprays or air blowers to increase the rate of evaporative heat loss from the pond. The pond could also be used as a cooling tower for an air-conditioning system when sprays or air blowers are used. Researchers at Kuwait Institute for

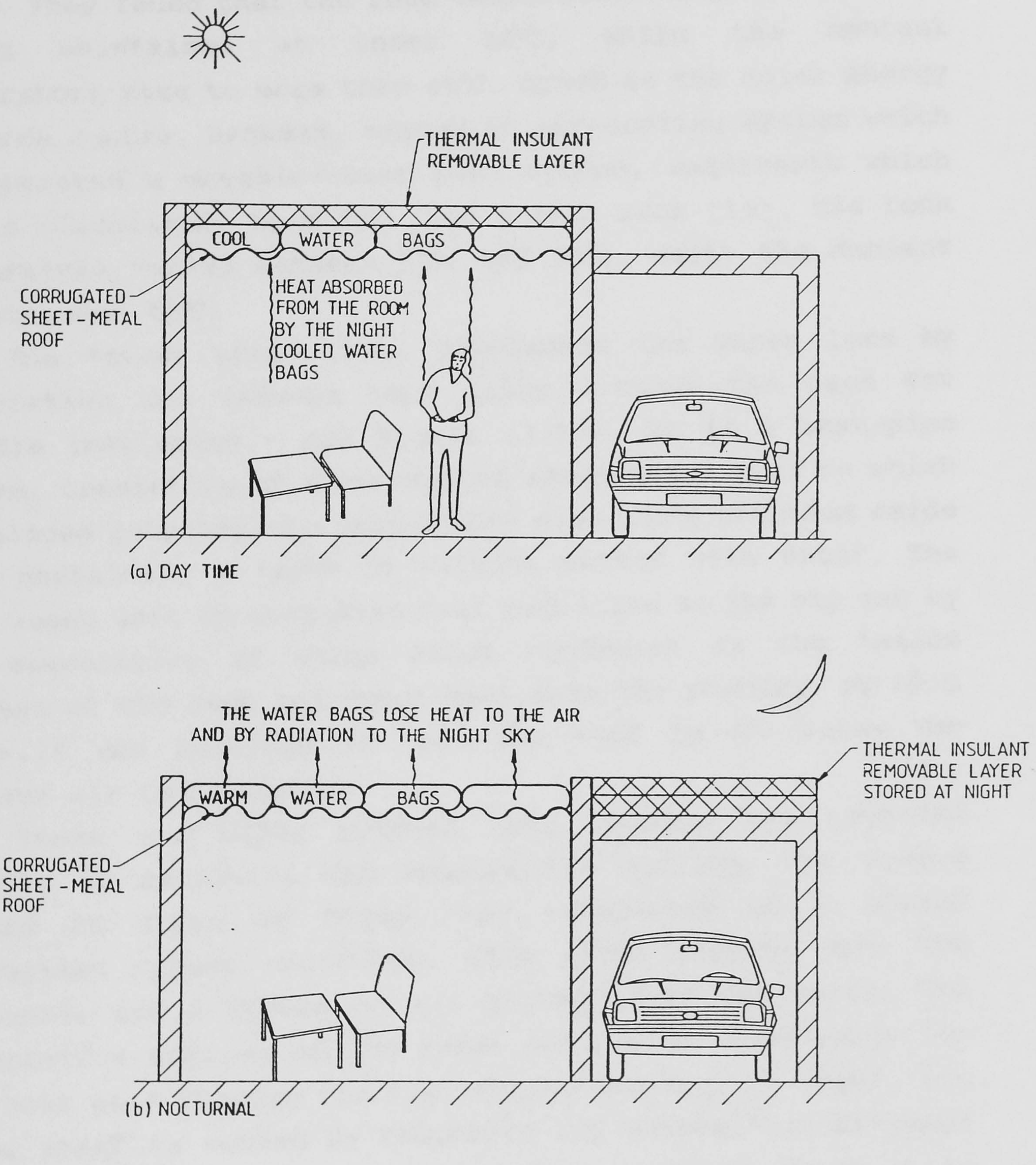

Figure 3.12: A roof pond cooling system.

Scientific Research (KISR)[18], have modelled and tested roof ponds on a corrugated metal roof and a concrete-slab roof of two test rooms, using brackish water and without covering the ponds. They found that the room temperature in both cases was always maintained at under 30°C, while the ambient temperature rose to more than 46°C. Ayoob at the Solar Energy Research Centre, Baghdad, tested an air-cooling system which incorporated a movable-cover pond system, underneath which air is circulated, by a fan into a test room [19], the room temperature varied between 27°C and 32°C, while the ambient air exceeded 46°C.

The "diode roof" [20], eliminates the water loss by evaporation and reduces heat gains without the need for movable insulation - see Figure (3.13). It is a heat-pipe system, consisting of a corrugated sheet-metal roof on which are placed polyethylene bags coated with white titanium oxide each containing a layer of pebbles wetted with water. The roof loses heat by long-wave heat radiation to the sky and by the evaporation of water which condenses on the inside surface of the bags and drops back onto the pebbles. By this means,it was possible to cool the roof to 4°C below the minimum air temperature.

There are other systems that utilise the combined effects of radiative and evaporative cooling. One system tested in Japan by Saito [21], consisted of a glazed corrugated copper collector. With water flowing down the collector and a stream of air blowing over the water, the evaporative cooling of the water more than compensates for the heat gain through the roof during the day. At night, the water which is cooled by radiation and evaporation extracts heat from another air stream flowing downward which is in contact with the lower surface of the collector. The air can be cooled by up to 4°C before it enters the room.

Dan & Chinnapa [22], described a method for cooling water by trickling it over the glass cover of a solar collector exposed to the night sky. The water was cooled by the

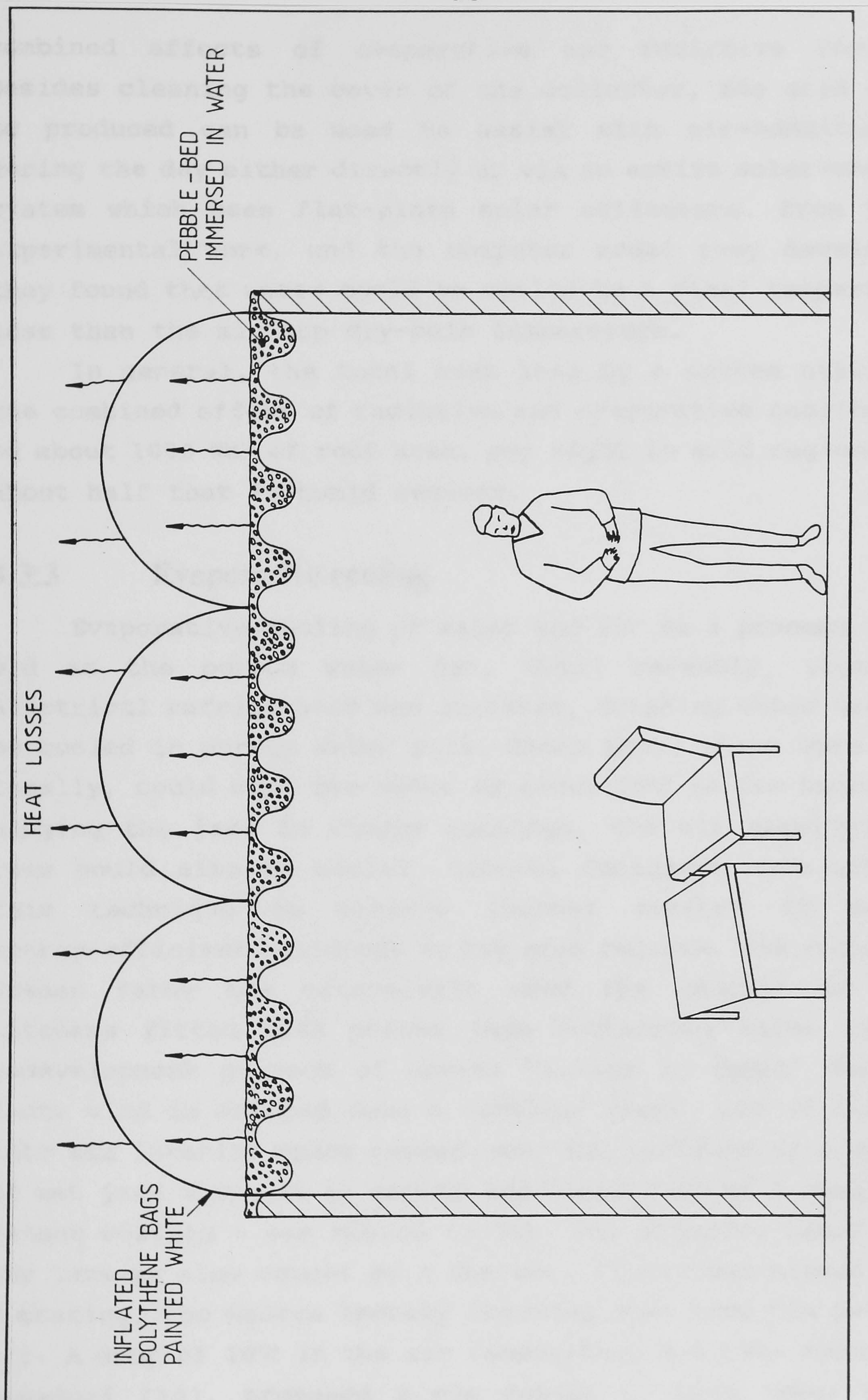

Figure 3.13: A vertical cross-section of a room with a Diode roof.

combined effects of evaporative and radiative cooling. Besides cleaning the cover of the collector, the cold water so produced can be used to assist with air-conditioning during the day either directly or via an active solar-cooling system which uses flat-plate solar collectors. From their experimental work, and the computer model they developed, they found that water could be cooled to a final temperature less than the minimum dry-bulb temperature.

In general, the total heat loss by a system utilising the combined effect of radiative and evaporative cooling can be about 1000 Wm^{-2} of roof area, per night in arid regions and about half that in humid regions.

3.3.3 Evaporative cooling

Evaporative cooling of water and air as a process is as old as the porous water jar. Until recently, when the electrical refrigerator was invented, drinking water used to be cooled in porous water pots. These pots, which were made locally, could cool the water by about 10°C in few hours. By hanging the jars in window openings, the air entering the room could also be cooled. Several designers have adopted this technique to achieve thermal comfort in modern energy-efficient buildings in hot arid regions. The architect Hassan Fathy has extensively used the concept of wind catchers fitted with porous jars containing water in the redevelopment project of Gourna Village in Egypt. The dry dusty wind is scooped down a vertical shaft, and on its way into the interior space passes over the surfaces of a series of wet jars where it is cooled and humidified as a result of latent cooling - see Figure (3.14). The dripping water from the jars is also caught by a charcoal filter-bed placed over a grating, the system thereby removing dust from the passing air. A drop of 10°C in the air temperature has been reported. Bahadori [10], proposed a new design of wind tower which includes conduits wetted by a water-spraying device.

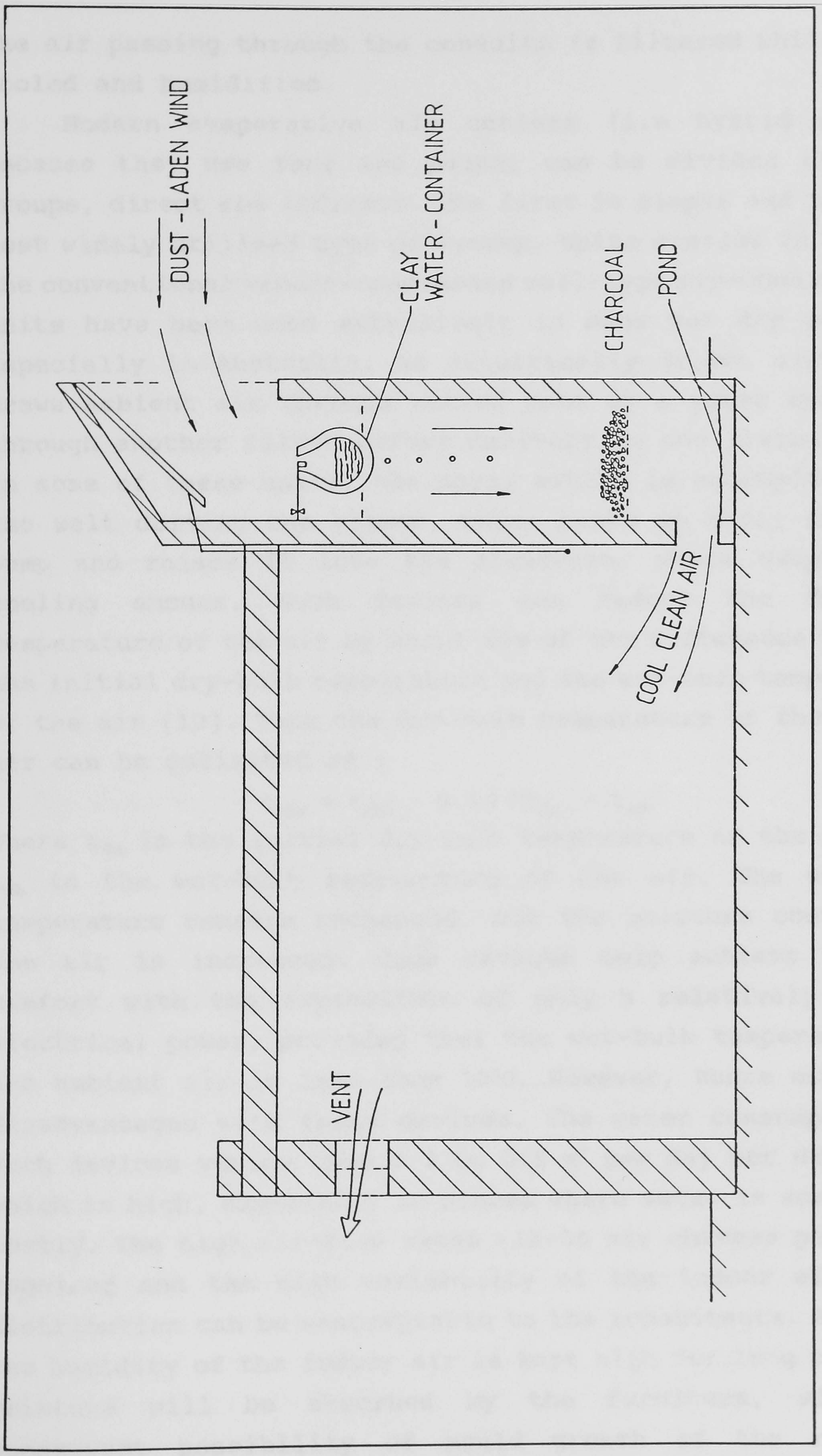

A wind scoop fitted with a porous (and hence wet outside surface) pot containing water.

Figure 3.14:

The air passing through the conduits is filtered while being cooled and humidified.

Modern evaporative air coolers (i.e hybrid systems because they use fans and pumps) can be divided into two groups, direct and indirect. The first is simple and thus the most widely utilised type of system. Units similar in size to the conventional vapour-compressed wall-type air-conditioning units have been used extensively in many hot dry regions, especially in Australia. An electrically driven air-blower draws ambient air through wetted pads or a water spray and through another filter before delivery to the living space. In some of these units, the spray action is accomplished by the belt driving the blower, which picks up water from the sump and raises it into the airstream, where evaporative cooling ensues. Such devices can reduce the dry-bulb temperature of the air by about 80% of the difference between the initial dry-bulb temperature and the wet-bulb temperature of the air [12]. Thus the dry-bulb temperature of the supply air can be estimated as :

$$t_{dbs} = t_{dbi} - 0.80\,(t_{dbi} - t_{wb})$$

where $\mathbf{t_{dbi}}$ is the initial dry-bulb temperature of the air and $\mathbf{t_{wb}}$ is the wet-bulb temperature of the air. The wet-bulb temperature remains unchanged, but the moisture content of the air is increased. Such devices help achieve thermal comfort with the expenditure of only a relatively little electrical power, provided that the wet-bulb temperature of the ambient air is less than 18°C. However, there are a few disadvantages with these devices. The water consumption of such devices varies from 0.3 to 0.5 m^3 per day per dwelling, which is high, especially in places where water is scarce and costly. The high air-flow rates (15-30 air changes per hour) required and the high variability of the indoor air-speed distribution can be unacceptable to the inhabitants. Also, if the humidity of the indoor air is kept high for long periods, moisture will be absorbed by the furniture, with the consequent possibility of mould growth if the relative

humidity stays at above 70%.

To improve the performance of direct evaporative coolers, the room air can be utilised to extract heat from the inlet air before it is evaporatively cooled, or from the building envelope by exhausting it through air gaps in the outer walls or double-glazed windows. Indirect evaporative air coolers can eliminate the increase in the moisture content of the air caused by the direct evaporative cooling method. In such devices, the evaporation process takes place in the exhaust air stream coming from the living space, and the supply air is cooled through a heat exchanger. The problem which has been encountered with these systems is the provision of a compact heat exchanger, with high effectiveness, which can withstand the deposition of salts and the ensuant high corrosion rates. A commercial unit - the Dricon - developed by the Commonwealth Scientific and Industrial Research Organisation (CSIRO) in Australia has overcome such problems: it has a plate-type heat exchanger, made of dimpled sheets of hydrophillic polymer and with a plate separation of 3 mm. The dimples provide turbulence while maintaining the narrow spacing between the plates. The evaporation takes place in the exhaust passage of the heat exchanger. Such devices can supply air which is within comfort conditions provided that the humidity ratio of the ambient air is less than 11.4 gkg^{-1} dry air, and the dew-point temperature is blow 18°C [12].

Anther method of indirect evaporative cooling employs a mass of water whose temperature has been reduced by evaporation and radiative cooling at night. This water is circulated in fan-coil units to extract sensible heat from the living space. Also finned-coil heat exchangers, which have high effectiveness, can be used in conjunction with a cooling tower to reduce the temperature of the air in the living space. The main problem here is that larger than usual heat exchangers are required due to the small temperature differences ensuing.

3.4 Active Solar-Cooling Techniques

3.4.1 Desiccant cooling systems

In hot humid regions, to maintain the room conditions within the comfort zone, the air supplied must be dehumidified. In vapour-compression air-conditioning systems, the supply air passes over chilled-water coils whose average temperature is less than the dew-point temperature of the air: thus some of the moisture in the air condenses while the air is being cooled. With air-conditioning systems which do not produce chilled water (in the range 4 to 10°C), as part of the cooling process, air can be dehumidified by the use of desiccants. These absorb moisture from the air, thus reducing its humidity ratio, but simultaneously the dry-bulb temperature of the air increases significantly, so it will then be necessary to cool the air before it is supplied to the living space. Also, the desiccant must be regenerated by supplying heat to it, to drive away the moisture which it has absorbed from the air. Suitable materials, with high affinities for water, are of the following groups:

(1) Solid desiccants such as activated charcoal, silica gel, alumina gel, zeolite, lithium chloride and calcium chloride.
(2) Liquid inorganic desiccants such as lithium chloride, lithium bromide and calcium chloride.
(3) Liquid organic desiccants such as glycerol, diethylene glycol and triethylene glycol

The dehumidification process can be continuous provided that there is a constant source of heat to regenerate the desiccant. Flat-plate solar collectors for heating water up to 80°C have been used successfully [22], to provide the heat for continuous regeneration. Alternatively, two beds of the desiccant can be used on a daily alternating cycle, so that while one bed is used for dehumidification the other bed is

regenerated by solar radiation. However the performance of the continuously regenerated desiccant does not deteriorate with time as much as that in the daily regenerating cycle. In a continuous dehumidification and cooling process (see Figure 3.15), a rotating desiccant bed absorbs moisture from the inlet air while being regenerated by the exhaust air stream. The dehumidified air is cooled by a heat exchanger, which heats the regenerating air stream. The regenerated air is further cooled by a direct or indirect evaporative-cooling process.

Desiccant air dryers and cooling systems, which use gas or waste heat for regeneration, are available commercially and it is relatively easy to convert such systems to be powered by solar energy. Such a system has recently been put into limited production for residential applications [23]. Jurinak et al. [24], have compared the performance of an open-cycle desiccant air-conditioning system for residential applications with an identical output vapour-compression cooling system and found that desiccant cooling is not yet economically competitive with that achievable with the vapour-compression system. Lof et al. [23], have tested a commercially available desiccant cooling-system (manufactured by ASK Corp. (American Solar King Corp.,USA)) using evacuated-tube solar collectors (manufactured by Sunmaster Inc.), and found that, under mild (≈15°C wet-bulb), conditions, cooling outputs of 6-7 Kw can be obtained by solar-heated water at 60-70°C with an average thermal coefficient of performance, (COP), in excess of unity. King & Maclaine-Cross [25], have carried out a parametric study on a high-performance solid-desiccant open-cooling cycle - see Figure (3.16(a)). They found that for the Air-conditioning and Refrigeration Institute (ARI) room and ambient conditions, such systems can have a thermal COP of ≈2.4 and a specific cooling effect of 25.3 $kJkg^{-1}$ dry air at a regeneration temperature of 65°C. With commercially available components, such systems can compete with vapour-compression

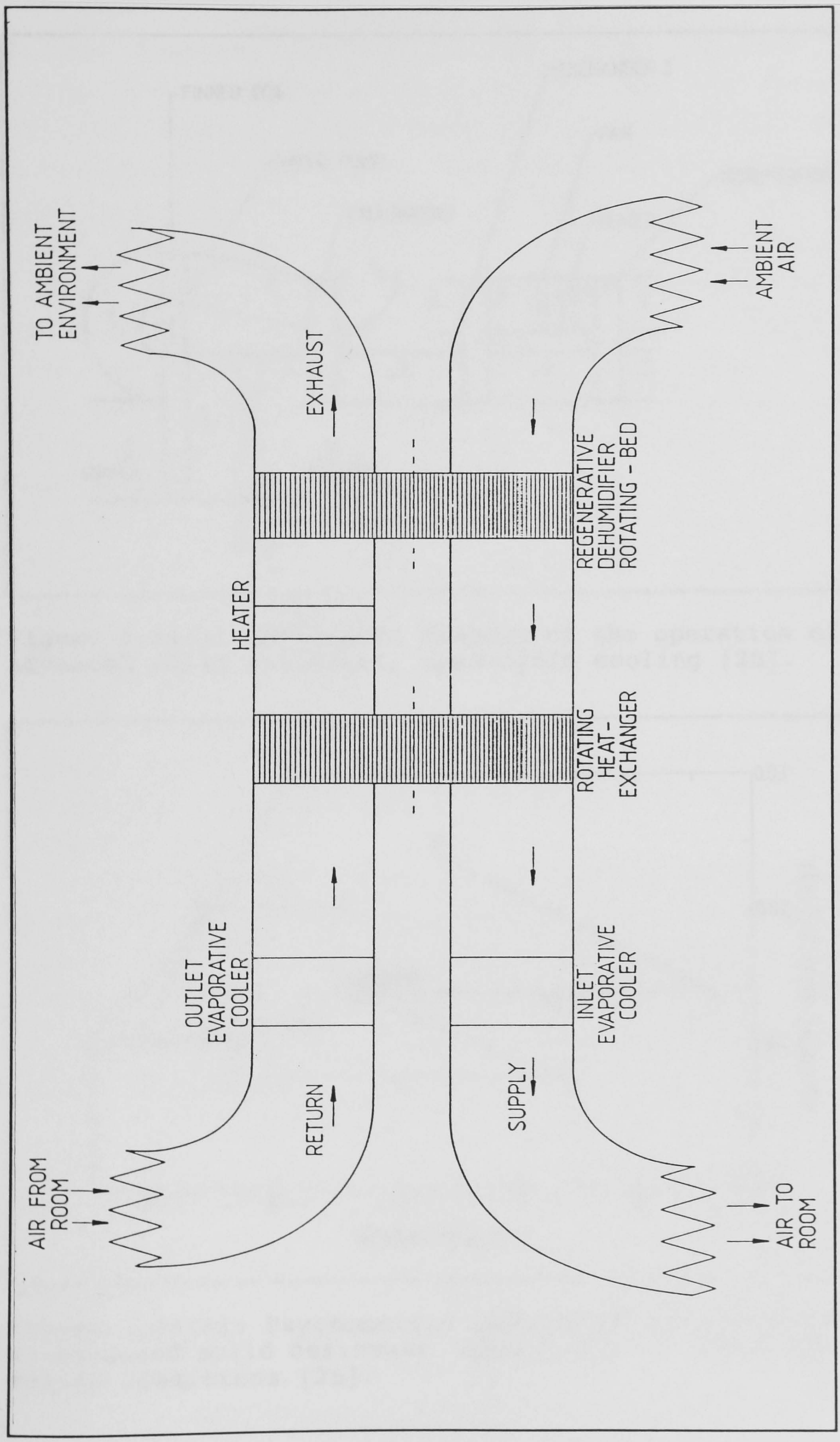

Figure 3.15: A continuous dehumidification-cooling process.

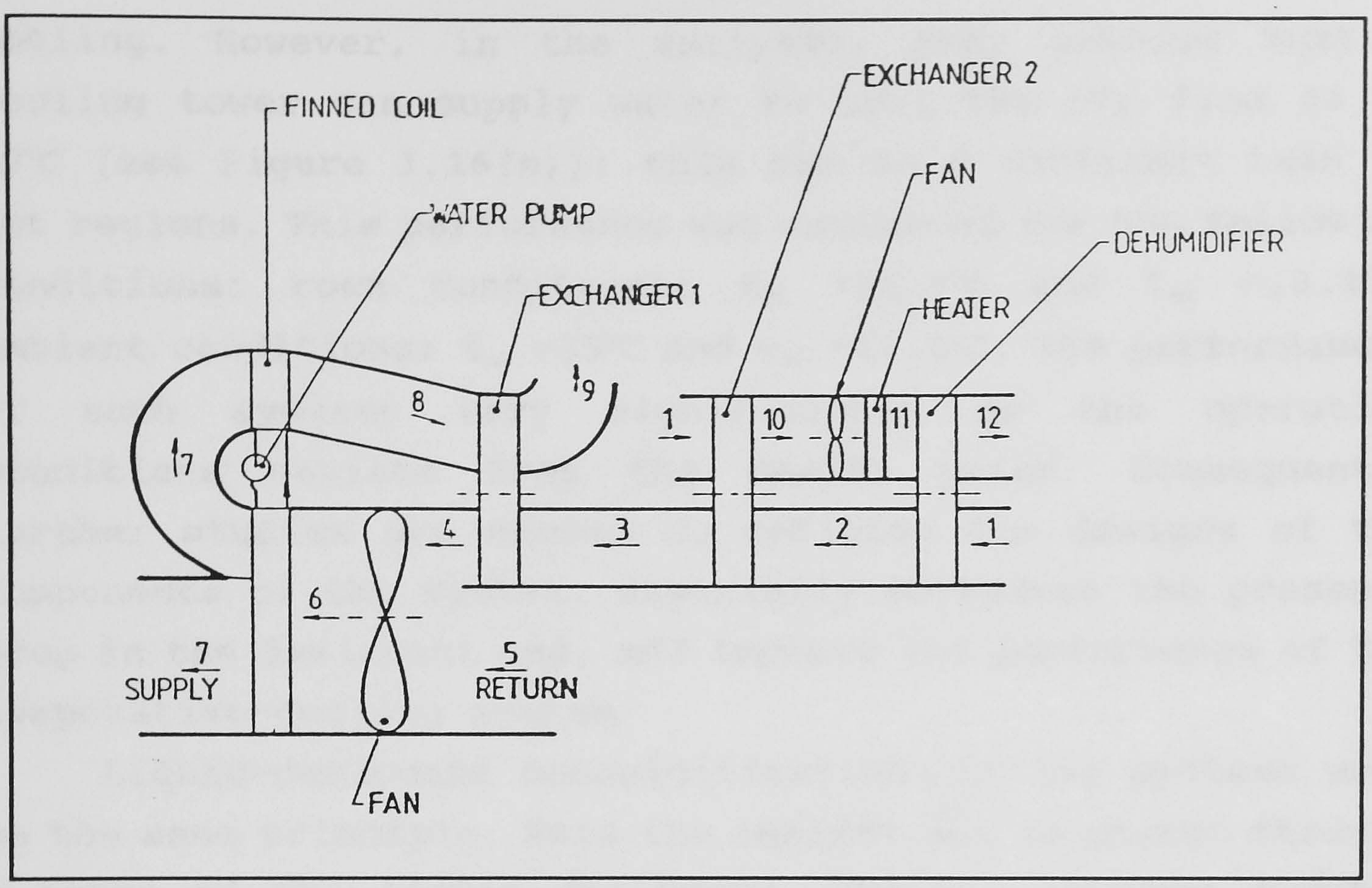

Figure 3.16(a): Schematic diagram of the operation of an advanced solid desiccant, open-cycle cooling [25].

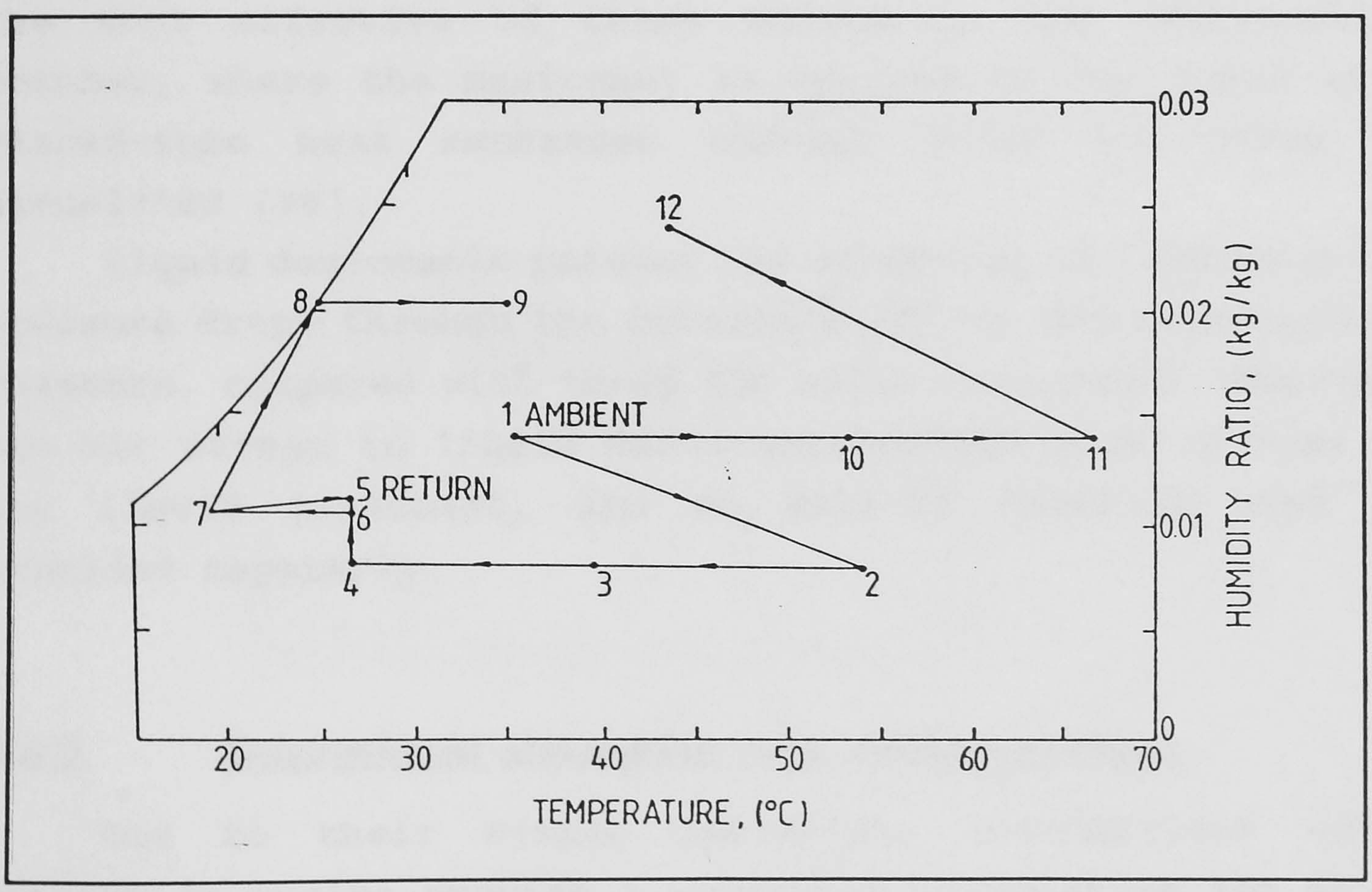

Figure 3.16(b): Psychometric diagram of the operation of an advanced solid desiccant, open-cycle cooling under ARI design conditions [25].

cooling. However, in the analysis, they assumed that a cooling tower can supply water to cool the air from 26 to 19°C (see Figure 3.16(b)): this can be a difficult task in hot regions. This performance was estimated for the following conditions: room conditions: t_{db} =26.7°C and t_{wb} =19.4°C; ambient conditions: t_{db} =35°C and t_{wb} =23.0°C. The performances of such systems vary significantly as the operating conditions deviate from the design point. Consequently further studies are needed to optimise the designs of the components of the system, especially to reduce the pressure drop in the desiccant bed, and improve the performance of the evaporative-cooling system.

Liquid-desiccant dehumidification-cooling systems work on the same principle. Here the ambient air is passed through a spray of the liquid desiccant. The air is then further cooled by direct or indirect evaporative cooling. the diluted desiccant liquid is regenerated in a variety of ways. One of the most effective of these occurs in the regenerating chamber, where the desiccant is sprayed on the pipes of a finned-tube heat exchanger through which hot water is circulated [26].

Liquid desiccants possess the advantage of incurring low pressure drops through the dehumidification and regeneration chambers, compared with those for solid desiccants. However, the air stream in liquid desiccant systems pick up some of the liquid desiccant, and so make-up solution must be provided regularly.

3.4.2 Intermittent absorptive solar-cooling systems

Due to their simple operation, intermittent solid absorption cycles provide a promising alternative for solar cooling. In these systems (see Figure 3.17), there is a pairing of absorbent and adsorbate such as Zeolite/water, activated carbon/methanol, and calcium chloride/ammonia. Each

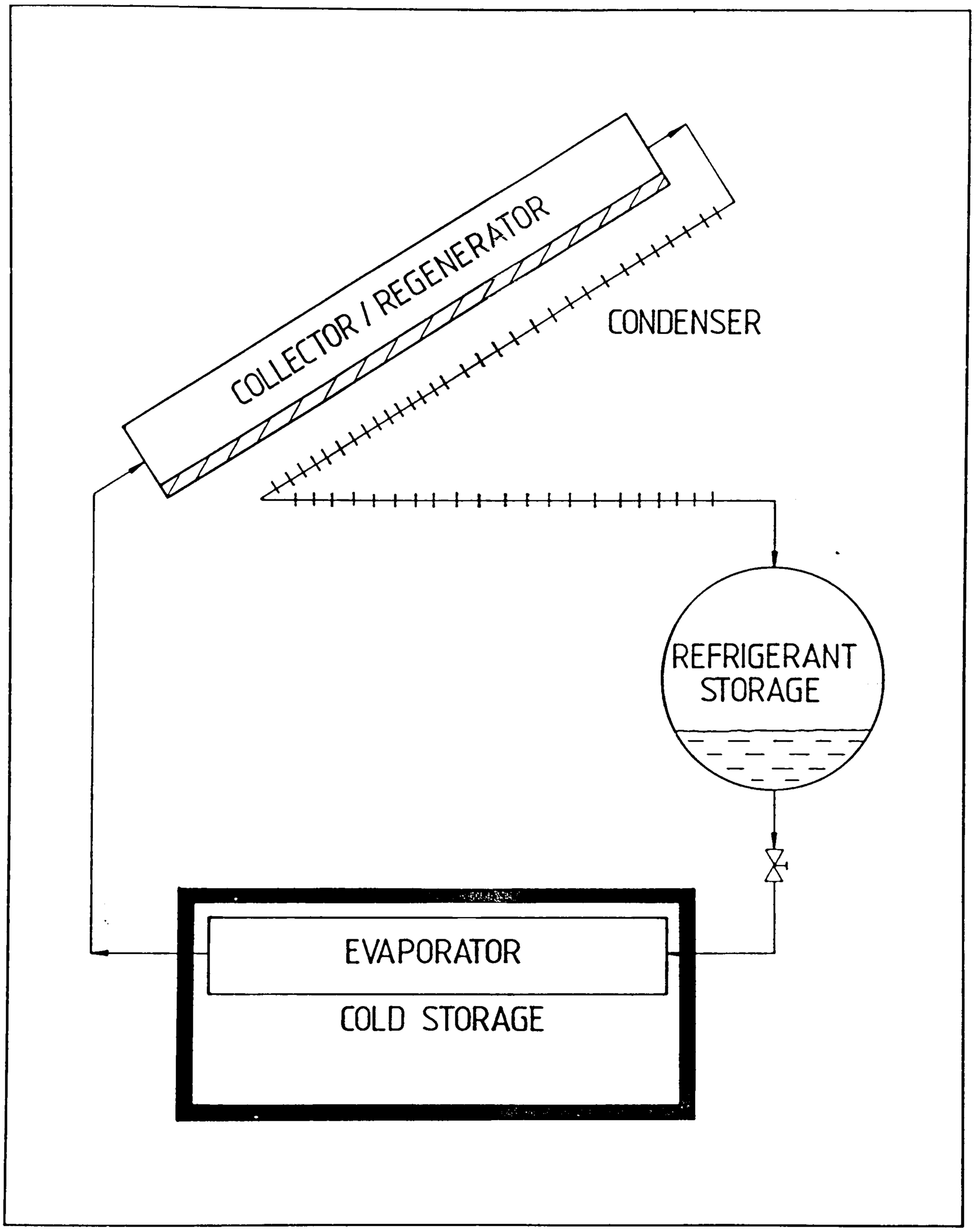

Figure 3.17: Schematic diagram of an intermittent solar adsorption-cooling system.

cycle consist of two-periods; heating/desorption/condensation and cooling /adsorption/evaporation. During the day, a collector containing the absorbent and adsorbate is heated by solar energy and the adsorbate evaporates (desorption) leaving the collector, subsequently condensing in a condenser. The condensate is collected in a reservoir. The process continues during the day and nearly all the adsorbate (i.e. refrigerant) evaporates from the collector and collects in the reservoir. During the night, the collector cools by radiation and convection, and the adsorbate is fed to the evaporator. The reduced pressure in the collector induces the evaporation of the refrigerant in the evaporator and the vapour is desorbed back into the collector. So the system must be completely airtight to prevent the suction of air into the system. When the refrigerant evaporates, the sensible cooling thus produced could be used to make ice or chilled water to be used the next day. Solar-powered solid absorbtion ice makers are already produced commercially (by eg Zeopower in the USA, Sun Ice in Denmark and BLM in France) with a solar COP of about 0.1 and ice-production rate of up to 7 kgm^{-2} of solar-collector plate per day [27,28].

The future of such ice-making machines in the field of air conditioning relies on the ability to store the "coolth" produce, in the form of ice, for summer air-conditioning. so ice is produce in a large ice-storage tank, which may be built underground beneath the house. The ice in the tank, which is produced the whole year round, should be sufficient to satisfy the total summer cooling load. The economic feasibility of such long-term storage needs to be investigated.

3.4.3 Absorption solar cooling

The most widely used of all active solar coolers is the vapour-absorption system. It is now commercially manufactured in sizes ranging from 5 to 70 Kw. The popularity of such

system is due to the fact that conventional gas or oil-fired vapour-absorption cooling systems are widely used and the change from gas or oil to solar energy is relatively easy. Absorption cooling is based on the principle that the refrigerant combines chemically with an absorbent to release heat during absorption while they absorb heat during evaporation. The system (see Figure 3.18) consists of a generator which contains a strong mixture of the absorbent and refrigerant. The refrigerant evaporates and condenses in or on the condenser. The cooled condensate then flows to the evaporator, through a throttling device, where it evaporates, thus absorbing heat from the fluid to be cooled. The vapour is subsequently absorbed and the strong mixture fed to the generator through a heat exchanger. Through the same heat exchanger the working fluid from the generator is fed to the absorber.

Suitable chemical solution for absorption cooling are water/ammonia where ammonia is the refrigerant, and lithium bromide/water, where water is the refrigerant. The water/ammonia system requires generating temperatures in the range 95-100°C and also needs a rectifying column to prevent water vapour from leaving with the ammonia vapour. For the solar operation of the water/ammonia system evacuated-tube collectors are needed and these are expensive. The lithium bromide/water system requires generating temperatures in the range 70-80°C without the need for rectifying column. Such systems can be used with flat-plate solar collectors and thus are more viable financially.

Extensive experiments on solar air-conditioning of buildings using the absorption cycle have been conducted. Al-Karaghouli et al. [29], have evaluated the cooling season performance of a house in Iraq fitted with a solar absorption cooling system, with an auxiliary kerosene heater. They found that when the house was kept at 28°C, and while the ambient air temperature exceeded 46°C, the solar fraction (i,e. the percentage of the total cooling load supplied utilising solar

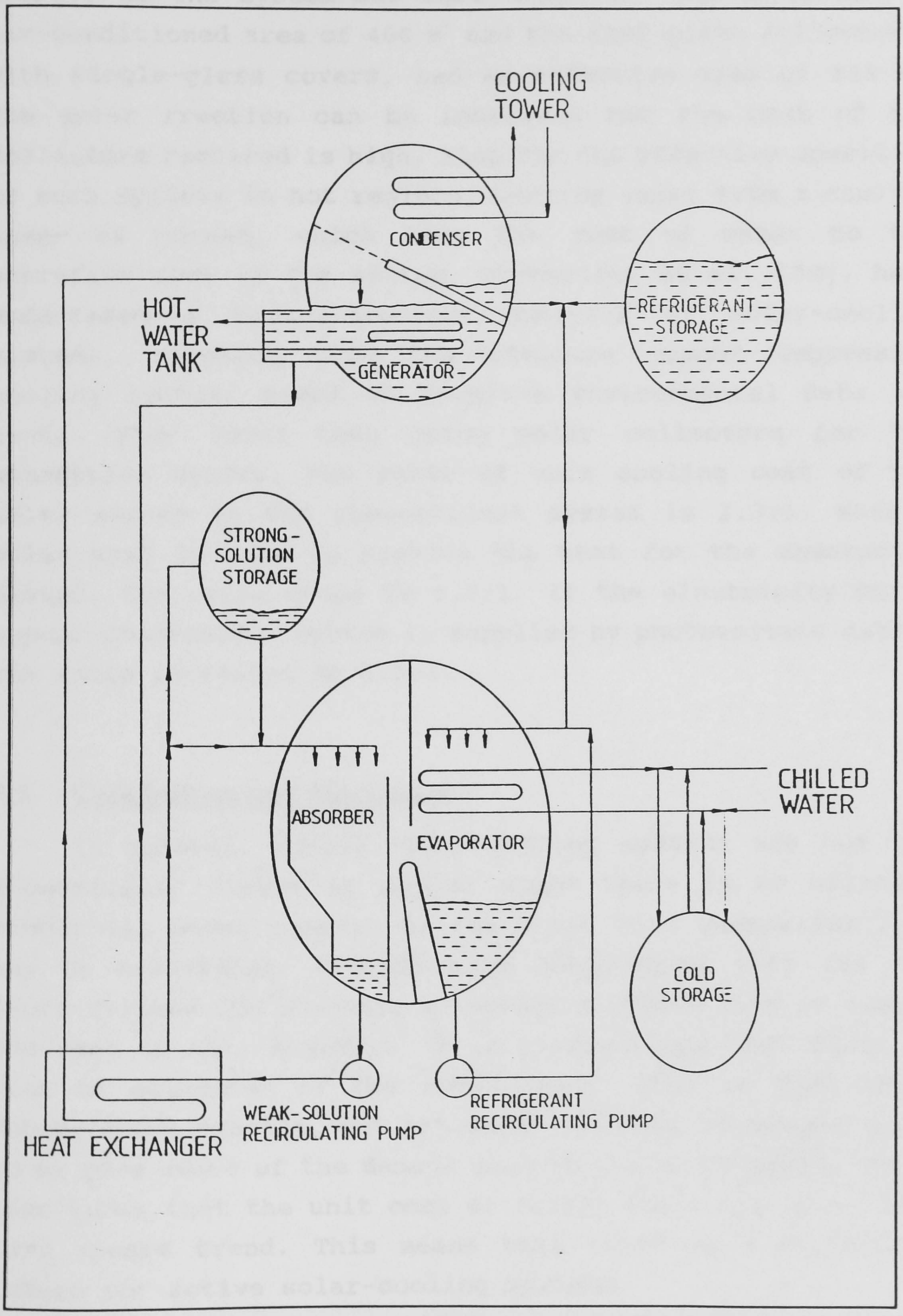

Figure 3.18: Schematic diagram of an absorption-cooling system.

energy) of the system was more than 51%. The house had an air-conditioned area of 400 m^2 and the flat-plate collectors, with single-glass covers, had an effective area of 243 m^2. The solar fraction can be increased but the cost of the collectors required is high. Also for the effective operation of such systems in hot regions, cooling water from a cooling tower is needed, which adds the cost of water to the operation cost of the system. Al-Marafie et al. [30], have undertaken a techno-economic analysis of solar-cooling systems, compared with the standard vapour-compression cooling system, based on Kuwait's environmental data and costs. They found that using solar collectors for the absorption system, the ratio of unit cooling cost of the solar system to the conventional system is 2.3:1. When a solar pond is used to provide the heat for the absorption system, the ratio drops to 1.7:1. If the electricity for a vapour-compression system is supplied by photovoltaic cells, the ratio increases to 3.3:1.

3.5 Conclusions and Discussion

In general, active solar-cooling systems are not yet economically viable in places where there is an existing electrical power supply. On the other hand generalisations may be misleading, because each environment with its own micro-climate and economic situation dictates what is viable and what is not. Nowadays it is acknowledged that there is cost of pollution of the environment. What is that cost? Nobody knows exactly, but estimates escalate as people start to be more aware of the damage done to the environment. It is also known that the unit cost of fossil fuels are on a long-term upward trend. This means that there is a worthwhile future for active solar-cooling systems.

Hybrid-and passive-cooling systems are influenced by the local climate and so successful incorporation of these

systems for the provision of comfort in residential buildings will depend to a large extent on the ingenuity of the local architect and engineer. The quality of the indoor environment produced by such systems and the habit and economical environment of the local people will influence the widespread use of such systems. However, most passive systems are economically viable, and in newly developed countries like the middle east this fact is still not understood even by most local architects. For this reason, regulations should be introduced to halt the spread of inadequate building designs which do not take heed of local conditions and the potential for low rates of energy consumption. This is especially pertinent in the Arab Gulf States, where the power used for the air-conditioning of buildings accounts for about 70% of the national electrical power production. This has forced a large expansion in the electricity production to meet the summer load, while for seven months of the year power stations run far below their capacity. Obviously, the cost of operation and maintenance of these stations is high, and will increase. A better distribution of seasonal electrical load to shorten the periods of high and low consumption rates would improve the systems' efficiencies, and reduce the need for further capital expenditures to accommodate new customers.

To encourage the introduction of more energy-efficient buildings, designers should understand the advantages to the customer and the society as a whole. Then they should be made aware of the techniques and tools available for designing energy-efficient buildings. Unfortunately, as yet in most developing countries there are no *energy* regulations for buildings and so this is where the first step should be taken. These should be simple and easy to understand and apply and give room for the designer to be creative in achieving a target level, while being easy to reinforce and check. Computerised techniques at the first stage will probably be too complicated to adopt. So manual techniques

and calculations (e.g F.Chart and solar-load ratio method (SLR)) or those which can be performed by programmable calculators, should be included in the energy regulations for the successful widespread deployment of these codes.

Generally, concern for energy consumption is only marginal in the majority of architectural-design practices, even in the developed countries. This is because, although energy conservation is an important concern at the macro-economic level, it is of little apparent concern at the micro-economic level. So why should the architect spend a lot of time and effort upon an aspect of the design which is not regarded as high priority by the customer. Also most of the energy calculations are performed during the final stages of the design process, by which time most of the structural decisions have been taken. Any changes at that stage will be cumbersome and time consuming. So for efficient design the energy considerations should be an essential part of the design process from the start, and not introduced as afterthoughts.

A wide variety of computerised energy-analysis tools are available and, thanks to the rapid development in computer technology in both hardware and software, many large programs have now been adapted to run on PCs. Examples of these are DOE 2.1C and Suncode [31,32]. Such programs will continue to be used by those who have an interest in the energy-efficient design. However if energy analysis is to be integrated in the design process of the ordinary designer, such energy-analysis tools must be incorporated into the larger computer-aided building-design packages. Such packages will make energy analysis easy to perform because much of the required data already exists in the systems. Computer-aided building-design systems are already in the development pipeline [33].

3.6 REFERENCES

1. P.O. Fanger, Thermal Comfort-Analysis and Applications in Environmental Engineering, McGraw-Hill, New York, 1972.

2. M.A. Humphreys, Desirable temperatures in dwellings. BRE Current paper 75/76, Garston, UK, 1976.

3. A. Bouchair & D. Fitzgerald, The optimum azimuth for a solar chimney in hot climates. Energy and Buildings, **12** (1988), pp 135-140.

4. A. Bowen, Bioclimatic-design approaches for Al Tihamat and Alhijaz, Saudia Arabia, Solar Energy and the Arab World. Pergamon Press, UK., 1983, pp.63-78.

5. J. Nayak, A. Srivastava, U. Singh & M. Sodha, The relative performances of different approaches to the passive cooling of roofs. Buildings and Environment, **17**(2)(1982), pp. 145-61.

6. N. Yardi & B. Jain, A solar house for hot and humid climates. In Proceedings of the 2nd International Passive and Low-Energy Architecture Conference, Crete, Greece,28 July 1983, pp. 73-82.

7. S. Groce, G. Degiorgio, L. Devita & L. Mazzarella, Steady-state thermal performance of a naturally ventilated cavity wall in a controlled-temperature cell. In Proceedings of the 6th International passive and Low-Energy Architecture Conference, Porto, Portugal, 27-31 July 1988, pp. 347-56.

8. F. Rohles, S. Konz & B. Jones, Ceiling fans as extenders of summer comfort envelope. ASHRAE Transactions 89, Part 1A (1983) pp. 245-63.

9. S. Chandra, P. Fairey, M. Houston & A. Keresteciogl u, Wing walls to improve natural ventilation. Full-scale results and design strategies. In 8th National Passive Solar Conference, Sante Fe, New Mexico, September 1983, pp. 855-60.

10. M.N. Bahadori, Natural air-conditioning systems. In Advances in Solar Energy, Vol. 3, Plenum Press, New York, 1986, pp. 283-356.

11. S. Barbera, G. Gammarata, L. Margani & L. Marletta, Performance analysis of a Mediterranean building retrofitted with solar chimney. In Proceedings of the 3rd International Passive and Low-Energy Architecture Conference, Mexico City, Mexico, 1984, pp. 879-88.

12. J.I. Yellott, Passive and hybrid cooling research. In Advances in Solar Energy, Vol. 1, Plenum Press, New York, 1982, pp. 241-63

13. E. Clark & P. Berdhal, Radiative cooling: resources and applications. In Proceedings of the Passive-cooling Workshop, Amherst, MA, 1980, pp. 177-212.

14. F. Murray, On Computation of saturation vapour pressure, Journal of Applied Meteorology, **16**(1967), pp. 203-4.

15. X. Berger, D. Buriot & F. Garnier, About the equivalent radiative temperature for clear skies. Solar Energy, **32**(6)(1984), pp. 725-33.

16. B. Givoni, Models of passive-cooling systems. In Proceedings of the 6th International Passive and Low-Energy Architecture Conference, Porto, Portugal, 27-31 July 1988, pp.521-6.

17. H. Hay, 100% natural thermal control. In Proceedings of the 3rd International Passive and Low-Energy Architecture Conference, Mexico City, Mexico, 1984, pp. 532-45.

18. K. Al-Jamal, O. Alameddine, H. Al- Shami & N. Shaban, Passive cooling evaluation of roof-pond systems. Solar and Wind Technology, **5**(1)(1988), pp. 55-6.

19. A.N. Ayoob, A retrofitting solar heating and cooling system. In Proceedings of the 6th International Passive and Low-Energy Architecture Conference, Porto, Portugal, 27-31 July 1988, pp.553-8.

20. X. Berger, M. Schenider, J. Deval, F. Kieno, C. Awanou & I. Donet, Thermal comfort in hot dry countries: radiative cooling by a diode roof. In Proceedings of the 3rd International Passive and Low-Energy Architecture Conference, Mexico City, Mexico, 1984, pp. 960-7.

21. Y. Saito, A simple air-conditioning system using a double roof. Paper No. B2:75, 1981, ISES Conference, Brighton, UK.

22. P. Dan & J. Chinnapa, The cooling effect of water flowing over an inclined surface exposed to the night sky. Solar and Wind Technology, **6**(1) (1989), pp. 41-50.

23. G. Lof, G. Cler & T. Brisbane, Performance of a solar desiccant cooling system. ASME J. Solar Energy Engineering, **110** (1988), pp. 165-71.

24. J. Jurinak, J. Mitchell & W. Beckman, Open-cycle desiccant air-conditioning as an alternative to vapour-compression cooling in residential applications. ASME J. Solar Energy Engineering, **106** (1984), pp. 252-60.

25. T.S. Kang & I.L. Maclaine-cross, High-performance solid-desiccant open cooling cycles. ASME J. Solar Energy Engineering, **111** (1989), pp. 176-83.

26. C.S. Peng & J. Howell, The performance of various types of regenerators for liquid desiccants. ASME J. Solar Energy Engineering, **106** (1984), pp. 133-41.

27. M. Pons & J. Guilleminot, Design of an experimental solar-powered solid-adsorption ice maker. ASME J. Solar Energy Engineering, **108** (1986), pp. 332-7.

28. J. Guilleminot & F. Meunier, Thermodynamic and economic optimisation of solar-powered solid adsorbent refrigerating units. Int.J. Solar Energy, **7** (1989), pp. 11-25.

29. A. Al-Karaghouli, N. Al-Hamaddani & W. Al-Sinan, Iraqi solar house cooling season performance evaluation, Solar and Wind Technology, **6**(1) (1989), pp. 29-40.

30. A. Al-Marafie, R. Suri & G. Matieshwari, Techno-economic performance analysis of solar cooling systems, Int. J. Energy Research, **12** (1988), pp. 393-401.

31. S. Hastings, Computer design tools for climate-responsive architecture, Solar and Wind Technology, **6**(4) (1989), pp. 357-63.

32. J. Clarke, Building energy simulation: The state-of-the-art, Solar and Wind Technology, **6**(4) (1989), pp. 345-55.

33. A. Dupange, Applying a solid-modelling language to built-form representation and evaluation, Solar and Wind Technology, **6**(4) (1989), pp. 333-44.

Chapter (4)

Mathematical Modelling of Heat Transfer Through Different Roof Constructions

Chapter (4)

Mathematical Modelling of Heat Transfer Through Different Roof Constructions

4.1 Introduction :

In order to obtain an optimised cooling strategy for buildings in hot climates, it was essential to compare the thermal performance of different passive techniques. In this chapter, mathematical models were developed and used to compare the effect of the following building roof constructions on heat gains into a room :

- Dry Roof - Uninsulated.
- Dry Roof - Insulated.
- Roof Pond.
- Roof Pond - Insulated Roof Slab.
- Roof Pond - Movable Insulating Cover.
- Shaded Dry Roof.
- Shaded Roof Pond.
- Air-Cooling of a Roof Slab which incorporates air channels.

In chapter 6, mathematical models for a single room, were used to investigate the combined effect of different roof designs with :

- Uninsulated walls, with concrete block or brick construction.
- Insulated walls.
- closed cavity walls.

and Ventilated cavity walls.

The following assumptions were used in the analysis:

- The densities, thermal conductivities, and specific heat capacities of the materials involved, remain constant within the temperature range under consideration.

- The edge effects are negligible.
- The water layer in a roof pond (2 - 4 cm deep) is isothermal.
- The temperature of the inside air is maintained at 26°C and there is no radiative heat exchange between the ceiling and the internal surfaces of the room.

The constant inside air temperature of 26°C, was chosen as an upper limit to thermally comfortable conditions. The models developed were compared in order to assess the thermal performance of the various roof construction, and so a constant value of internal air temperature was considered reasonable for this purpose.

The ambient weather data used in the analysis, is that for Muscat - Oman, on 17-6-88, which can be classified as very hot (see Table 1 - Appendix A). A comparison of the effectiveness of the different roof constructions has also been conducted for a less severe climate, namely that for Muscat on 21-3-88 - (see Table 2 - Appendix A).

The values of the properties of the materials used in the analysis of the different roof constructions are shown in Table 3 - Appendix A.

4.2 Dry Roof Analysis :

A dry uninsulated roof slab is taken as the base case, which consists of a steel-reinforced concrete slab, 150mm thick. This type of construction is commonly used in modern houses in Oman. The analysis aims at finding the temperature variations occurring within the roof, and the consequent heat flows, through a 24-hour period.

4.2.1 Heat gains and losses in a dry roof

For a dry roof, the following heat exchange processes occur between the outside surface of the roof and the outside environment :

- Convective heat exchange with the ambient air.
- Long-wave radiation heat exchange with the sky.
- Solar heat gain into the roof during the day.

There is also a convective heat exchange process between the ceiling and the air inside the room.

4.2.1.1 Convective heat exchange with the ambient air

The amount of heat gained or lost, via convection, by the roof to the ambient air depends on the temperature difference between the outside surface of the roof and the ambient air, and also on the external convective heat transfer coefficient. Thus the convective heat gain rate (per meter square of roof area), from the outside air to the roof is given as :

$$Q_{conv_o} = h_o \, (T_{ao} - T_{ro})$$

Where h_o is the external convective heat transfer coefficient ($W\ m^{-2}\ K^{-1}$)

T_{ao} is the temperature of the ambient air (K)

T_{ro} is the temperature of the outside surface of the roof (K)

Thus if the temperature of the outside surface of the roof, T_{ro}, is higher than that of the ambient air, the roof will

lose heat to the air, and visa versa.

The external convective heat transfer coefficient, h_o, is affected by the wind speed over the roof, the temperature difference between the roof and the ambient air, and the dimensions of the roof. In this analysis, the correlations used by Gandrille and Hammond [1], are employed. These correlations are derived from full-scale measurements, and take account of the roof dimensions, the variations in wind speed and temperature difference between the roof and ambient air. They are also valid over the full-range of laminar, transitional and turbulent flow. A geometric mean of the buoyancy-driven and forced (wind-driven) components of the convective heat transfer coefficient is employed to give :

$$h_o = \frac{(Nu_p^3 + Nu_b^3)^3 . k_a}{L_{c_o}}$$

$\mathbf{k_a}$ is the thermal conductivity of the air (W $m^{-1}K^{-1}$)

L_{c_o} is The characteristic length of the roof. This is analogous with the concept of the "hydraulic diameter" widely used in fluid mechanics, and is computed as :

$$L_{c_o} = \frac{4 \times ROOF\ AREA}{ROOF\ PERIMETER} \quad (m)$$

$\mathbf{Nu_p}$ is the Nusselt number representing the parallel flow component (wind-driven)

and $\mathbf{Nu_b}$ is the Nusselt number representing the buoyancy-driven component.

$$Nu_p = 0.59\, Re^{\frac{1}{2}} \qquad if \quad Re \le 2.86\times10^5$$

OR

$$Nu_p = \left[\left(059\, Re^{\frac{1}{2}}\right)^6 + \left(0.032\, Re^{\frac{4}{5}} - 745\right)^6\right]^{\frac{1}{6}} \qquad if \quad Re > 2.86\times10^5$$

Where **Re** is the Reynold number defined as :

$$Re = \frac{\rho_a . v_a . L_{c_o}}{\mu_a}$$

ρ_a is the density of air (1.145 kgm^{-3})

$\mathbf{V_a}$ is the air speed (ms^{-1})

μ_a is the coefficient of dynamic viscosity of air ($kgm^{-1}s^{-1}$)

The Nusselt number representing the buoyancy-driven component, $\mathbf{Nu_b}$ is defined as :

$$Nu_b = \left[\left(0.54\,(Gr_o \times Pr)^{\frac{1}{4}}\right)^6 + \left(0.14\,(Gr_o \times Pr)^{\frac{1}{3}}\right)^6\right]^{\frac{1}{6}}$$

Pr is the Prandtl number for air, assumed to have a value of 0.707

and $\mathbf{Gr_o}$ is the Grashof number on the outside surface of the roof, defined as :

$$Gr_o = \frac{g . \beta_o . \Delta T_o . \rho_a^2 . L_{c_o}^{\ 3}}{\mu_a^2}$$

$\mathbf{g}$ is the acceleration due to gravity (ms^{-2})

β_o is the coefficient of thermal expansion of the outside air film, defined as :

$$\beta_o = \frac{1}{\left(\frac{T_{ao} + T_{ro}}{2}\right)} \qquad (K^{-1})$$

Where $\mathbf{T_{ao}}$ is the ambient air temperature (K)

and $\mathbf{T_{ro}}$ is the temperature of the outside surface of the roof (K)

$\Delta\mathbf{T_o}$ is the temperature difference between the outside surface of the roof and the ambient air (K)

4.2.1.2 Long-wave radiation heat exchange between the roof and the sky :

The temperature beyond the atmosphere in outer space should be about 3 K, but in practice, even for a clear sky with no clouds present, the effective temperature of the sky is approximately -45 °C. The effective temperature of the sky is increased with the increase of the amount of water vapour and dust in the atmosphere, because more heat is reflected back to the ground. In general, the effective temperature of the sky, $\mathbf{T_{sky}}$, (in K), [2], is :

$$T_{sky} = \varepsilon_{sky}^{.25} \times T_{ao}$$

Where $\mathbf{T_{ao}}$ is the ambient air temperature (K)

and $\boldsymbol{\epsilon_{sky}}$ is the average emissivity of the atmosphere.

The average emissivity of the atmosphere is almost a linear function of the dew point temperature, $\mathbf{t_{dp}}$ (in °C), and can be expressed as [3] :

$$\varepsilon_{sky} = 0.74 + (0.006 \times t_{dp})$$

The dew point temperature of the ambient air, (°C), can be computed from the ambient air temperature, $\mathbf{t_{ao}}$ (in °C), and the relative humidity, $\boldsymbol{\phi}$, by the expression suggested by Murray [4]:

$$t_{dp} = \frac{\left\{ 237.3 \times \left[\ln\phi + \frac{17.27\ t_{ao}}{t_{ao} + 237.3} \right] \right\}}{\left[17.27 - \ln\phi + \frac{17.27\ t_{ao}}{t_{ao} + 237.3} \right]}$$

In the expression above, the relative humidity, ϕ, has the range of $0 \leq \phi \leq 1$.

When the sky is partly covered with clouds, its effective radiative temperature rises until, with complete coverage by relatively low clouds, it becomes virtually the same as the air temperature. Using the cloud-cover correction factor, C_s, developed by Clark and Berdhal [3], and defined as :

$$C_s = 1.0 + 0.022n + 0.0035n^2 + 0.00028n^3$$

Where **n** is the cloud-cover area in tenths (1-10) of the sky dome, the net rate of heat loss by radiation, $Qrad_{net}$, from a horizontal flat roof to the sky is :

$$Qrad_{net} = \sigma \cdot \varepsilon_r \left(T_{ro}^4 - C_s \cdot T_{sky}^4 \right)$$

Where σ is Stefan-Boltzmann constant.

ϵ_r is the emissivity of the roof.

T_{ro} is the temperature of the outside surface of the roof (K)

and T_{sky} is the apparent temperature of the sky (K)

4.2.1.3 Solar heat gain:

The amount of solar radiation absorbed by the roof depends on the absorptance of the roof and the solar radiation falling on it. Thus the heat gain due to solar radiation, $Qsol_r$, can be expressed as :

$$Qsol_r = \alpha_r . I$$

Where α_r is the absorptance of the roof. The absorptance of concrete is in the range of 0.4 - 0.6, and thus a value of 0.5 is assumed in this analysis.

and **I** is the total hourly solar radiation falling on the roof ($W\ m^{-2}$)

The total hourly solar radiation could be estimated from the monthly averaged daily global radiation, in accordance with Duffie and Beckman's " Solar Energy For Thermal Processes" [5], as follows:

$$I = \frac{r . H}{3.6}$$

H is the monthly averaged daily global radiation for the day and location under consideration ($kJ\ m^{-2}\ day^{-1}$). In the analysis, the average for June - 88, at Muscat, was used.

r is the ratio of the total radiation for the hour to that of the whole day.

$$r = \frac{\pi}{24} . (a + b.\cos(\omega)) . \left[\frac{\cos(\omega) - \cos(\omega_s)}{\sin(\omega_s) - \frac{\pi}{180} . \omega_s . \cos(\omega_s)} \right]$$

Where **a** = $0.4090 + 0.5016 \sin(\omega_s - 60)$

b = $0.6609 - 0.4767 \sin(\omega_s - 60)$

ω is the hour angle of the sun (deg.), given as :

$$\omega = \left(\frac{360}{24} \right) . (h - 12)$$

h is the time of the day (solar time)

and ω_s is the sun set hour angle (deg.), given as :

$$\omega_s = acos\left(-\tan(\phi)\tan(\delta)\right)$$

Where ϕ is the latitude of the location (deg.)

and δ is the declination angle of the sun (deg.), given as:

$$\delta = 23.45 \cdot \sin\left[360 \cdot \frac{284 + day}{365}\right]$$

day is the day of the year under consideration (1-365).

4.2.1.4 Convective heat exchange between the ceiling and the inside air :

The amount of heat gained or lost by the ceiling to the inside air depends on the temperature difference between the air and the ceiling, and on the inside convective heat transfer coefficient. Thus the convective heat gain rate (Wm^{-2}), from the inside air to the ceiling, is given by :

$$Q_{conv_i} = h_i\left(T_{ai} - T_c\right)$$

Where h_i is the internal convective heat transfer coefficient ($W\ m^{-2}\ K^{-1}$)

T_{ai} is the temperature of the room air (K)

T_c is the temperature of the surface of the ceiling (K)

The inside heat transfer coefficient is buoyancy driven, and depends on whether the surface of the ceiling is warmer or cooler than the air inside the room. The correlations used in this analysis, are those given in [6], where the inside convective heat transfer coefficient, $\mathbf{h_i}$, is given as :

$$h_i = \frac{Nu_i \times k_a}{L_{c_i}}$$

Where

$\mathbf{k_a}$ is the thermal conductivity of the air (W $m^{-1}K^{-1}$)

L_{c_i} is the characteristic length of the ceiling. In these correlations, L_{c_i} is defined as:

$$L_{c_i} = \frac{AREA}{PERIMETER} \qquad (m)$$

and $\mathbf{Nu_i}$ is the Nusselt number, which describes the temperature gradient at the ceiling. This depends on the temperature difference and the direction of the temperature gradient between the surface of the ceiling and the inside air, and is given as :

$$Nu_i = \left\{ \begin{array}{ll} \left\{ \begin{array}{ll} 0.54.(Gr_i x Pr)^{\frac{1}{4}} & 10^4 \leq (Gr_i x Pr) \leq 10^7 \\ 0.15.(Gr_i x Pr)^{\frac{1}{3}} & 10^7 \leq (Gr_i x Pr) \leq 10^{11} \end{array} \right\} & T_c < T_{ai} \\ 0.27.(Gr_i x Pr)^{\frac{1}{4}} & T_c \geq T_{ai} \end{array} \right\}$$

$\mathbf{Gr_i}$ is the Grashof number at the ceiling surface, defined as:

$$Gr_i = \frac{g.\beta_i.\Delta T_i.\rho_a^2.{L_{c_i}}^3}{\mu_a^2}$$

β_i is the coefficient of thermal expansion of the air film at the surface of the ceiling, defined as :

$$\beta_i = \frac{1}{\left(\frac{T_{ai} + T_c}{2}\right)} \qquad (K^{-1})$$

and $\mathbf{\Delta T_i}$ is the temperature difference between the surface of the ceiling and the inside air (K)

4.2.2 Mathematical simulation of the temperature variations in a dry roof, through a 24-hour period of analysis

A one-dimensional Implicit Finite Difference Method was used to simulate the temperature variations in the roof slab, through a 24-hour period. This method is used because it is unconditionally stable. Figure (4.1) shows the nodal distribution diagram used in the analysis. The nodal equations assumed, are shown in Appendix A.

4.2.3 Simulation result

The result of the simulation for the base case of the dry uninsulated roof slab (Figure 4.2) show that the ceiling temperature stays higher than that of the room, throughout the day. This means that there is a continuous heat gain into the room through the roof. The outside surface of the roof reaches a maximum temperature of about 55 °C at around 3 pm, and the ceiling reaches a maximum temperature of about 44 °C after a time lag of about 3 hours, i.e. at 6 pm. During the day, there is a total heat gain into the room, through the roof, of about 10 MJ m^{-2} day^{-1}.

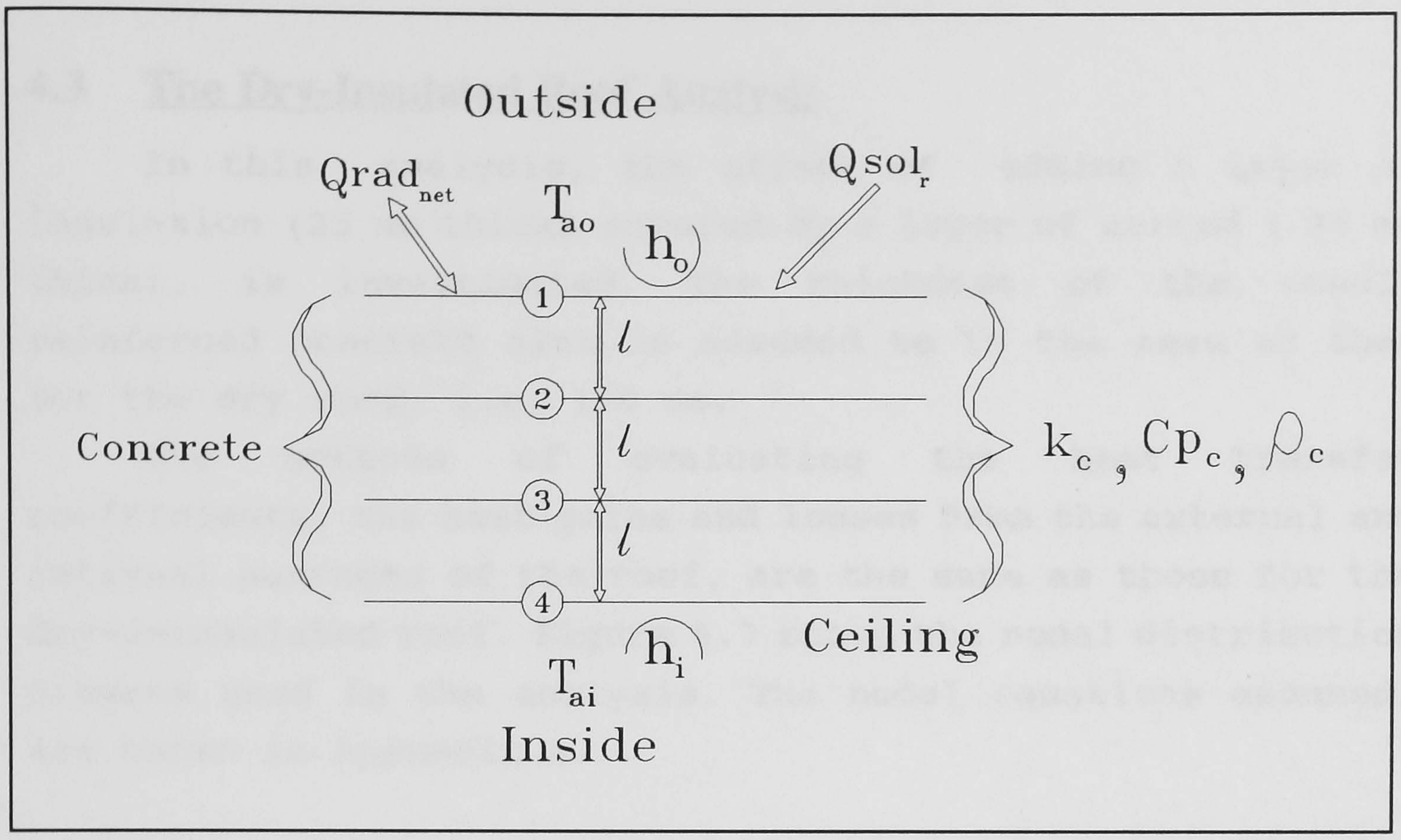

Figure 4.1 : The nodal diagram for a dry-uninsulated roof slab.

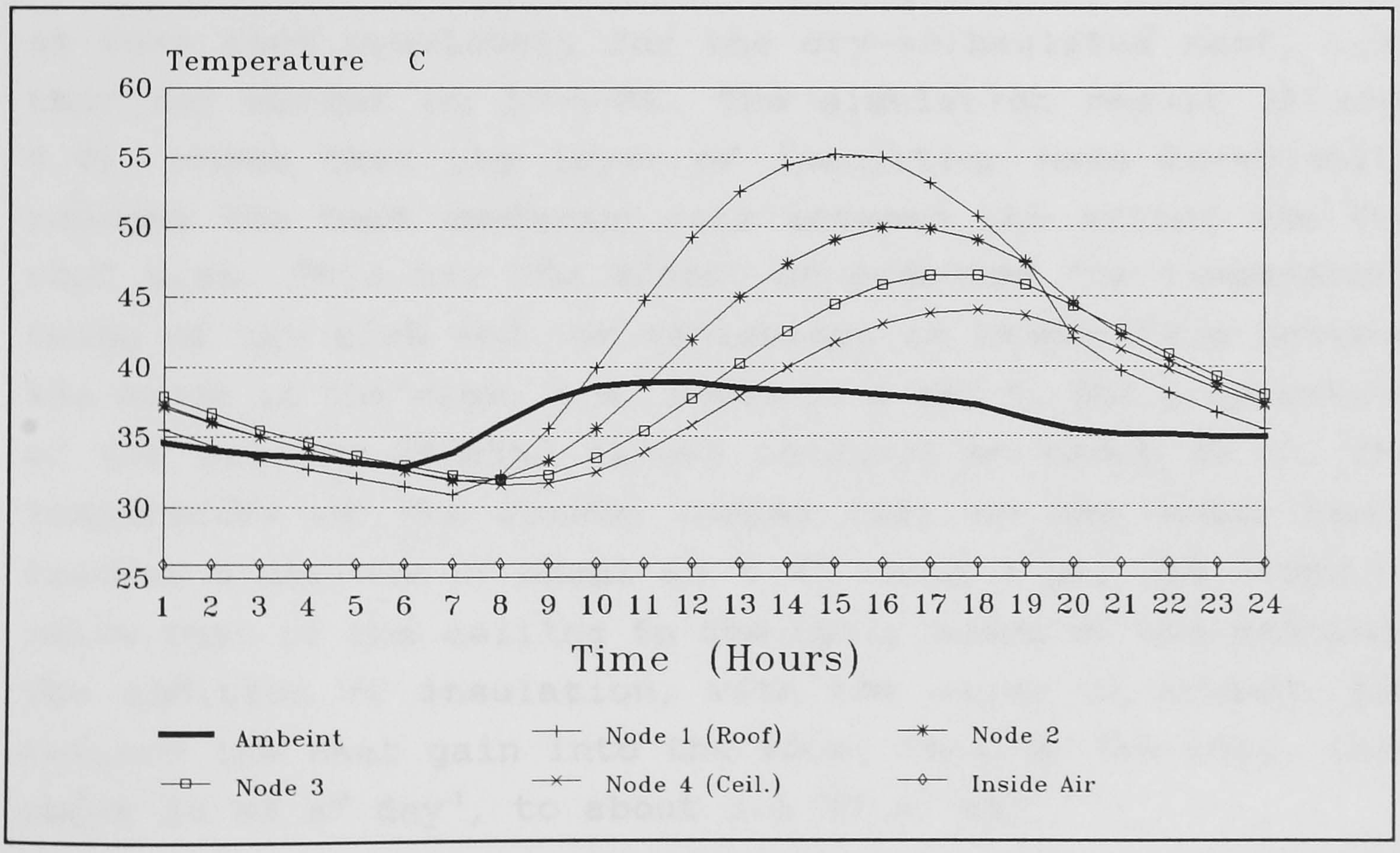

Figure 4.2 : The simulated 24-hour nodal temperature variations for the dry-uninsulated roof slab when the internal air temperature is maintained at 26 °C and the weather data for Muscat on 17-6-1988 is used.

4.3 The Dry-Insulated Roof Analysis

In this analysis, the effect of adding a layer of insulation (25 mm thick) covered by a layer of screed (25 mm thick), is investigated. The thickness of the steel-reinforced concrete slab is assumed to be the same as that for the dry roof, i.e. 150 mm.

The methods of evaluating the heat transfer coefficients, the heat gains and losses from the external and internal surfaces of the roof, are the same as those for the dry-uninsulated roof. Figure 4.3 shows the nodal distribution diagram used in the analysis. The nodal equations assumed, are shown in Appendix A.

4.3.1 Simulation result

A simulation was carried out using the same weather data as that used previously for the dry-uninsulated roof, i.e. that for Muscat on 17-6-88. The simulation result (Figure 4.4), shows that the layer of insulation have drastically reduced the heat exchange rate between the screed and the roof slab. This has the effect of reducing the temperature swing of the slab and the variations in temperature between the nodes in the slab, i.e. nodes 3, 4 and 5. The temperature of the ceiling remains almost constant at about 29 °C. The temperature of the screed (nodes 1&2) on the other hand, reaches a maximum of about 65 °C at about 2 pm, and drops to below that of the ceiling in the early hours of the morning. The addition of insulation, with the layer of screed, has reduced the heat gain into the room, through the roof, from about 10 MJ m^{-2} day^{-1}, to about 3.5 MJ m^{-2} day^{-1}.

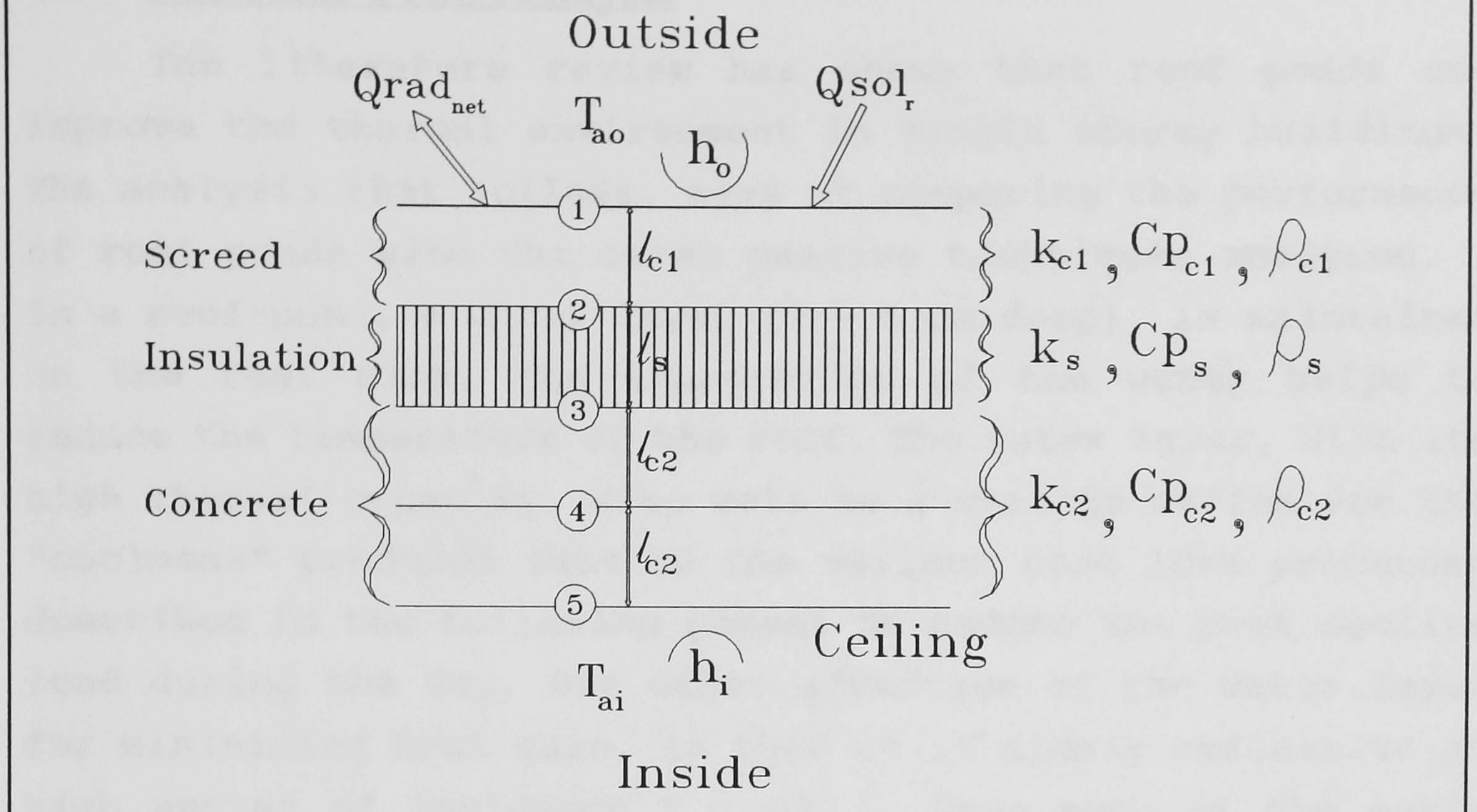

Figure 4.3 : The nodal distribution diagram for the dry-insulated roof.

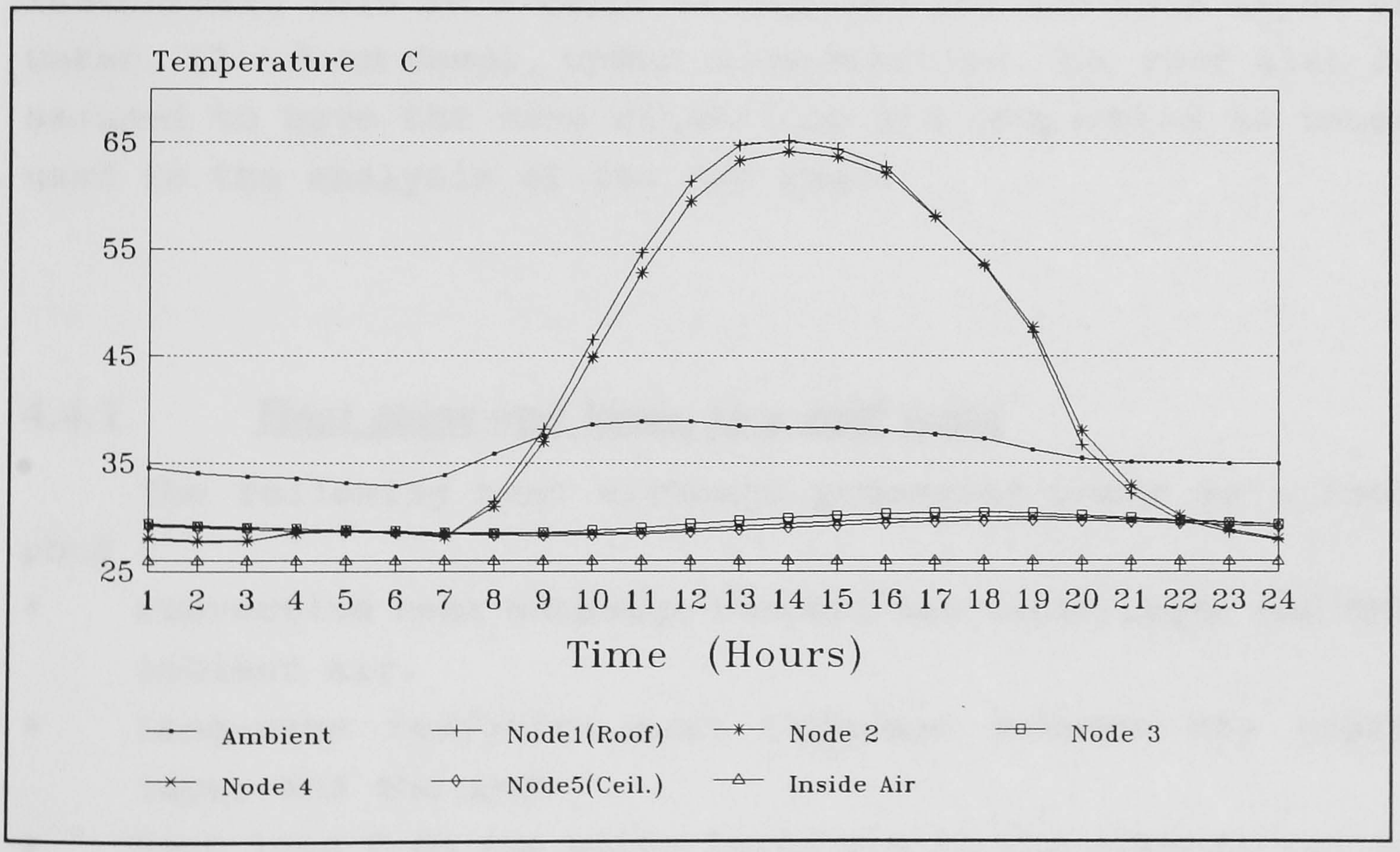

Figure 4.4 : The simulated 24-hour nodal temperature variations for the dry-insulated roof slab when the internal air temperature is maintained at 26 ºC and the weather data for Muscat on 17-6-1988 is used.

4.4 The Roof-Pond Analysis

The literature review has shown that roof ponds can improve the thermal environment in single storey buildings. The analysis that follows, aims at comparing the performance of roof ponds with the other passive techniques analyzed. In a roof-pond, a water layer (2 - 5 cm deep), is maintained on the roof slab. The evaporation of the water helps to reduce the temperature of the roof. The water layer, with its high thermal capacity, also acts as a storage medium for the "coolness" produced (due to the various heat loss processes described in the following pages) to reduce the peak cooling load during the day. One other advantage of the water layer for minimising heat gain, is that it is highly reflective at high angles of incidence (> 60°). Thus much of the early morning and late afternoon solar radiation is reflected by the water layer.

In this analysis, it is assumed that the water layer is isothermal. This is a valid assumption for the thin layer of water, (2 - 5 cm deep), under consideration. The roof slab is assumed to have the same dimensions and properties as those used in the analysis of the dry roof.

4.4.1 Heat gains and losses in a roof pond

The following heat exchange processes occur in a roof pond :

- Convective heat exchange between the water layer and the ambient air.
- Long-wave radiation heat exchange between the water layer and the sky.
- Heat loss from the water layer due to the evaporation of water.
- Solar heat gain by the water layer during the day.
- Solar heat gain by the roof slab during the day.

- Convective heat exchange process between the water layer and the roof slab, and
- Convective heat exchange process between the ceiling and the air inside the room.

The Convective heat exchange rates between the water layer and the ambient air, and that between the ceiling and the inside air are derived as for the dry roof. The long-wave heat exchange rate between the water layer and the sky is also derived as for the dry roof.

4.4.1.1 Heat loss by evaporation

The rate of heat loss by evaporation, $\mathbf{Q_{evap}}$ (W m^{-2}), depends on the rate of evaporation and the latent heat of evaporation of the water. That is :

$$Q_{evap} = \dot{m}_v \times h_{fg}$$

Where $\mathbf{\dot{m}_v}$ is the mass transfer of vapour per unit area and time ($kgm^{-2}s^{-1}$)

and $\mathbf{h_{fg}}$ is the latent heat of evaporation of water (Jk^{-1})

The rate of evaporation of water can be determined from [7]:

$$\dot{m}_v = h_m \, (W_{sat} - W_o)$$

Where $\mathbf{h_m}$ is the mass transfer coefficient. This is given by the Lewis relation [7] and further approximated to :

$$h_m = \frac{h_o}{Cp_a}$$

$\mathbf{h_o}$ is the convective heat transfer coefficient between the water layer and the ambient air ($Wm^{-2}K^{-1}$)

$\mathbf{Cp_a}$ is the specific heat capacity of air ($Jkg^{-1}K^{-1}$)

W_{sat} is the humidity ratio of the moist air in contact with the water surface. This air is assumed to be saturated. The saturation vapour pressure at this location, P_{sw}, is then a function of the water temperature only and is given by [4] viz :

$$P_{sw} = 10^{30.59051 - 8.2 \log T_w + 2.4804 \times 10^{-3} T_w - \frac{3142.31}{T_w}}$$

T_w is the temperature of the water layer (K)

The humidity ratio of this saturated air, W_{sat}, is given by [8]:

$$W_{sat} = \frac{0.622 \times P_{sw}}{p_g}$$

Where p_g is the partial pressure of the dry air (gas). This is given as :

$$p_g = P_t - p_v$$

P_t is the total pressure of the air assumed atmospheric.

and p_v is the partial pressure of the water vapour, given as:

$$p_v = \phi \, P_{sa}$$

ϕ is the relative humidity of the ambient air.

and P_{sa} is the saturation vapour pressure of the ambient air

$$P_{sa} = 10^{30.59051 - 8.2 \log T_{ao} + 2.4804 \times 10^{-3} T_{ao} - \frac{3142.31}{T_{ao}}}$$

T_{ao} is the temperature of the ambient air (K)

The humidity ratio of the ambient air, W_o, is :

$$W_o = \frac{0.622 \times p_v}{p_g}$$

The latent heat of evaporation of the water, h_{fg}, can be related to the water temperature. Following Ref.[9], we have:

$$h_{fg} = (2502.555 - 2.40516\,T_w) \times 10^3$$

Thus the heat loss by evaporation can be written as :

$$Q_{evap} = \frac{h_o}{Cp_a} \cdot (W_{sat} - W_o) \cdot h_{fg}$$

4.4.1.2 Solar heat gain by the water layer

All of the thermal models encountered in the literature review, which are used to simulate heat gains and losses in a roof pond [10,11], have assumed that the solar heat radiation absorbed by the water layer is negligible. But although the amount of solar radiation absorbed by the water layer could be small, the water layer has a modifying effect on the amount of solar radiation absorbed by the roof slab. First, when the sun is low in the sky, i.e. the altitude of the sun is less than about 30°, much of the beam solar radiation will be reflected by the water layer. However, when the sun is low in the sky, the intensity of solar radiation is low, and thus the net reflective losses of the direct solar radiation component is relatively small. Second, virtually all of the long-wave spectral band of solar radiation (> 1.2 μm), representing about 20 % of the solar intensity, which is not reflected at the surface will be absorbed by the first few centimetres of the water layer [12]. Thus this part of the solar spectrum may not reach the roof slab. For these reasons, it was considered desirable to take account of the reflected, absorbed and transmitted components of the solar radiation falling on the water pond, despite the amount of work involved. The methodology used is similar to that described by Duffie and Beckman in " Solar Energy For Thermal Processes" [5], for estimating the

reflected, absorbed and transmitted components of the solar radiation falling on a sheet of glass.

The diffuse component of the solar radiation, falling on a horizontal surface is assumed to come with equal intensity from all parts of the sky. The absorptance of the water pond to this radiation is considered equivalent to that of beam radiation falling at an incident angle of 60° [5]. Since the absorptance of the water layer to the beam component of solar radiation depends on the angle of incidence of the beam, it thus depends on the time of the day and the day of the year. Part of the beam radiation transmitted by the water layer is reflected back, through the water, by the roof. The amount of this reflected radiation depends on the reflectivity of the roof, which will be influenced by the non-specular nature of the roof surface. Generally, the total solar heat radiation absorbed by the water layer, Q_{sol_w} (in Wm^{-2}), see Figure 4.5 - can be expressed as :

$$Q_{sol_w} = \alpha_{w_b} . I_b . [1 + \rho_r . \tau_{w_b}] + \alpha_{w_d} . I_d . [1 + \rho_r . \tau_{w_d}]$$

Where

α_{w_b} is the absorptance of the water layer to direct solar radiation

α_{w_d} is the absorptance of the water layer to diffuse solar radiation.

I_b is the hourly direct solar radiation (Wm^{-2})

I_d is the hourly diffuse solar radiation (Wm^{-2})

ρ_r is the reflectance of the roof slab.

τ_{w_b} is the total transmittance of the water layer to the incident direct solar radiation.

τ_{w_d} is the total transmittance of the water layer to the incident diffuse solar radiation.

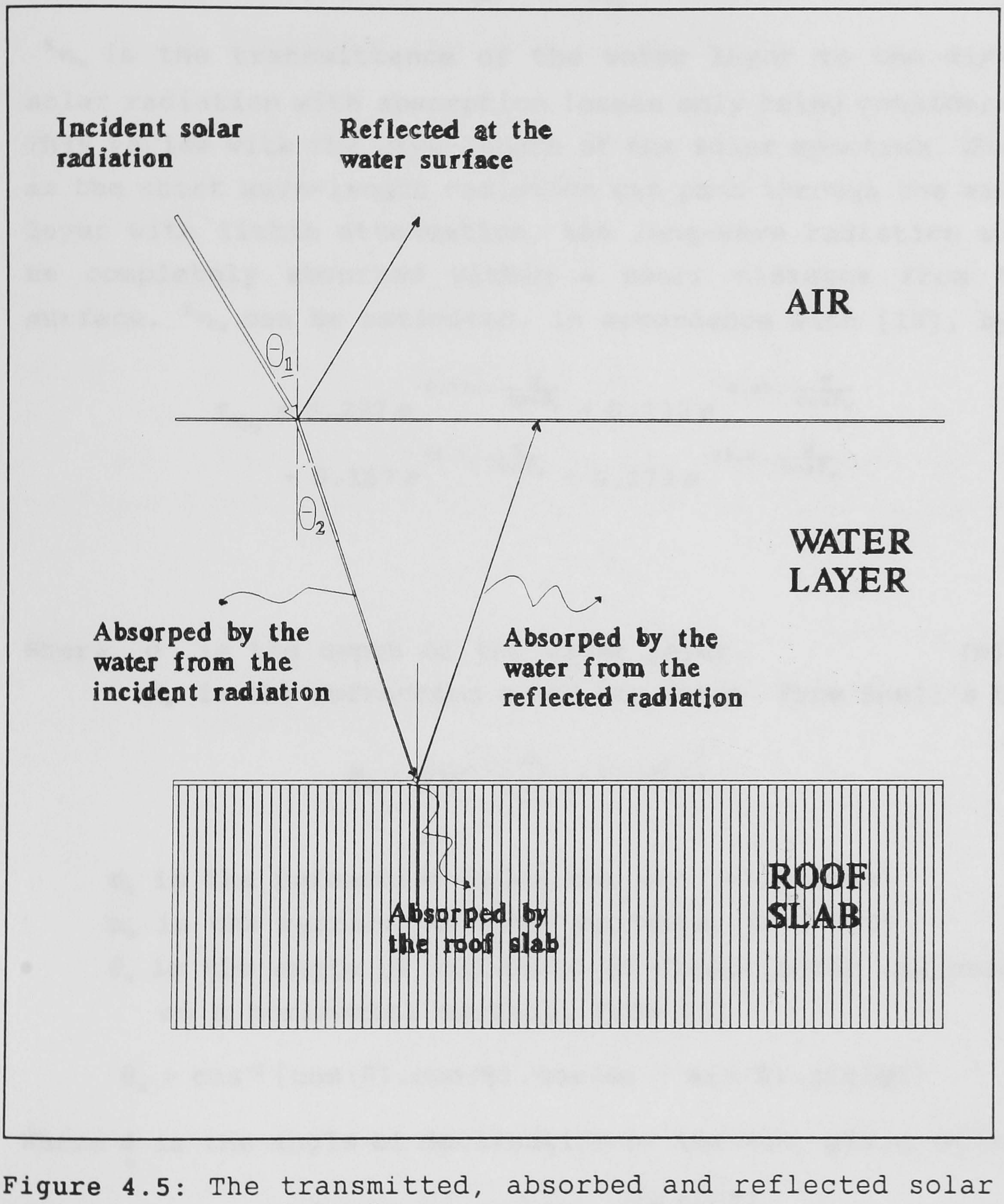

Figure 4.5: The transmitted, absorbed and reflected solar radiation in roof pond.

The ratio of the direct solar radiation absorbed by the water layer to that passing through the surface is given by:

$$\alpha_{wb} = 1 - \tau_{w_{b_a}}$$

$\tau_{w_{b_a}}$ is the transmittance of the water layer to the direct solar radiation with absorption losses only being considered. This varies with the wave-length of the solar spectrum. Where as the short wave-length radiation can pass through the water layer with little attenuation, the long-wave radiation will be completely absorbed within a short distance from the surface. $\tau_{w_{b_a}}$ can be estimated, in accordance with [13], by :

$$\tau_{w_{b_a}} = 0.237\, e^{-0.032 . \frac{d}{\cos\theta_w}} + 0.193\, e^{-0.45 . \frac{d}{\cos\theta_w}} + 0.167\, e^{-3.0 . \frac{d}{\cos\theta_w}} + 0.179\, e^{-35.0 . \frac{d}{\cos\theta_w}}$$

Where **d** is the depth of the water layer. (m)

θ_w is the refraction angle for water. From Snell's Law

$$\theta_w = \sin^{-1}\left[\frac{n_a}{n_w} . \sin(\theta_a)\right]$$

$\mathbf{n_a}$ is the refractive index for air (=1.000289)

$\mathbf{n_w}$ is the refractive index for water (= 1.333)

θ_a is the angle of incidence of direct solar radiation on a horizontal surface. From [5]

$$\theta_a = \cos^{-1}[\cos(\delta).\cos(\phi).\cos(\omega) + \sin(\delta).\sin(\phi)]$$

Where δ is the angle of declination of the sun, given as [5]:

$$\delta = 23.45 \sin\left[360 . \frac{284 + Day}{365}\right]$$

Day is the day of the year under consideration (1-365).

ϕ is the latitude of the location under consideration.

ω is the hour angle of the sun, given as :

$$\omega = \frac{360}{24} . (h-12)$$

h is the hour of the day - solar time.

The transmittance of the water layer to the diffuse solar radiation with absorption losses only being considered, $\tau_{w_{d_a}}$, is given by [13]:

$$\tau_{w_{d_a}} = 0.237 e^{-0.042 d} + 0.193 e^{-0.592 d} + 0.167 e^{-3.95 d} + 0.179 e^{-46 d}$$

Where **d** is the depth of the water layer. (m)

The total transmittance of the water layer to the incident direct solar radiation can be expressed as [5]:

$$\tau_{w_b} = \tau_{w_{b_a}} \times \tau_{w_{b_r}}$$

$\tau_{w_{b_r}}$ is the transmittance of the water layer, to beam radiation, with reflection losses only being considered.

$$\tau_{w_{b_r}} = \frac{1}{2} . \left[\frac{1 - r_{pa}}{1 + r_{pa}} + \frac{1 - r_{pe}}{1 + r_{pe}} \right]$$

$\mathbf{r_{pa}}$ is the reflection of the parallel component of beam radiation on the water surface

$$r_{pa} = \frac{\tan^2(\theta_w - \theta_a)}{\tan^2(\theta_w + \theta_a)}$$

And $\mathbf{r_{pe}}$ is the reflection of the perpendicular component of beam radiation on the water surface

$$r_{pe} = \frac{\sin^2(\theta_w - \theta_a)}{\sin^2(\theta_w + \theta_a)}$$

The total transmittance of the water layer to the diffuse solar radiation can be expressed as:

$$\tau_{w_d} = 0.89\ \tau_{w_{d_a}}$$

4.4.1.3 Solar heat gain by the roof slab

Part of the solar radiation transmitted through the water layer is absorbed by the roof slab and the rest is reflected back through the water - see Figure 4.5. In order to reduce the solar heat gain by the roof slab, it is desirable for the top surface to be highly reflective. But without periodic cleaning, the reflectivity of the dust, collecting on top of the slab, will dominate. Thus in this analysis, it is assumed that the slab has a reflectivity of 0.5 (i.e. that of the clay sediment). Neglecting the solar radiation reflected back by the top surface of the water layer, the solar heat gain by the roof slab, Q_{sol_r} , can be estimated by:

$$Q_{sol_r} = \alpha_r\,(\tau_{w_b}.\,I_b + \tau_{w_d}.\,I_d)$$

Where α_r is the absorptance of the roof.

4.4.1.4 Convective heat exchange between the roof slab and the water layer

The heat exchange rate between the water layer and the roof slab (Wm^{-2}), is given by :

$$Q_{conv_w} = h_w\,\Delta T$$

Where h_w is the convective heat transfer coefficient between the slab and the water ($Wm^{-2}K^{-1}$)

ΔT is the temperature difference between the water and the top surface of the slab (K)

The heat transfer coefficient is buoyancy driven, and depends on whether the surface of the slab is warmer or cooler than the water. The convective heat transfer coefficient, $\mathbf{h_w}$, is given as:

$$h_w = \frac{Nu \times k_w}{L_{c_r}}$$

Where $\mathbf{K_w}$ is the thermal conductivity of the water ($Wm^{-1}K^{-1}$)

L_{c_r} is the characteristic length of the slab. In these correlations, $\mathbf{L_{c_r}}$ is defined as:

$$L_{c_r} = \frac{AREA}{PERIMETER} \qquad (m)$$

and **Nu** is the Nusselt number, which describes the temperature gradient at the top surface of the slab. This depends on the temperature difference between the surface and the water, and is given as :

$$Nu = \begin{cases} \left\{ \begin{array}{ll} 0.54.(Gr_w x Pr_w)^{\frac{1}{4}} & 10^4 \le (Gr_w x Pr_w) \le 10^7 \\ 0.15.(Gr_w x Pr_w)^{\frac{1}{3}} & 10^7 \le (Gr_w x Pr_w) \le 10^{11} \end{array} \right\} & T_r < T_w \\ 0.27.(Gr_w x Pr_w)^{\frac{1}{4}} & T_r \ge T_w \end{cases}$$

$\mathbf{Pr_w}$ is the Prandtl number for water.

$\mathbf{Gr_w}$ is the Grashof number at the surface, defined as:

$$Gr_w = \frac{g \cdot \beta \cdot \Delta T \cdot \rho_w^2 \cdot L_{c_r}^3}{\mu_w^2}$$

ρ_w is the density of water (kgm^{-3})

μ_w is the absolute viscosity of water ($kgm^{-1}s^{-1}$)

and β is the coefficient of thermal expansion of the water film at the surface, defined as :

$$\beta = \frac{1}{\left(\frac{T_r + T_w}{2}\right)} \qquad (K^{-1})$$

4.4.2 Mathematical simulation of the temperature variations in a roof pond

A similar procedure was used in simulating the temperature variations in the roof pond, through a 24-hour period of analysis, as that used for the dry roof. Figure 4.6 shows the nodal distribution diagram used in the analysis. The nodal equations assumed are shown in Appendix A.

The result of the simulation (Figure 4.7), using the weather data for Muscat on 17-6-88, shows that the water layer has inhibited the sharp rise in the temperature of the outer surface of the roof during the day. Compared with a maximum outer surface temperature of 55 °C for the dry-uninsulated roof, and 65 °C for the dry-insulated roof, the maximum temperature reached by the water layer and the outside surface of the roof in the roof pond, is about 39 °C. This is about the same as the maximum ambient air temperature for the day. During the early hours of the morning, the water temperature drops to about 25 °C. This is lower than the inside air temperature, maintained at 26 °C. The ceiling temperature fluctuates between a maximum of about 34 °C, at around 5 pm, and a minimum of about 26 °C, at 8 am. Compared with the dry-insulated roof, the swing in the ceiling temperature is much greater, but the average temperatures are about the same. The net heat gain into the room, via the roof, is thus about the same as that for the dry-insulated roof.

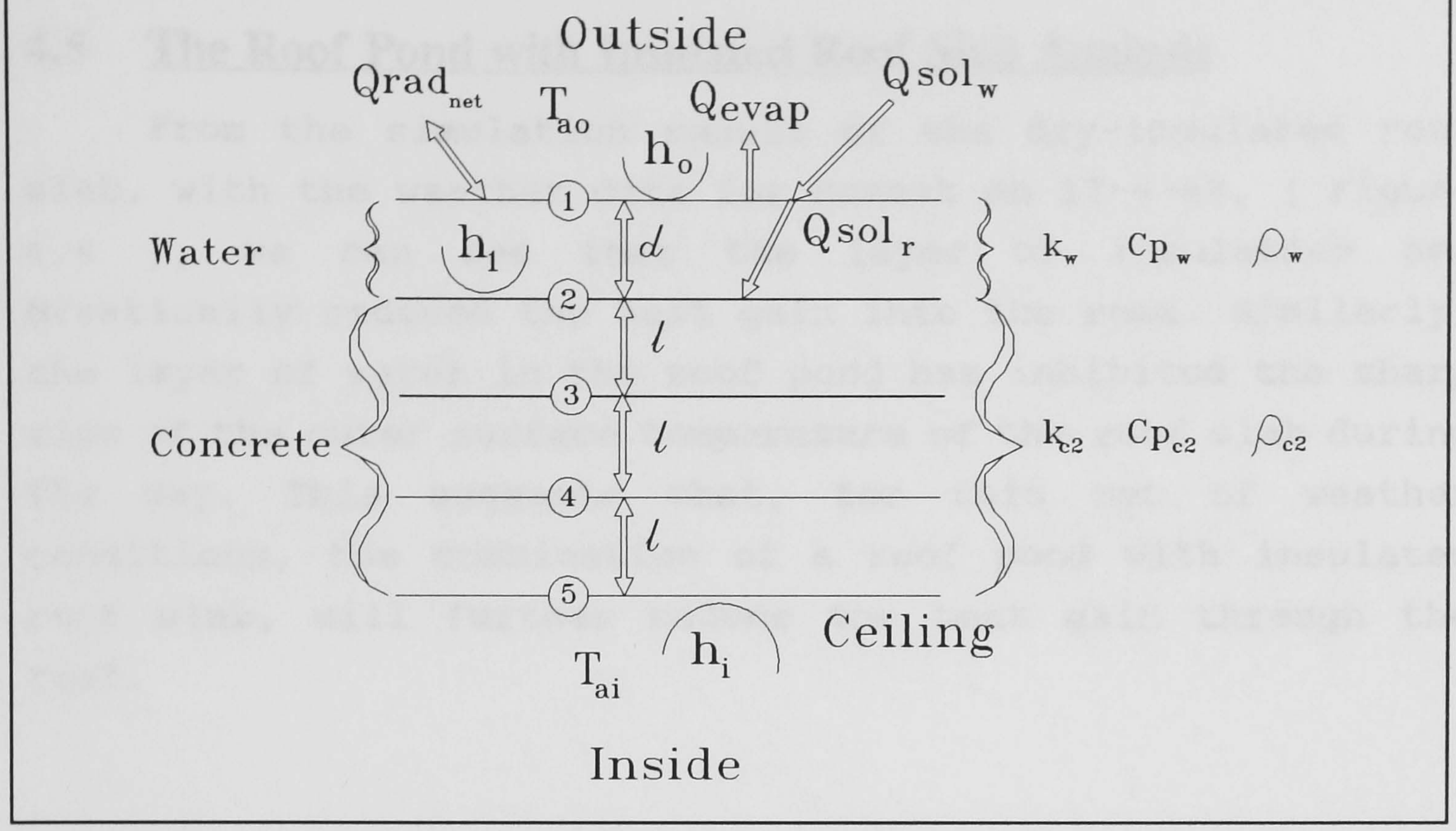

Figure 4.6 : The nodal diagram for a Roof-Pond.

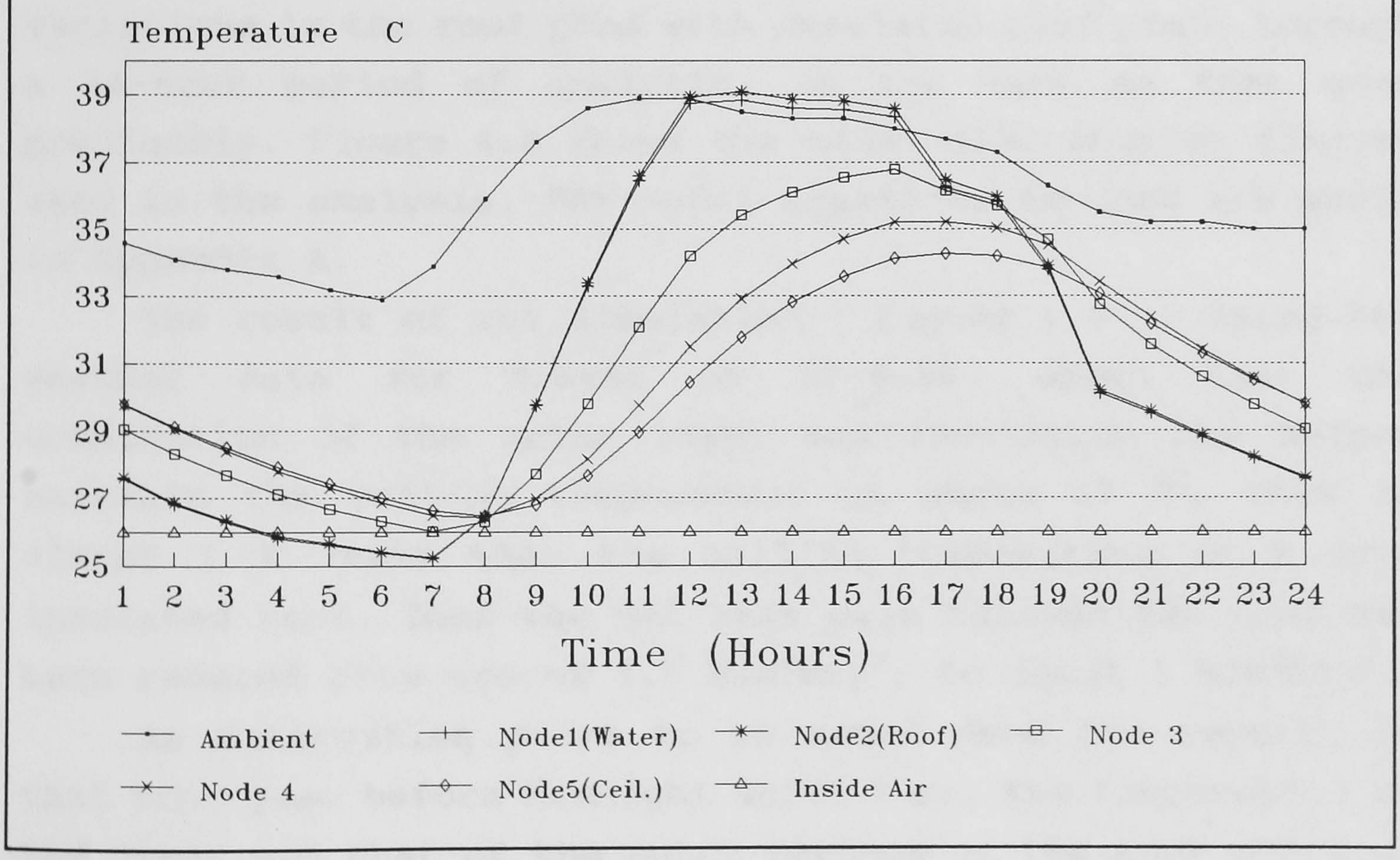

Figure 4.7: The simulated 24-hour nodal temperature variations for the roof pond when the internal air temperature is maintained at 26 ℃ and the weather data for Muscat on 17-6-1988 is used.

4.5 The Roof Pond with Insulated Roof Slab Analysis

From the simulation result of the dry-insulated roof slab, with the weather data for Muscat on 17-6-88, (Figure 4.4), we can see that the layer of insulation has drastically reduced the heat gain into the room. Similarly, the layer of water in the roof pond has inhibited the sharp rise of the outer surface temperature of the roof slab during the day. This suggests that, for this set of weather conditions, the combination of a roof pond with insulated roof slab, will further reduce the heat gain through the roof.

4.5.1 Mathematical simulation of the temperature variations in a roof pond with insulated roof slab

The procedure used in simulating the temperature variations in the roof pond with insulated roof slab, through a 24-hour period of analysis, is the same as that used previously. Figure 4.8 shows the nodal distribution diagram used in the analysis. The nodal equations assumed are shown in Appendix A.

The result of the simulation (Figure 4.9), using the weather data for Muscat on 17-6-88, shows that the combination of the water layer and insulation has helped maintain the ceiling temperature at about 27 °C. This is almost 3 °C lower than the ceiling temperature in a dry-insulated roof. Thus the net heat gain through the roof has been reduced from around 3.5 $MJm^{-2}day^{-1}$, to about 1 $MJm^{-2}day^{-1}$.

An interesting point to be noted from the result, is that from just before Midnight until 7 am, the temperature of the water and that of the outer surface of the roof stays at around 25 °C. Thus although this temperature is lower than that of the inside air, maintained at 26 °C, the layer of insulation inhibits the heat loss from the room to the cooler

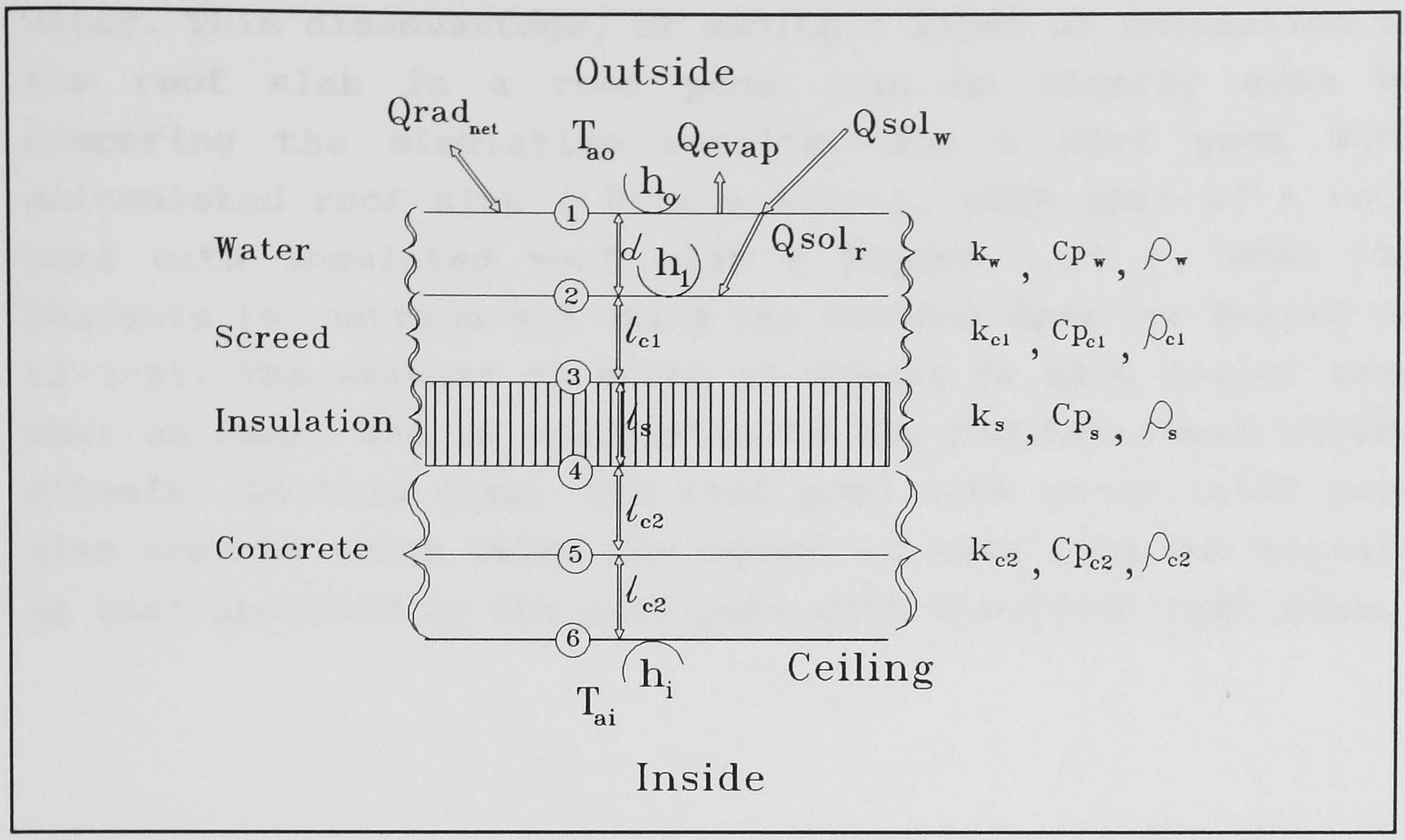

Figure 4.8: The nodal distribution diagram for a roof-pond with insulated roof slab.

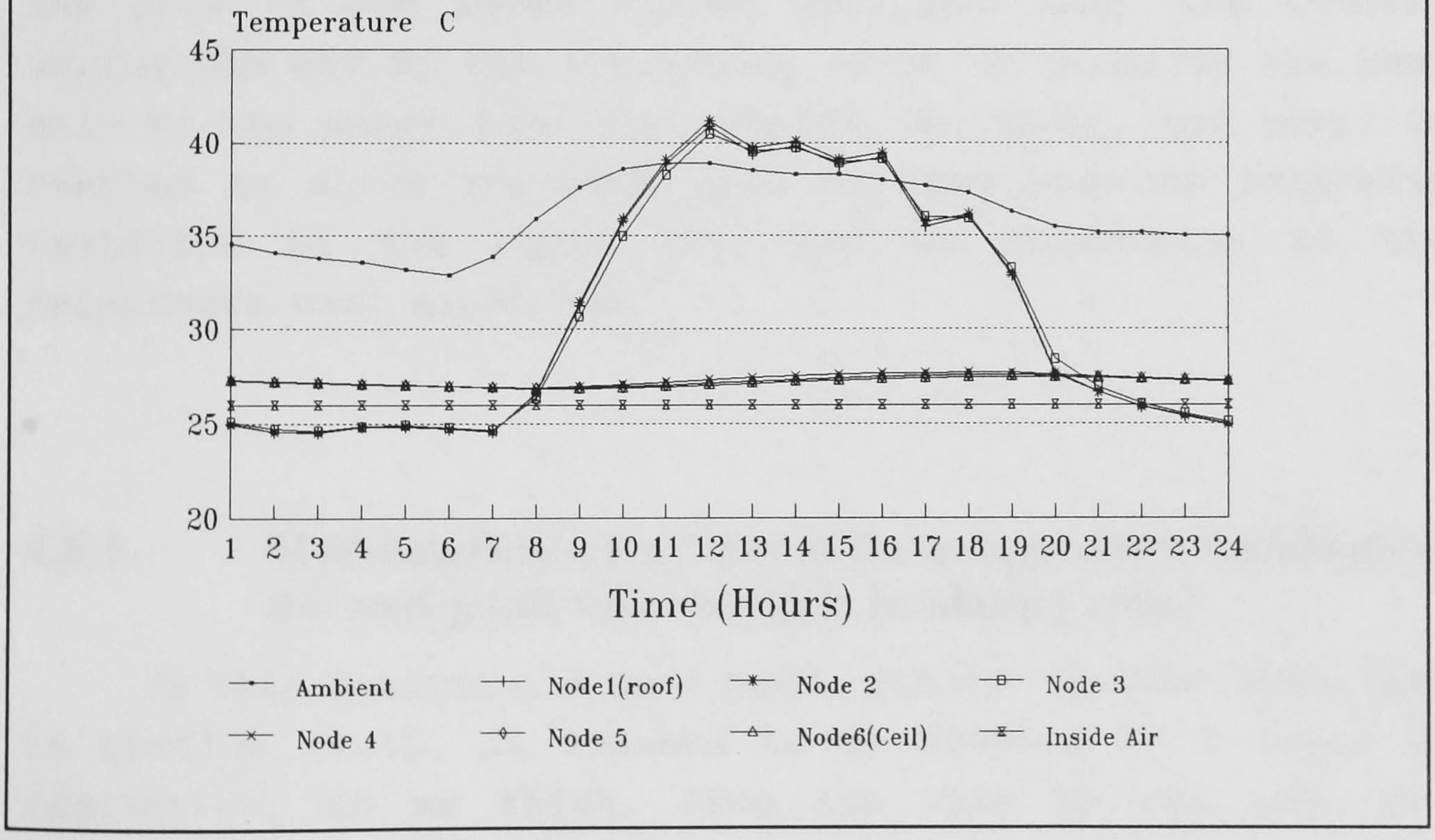

Figure 4.9: The simulated 24-hour nodal temperature variations for the roof pond with insulated roof slab when the internal air temperature is maintained at 26 °C and the weather data for Muscat on 17-6-1988 is used.

water. This disadvantage, of adding a layer of insulation to the roof slab in a roof pond, can be clearly seen by comparing the simulation results, for a roof pond with uninsulated roof slab (Figure 4.10), with that of a roof pond with insulated roof slab (Figure 4.11), when the analysis is carried out using the weather data for Muscat on 21-3-88. The weather on March at Muscat is much cooler than that on June, and is comparable to the Mediterranean summer climate. In this case, the roof pond with uninsulated roof slab absorbs about twice the amount of heat from the inside, as that absorbed by the roof pond with insulated roof slab.

4.6 The Roof Pond With Movable Insulating Cover

The ***Sky Therm*** system, first suggested by Hay, is a roof pond with movable insulating cover. For cooling in summer, the pond or the water filled polythene bags are covered during the day by the insulating cover to minimise the heat gain to the water from the outside. At night, the cover is removed to allow the roof pond to lose heat by long-wave radiation to the night sky, and by convection to the relatively cool night air.

4.6.1 Mathematical simulation of the temperature variations in the roof pond with movable insulating cover

In this analysis, a roof pond, similar to that described in section (4.4), is assumed to be covered by a layer of insulation, 50 mm thick, from sun rise to sun set. The insulation material have the same properties as that used in insulating the roof slab, and a reflectivity of 0.7.

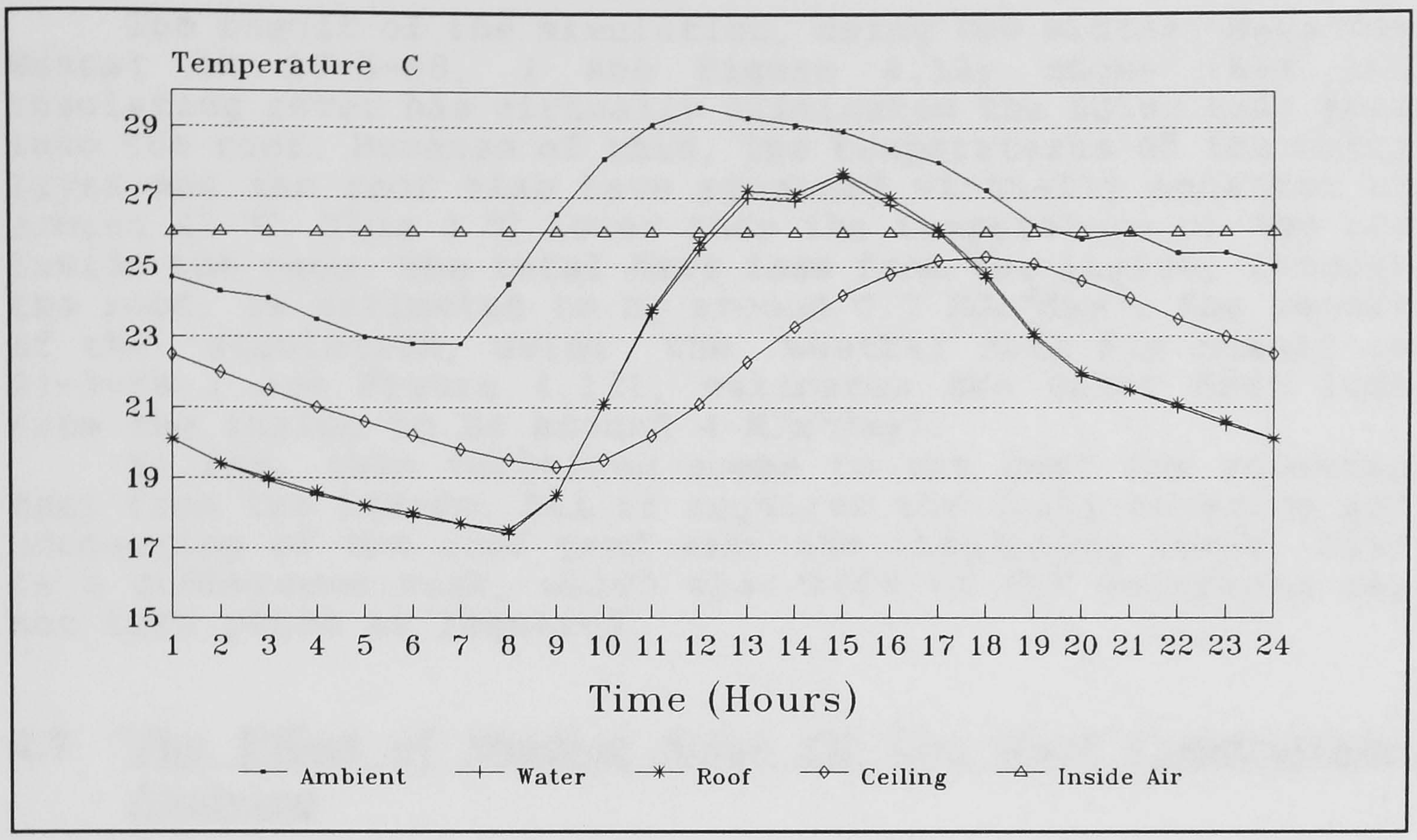

Figure 4.10: The simulated 24-hour nodal temperature variations for the roof pond with uninsulated roof slab when the internal air temperature is maintained at 26 °C and the weather data for Muscat on 21-3-1988 is used.

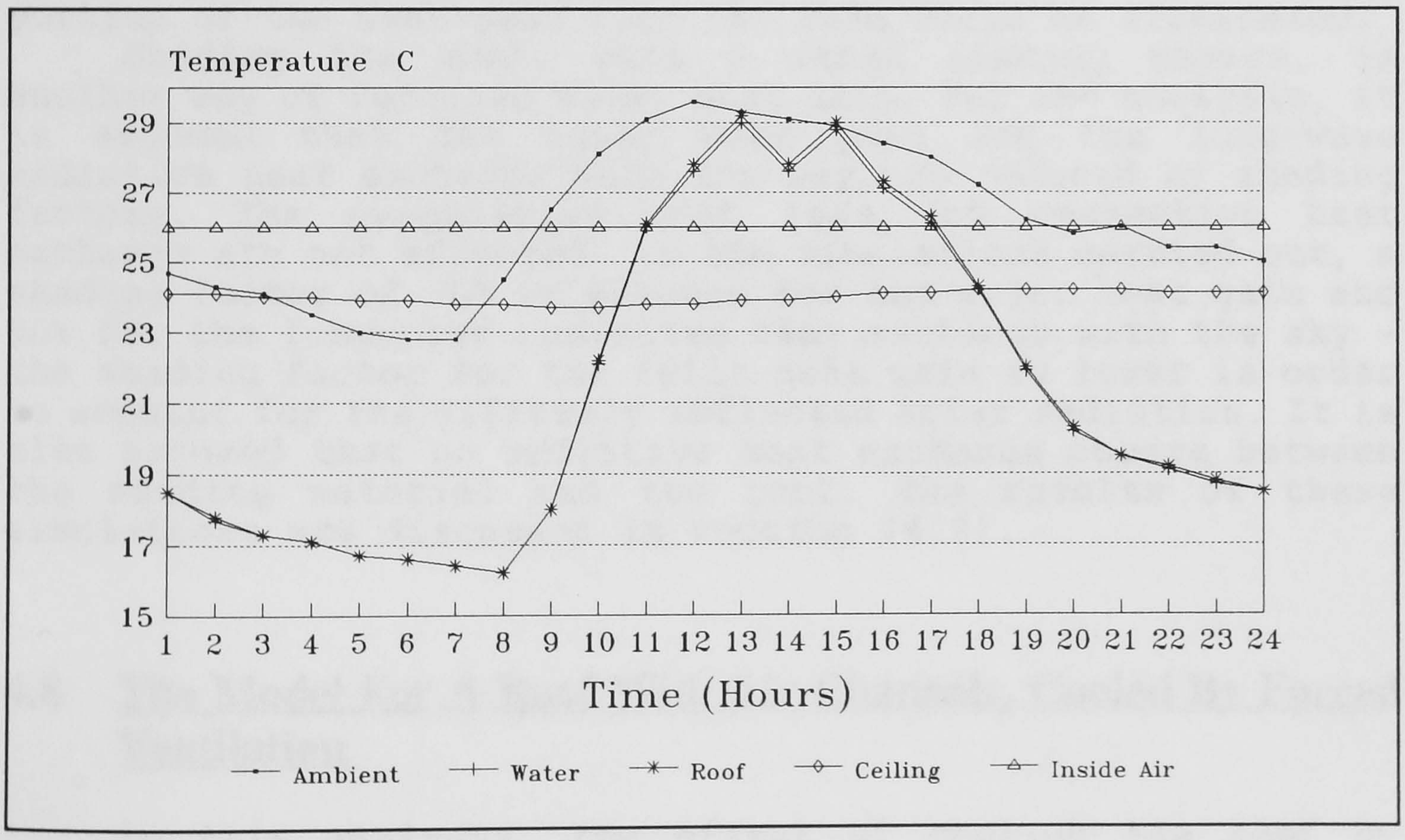

Figure 4.11: The simulated 24-hour nodal temperature variations for the roof pond with insulated roof slab when the internal air temperature is maintained at 26 °C and the weather data for Muscat on 21-3-1988 is used.

The result of the simulation, using the weather data for Muscat on 17-6-88, (see Figure 4.12) shows that the insulating cover has virtually eliminated the solar heat gain into the roof. Because of this, the temperatures of the water layer and the roof slab have remained virtually constant at around 25 °C. This 1 °C lower than the temperature of the air inside the room. The total ***heat loss*** from the inside, through the roof, is estimated to be around 0.7 $MJm^{-2}day^{-1}$. The result of the simulation, using the weather data for Muscat on 21-3-88 (see Figure 4.13), estimates the total heat loss from the inside to be around 4 $MJm^{-2}day^{-1}$.

So far, this technique seems to the best for removing heat from the inside. But it requires the daily covering and uncovering of the roof pond with the insulating cover. This is a cumbersome task, which when left to the occupants may not take place as required

4.7 The Effect of Shading Some Of The Roof Constructions Analyzed

The analysis of the roof pond with the movable insulating cover, has shown that the solar heat gain is the most influential heat transfer process. By minimising its effect,(and ignoring other heat gains into the room, i.e. through the walls and those generated internally) the temperature of the roof slab would stabilise and a large portion of the heat gain into the room would be eliminated.

Shading the roof, with a fixed shading device, is another way of reducing solar heat gain. For the analysis, it is assumed that the solar heat gain and the long-wave radiative heat exchange with the sky are reduced by shading factors. The evaporative heat loss and convective heat exchange are not affected. In the simulations carried out, a shading factor of 70% is assumed for the solar heat gain and 90% for the long-wave radiative heat exchange with the sky - the shading factor for the solar heat gain is lower in order to account for the diffusely reflected solar radiation. It is also assumed that no radiative heat exchange occurs between the shading material and the roof. The results of these simulations are discussed in section (4.9).

4.8 The Model For A Roof With Air Channels, Cooled By Forced Ventilation

in this analysis, the effect of cooling the roof by forcing ambient air through channels in the roof when the temperature of the air is lower than that of the roof slab, is investigated. This construction technique is used, in some Mediterranean countries, in order to reduce the weight of the

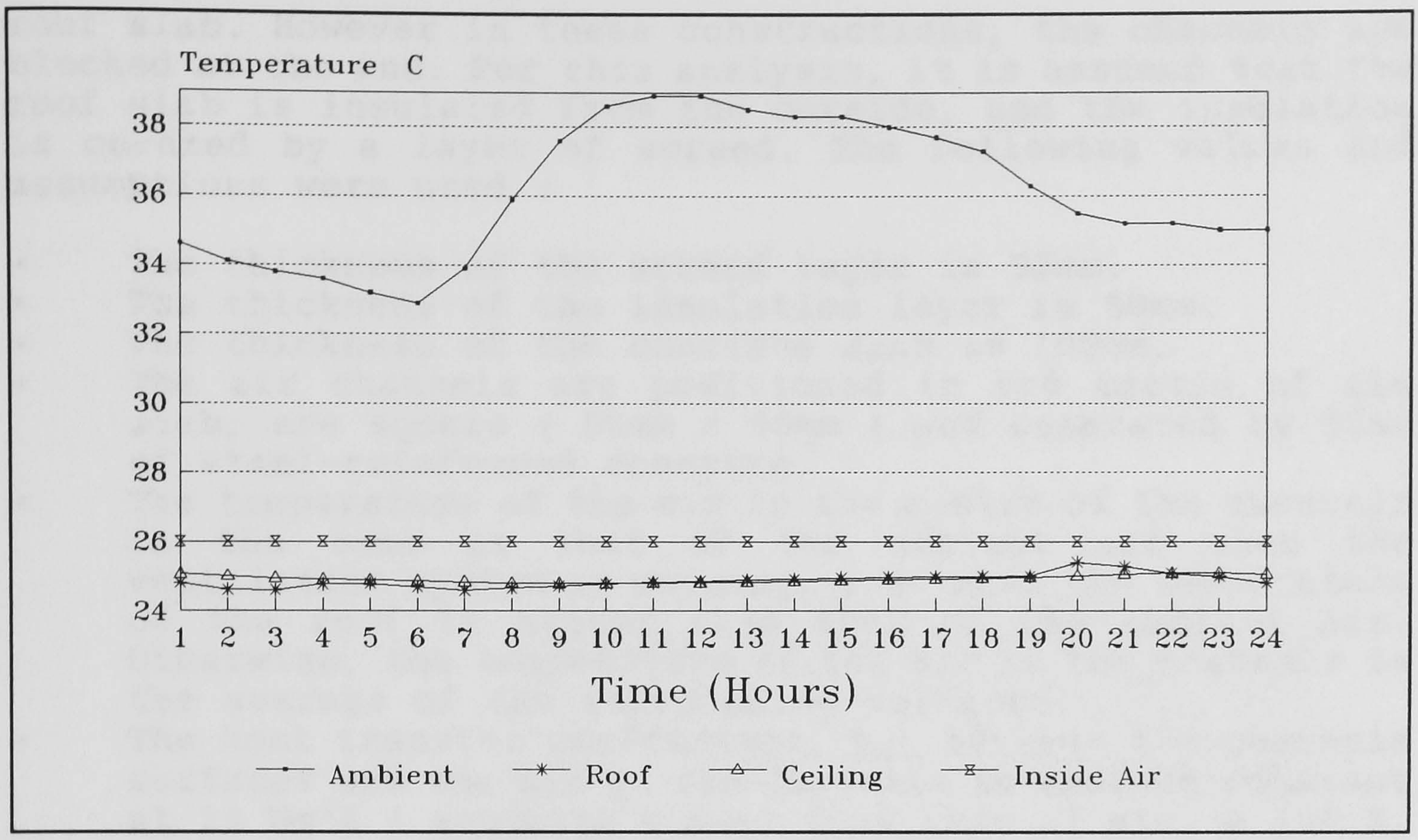

Figure 4.12: The simulated 24-hour nodal temperature variations for the roof pond with movable insulating cover when the internal air temperature is maintained at 26 °C and the weather data for Muscat on 17-6-1988 is used.

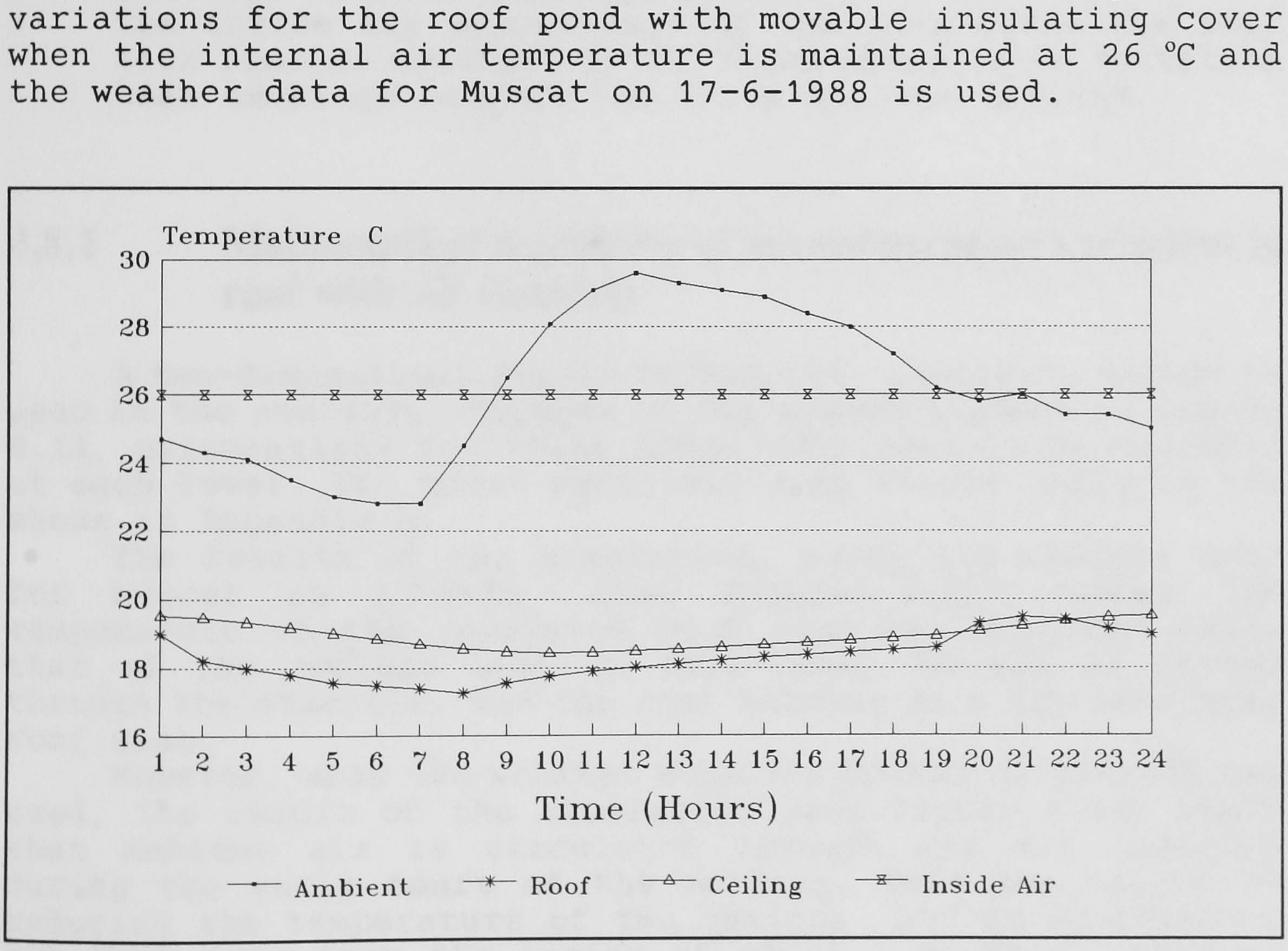

Figure 4.13: The simulated 24-hour nodal temperature variations for the roof pond with movable insulating cover when the internal air temperature is maintained at 26 °C and the weather data for Muscat on 21-3-1988 is used.

roof slab. However in these constructions, the channels are blocked at the end. For this analysis, it is assumed that the roof slab is insulated from the outside, and the insulation is covered by a layer of screed. The following values and assumptions were used :

- The thickness of the screed layer is 50mm.
- The thickness of the insulation layer is 50mm.
- The thickness of the concrete slab is 100mm.
- The air channels are positioned in the centre of the slab; are square (50mm x 50mm) and separated by 50mm of steel-reinforced concrete.
- The temperature of the air in the centre of the channels is the same as that of the ambient air when the ventilation system is working, i.e. when the temperature of the roof is higher than that of the ambient air. Otherwise, the temperature of the air in the channels is the average of the surrounding surfaces.
- The heat transfer coefficient, $\mathbf{h_{ch}}$, between the channels surfaces and the air in the channels is assumed constant at 25 $Wm^{-2}K$ (assuming a mass flow rate of air, @ 300 K, of about 0.0025 kgs^{-1} per channel).
- The edge effects are negligible.
- The inside air temperature of the room below the roof slab remains constant at 26 ºC and there is no radiation heat exchange between the walls and the ceiling.

4.8.1 Mathematical simulation of the temperature variations in roof with air channels

A two-dimensional Finite Difference, implicit, method is used in the analysis. Because of the symmetry shown in Figure 4.14, calculations for three nodes only need to be executed at each level. The nodal equations used in the analysis are shown in Appendix A.

The results of the simulation, using the weather data for Muscat on 17-6-88, (see Figure 4.15), shows the temperature of the insulated roof slab has remained below that of the ambient air. In this case, no air is forced through the channels, and the roof behaves as a dry insulated roof slab.

However, when the weather data for Muscat on 21-3-88 was used, the result of the simulation (see Figure 4.16) shows that ambient air is circulated through the air channels during the early hours of the morning. This has helped in reducing the temperature of the ceiling and in achieving a net **heat loss** from the inside of about 1 $MJm^{-2}day^{-1}$. This is compared with a net **heat gain** of about 1 $MJm^{-2}day^{-1}$ for the dry insulated roof, during the same period of analysis.

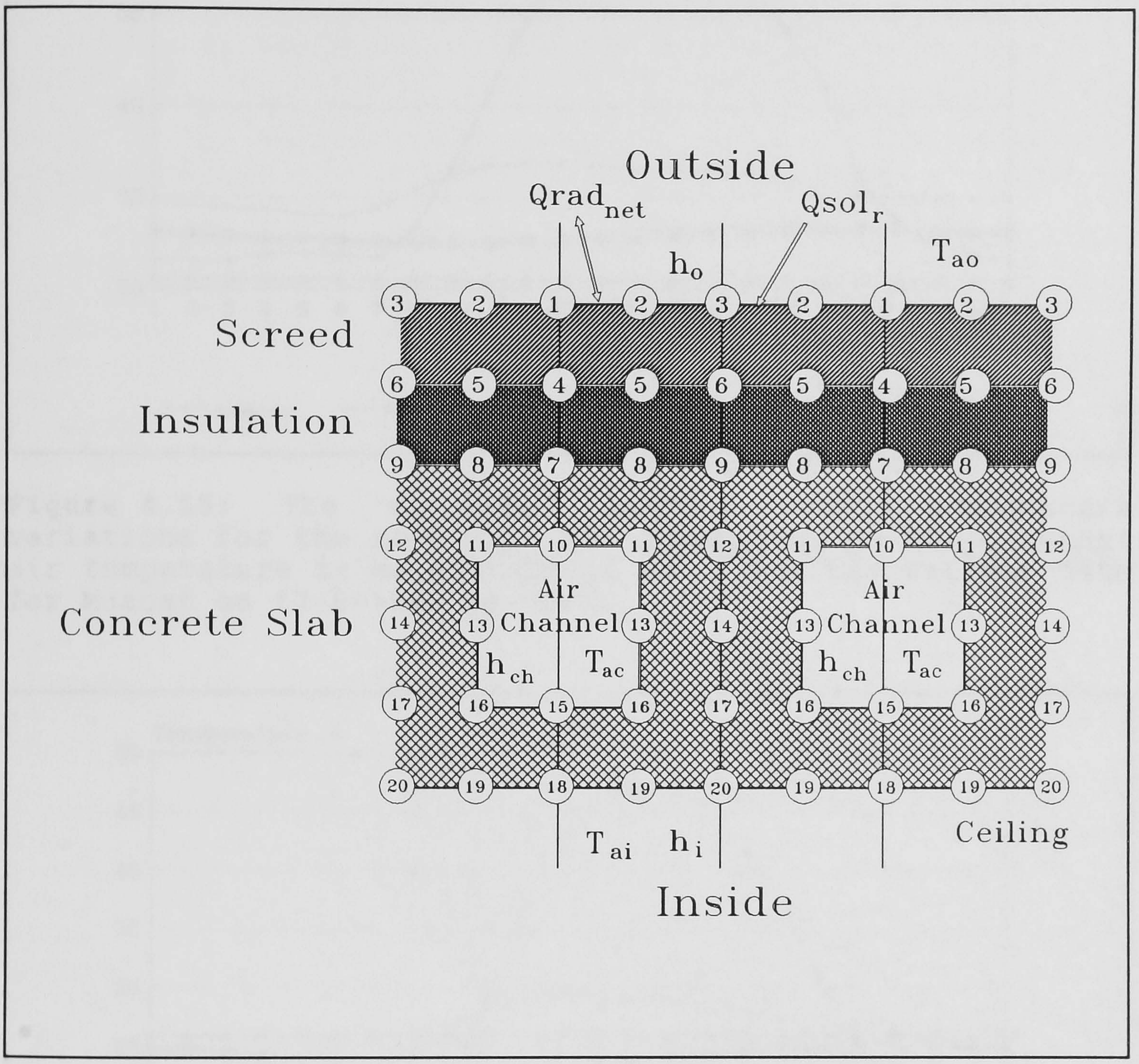

Figure 4.14 : The nodal distribution diagram for a roof with air channels.

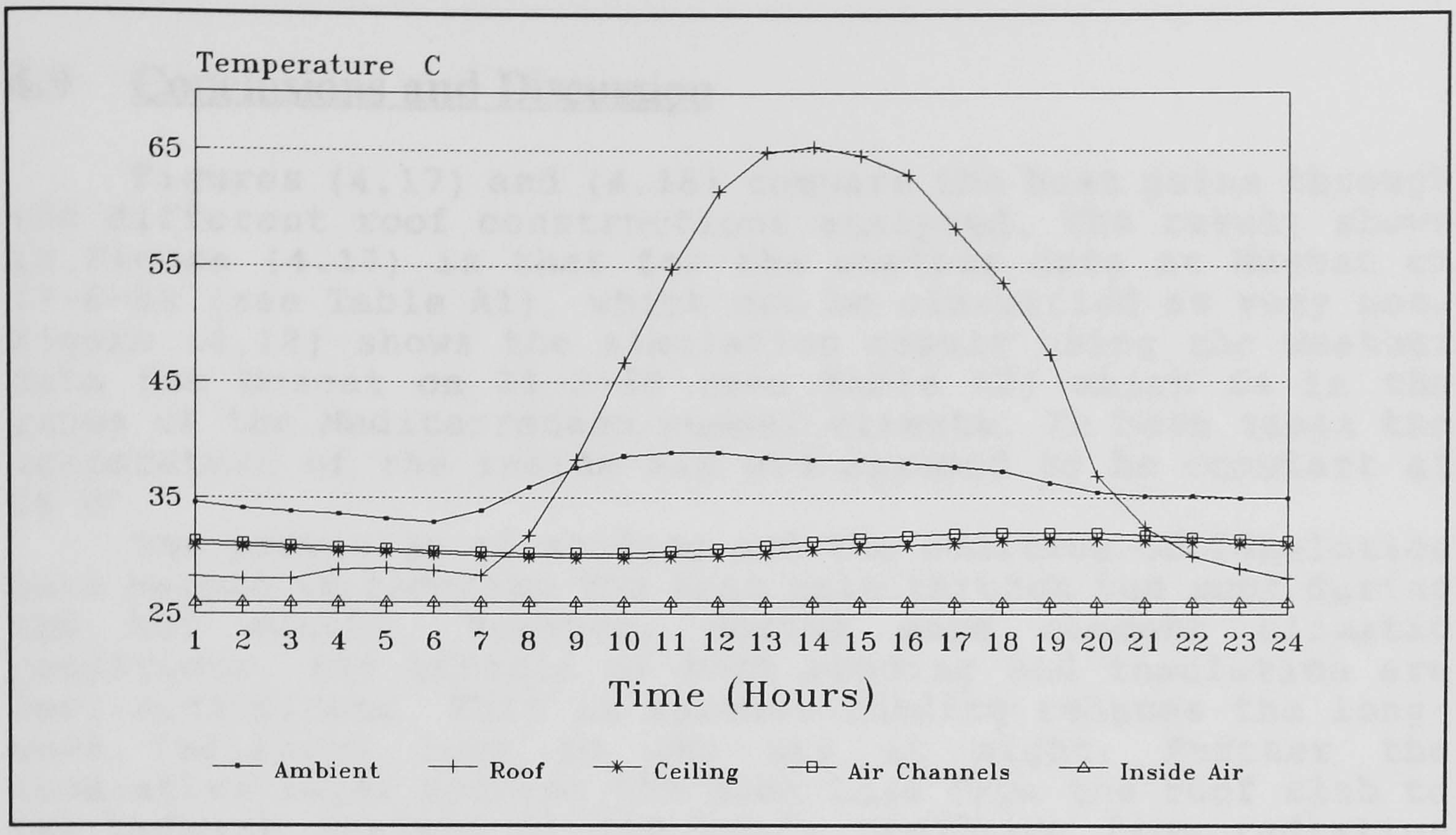

Figure 4.15: The simulated 24-hour nodal temperature variations for the roof with air channels when the internal air temperature is maintained at 26 °C and the weather data for Muscat on 17-6-1988 is used.

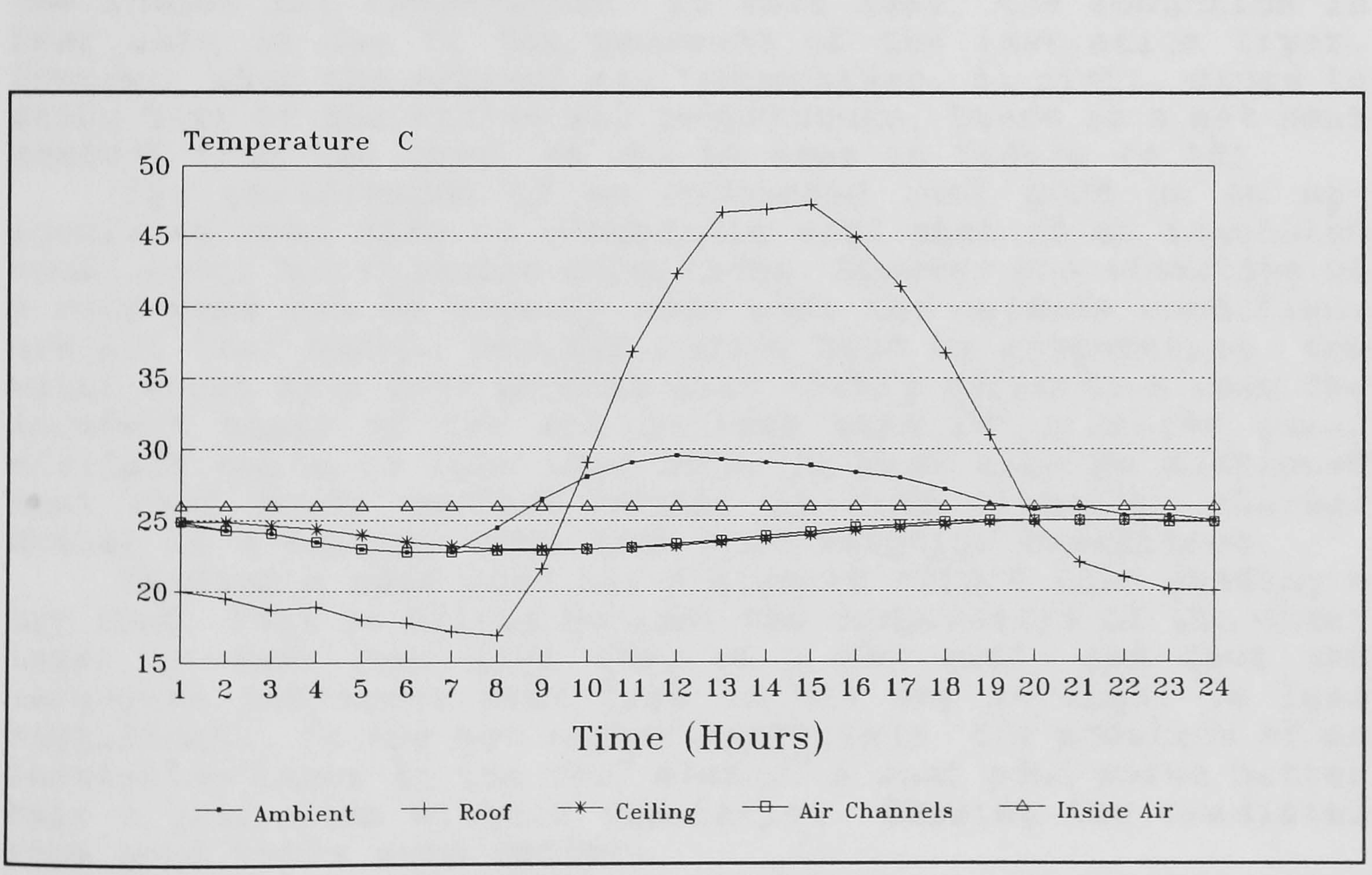

Figure 4.16: The simulated 24-hour nodal temperature variations for the roof with air channels when the internal air temperature is maintained at 26 °C and the weather data for Muscat on 21-3-1988 is used.

4.9 Conclusions and Discussion

Figures (4.17) and (4.18) compare the heat gains through the different roof constructions analyzed. The result shown in Figure (4.17) is that for the weather data at Muscat on 17-6-88 (see Table A1), which can be classified as very hot. Figure (4.18) shows the simulation result using the weather data for Muscat on 21-3-88 (see Table A2) which is in the range of the Mediterranean summer climate. In both cases the temperature of the inside air was assumed to be constant at 26 c°.

The provision of shading and the addition of insulation have helped in reducing the heat gain through the roof during the hot months. However, during more clement climatic conditions, the effects of both shading and insulation are less significant. This is because shading reduces the long-wave radiation loss to the sky at night. Further the insulation layer reduces the heat loss from the roof slab to the outside surface of the roof, resulting from radiation heat loss to the sky at night. These effects can be clearly seen by comparing Figures (4.17) and (4.18).

The roof with air channels does not function as required when the ambient air temperature does not drop below that of the inside air temperature. In this case, the reduction in heat gain is due to the presence of the insulation layer. However, when the ambient air temperature, at night, drops to below that of the inside air temperature, there is a net heat removal from the room, as can be seen in Figure (4.18).

The performance of an uncovered roof pond on an un-insulated roof slab is comparable with that of an insulated roof, under hot climatic conditions. However the advantage of a roof pond can be clearly seen when the outside conditions are not that harsh. Besides losing heat by evaporation, the water layer in a roof pond is also highly reflective when the incident angle of the sun is less than 60° (i.e the solar altitude angle is less than 30°). It must also be mentioned that roof ponds perform better in arid climates, whereas Muscat is a coastal town with high relative humidities.

Shading a roof pond has a greater effect than shading a dry roof. This is mainly because the temperature of the water layer is much less than that of a dry roof, and thus the long-wave radiation heat loss to the sky at night is less significant. In the hot summer conditions, the addition of an insulation layer to the roof slab of a roof pond works better than a roof pond without insulation. Shading the insulated roof pond works even better.

But the best performer, of all the roof constructions analyzed, is a roof pond covered by an insulation layer during the day and uncovered at night. Even under the harsh conditions in June, there has been a net heat loss from the inside with this roof construction. However, the task of insulating the roof pond during the day, and uncovering it at

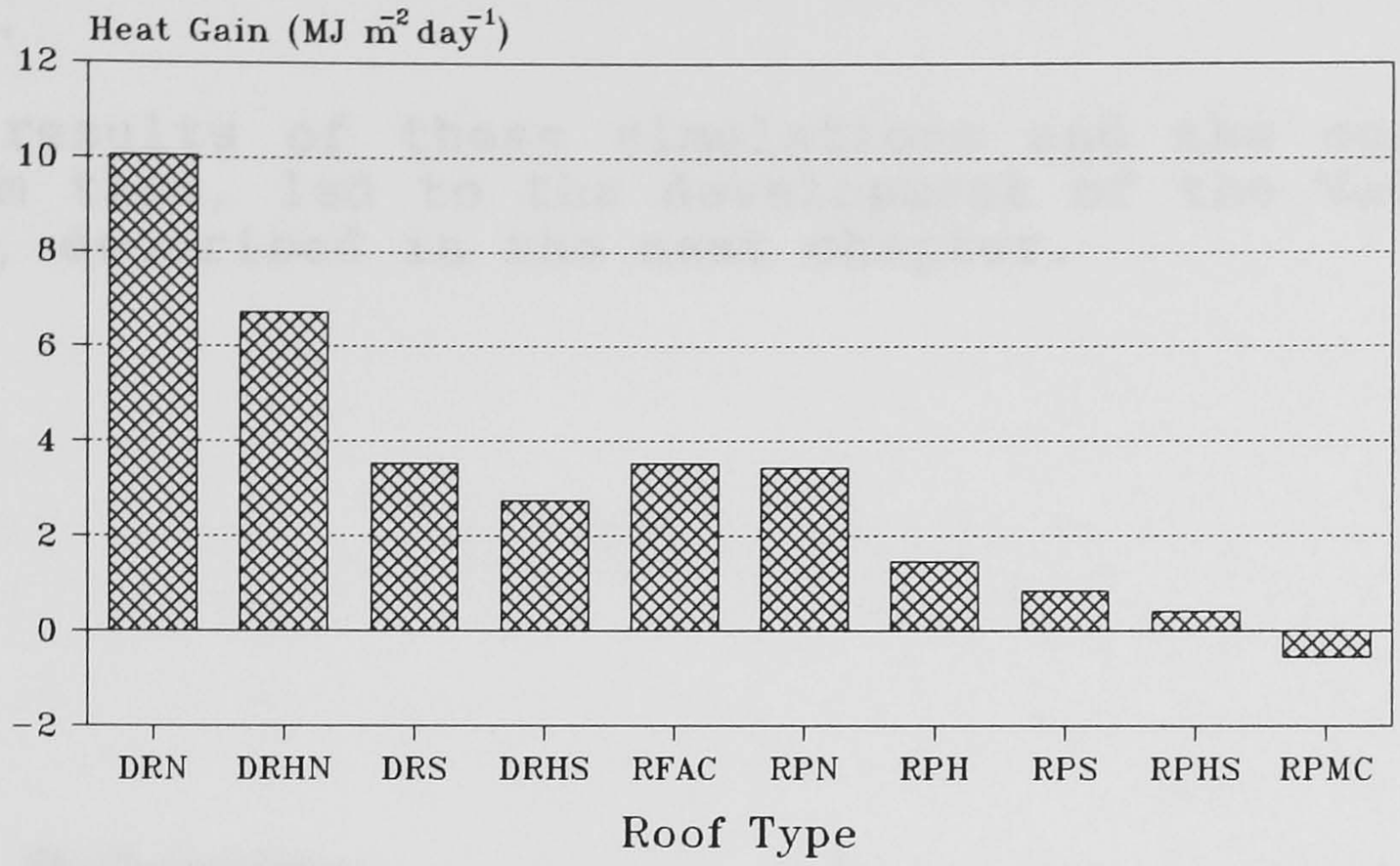

Figure 4.17 : Comparative analysis of heat gains through the different roof constructions - Muscat 17/6/1988.

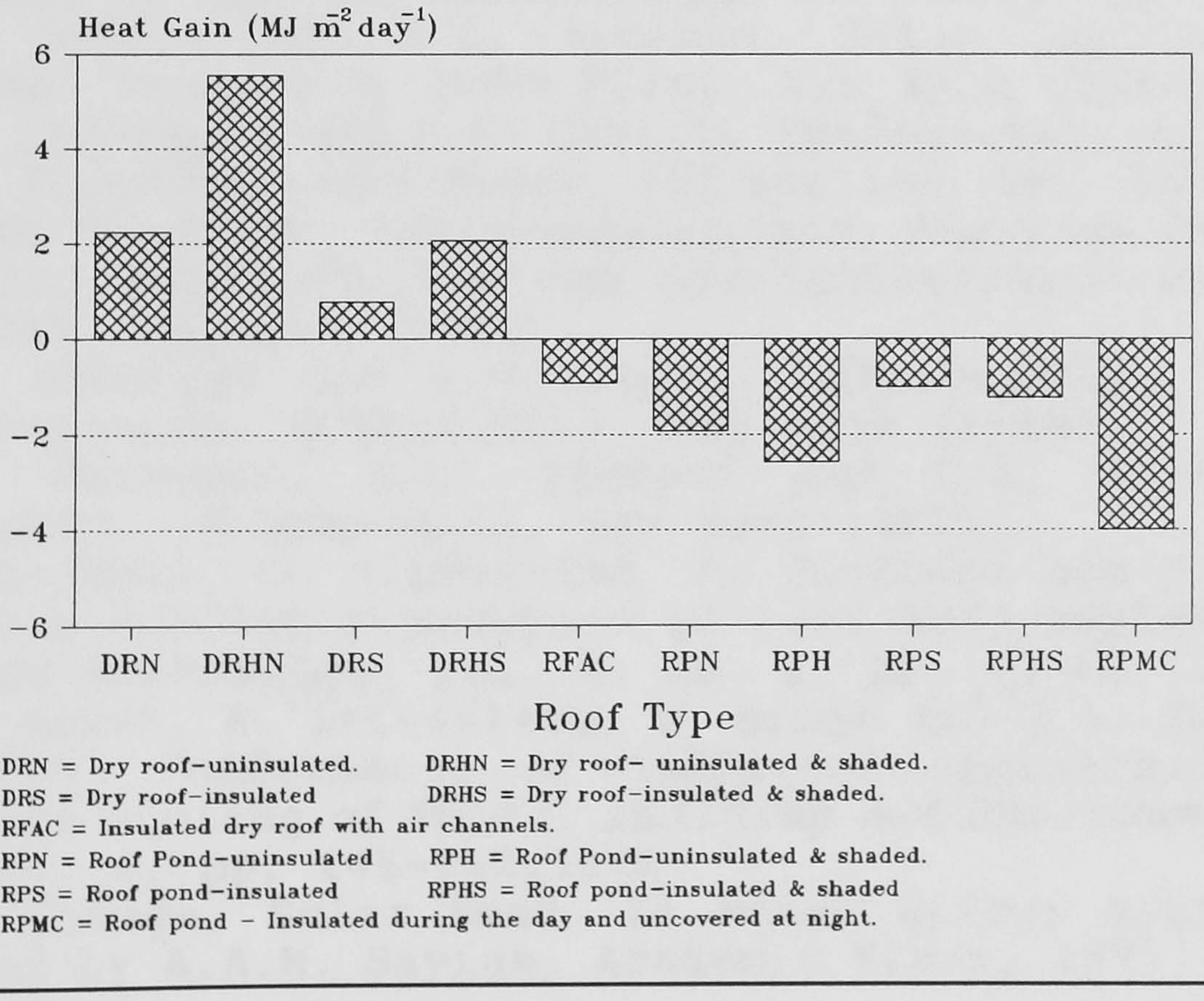

Figure 4.18 : Comparative analysis of heat gains through the different roof constructions - Muscat 21/3/1988.

night is cumbersome and may not take place if left to the occupants.

The results of these simulations and the conclusions drawn from them, led to the development of the **Water Diode Roof Pond**, described in the next chapter.

4.10 References

1. T.Gandrille, G.P. Hammond, and C. Melo, An Intermediate-level Model of External Convection for Building Energy Simulation, ***Energy and Buildings***, **12** (1988), pp. 53-66.
2. J.I. Yellott, Passive and Hybrid Cooling Research, In *Advances in Solar Energy*, Vol. 1, Plenum Press, New York, 1982, pp. 241-263.
3. E. Clark and P. Berdhal, Radiative Cooling : Resources and Applications, In *Proceedings of the Passive-Cooling Workshop*, Amherst, MA, 1980, pp. 177-212.
4. F. Murray, On Computation of Saturation Vapour Pressure, ***Journal of Applied Meteorology***, **16** (1967), pp. 203-204.
5. J.A. Duffie and W.A. Beckman, Solar Engineering of Thermal Processes, John Wiley, New York (1980).
6. F.P. Incropera and D.P. DeWitt, Fundamentals of Heat and Mass Transfer, John Wiley, 2nd edition, New York (1985).
7. ASHRAE Handbook, 1981 Fundamentals, American Society of Heating Refrigeration and Air-conditioning Engineers, Atlanta, Georgia (1981).
8. W.F. Stoecker and J.W. Jones, Refrigeration and Air-conditioning, McGraw-Hill, New York (1982).
9. T.K. Sherwood, R.L. Pigford and C.R. Wilke, Mass Transfer, McGraw-Hill, New York (1975).
10. K. AL-Jamal, O. Alameddine, H. AL-Shami and N. Shaban, Passive Cooling Evaluation of Roof Pond Systems, ***Solar & Wind Technology***, Vol. 5, No. 1, pp. 55-65, 1988.
11. J.K. Nayak, A. Srivastsva, U. Singh and M.S. Sodha, The Relative Performance of Different Approaches to the Passive Cooling of Roofs, ***Building and Environment***, Vol. 17, No. 2, pp. 145-162,1982.
12. S.B. Savage, Solar Pond, In Solar Energy Engineering, Edited by A.A.M. Sayigh, Academic Press, 1977, pp. 217-232.
13. A. Rabl and C.E. Nielsen, Solar Ponds for Space Heating, ***Solar Energy***, Vol. 17, No. 1, 1975, pp. 1-12.

Chapter (5)

The Water Diode Roof Pond

Chapter (5)

The Water Diode Roof Pond

5.1 Introduction

In the previous chapter, the simulation results suggested that a roof pond, covered by an insulating layer during the day and un-covered at night, was the better technique, of those analyzed, for removing heat from a room in the climatic conditions assumed. By covering the roof pond during the day, the effects of the major source of heat gain - solar radiation - are minimised. Also the convective heat exchange with the ambient air is eliminated. However, we are also eliminating simultaneously the evaporative cooling process and the long-wave radiative heat exchange with the sky. Figure (5.1) shows the magnitude of these heat gains and losses for an un-covered, un-insulated roof pond. The net effect of covering the roof pond during the day, and un-covering it at night, is to reduce direct solar gain while the water pond and the roof slab beneath it serve as a heat sink, absorbing heat from the room and discharging it, at night to the ambient air and by radiation to the sky at night. But the daily task of covering the roof pond with a thick insulating layer during the day and un-covering it at night, has prevented the widespread use of this widely documented technique, developed by H. Hay in the mid-1960s.

From the other techniques analyzed, the roof pond with insulated roof slab performed well in reducing heat gain through the roof, but the insulation layer also reduces the heat loss from the roof slab, and thus from the room, when the water pond is at a lower temperature than the slab. On the other hand, the roof pond with un-insulated roof slab allows more heat gain during the day and more heat loss at night. Similarly, shading devices reduce solar heat gain during the day, but also reduce the long-wave radiation heat loss to the sky at night.

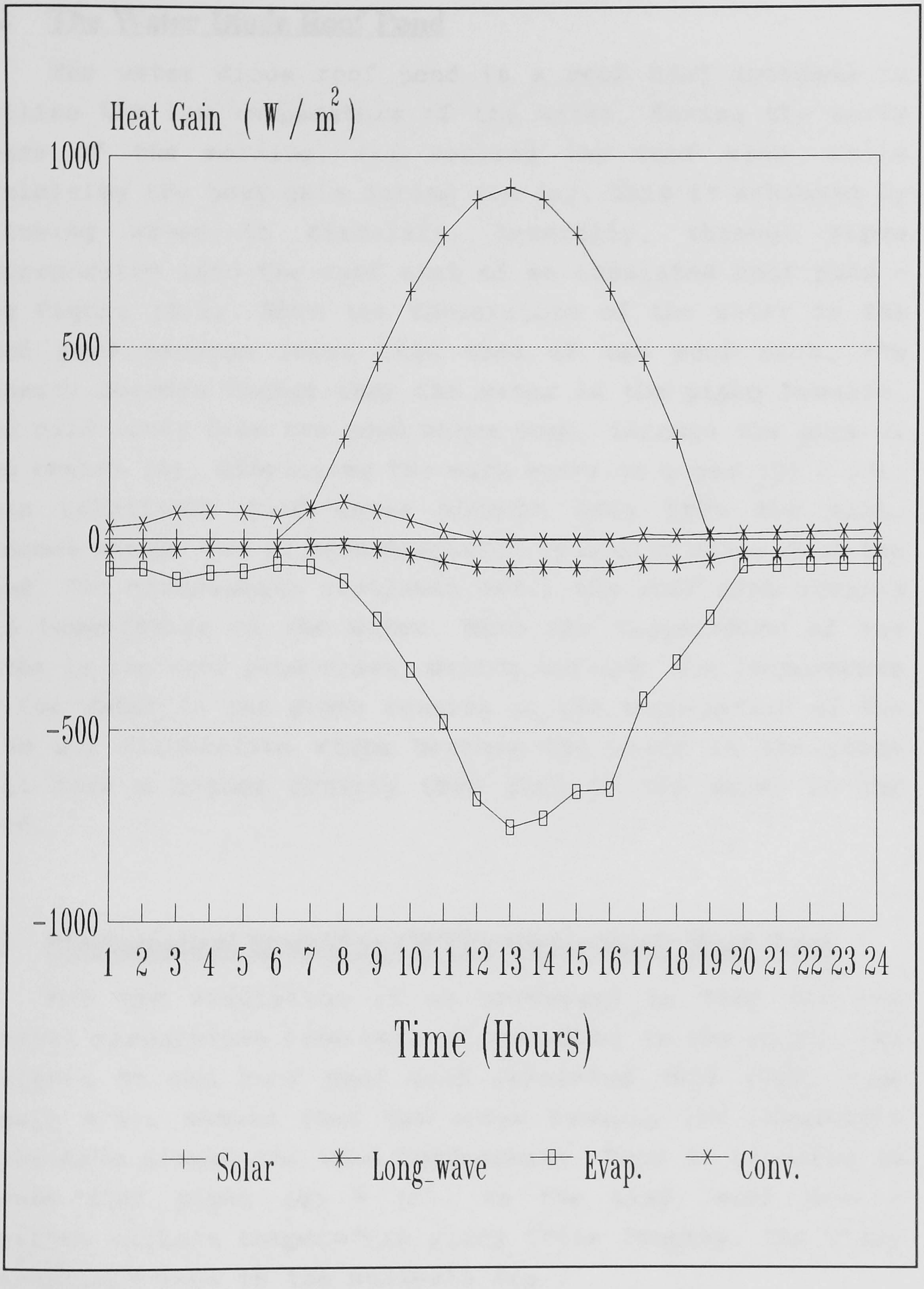

Figure 5.1: Heat gains and loses from an uncovered roof pond with un-insulated roof slab.

5.2 The Water Diode Roof Pond

The water diode roof pond is a roof pond designed to utilise the low temperature of the water, during the early hours of the morning, for cooling the roof slab, while minimising the heat gain during the day. This is achieved by allowing water to circulate, naturally, through pipes incorporated into the roof slab of an insulated roof pond - see Figure (5.2). When the temperature of the water in the roof pond becomes lower than that of the roof slab, its density becomes higher than the water in the pipes beneath. The cold water from the pond moves down, through the pipe in the centre (A), displacing the warm water in pipes (B) & (C). This relatively cold water absorbs heat from the slab, becomes warmer and is then displaced by cooler water from the pond. The circulation continues until the roof slab attains the temperature of the water. When the temperature of the water in the roof pond rises, during the day, the temperature of the water in the pipes remains at the temperature of the slab and circulation stops because the water in the pipes will have a higher density than that of the water in the pond.

5.3 Mathematical Modelling Of The Water Diode Roof Pond

For the simulation it is necessary to find out the natural circulation flow rate of the water in the pipes. The analysis of the roof pond with insulated roof slab, (see Figure 4.9), showed that the nodes beneath the insulation layer have almost the same temperature. Thus it is valid to assume that pipes (B) & (C), in the slab, will have a constant surface temperature along their lengths. The other assumptions used in the analysis are :

- The temperature of the water in the central pipe, (A), is the same as that of the water pond if the temperature of the water pond is lower than that of the slab.

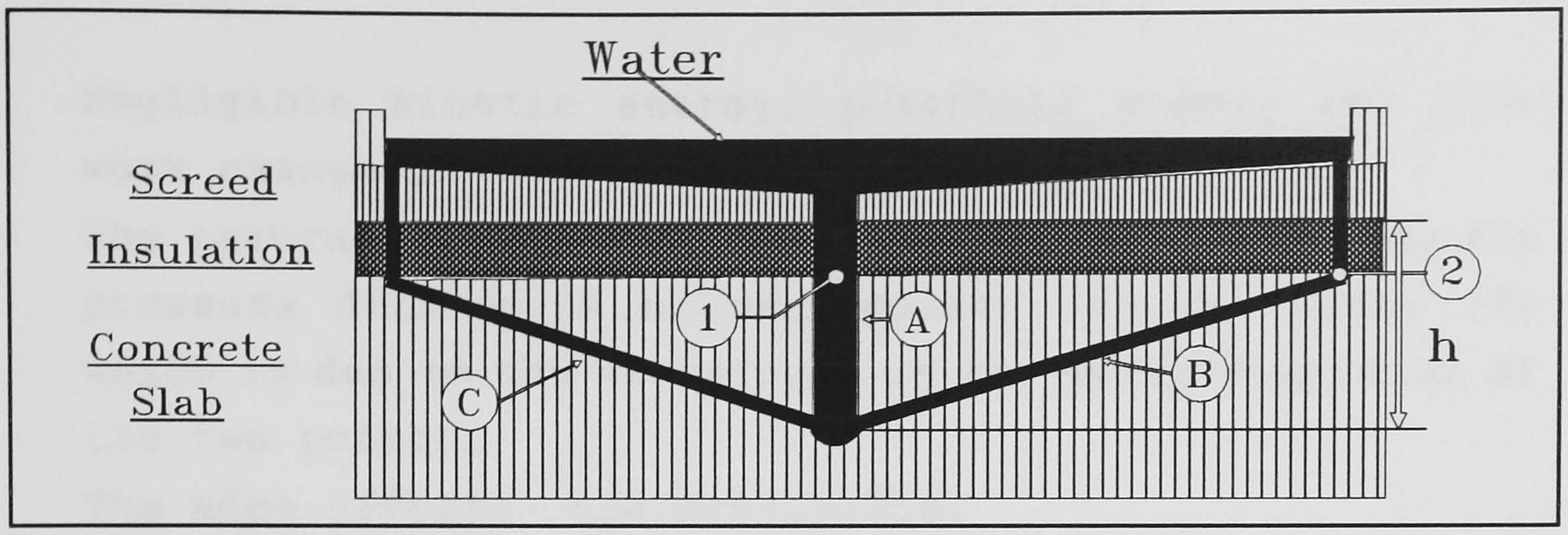

Figure 5.2 : A cross-section of a water diode roof pond.

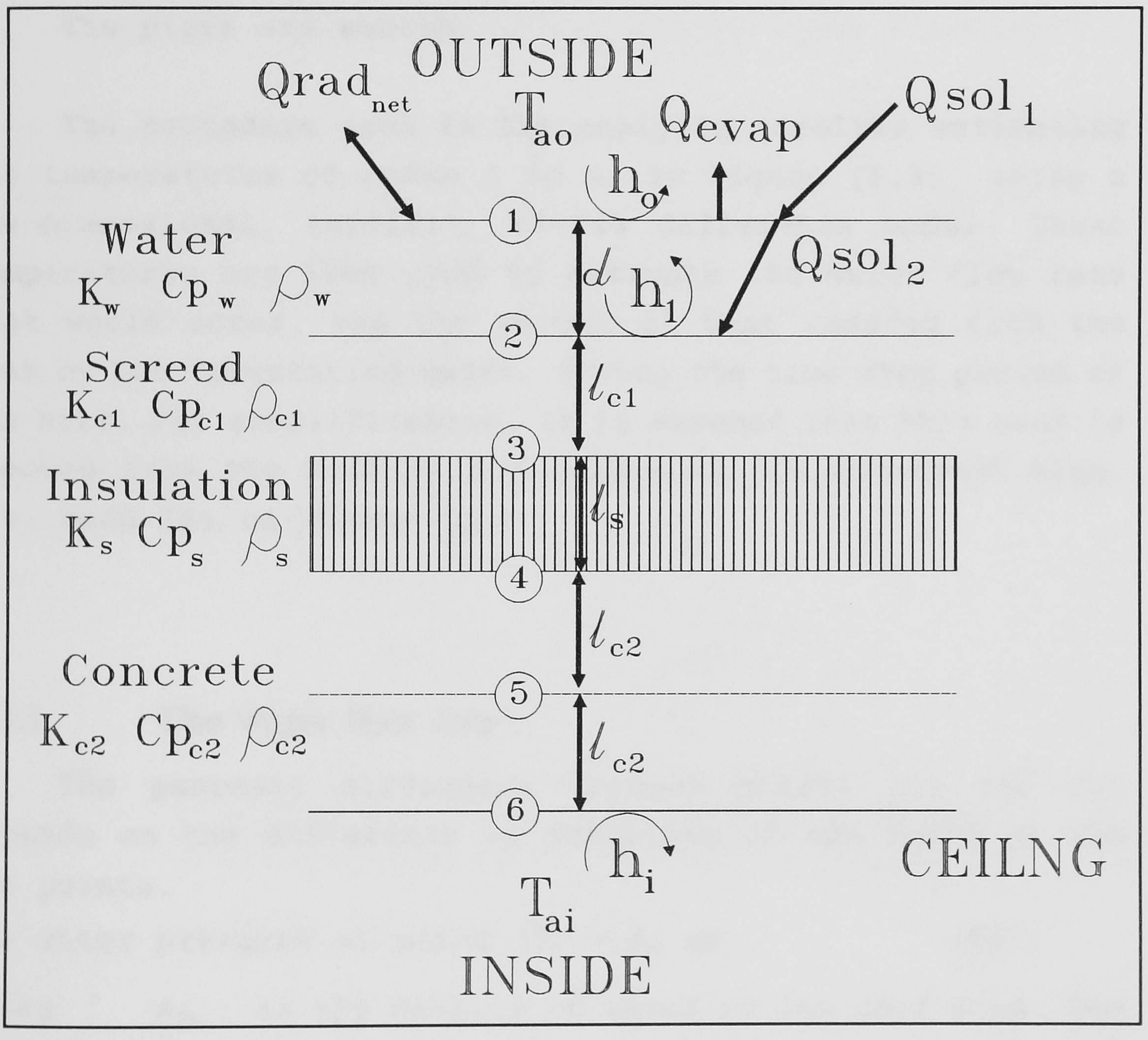

Figure 5.3:A cross-section of a roof pond with an insulated roof slab.

- Negligible kinetic energy, potential energy and flow work changes.
- The natural water circulation in the pipe is due to the pressure difference between points (1) and point (2) which is due to the difference in the water densities at the two points.
- The edge effects are negligible.
- The thermal resistance of the pipes walls is negligible (copper pipes are used).
- The pipes are smooth.

The procedure used in the analysis involves estimating the temperatures of nodes 1 to 6, in Figure (5.3), using a one-dimensional, implicit, finite difference model. These temperatures are then used to estimate the water flow rate that would occur, and the amount of heat removed from the slab by the circulating water, during the time step period of one hour. For simplification, it is assumed that this heat is removed from the node in the centre of the insulated slab, i.e. Node (5) in Figure (5.3).

5.3.1 The water flow rate :

The pressure difference between points (1) and (2) depends on the difference in densities of the water at the two points.

The water pressure at point (1) $= \rho_{T1}\ gh$ (Nm^{-2})

Where ρ_{T1} is the density of water in the roof pond. The following correlation is used to find the water density at a given temperature, T, for the temperature range, 5 C° to 50 C° :

$$\rho_T = 1000.1 - 0.0135\ T - 0.0045\ T^2$$

g is the acceleration due to gravity. (ms^{-2})

h is the depth of the water column, taken as the distance between the top surface of the insulation, Node (3), and the centre of the insulated roof slab, Node (5). The assumption used here is that the temperature of the water in the insulated section of the pipe, above point (2), will have the same temperature as that at point (2), since the heat loss from the water to the insulation layer is negligible. This is a valid assumption when there is water circulation.

The water pressure at point (2) = ρ_{T4} gh (Nm^{-2})

Where ρ_{T4} is the density of the water at point (2), corresponding to Node(4) in Figure (5.3).

The pressure difference across pipe (B) or (C) is thus;

$$P_d = (\rho_{T1} - \rho_{T4})\ gh \qquad (Nm^{-2})$$

The mass flow rate of the water, circulating naturally in a single pipe is given by [1]:

$$\dot{m} = A \times V = A \times \sqrt{\frac{2 \times P_d}{\rho_0}}$$

Where **A** is the cross-sectional area of the pipe.

V is the velocity of the water in the pipe.

and ρ_0 is the density of water at 4 C^0.

As mentioned before, when the temperature of the water pond becomes higher than that of the water in the pipes, the circulation stops.

5.3.2 The heat removal rate from the slab by the circulating water

The heat absorbed from the slab by the circulating water in a single pipe is given by;

$$\dot{q} = \dot{m} \cdot C_p (T_{w_o} - T_{w_i})$$

C_p i s the specific heat capacity of water, assumed constant.

T_{wo} is the temperature of the water at point (2).

T_{wi} is the temperature of the water at point (1).

The temperature of the water at point (1) is assumed to be the same as that in the water pond. The temperature of the water at point (2) is worked out as follows :

We have already assumed that the surface temperature along the pipe is constant, and is the same as that of the insulated slab. For a fully developed laminar flow in a pipe with constant surface temperature the Nusselt number Nu_D is 3.66 [2]. Thus the average heat transfer coefficient in the pipe is

$$\bar{h} = \frac{Nu_D \times k_w}{D_h} = \frac{3.66 \times k_w}{D_h}$$

k_w is the thermal conductivity of the water in the pipe, assumed constant.

D_h is the diameter of the pipe.

The temperature difference between the insulated slab and the water at point (2) is given by [1]:

$$(T_s - T_{w_o}) = (T_s - T_{w_i})\ e^{\left(\frac{-\pi\ D_h\ L\ \bar{h}}{\dot{m}\ C_p}\right)}$$

T_s is the temperature of the insulated slab. This is taken as the average of nodes (4), (5) & (6).

L is the length of the pipe (B) or (C).

The heat removed by the water circulating in both pipes (B) & (C) is twice the amount calculated above.

The heat removal rate from the slab is also influenced by the following factors:

- The diameter of pipes (B) & (C) - D (m).
- The distance between the pipes in the slab.

In the analysis of the previous roof construction, it has been assumed that the width of the node is unity, i.e. 1 m . If this assumption is used here, it would mean that the spacing between two sets of pipes (PS) is 1 m . Varying the width of the node is used in this analysis to simulate the effect of changing the distance between two sets of pipes. The speed of response to temperature changes in the water pipes and the surrounding nodes, will be increased by reducing the width of the node, and thus its volume. This means that for a particular pipe diameter, there is an optimum distance between two sets of pipes. Similarly, using pipes with larger diameters will increase the water flow rates in the pipes and thus the rate of heat removal from the slab.

5.4 Simulation Result

Simulations were carried out in order to compare the thermal performance of the Water Diode roof pond with the other roof constructions previously investigated. Also the effects of pipes diameter and spacing are investigated. Figure (5.4) shows the flow chart for the program used in the analysis.

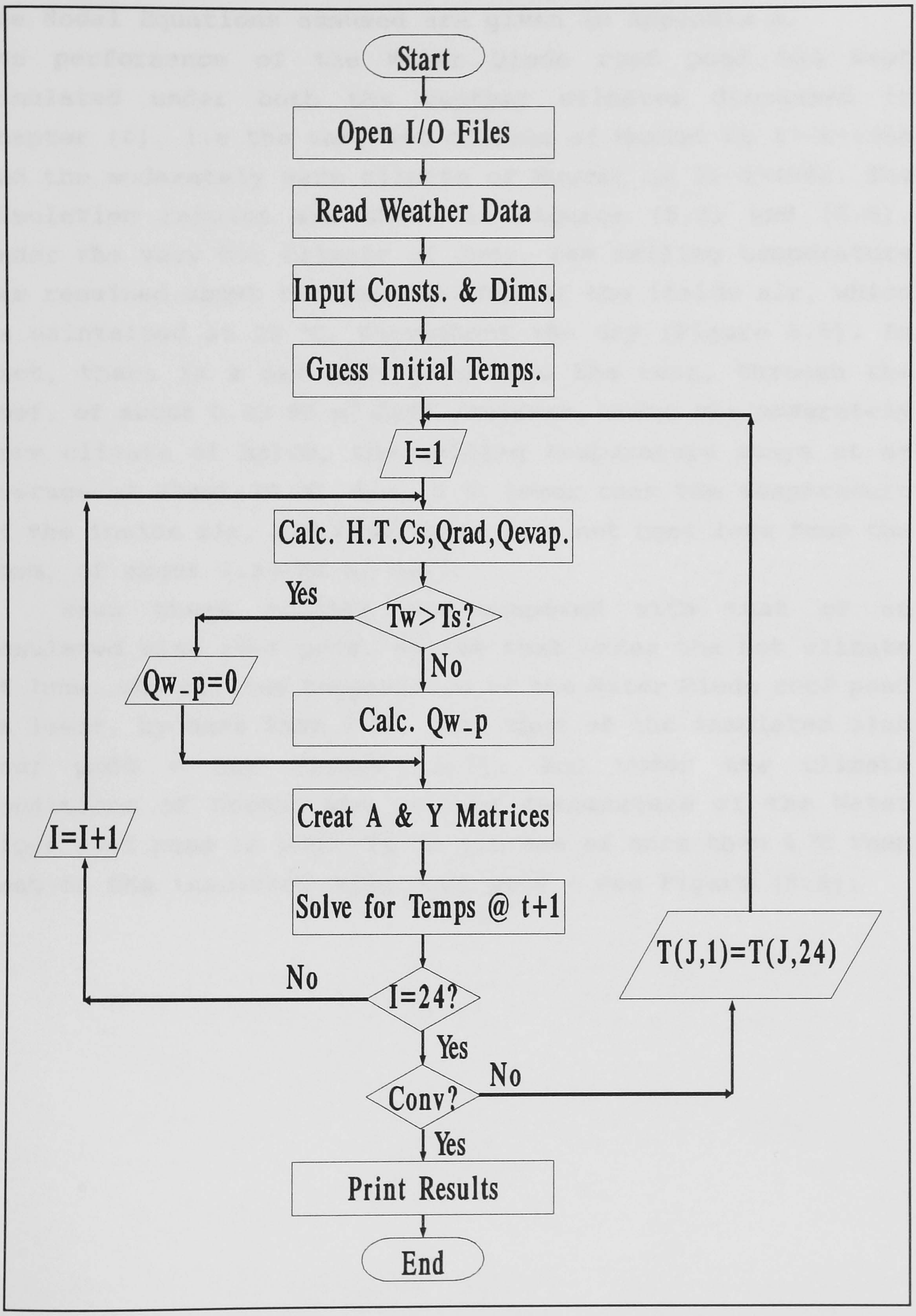

Figure 5.4: The flow chart of the computer program used in the analysis of the Water Diode roof pond.

The Nodal Equations assumed are given in Appendix A.

The performance of the Water Diode roof pond has been simulated under both the weather climates discussed in Chapter (4), i.e the very hot climate of Muscat on 17-6-1988 and the moderately warm climate of Muscat on 21-3-1988. The simulation results are shown in Figures (5.5) and (5.6). Under the very hot climate of June, the ceiling temperature has remained about the same as that of the inside air, which is maintained at 26 °C, throughout the day (Figure 5.5). In fact, there is a net heat gain into the room, through the roof, of about 0.23 MJ m^{-2} day^{-1}. However, under the moderately warm climate of March, the ceiling temperature stays at an average of about 20 °C, i.e. 6 °C lower than the temperature of the inside air, and thus there is a net heat *loss* from the room, of about 3.25 MJ m^{-2} day^{-1}.

When these results are compared with that of an insulated slab roof pond, we see that under the hot climate of June, the ceiling temperature of the Water Diode roof pond is lower, by more than 1 °C, than that of the insulated slab roof pond - see Figure (5.7). And under the climate conditions of March, the ceiling temperature of the Water Diode roof pond is lower by an average of more than 4 °C than that of the insulated slab roof pond - see Figure (5.8).

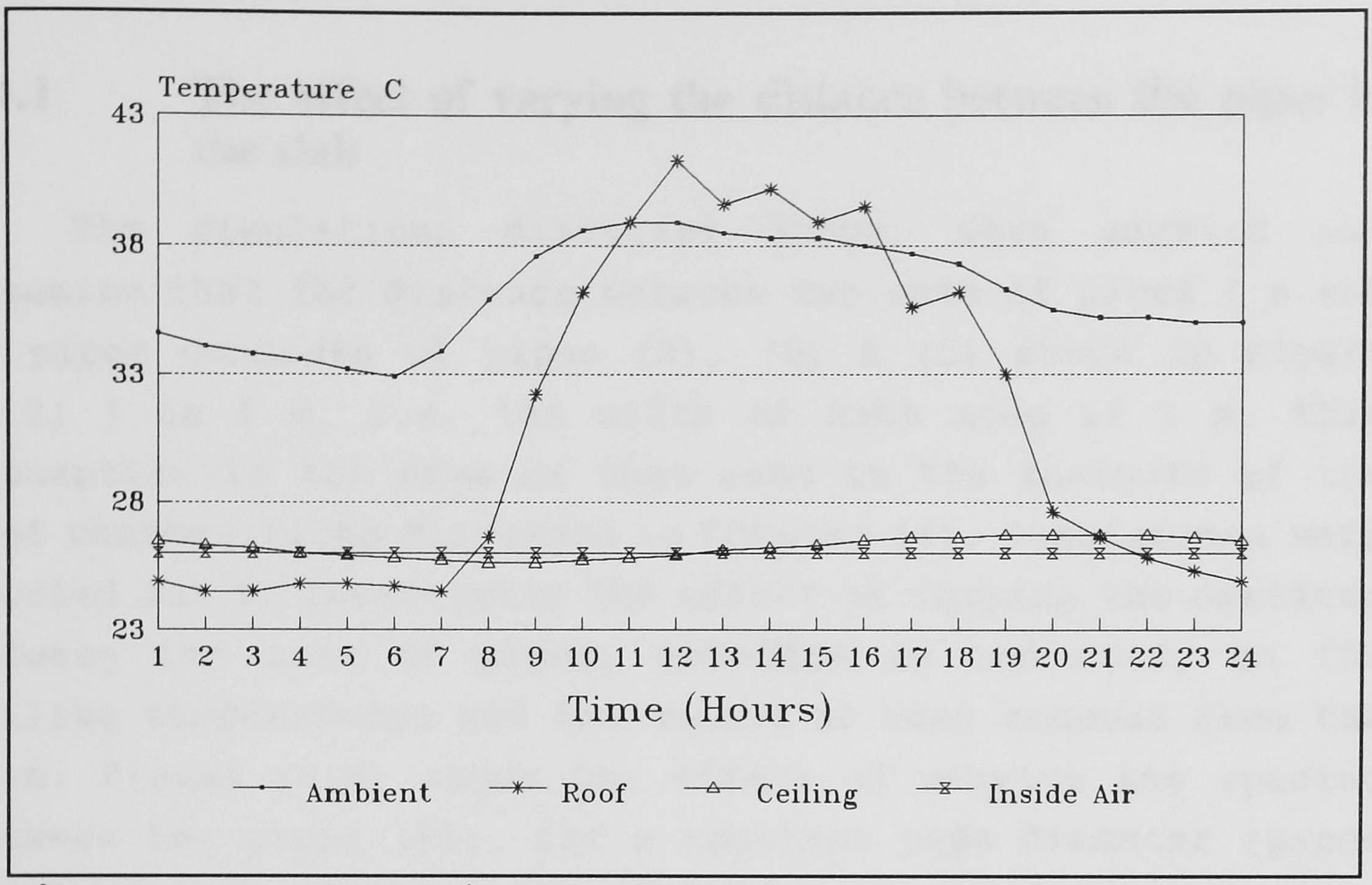

Figure 5.5: The simulated 24-hours nodal temperature variation in a Water Diode Roof Pond when the internal air temperature is maintained at 26 °C and the weather data for Muscat on 17-6-1988 is used. (PS= 1m ,D= .025m)

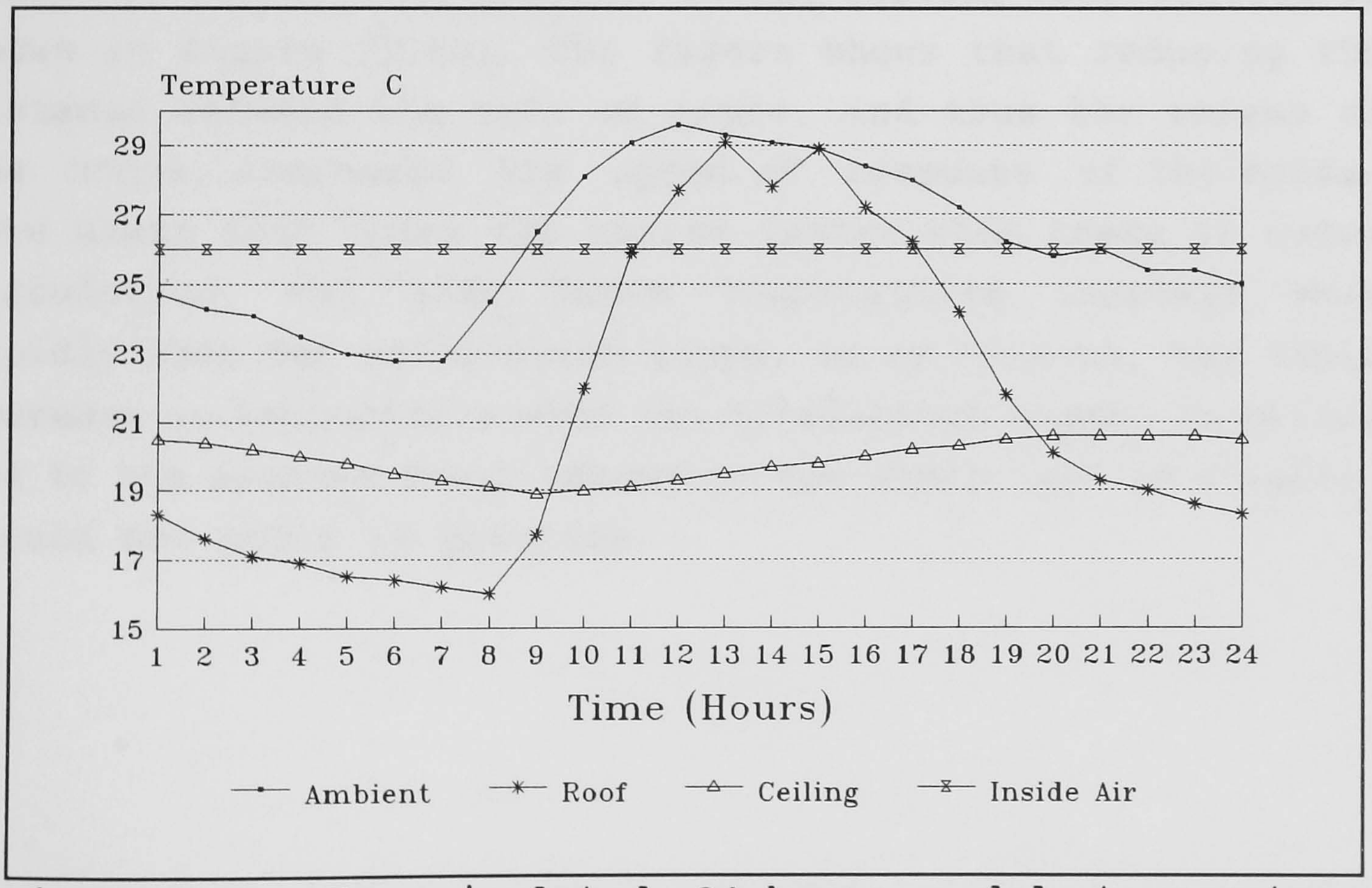

Figure 5.6: The simulated 24-hours nodal temperature variation in a Water Diode Roof Pond when the internal air temperature is maintained at 26 °C and the weather data for Muscat on 21-3-1988 is used. (PS= 1m ,D= .025m)

5.4.1 The effect of varying the distance between the pipes in the slab

The simulations discussed above, were carried out assuming that the distance between two sets of pipes (a set of pipes consists of pipes (A), (B) & (C) shown in Figure (5.2)) is 1 m, i.e. the width of each node is 1 m. This assumption is the same as that used in the analysis of the roof constructions discussed in Chapter (4). Simulations were carried out to investigate the effect of varying the distance between the sets of pipes, embedded in the roof, on the ceiling temperatures and the amount of heat removed from the room. Figure (5.9) shows the effect of varying the spacing between the pipes (PS), for a constant pipe diameter (pipes (B) & (C)), of 0.025 m, on the net heat gain into the room, using the weather data for Muscat on 17-6-1988. The figure shows that there is an optimum spacing of about 0.67 m. The effect of varying the spacing, on the ceiling temperatures is shown in Figure (5.10). The figure shows that reducing the distance between the sets of pipes, and thus the volume of the nodes, increases the speed of response of the nodes. This means that nodes are cooled faster when there is water circulation, but also there temperatures increase more rapidly when the circulation stops. In my opinion, the rapid ***increase*** in temperature when the circulation stops, is mainly due to the assumed lower volume of the nodes, and in a sense, should not occur in practice.

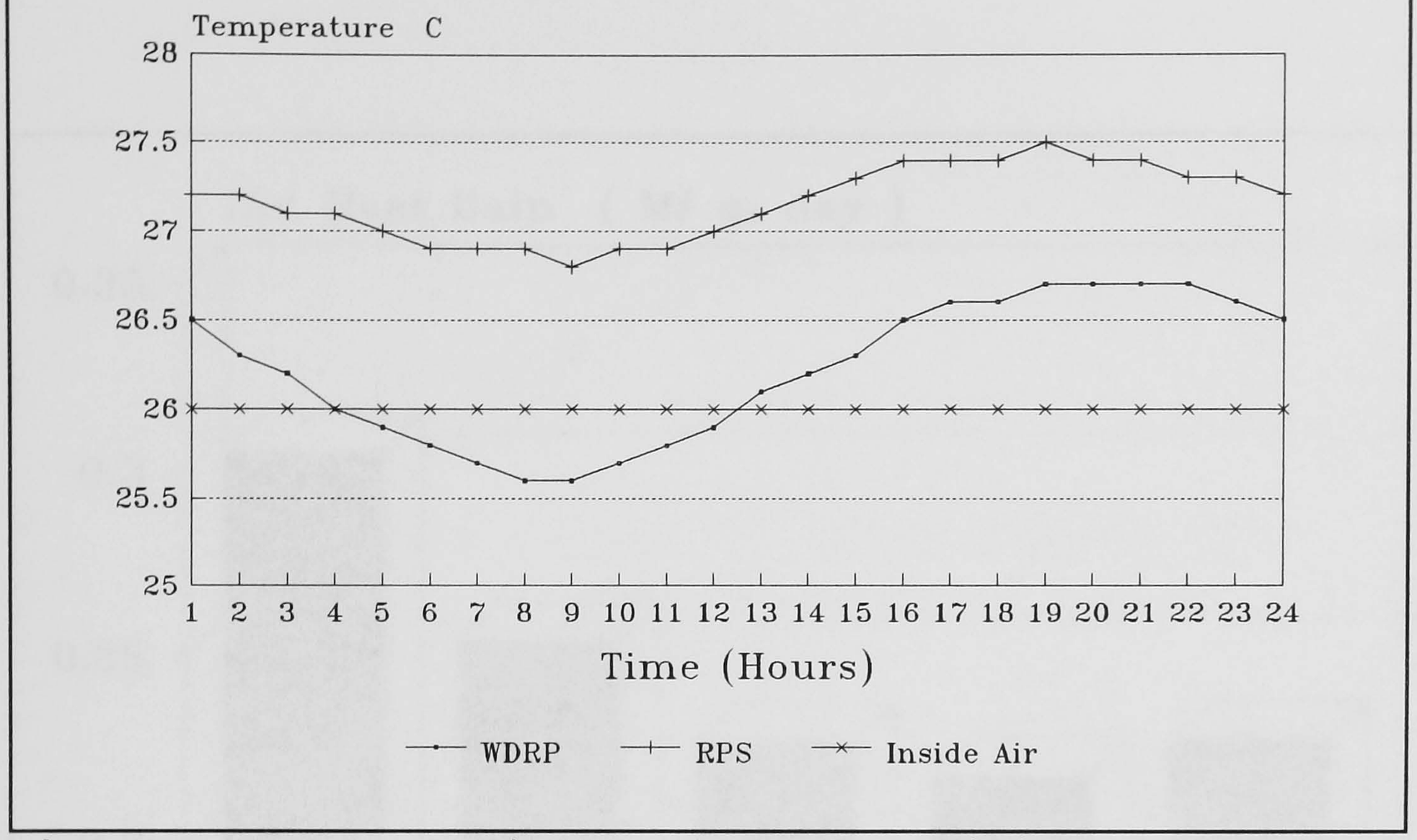

Figure 5.7: A comparison between the ceiling temperatures of a Water Diode Roof Pond, with that of a roof pond with an insulated roof slab when the weather data for Muscat on 17-6-88 is used.

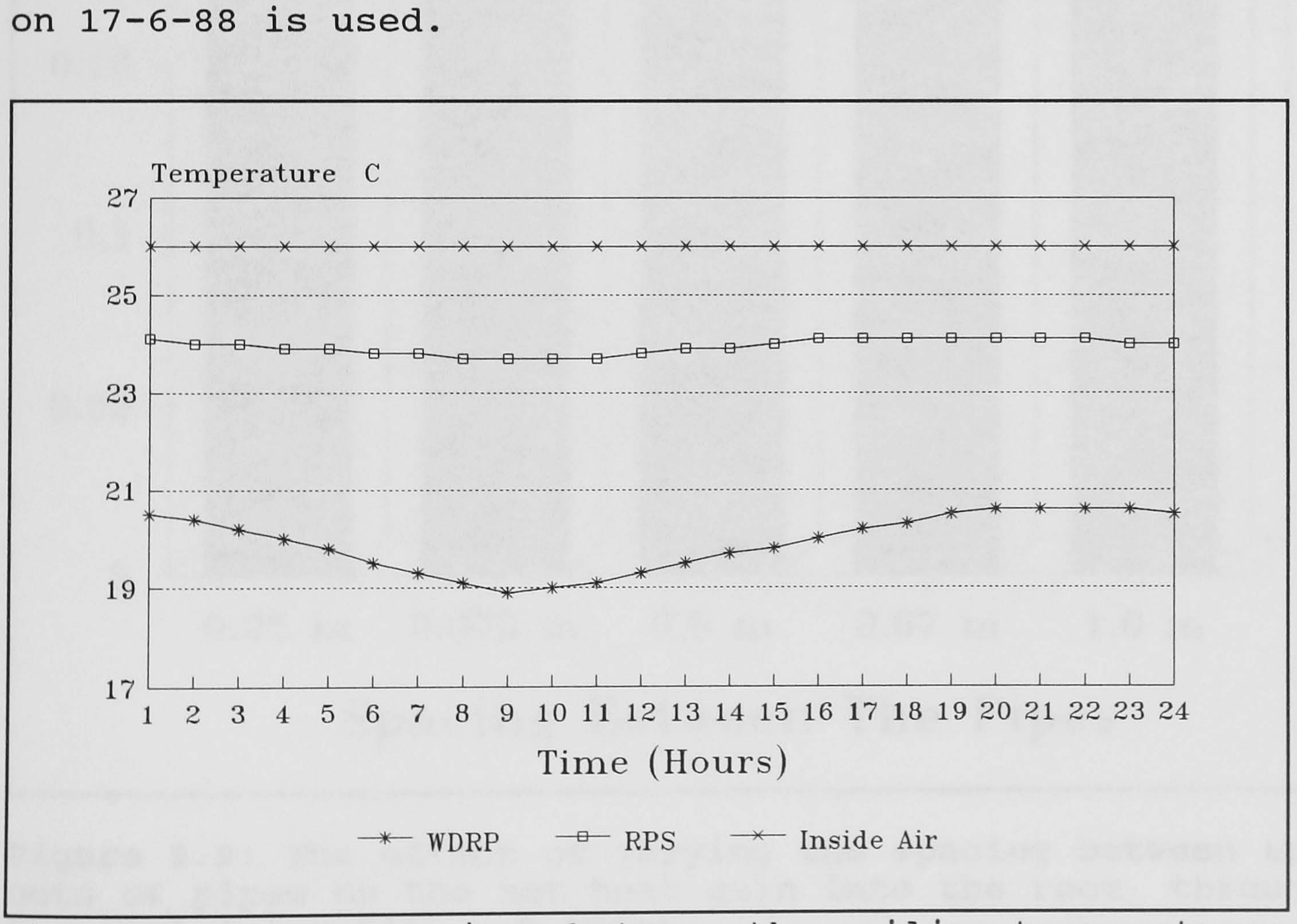

Figure 5.8: A comparison between the ceiling temperatures of a Water Diode Roof Pond, with that of a roof pond with an insulated roof slab when the weather data for Muscat on 21-3-88 is used.

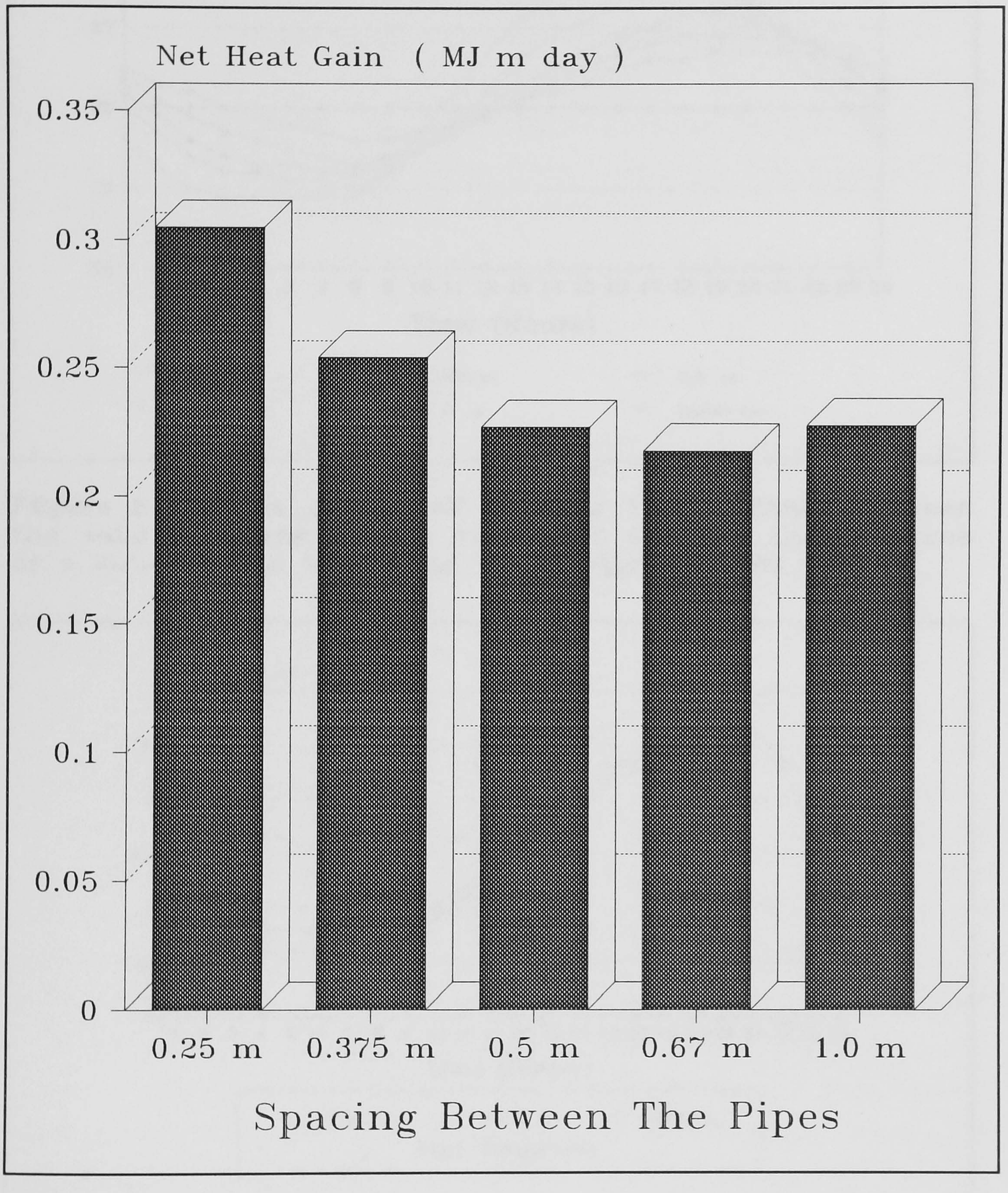

Figure 5.9: The effect of varying the spacing between the sets of pipes on the net heat gain into the room, through the roof (pipe dia. = 0.025m).

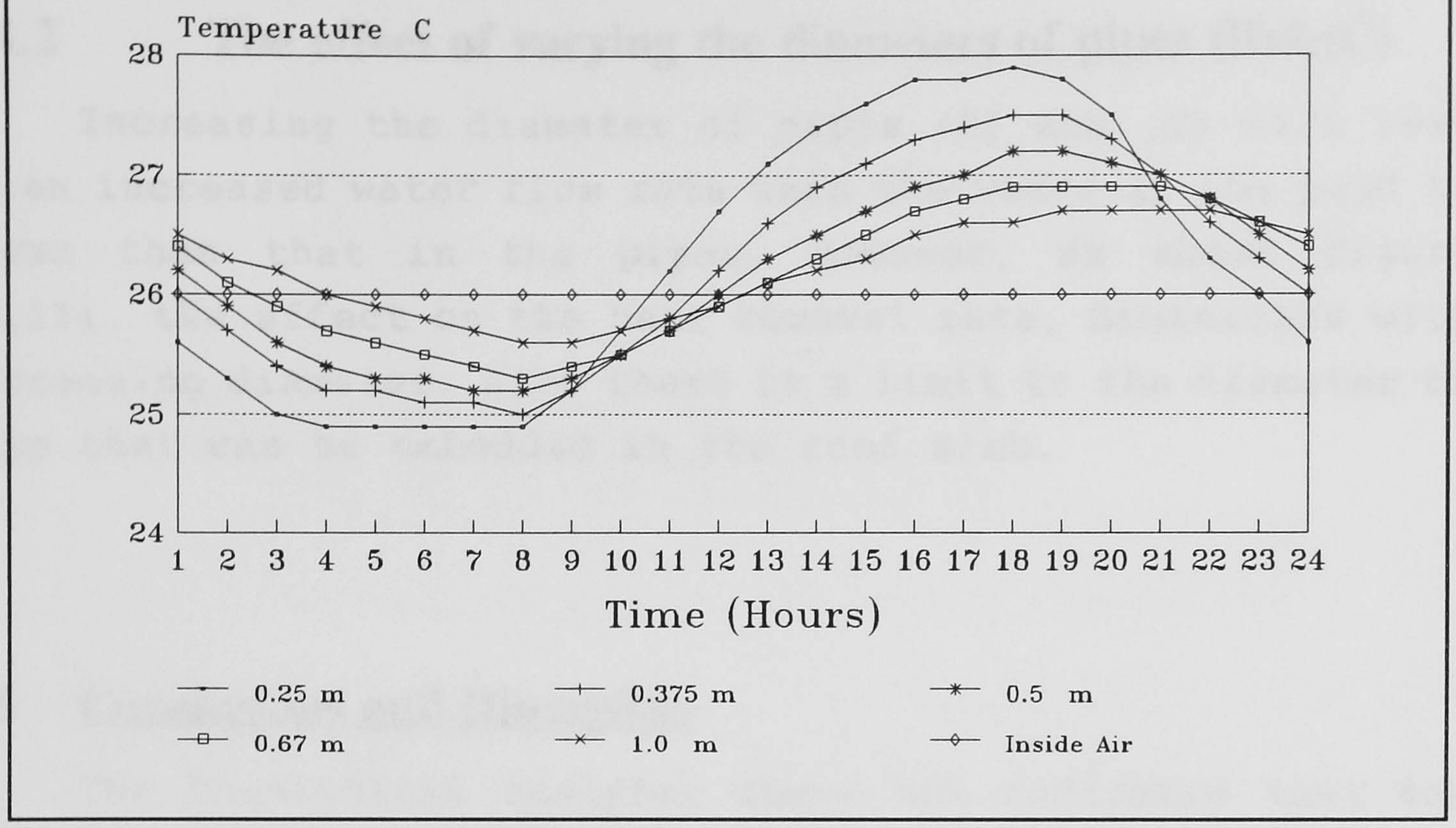

Figure 5.10: The effect of varying the distance between the sets of pipes on the simulated ceiling temperatures of a Water Diode Roof Pond for a pipe dia. of 0.025m.

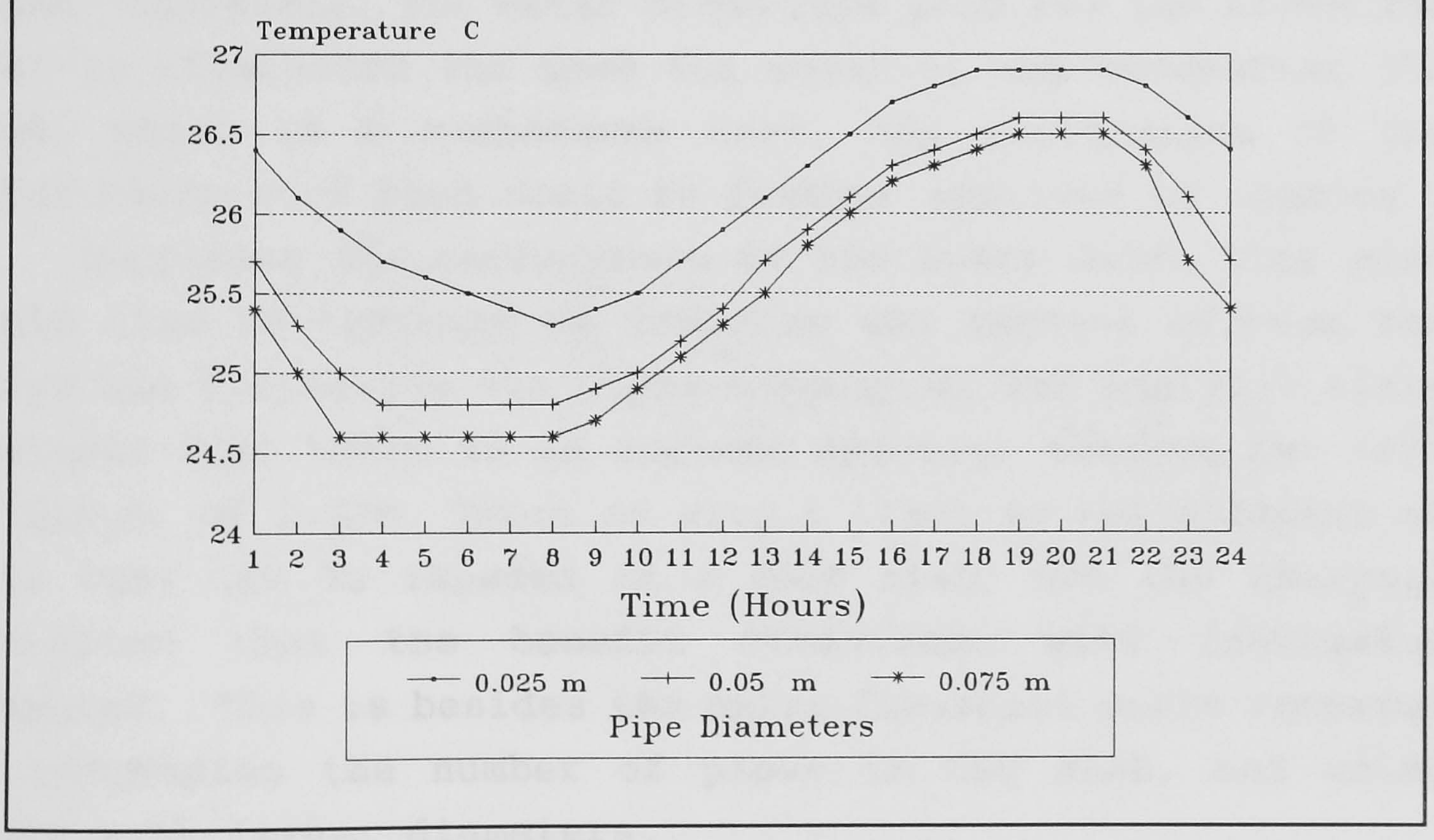

Figure 5.11: The effect of varying the pipe diameter on the simulated ceiling temperature of a Water Diode Roof Pond, for a pipes spacing of 0.67m.

5.4.2 The effect of varying the diameters of pipes (B)&(C)

Increasing the diameter of pipes (B) and (C) will lead to an increased water flow rate when the water in the pond is lower than that in the pipes. However, as shown Figure (5.11), the effect on the heat removal rate, diminishes with increasing diameter. Also there is a limit to the diameter of pipe that can be embedded in the roof slab.

5.5 Conclusions and Discussion

The theoretical analysis above has indicated that the idea of the Water Diode roof pond is feasible. In fact, as can be seen from Figures (5.12) and (5.13), its performance is better than all of the roof constructions analyzed, except that of a roof pond covered during the day and uncovered at night. Obviously, the Water Diode roof pond has the advantage that it eliminates the need for covering and uncovering the pond, which is a cumbersome task. The performance of the Water Diode roof pond could be further improved by shading.

Improving the performance of the Water Diode roof pond could also be achieved by reducing the spacing between the pipes and increasing the pipes diameters. The analysis above suggests that there is an optimum spacing, between two sets of pipes, of 0.67m. There is also a limit to the diameter of pipe that can be impeded in a roof slab, and the analysis indicates that the benefit diminishes with increasing diameter. This is besides the extra financial costs incurred by increasing the number of pipes in the slab, and using pipes with larger diameters.

The next step is to test the idea of the Water Diode roof pond, experimentally. But to achieve a better understanding of the roof's performance, it was considered essential to analyze first, the heat gains through the walls.

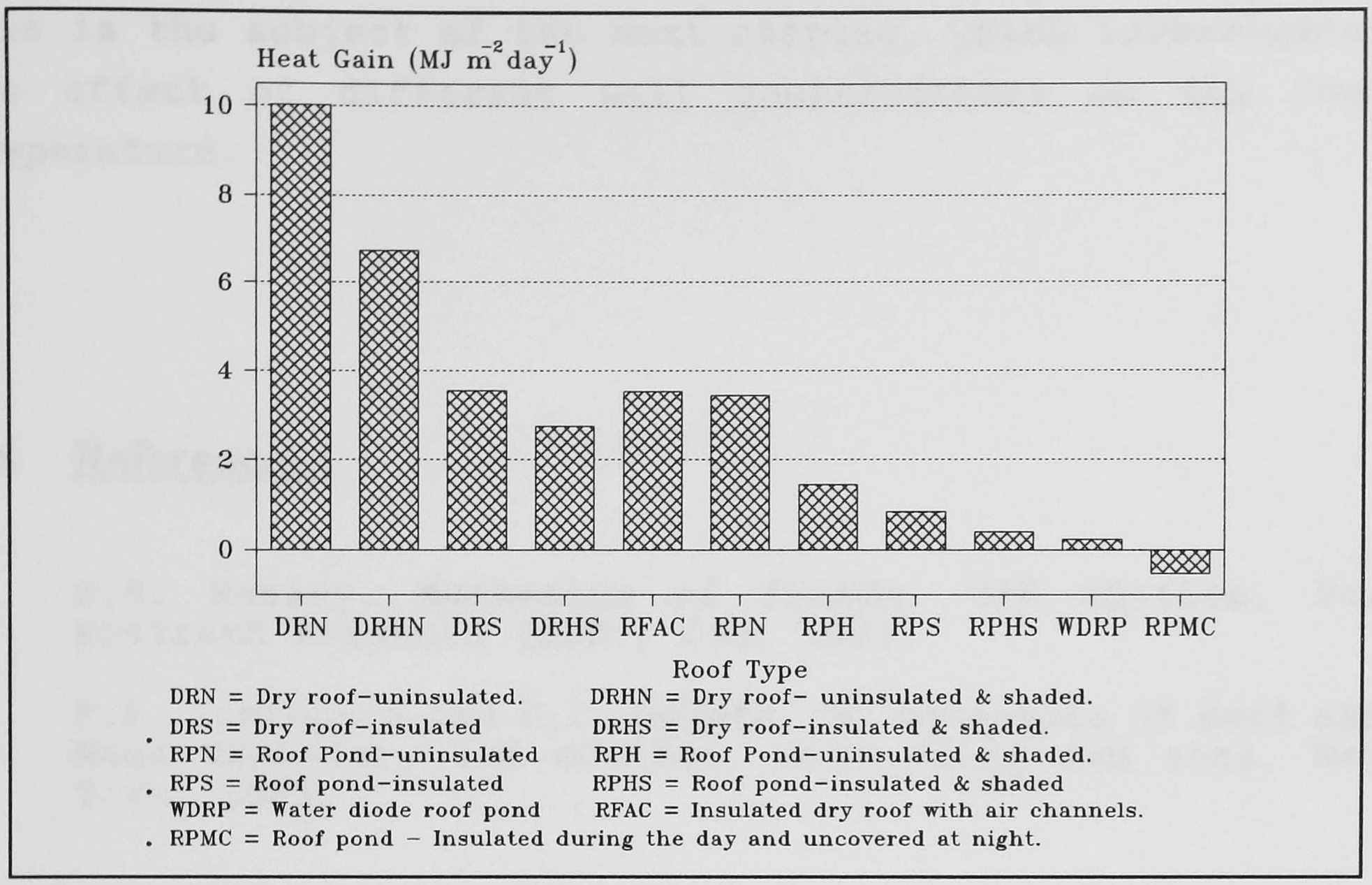

Figure 5.12: Comparative analysis of heat gains through the different roof constructions, using the weather data for Muscat on 17-6-1988.

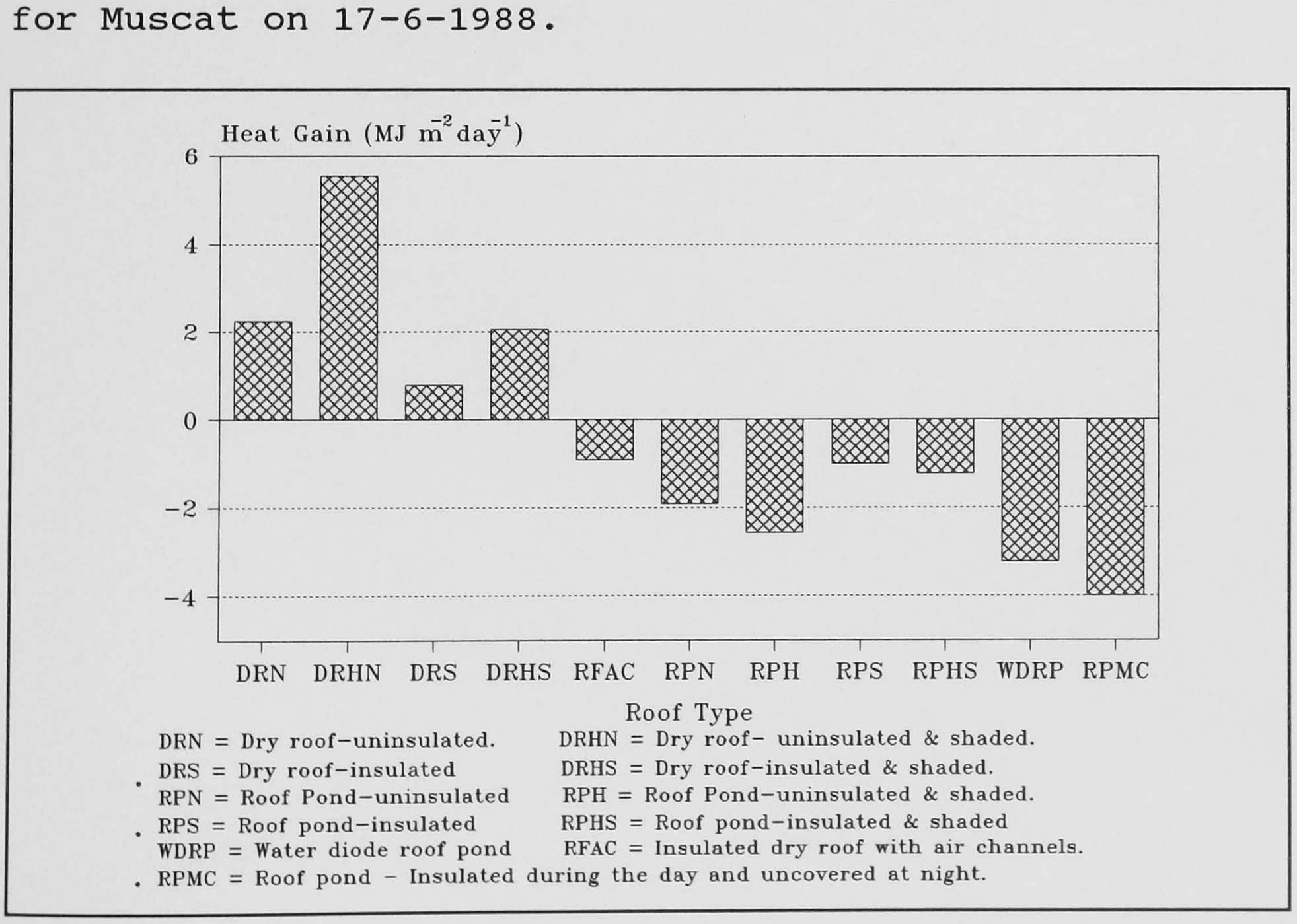

Figure 5.13: Comparative analysis of the heat gains through the different roof constructions, using the weather data for Muscat on 21-3-1988.

This is the subject of the next chapter, which investigates the effect of different wall constructions on the room temperature.

5.6 References :

1. B.S. Massey, Mechanics of Fluids, 5th edition, Van Nostrand Reinhold (U.K.) Ltd, 1983.

2. F.P. Incropera and D.P. DeWitt, Fundamentals of Heat and Mass Transfer, 2nd edition, John Wiley and sons, New York, 1983.

Chapter (6)

Mathematical Modelling Of Heat Transfer Through Different Wall Constructions

Chapter (6)

Mathematical Modelling Of Heat Transfer Through Different Wall Constructions

6.1 Introduction

In the previous two chapters (4 & 5), mathematical models we developed in order to assess and compare the effectiveness of different roof constructions, in reducing the heat gain in buildings in hot climates. In the first part of this chapter, a similar analysis is carried out, in order to asses and compare the thermal performance of different wall constructions. The second part of the chapter will include an analysis of the combined effects of the different roofs and walls on the heat gains in air conditioned rooms. The thermal performance of the following wall constructions will be investigated :

1- A single leaf, hollow concrete block, wall.
2- A double leaf, hollow concrete block, wall with 50mm uninsulated closed cavity.
3- A double leaf, hollow concrete block, wall with 50mm naturally ventilated cavity.
4- A double leaf, hollow concrete block, wall with 50mm insulated cavity.
5- A double leaf wall, the inner leaf is constructed from hollow concrete block and the outer leaf is constructed from brick. The 50mm closed cavity is uninsulated.
6- The same as 5, but with naturally ventilated cavity.
7- The same as 5, but with insulated cavity.
8- A double leaf brick wall, with 50mm uninsulated closed cavity.
9- The same as 8, but with naturally ventilated cavity.
10- The same as 8, but with insulated cavity.
11- A single leaf, brick wall.

6.2 Heat Gains and Loses in Vertical Wall

The following heat exchange processes occur between a wall and its surrounding environments :

- Solar heat gain into the external wall surface.
- Long-wave radiation heat exchange between the outside surface of the wall and the outside environment, i.e. the sky and the ground.
- Convective heat exchange between the outside surface of the wall and the ambient air.
- Convective heat exchange between the inside surface of the wall and the room air.
- Long-wave radiation heat exchange between the inside surface of the wall and the other internal surfaces of the room.

6.2.1 Solar heat gain

The amount of solar radiation absorbed by a wall depends on the absorptivity of its surface to solar radiation, and on the total solar radiation falling on it. The absorptivity of the wall depends on its surface finish, and to some extent on the dust that will eventually collects on it, a problem most noticeable in hot arid climates. Surfaces painted white have an absorptivity in the range of 0.2 - 0.4, and for this analysis a value of 0.36 is assumed. The absorptivity of bricks to solar radiation varies within the range of 0.3 - 0.8, depending on the type of brick used. In this analysis, the brick work is assumed to have an absorptivity of 0.65.

The total solar radiation falling on the wall, depends on the latitude of the location, the orientation of the wall, the time of day and day of the year and the clarity of the sky. This is neglecting any shading or enhancing effects of neighbouring structures. Generally, the total solar radiation falling on the wall can be divided into three components; the

direct, or beam component, the **diffuse** component and that diffusely **reflected from the ground.** The proportion of each component depends on many factors, such as the clarity of the sky, the orientation of the surface, the time of day and day of the year and the reflectivity of the surrounding environment. To estimate these components, from the monthly averaged, daily global radiation, we must first estimate the proportions of the beam and diffuse components falling on a horizontal surface. The procedure described in [1], is used in this analysis.

The total hourly solar radiation, **I** (in Wm^{-2}), falling on a horizontal surface could be estimated from the monthly averaged daily global radiation, as follows:

$$I = \frac{r \,.\, H}{3.6}$$

H is the monthly averaged daily global radiation for the day and location under consideration ($kJm^{-2}day^{-1}$). In the analysis, the average for June - 88, at Muscat, was used.

r is the ratio of the total radiation for the hour to that of the whole day.

$$r = \frac{\pi}{24} \,.\, (a + b.\cos(\omega)) \,.\left[\frac{\cos(\omega) - \cos(\omega_s)}{\sin(\omega_s) - \frac{\pi}{180} \,.\, \omega_s \,.\cos(\omega_s)}\right]$$

Where **a** = $0.4090 + 0.5016 \sin(\omega_s - 60)$

b = $0.6609 - 0.4767 \sin(\omega_s - 60)$

ω is the hour angle of the sun (deg.), given as :

$$\omega = \left(\frac{360}{24}\right) \,.\, (h - 12)$$

h is the time of the day (solar time)

and ω_s is the sun set hour angle (deg.), given as :

$$\omega_s = acos(-\tan(\phi)\tan(\delta))$$

Where ϕ is the latitude of the location (deg.)

and δ is the declination angle of the sun (deg.), given as:

$$\delta = 23.45 \cdot \sin\left[360 \cdot \frac{284 + day}{365} \right]$$

day is the day of the year under consideration.

The hourly diffuse solar radiation, I_d (in Wm^{-2}), falling on a horizontal surface is given by :

$$I_d = \frac{r_d \cdot H_d}{3.6}$$

Where r_d is the ratio of the diffuse solar radiation for the hour to that of the whole day. This is given by Lui and Jordan as :

$$r_d = \frac{\pi}{24} \cdot \frac{\cos(\omega) - \cos(\omega_s)}{\sin(\omega_s) - \frac{\pi \omega_s}{180} \cdot \cos(\omega_s)}$$

and H_d is the monthly averaged, daily diffuse solar radiation (in $kJm^{-2}day^{-1}$). This is estimated using the Collares-Pereira Rabl correlation, given in [1] as :

$$H_d = H \cdot [0.775 + 0.00606(\omega_s - 90) - [0.505 + 0.00455(\omega_s - 90)]\cos(115\bar{K}_T - 103)]$$

$\bar{k}_T$ is the monthly averaged clearness index.

$$\bar{k}_T = \left(\frac{monthly averaged daily radiation on a horizontal surface}{monthly averaged daily extraterrestrial radiation} \right)$$

The hourly beam solar radiation (in Wm^{-2}), falling on a horizontal surface, is thus given by :

$$I_b = I - I_d$$

The next step is to find the hourly total solar radiation falling on a vertical surface. The beam component of the solar radiation falling on a vertical surface is given by :

$$I_{b_{vs}} = I_b \cdot R_b$$

Where $\mathbf{R_b}$ is the ratio of the beam radiation on a vertical wall to that on a horizontal surface. This is given as :

$$R_b = \frac{\cos\theta}{\cos\theta_z}$$

$$= \frac{\cos\delta\sin\phi\cos\gamma\cos\omega + \cos\delta\sin\gamma\sin\omega - \sin\delta\cos\phi\cos\gamma}{\cos\phi\cos\delta\cos\omega + \sin\phi\sin\delta}$$

Where γ is the surface azimuth angle, defined as the deviation of the of the normal to the surface from the local meridian, zero due south, east -ve and west +ve; $-180^\circ \leq \gamma \leq 180^\circ$.

For a clear sky, most encountered in hot arid climates, the diffuse solar radiation coming from the sky can be divided into three parts [1]. The **isotropic**, received uniformly from all of the sky dome; the **circumsolar diffuse**, concentrated in the part of the sky around the sun; and the **horizon brightening**, concentrated near the horizon. There are many correlations developed for estimating the diffuse component of the solar radiation falling on an inclined surface [2]. They vary in the way they account for each of the three parts of the diffuse radiation. The research work carried out in Saudi Arabia by Abdelrahman et al. [3] comparing the isotropic model of Liu and Jordan and the anisotropic models of Hay and Klucher, with actual data suggests that the difference between the three models is quite small, and therefore one can use any of the three models.

The correlation used in this analysis is that suggested by Reindl et al. [4], which is a modified version of the Hay and Davies correlation and the Klucher correlation. The hourly diffuse solar radiation, falling from the sky, on a vertical surface is given as:

$$I_{d_{vs}} = I_d \{(0.5 + 0.177f)(1 - A_i) + A_i R_b\}$$

Where $\mathbf{I_d}$ is the hourly diffuse solar radiation falling on a horizontal surface.

f is a factor, defined as :

$$f = \sqrt{\frac{I_b}{I}}$$

$\mathbf{I_b}$ is the hourly direct solar radiation falling on a horizontal surface.

$\mathbf{I}$ is the hourly total solar radiation falling on a horizontal surface.

And $\mathbf{A_i}$ is an anisotropy index, which is a function of the transmittance of the atmosphere for beam radiation, given as :

$$A_i = \frac{I_b}{I_o}$$

Where $\mathbf{I_o}$ is the hourly extraterrestrial solar radiation falling on a horizontal surface. This is given in [1] as :

$$I_o = \frac{12\times3600}{\pi} G_{sc}\left(1 + 0.033\cos\frac{360n}{365}\right)$$

$$\times\left[\cos\phi\cos\delta(\sin\omega_2 - \sin\omega_1) + \frac{\pi(\omega_2 - \omega_1)}{180}\sin\phi\sin\delta\right]$$

Where $\mathbf{G_{sc}}$ is the solar constant (= 1367 Wm^{-2}).

$\mathbf{n}$ is the number of the day (1 - 365).

ω_1 is the hour angle of the sun, at the beginning of the hour.

And ω_2 is the hour angle of the sun, at the end of the hour.

The ground reflected component of the solar radiation falling on a vertical surface, depends on the total solar radiation incident on the ground, **I**, and on the reflectivity of the ground, ρ_g, and thus can be expressed as :

$$I_{refl_{vs}} = 0.5\,(I.\,\rho_g)$$

So, the hourly total solar radiation falling on a vertical surface, can be expressed as :

$$I_{vs} = (I_b + I_d A_i)\,R_b + I_d(1-A_i)(0.5+0.177f) + 0.5\,(I\rho_g)$$

The model above, is termed the **HDKR** model (the Hay, Davies, Klucher, Reindl model).

6.2.2 Long-wave radiation heat exchange with the outside

A vertical wall exchanges long-wave heat radiation with the sky and with the part of the ground it sees. It is exposed to half of the sky dome, and can see half of the circular plane of the ground. The long-wave heat radiation falling on the outside surface of the wall can be divided into three parts; that emitted from the sky and falling directly on the wall; that emitted by the sky and reflected by the ground onto the wall; and that emitted by the ground. The sky temperature has been discussed earlier in Chapter 4 (4.2.1.2). The upper-surface temperature of the ground is assumed to be the same as that of the ambient air. Thus the net heat loss from the outside surface of the wall, by long-wave heat radiation, to the sky and the ground, (in Wm^{-2}), can be expressed as :

$$Q_{rad_{net}} = \varepsilon_w \sigma \left\{ T_{wo}^{\,4} - 0.5 \left[\varepsilon_s C_s T_{sky}^{\,4} (1 + \rho_g) + \varepsilon_g T_{ao}^{\,4} \right] \right\}$$

Where σ is Stefan-Boltzmann constant.

ϵ_w is the emissivity of the wall.

ϵ_s is the emissivity of the sky.

ϵ_g is the emissivity of the ground.

ρ_g is the reflectivity of the ground (= 1-ϵ_g).

C_s is the cloud correction factor (see 4.2.1.2).

T_{wo} is the temperature of the outside surface of the wall. (K).

T_{sky} is the apparent temperature of the sky (K).

And T_{ao} is the ambient air temperature (K).

6.2.3 Convective heat exchange between the outside surface of the wall and the ambient air

The convective heat exchange rate between the outside surface of the wall and the ambient air is influenced by the wind speed at the surface of the wall, the direction of the wind relative to the wall, the temperature difference between the outside surface of the wall and the ambient air, and the dimensions of the wall. In general, the rate of heat loss from the outside surface of the wall, by convection to the ambient air (in Wm^{-2}), can be expressed as :

$$Q_{conv_{wo}} = h_{wo} \ (T_{wo} - T_{ao})$$

Where h_{wo} is the convective heat transfer coefficient between the wall and the ambient air ($Wm^{-2}K^{-1}$)

T_{wo} is the temperature of the outside surface of the wall. (K)

And T_{ao} is the temperature of the ambient air (K)

The heat transfer coefficient has two main components; the **buoyancy-driven**, which is caused by the temperature difference between the outside surface of the wall and the ambient air; and the wind-driven or **forced** component, which is caused by the wind flow. The procedure described by Gandrille et al. [5], is used in this analysis, for the reasons discussed earlier in 4.2.1.1. Here, the heat transfer

coefficient is taken as the geometric mean of the buoyancy and forced components, and is expressed as:

$$h_{wo} = \frac{(Nu_f^3 + Nu_b^3)^3 \cdot k_a}{L_{c_{wo}}}$$

$\mathbf{k_a}$ is the thermal conductivity of the air $(Wm^{-1}K^{-1})$

$L_{c_{wo}}$ is The characteristic length of the outside surface of the wall, and is computed as :

$$L_{c_{wo}} = \frac{4 \times AREA}{PERIMETER} \quad (m)$$

$\mathbf{Nu_f}$ is the Nusselt number representing the wind-driven component of the heat transfer coefficient.

and $\mathbf{Nu_b}$ is the Nusselt number representing the buoyancy-driven component of the heat transfer coefficient.

The Nusselt number representing the buoyancy-driven component, $\mathbf{Nu_b}$ is defined as :

$$Nu_b = \left[\left(0.54\,(Gr_{wo} \times Pr)^{\frac{1}{4}}\right)^6 + \left(0.14\,(Gr_{wo} \times Pr)^{\frac{1}{3}}\right)^6\right]^{\frac{1}{6}}$$

Pr is the Prandtl number for air, assumed to have a value of 0.707 for the range of ambient conditions experienced.

and $\mathbf{Gr_{wo}}$ is the Grashof number on the outside surface of the wall, defined as :

$$Gr_{wo} = \frac{g \cdot \beta_{wo} \cdot \Delta T_{wo} \cdot \rho_a^2 \cdot L_{c_{wo}}^3}{\mu_a^2}$$

g is the acceleration due to gravity (ms^{-2})

β_{wo} is the coefficient of thermal expansion of the outside air film, defined as :

$$\beta_{wo} = \frac{1}{\left(\frac{T_{ao} + T_{wo}}{2}\right)} \qquad (K^{-1})$$

Where $\mathbf{T_{ao}}$ and $\mathbf{T_{wo}}$ are expressed in Kelvin.

And $\mathbf{\Delta T_{wo}}$ is the temperature difference between the outside surface of the roof and the ambient air (K)

The forced component of the heat transfer coefficient, depends on the direction of the wind, relative to the wall. If the wind flow is parallel to the wall, then the Nusselt Number representing the forced component is expressed as :

$$Nu_f = Nu_p = 0.59\,Re^{\frac{1}{2}} \qquad for\ Re \leq 2.86\times10^5$$

OR

$$Nu_f = Nu_p = \left[\left(059\,Re^{\frac{1}{2}}\right)^6 + \left(0.032\,Re^{\frac{4}{5}} - 745\right)^6\right]^{\frac{1}{6}} \qquad for\ Re > 2.86\times10^5$$

Where **Re** is the Reynold number defined as :

$$Re = \frac{\rho_a . v_a . L_{wo}}{\mu_a}$$

$\boldsymbol{\rho_a}$ is the density of air (1.145 kgm^{-3})

$\mathbf{V_a}$ is the air speed (ms^{-1})

$\boldsymbol{\mu_a}$ is the absolute viscosity of air ($kgm^{-1}s^{-1}$)

$\mathbf{L_{wo}}$ is the surface length in the streamwise direction (m)

If the direction of the wind is perpendicular to the wall, then the flow will be completely separated if the wall is in the lee-ward direction of the wind, and stagnation flow occurs at the wall facing the wind. For a completely separated flow, the Nusselt Number representing the forced component of the heat transfer coefficient, is expressed as:

$$Nu_f = Nu_s = 0.20\ Re^{\frac{2}{3}}$$

The characteristic length, $L_{c_{wo}}$, is used for computing the Reynold Number in this case.

And for stagnation flow, the Nusselt Number is expressed as:

$$Nu_f = Nu_{st} = 0.14\ Re^{0.69}$$

The characteristic length, $L_{c_{wo}}$, is also used here for computing the Reynold Number.

For a combined flow, when the wind direction is neither parallel nor perpendicular, a weighting function is used to give :

$$Nu_f = \cos^2\theta\, Nu_{s/st} + (1 - \cos^2\theta)\, Nu_p$$

Where θ is the angle between the oncoming flow and the normal to the surface. Knowing the wind direction (**WD** in degrees), θ is worked out as follows:

$$\theta = |WD - \gamma|$$

The separation flow correlation is used if θ is in the range : $90 < \theta < 270$.

Although the computer program used in the analysis, was developed to take account of the changing hourly direction of the wind, the lack of actual data meant that the prevailing direction of the wind for the month (060°) was used instead.

6.2.4 Convective heat exchange between the inside surface of the wall and the room air

The convective heat gain rate (Wm^{-2}), from the room air to the inside surface of the wall, is given by :

$$Q_{conv_{wi}} = h_{wi} (T_{ai} - T_{wi})$$

Where **h_{wi}** is the convective heat transfer coefficient between the inside surface of the wall and the room air ($Wm^{-2}K^{-1}$)

T_{ai} is the temperature of the room air (K)

T_{wi} is the temperature of the inside surface of the wall (K)

The inside heat transfer coefficient is buoyancy driven, and can be expressed as :

$$h_{wi} = \frac{Nu_{wi} \times k_a}{L_{c_{wi}}}$$

Where **k_a** is the thermal conductivity of the air ($Wm^{-1}K^{-1}$)

$L_{c_{wi}}$ is the characteristic length of the ceiling.

In these correlations, $L_{c_{wi}}$ is defined as:

$$L_{c_{wi}} = \frac{AREA}{PERIMETER} \qquad (m)$$

AND **Nu_{wi}** is the Nusselt number, which describes the temperature gradient at the surface. The correlation used here is that developed by Churchill and Chu and recommended in [6]. This is given as :

$$Nu_{wi} = \left\{ 0.825 + \frac{0.387 \, (Gr_{wi} \times Pr)^{\frac{1}{6}}}{\left[1 + \left(\frac{0.429}{Pr} \right)^{\frac{9}{16}} \right]^{\frac{8}{27}}} \right\}^2$$

Pr is the Prandtl number for air, assumed to have a value of 0.707

$\mathbf{Gr_{wi}}$ is the Grashof number at the inside surface of the wall, defined as:

$$Gr_{wi} = \frac{g \cdot \beta_{wi} \cdot \Delta T_{wi} \cdot \rho_a^2 \cdot {L_{c_{wi}}}^3}{\mu_a^2}$$

β_{wi} is the coefficient of thermal expansion of the air film at the inside surface of the wall, defined as:

$$\beta_{wi} = \frac{1}{\left(\frac{T_{ai} + T_{wi}}{2}\right)} \qquad (K^{-1})$$

Where $\mathbf{T_{ao}}$ and $\mathbf{T_{wo}}$ are expressed in Kelvin.

And $\mathbf{\Delta T_{wi}}$ is the temperature difference between the surface of the wall and the room air (K)

6.2.5 Long-wave radiation heat exchange between the inside surface of the wall and the other internal surfaces

The internal surface of the wall will exchange long-wave heat radiation with all of the other internal surfaces of the room. The amount of heat it loses to or gains from a particular surface will depend on the temperature difference between the surfaces and the view factor. To simplify the calculation required, it is assumed that the long-wave heat radiation exchange occurs between the inside surface of the wall, and an imaginary surface that has the average temperature of all of the internal surfaces of the room, and has a view factor of 1. Thus the heat gain into the wall, by long-wave radiation from the internal surfaces of the room (in Wm^{-2}), can be expressed as:

$$Q_{rad_{si}} = h_r \left(T_{si} - T_{wi} \right)$$

Where $\mathbf{T_{si}}$ is the average temperature of all of the internal surfaces of the room. (K)

$\mathbf{T_{wi}}$ is the temperature of the inside surface of the wall. (K)

And $\mathbf{h_r}$ is the radiation heat transfer coefficient between the inside surface of the wall, and the assumed surface that has the average temperature of the internal surfaces of the room. $\mathbf{h_r}$ is computed from :

$$h_r = 4\,\sigma\,\varepsilon_w\,T_{si}^3$$

6.2.6 Heat transfer in the air gap of a closed cavity in a vertical wall

The uninsulated double leaf wall constructions are assumed to have an air gap, 50mm wide, between the two leaves. For air-filled cavities, where the ratio of the height of the wall to the space between the two leaves is greater than 40, the heat transfer regimes encountered change, with increasing temperature difference between the two leaves, from conduction to turbulent transition and then to turbulent boundary-layer. Also radiative heat transfer will occur between the facing surfaces of the cavity. In this analysis, the conductive/ convective heat transfer is estimated using the correlations developed by Elsharbiny et al., and recommended in [7]. In these, the Nusselt number is given as the maximum of the Nusselt number which applies to the conduction, turbulent transition regime and the turbulent boundary layer regime. That is :

$$Nu = Max\left[Nu_{ct}, Nu_t\right]$$

Where $\mathbf{Nu_{ct}}$ is the Nusselt number which applies to the conduction, turbulent transition regime, given as:

$$Nu_{ct} = \left[1 + \left\{\frac{0.104\,Ra^{0.293}}{1 + \left(\frac{6310}{Ra}\right)^{1.36}}\right\}^3\right]^{\frac{1}{3}}$$

And $\mathbf{Nu_t}$ is the Nusselt Number which applies to the turbulent boundary-layer regime, given as:

$$Nu_t = 0.0605\ Ra^{\frac{1}{3}}$$

Ra is the Rayleigh number, given as:

$$Ra = \frac{g\beta\,(\Delta T)\,s^3}{\nu\,\alpha}$$

Where **β** is the coefficient of thermal expansion of the air in the cavity. (K^{-1})

ΔT is the temperature difference between the two surfaces. (K)

s is the space between the two leaves (m)

ν is the kinematic viscosity of the air in the cavity. (m^2s^{-1})

And **α** is the thermal diffusivity of the air in the cavity. (m^2s^{-1})

The fluid properties are evaluated at the average temperature of the two surfaces. The conductive / convective heat transfer coefficient is then obtained from :

$$h_{cv} = \frac{Nu\,.\,k_a}{s}$$

And the conductive / convective heat transfer rate (in Wm^{-2}), between the sides of the cavity is obtained from :

$$Q_{cd/cv} = h_{cv}\,(\Delta T)$$

The radiative heat transfer rate (in Wm^{-2}), between the two sides of the cavity is estimated from :

$$Q_{rad_{cv}} = \frac{\sigma\,(T_{cvo}^4 - T_{cvi}^4)}{\frac{1}{\varepsilon_{cvo}} + \frac{1}{\varepsilon_{cvi}} - 1}$$

Where **σ** is Stephan-Boltzmann constant.

T_{cvo} is the temperature of the outer surface of the cavity. (K)

T_{cvi} is the temperature of the inner surface of the cavity. (K)

ϵ_{cvo} is the emissivity of the outer surface of the cavity.

And ϵ_{cvi} is the emissivity of the inner surface of the cavity.

This is the standard derived expression for radiative heat transfer between two infinite planes.

6.2.7 Heat transfer in the air gap of a ventilated cavity in a vertical wall

The analysis of a ventilated cavity wall construction, aims at estimating the benefit of allowing the hot air in the cavity to escape to the outside, through openings at the top of the wall, to be replaced by cooler ambient air, from openings at the bottom of the wall. The circulation thus caused, will remove heat from the cavity when the ambient air is cooler than the air in the cavity in a similar manner to a solar chimney. To estimate the maximum benefit that could be achieved, the reverse, warming process, is assumed to be inhibited by a device, located at the bottom of the wall, that only allows upward flow.

In a ventilated cavity, the air in the cavity will exchange heat, via convection, with the two sides of the cavity. The Nusselt number correlation recommended, in [7], for use with such cavities is :

$$Nu = \left[(0.0417\,Ra)^{-1.9} + \left(0.68\,Ra^{\frac{1}{4}}\right)^{-1.9} \right]^{-\frac{1}{1.9}}$$

Where **Ra** is the Rayleigh number, given in these correlations as:

$$Ra = \frac{g\beta\,(\overline{T}_w - T_{acv})\,s^3}{\nu\,\alpha} \cdot \frac{s}{H}$$

Where β is the coefficient of thermal expansion of the air in the cavity. (K^{-1})

$\bar{T}_w$ is the average temperature of the two surfaces.

T_{acv} is the temperature of the air in the cavity.

s is the space between the two leaves (m)

ν is the kinematic viscosity of the air in the cavity. (m^2s^{-1})

And α is the thermal diffusivity of the air in the cavity. (m^2s^{-1})

The heat transfer coefficient is then obtained from :

$$h_{cv} = \frac{Nu \,.\, k_a}{s}$$

And the heat gained by the air in the cavity form the two sides (in Wm^{-2}) is estimated from :

$$Q_{conv} = h_{cv}\,(T_{cvo} - T_{acv}) + h_{cv}\,(T_{cvi} - T_{acv})$$

Where T_{cvo} is the temperature of the outer surface of the cavity. (K)

T_{cvi} is the temperature of the inner surface of the cavity. (K)

And T_{acv} is the temperature of the air in the cavity. (K)

Besides the convective and radiative heat transfer processes that occur in a closed cavity, there is a heat removal from the cavity by the air flow. The heat removal rate, from the cavity, will depend on the mass flow rate of the air. This is influenced by the temperature difference between the air in the cavity and the ambient air, and is also affected by the wind speed and direction. For the sake

of simplicity, the wind effects are neglected, and thus the air flow in cavity is assumed to thermally induced and one-directional. This thermally induced, air mass flow rate is estimated from [6] :

$$\dot{m} = A \times V = A \times \sqrt{\frac{2 \times P_d}{\rho_o}}$$

Where **A** is the cross-sectional area of the cavity (m^2)

V is the velocity of the air in the cavity (ms^{-1})

$\mathbf{P_d}$ is the pressure difference between the openings at the top and bottom of the wall (Nm^{-2})

And $\boldsymbol{\rho_o}$ is the density of air at 273 K (kgm^{-3})

The stack pressure difference, $\mathbf{P_d}$, is estimated from [8]:

$$P_d = 0.0342 \times P_{at} \times h \times \left(\frac{1}{T_{ao}} - \frac{1}{T_{ac}} \right)$$

Where $\mathbf{P_{at}}$ is the atmospheric pressure (Nm^{-2})

h is the distance between the top and bottom openings in the wall (m)

$\mathbf{T_{ao}}$ is the ambient air temperature (K)

And $\mathbf{T_{ac}}$ is the temperature of the air in the cavity (K)

The amount of heat removed, from the air in the air gap is thus:

$$Q_{vent} = \dot{m}_a \, Cp_a \, (T_{ac} - T_{ao})$$

The radiative heat exchange between the two sides of the cavity is estimated in a similar manner to that of a closed cavity.

6.2.8 Heat exchange between the floor and the room air

The floor of the room is assumed to be cover by a layer of concrete, 10 cm deep. The ground below the room is taken to be at a constant temperature of 26 °C. Thus the room will exchange heat with the ground by conduction through the floor, whereas the top surface of the floor will exchange heat by convection with the room air, and by radiation with the other internal surfaces. The convective heat transfer coefficient between the room air and the floor is buoyancy driven, and depends on whether the surface of the floor is warmer or cooler than the air inside the room. The correlations used in this analysis, are those given in [6], where the convective heat transfer coefficient, $\mathbf{h_f}$, is given as:

$$h_f = \frac{Nu_f \times k_a}{L_{c_f}}$$

Where $\mathbf{k_a}$ is the thermal conductivity of the air $(Wm^{-1}K^{-1})$

L_{c_f} is the characteristic length of the floor. In these correlations, L_{c_f} is defined as:

$$L_{c_f} = \frac{AREA}{PERIMETER} \qquad (m)$$

AND $\mathbf{Nu_f}$ is the Nusselt number, which describes the temperature gradient at the floor. This depends on the temperature difference and the direction of the temperature gradient between the surface of the floor and the inside air, and is given as :

$$Nu_f = \begin{cases} \left.\begin{cases} 0.54.(Gr_f x Pr)^{\frac{1}{4}} & 10^4 \le (Gr_f x Pr) \le 10^7 \\ 0.15.(Gr_f x Pr)^{\frac{1}{3}} & 10^7 \le (Gr_f x Pr) \le 10^{11} \end{cases}\right\} T_f > T_{ai} \\ 0.27.(Gr_f x Pr)^{\frac{1}{4}} \qquad T_f \le T_{ai} \end{cases}$$

$\mathbf{Gr_f}$ is the Grashof number at the floor surface, defined as:

$$Gr_f = \frac{g \cdot \beta_f \cdot \Delta T_f \cdot \rho_a^2 \cdot L_{c_f}^{\ 3}}{\mu_a^2}$$

β_f is the coefficient of thermal expansion of the air film at the surface of the floor, defined as :

$$\beta_f = \frac{1}{\left(\frac{T_{ai} + T_f}{2}\right)} \qquad (K^{-1})$$

Where $\mathbf{T_{ai}}$ and $\mathbf{T_f}$ are expressed in Kelvin.

$\mathbf{T_f}$ is the temperature at the surface of the floor (K)

And $\mathbf{\Delta T_f}$ is the temperature difference between the surface of the floor and the inside air (K)

The radiative heat exchange between the floor and the other internal surfaces of the room is worked out in a similar manner to that used for the walls.

6.3 The Method Used In The Analysis

A room with the dimensions, 5m x 5m x 2.5m, with its southerly wall facing exactly south, and with no doors or windows, is assumed in the analysis. The room is not air-conditioned, and there are no additional heat gains or loses into the room, except those through the walls, roof and floor. This means that, unlike the assumption used previously in Chapters (4 & 5) of a constant internal air temperature, in this analysis the internal air temperature of the room will vary throughout the day. The performance of the different wall constructions will be compared by comparing the internal air temperatures in the room. The room is assumed to have a dry insulated roof, similar to that analyzed in section 4.3, and the ground temperature is assumed to be constant at 26 °C.

A one-dimensional implicit finite difference model was used to simulate the temperature variations in the walls, roof, floor and the internal air, through a period of 24-hours. The nodal distribution diagram assumed in the analysis of a room with double leaf walls, is shown in Figure (6.1).

Walls with an outer leaf of concrete block are assumed to be painted, white (the solar radiation absorptivity of white paint is taken as 0.36). On the other hand, walls with an outer layer of brick are assumed to be without paint or plaster, as actually happens in practice (the solar radiation absorptivity of bricks is taken as 0.65) . The effect of the plaster layer, in concrete block leaves, on the heat transfer process is assumed negligible.

The thermal performance of the different wall constructions are simulated under both; the very hot climate of Muscat in June and the clement climate for the same place in March. This is because, as realised in Chapter (4), the performance of the different constructions may vary under different climatic conditions.

6.4 Simulation Results

The model was used to simulate the temperature variations, through a 24-hours period, in a room the walls of which are constructed from the 11 different wall configurations mentioned in 6.1. The analysis is used to compare the effectiveness of closed cavities, ventilated cavities and the addition of insulation, in maintaining a low room air temperature. The analysis is also used to compare the thermal performance of concrete blocks and brick work.

The thermal properties of the materials used, are shown in Appendix A.

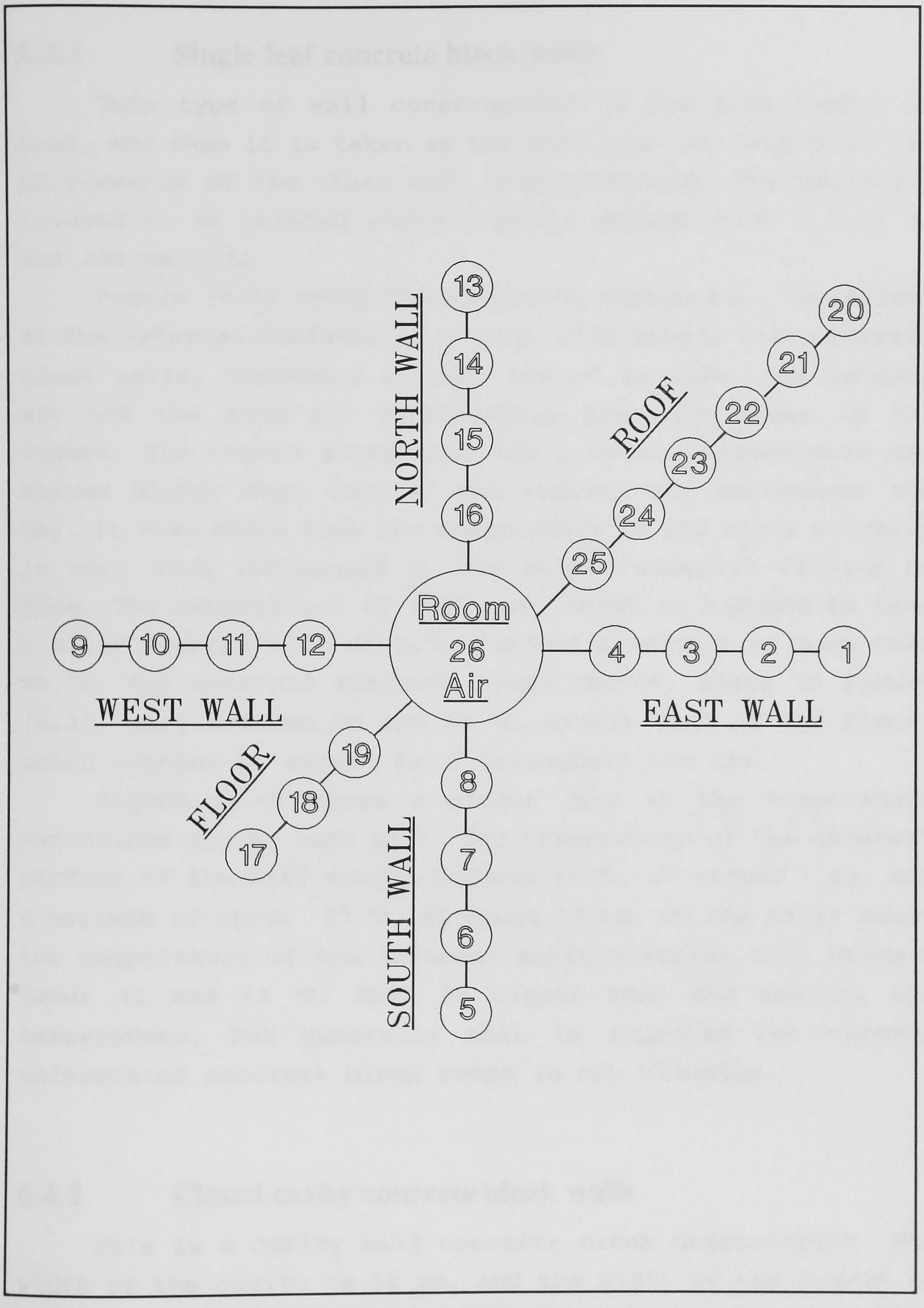

Figure 6.1: The nodal distribution diagram used in the one-dimensional Finite Difference analysis of heat transfer in a room.

6.4.1 Single leaf concrete block walls

This type of wall construction is the most common in Oman, and thus it is taken as the base case for comparing the performance of the other wall configurations. The walls are assumed to be painted white (solar absorptivity = 0.36), and 200 mm wide.

Figure (6.2) shows the simulated temperature variations of the external surfaces of a room, with single leaf concrete block walls, through a 24-hour period in June. The ambient air and the room air temperatures are also shown in the figure. The figure shows that the room air temperature has stayed higher than that of the ambient air throughout the day. It also shows that the temperature of the outer surfaces is very much influenced by the solar radiation falling on them. The temperature of the roof, which is assumed to have a solar absorptivity of 0.5, reaches a maximum of more than 65 °C. The internal surfaces temperatures, shown in Figure (6.3), vary between 39 and 44 °C, except that of the floor, which remains at around 33 °C throughout the day.

Figure (6.4) shows a closer look at the temperature variations of the east wall. The temperature of the external surface of the wall varies between 40 °C, at around 7 am, and a maximum of about 53 °C, at about 11 am. On the other hand, the temperature of the internal surface varies only between about 41 and 43 °C. This is higher than the ambient air temperature, but generally this is expected for closed, uninsulated concrete block rooms in hot climates.

6.4.2 Closed cavity concrete block walls

This is a cavity wall concrete block construction. The width of the cavity is 50 mm, and the width of the leaves is 100 mm each. Figure (6.5) shows the simulated temperature variations, in an east-facing closed cavity wall. Comparing

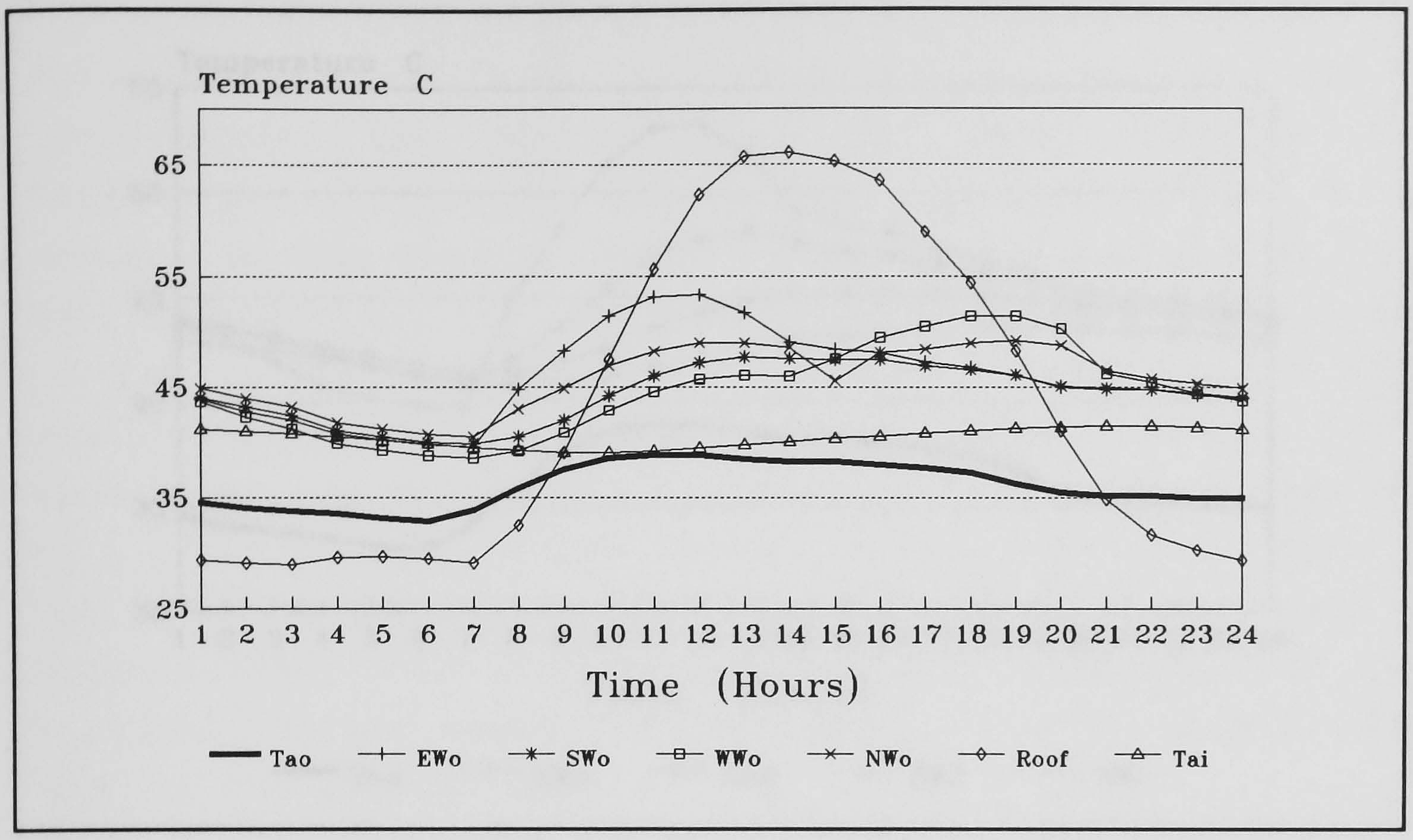

Figure 6.2: The simulated temperature variations of the external surfaces of a room with concrete block walls, through a 24-hour period, using the weather data for Muscat on 17-6-88.

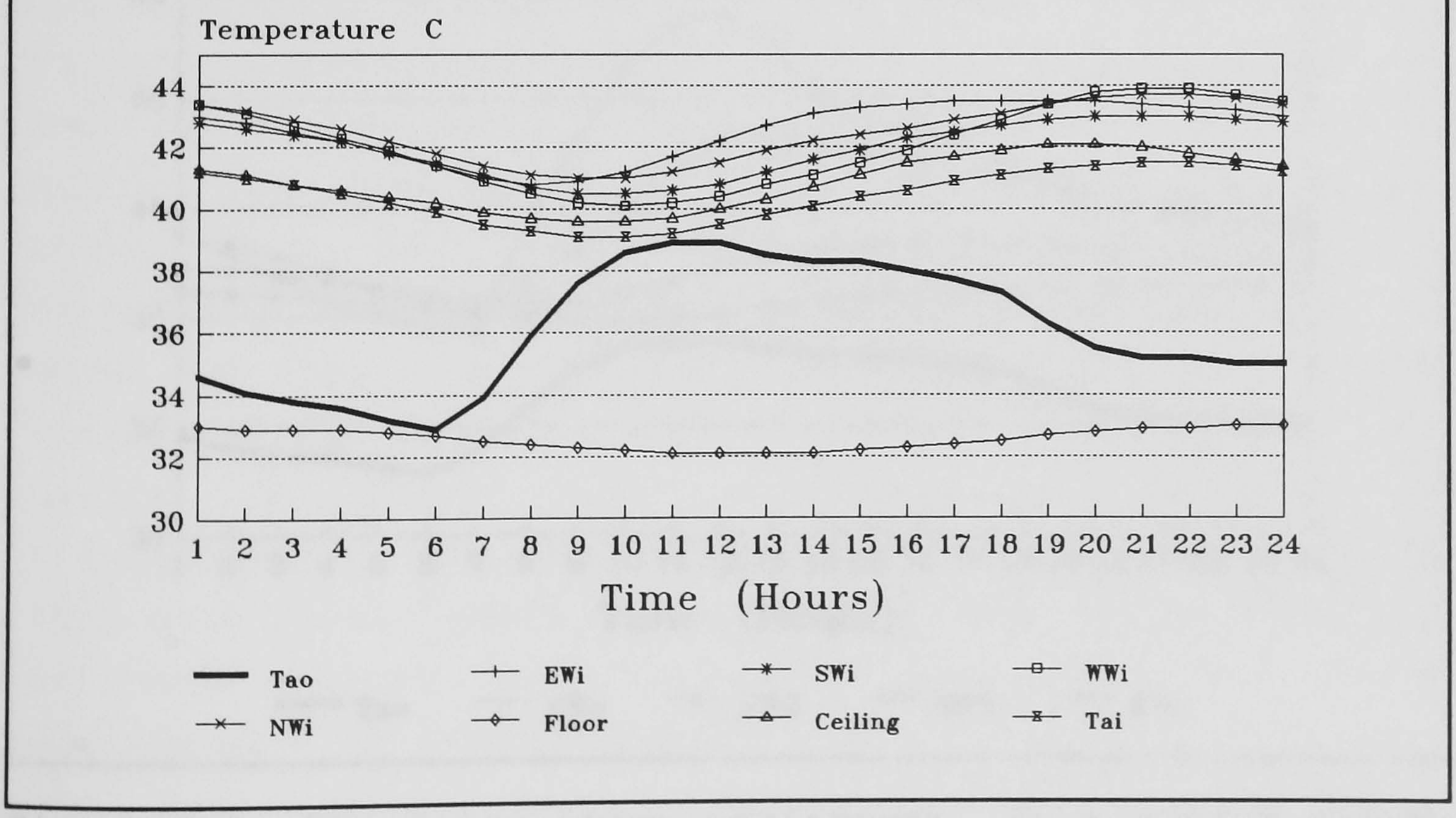

Figure 6.3: The simulated temperature variations of the internal surfaces of a room with concrete block walls, through a 24-hour period, using the weather data for Muscat on 17-6-88.

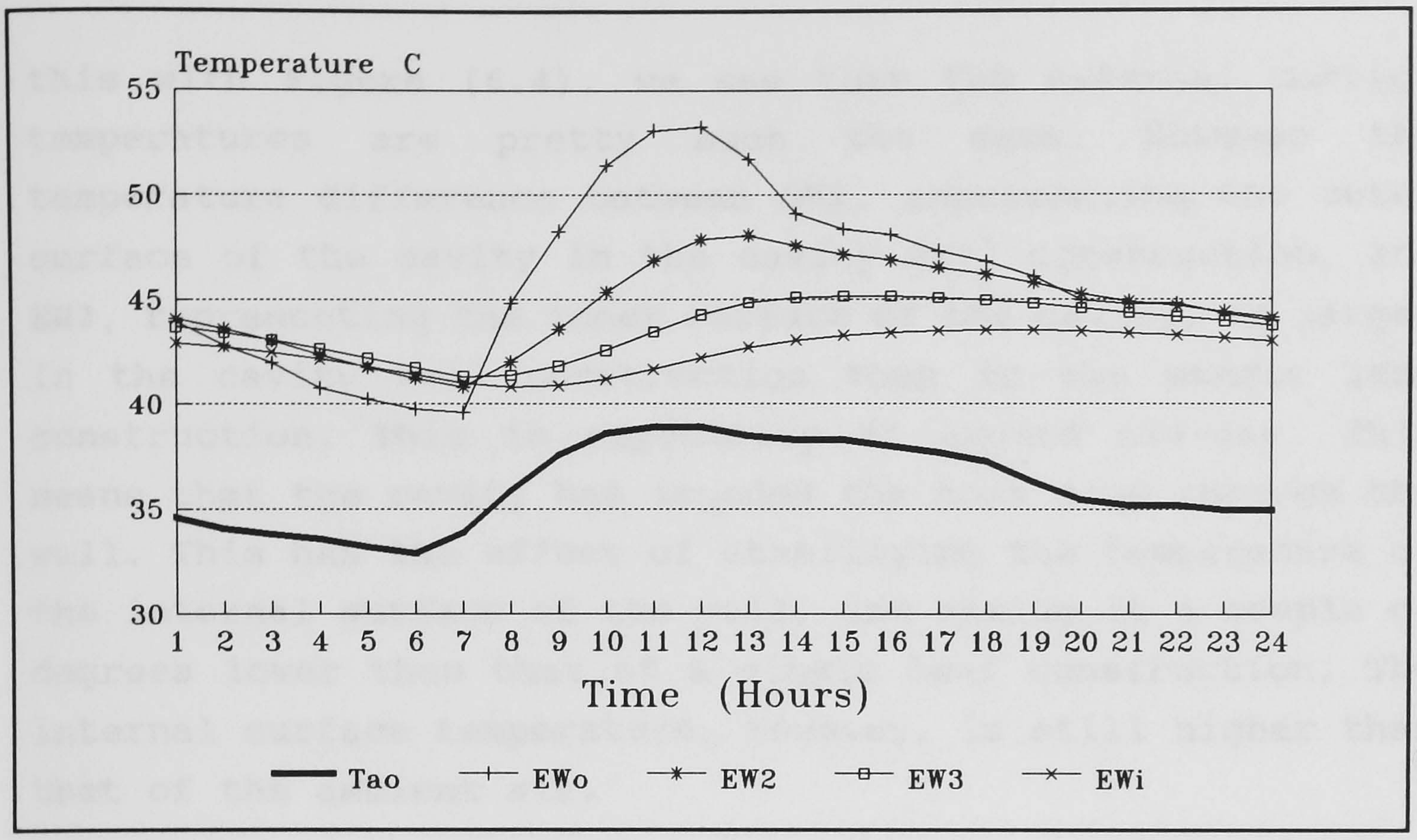

Figure 6.4: The temperature variations, in a single leaf concrete block wall, facing east, through a 24-hour period, using the weather data for Muscat on 17-6-1988.

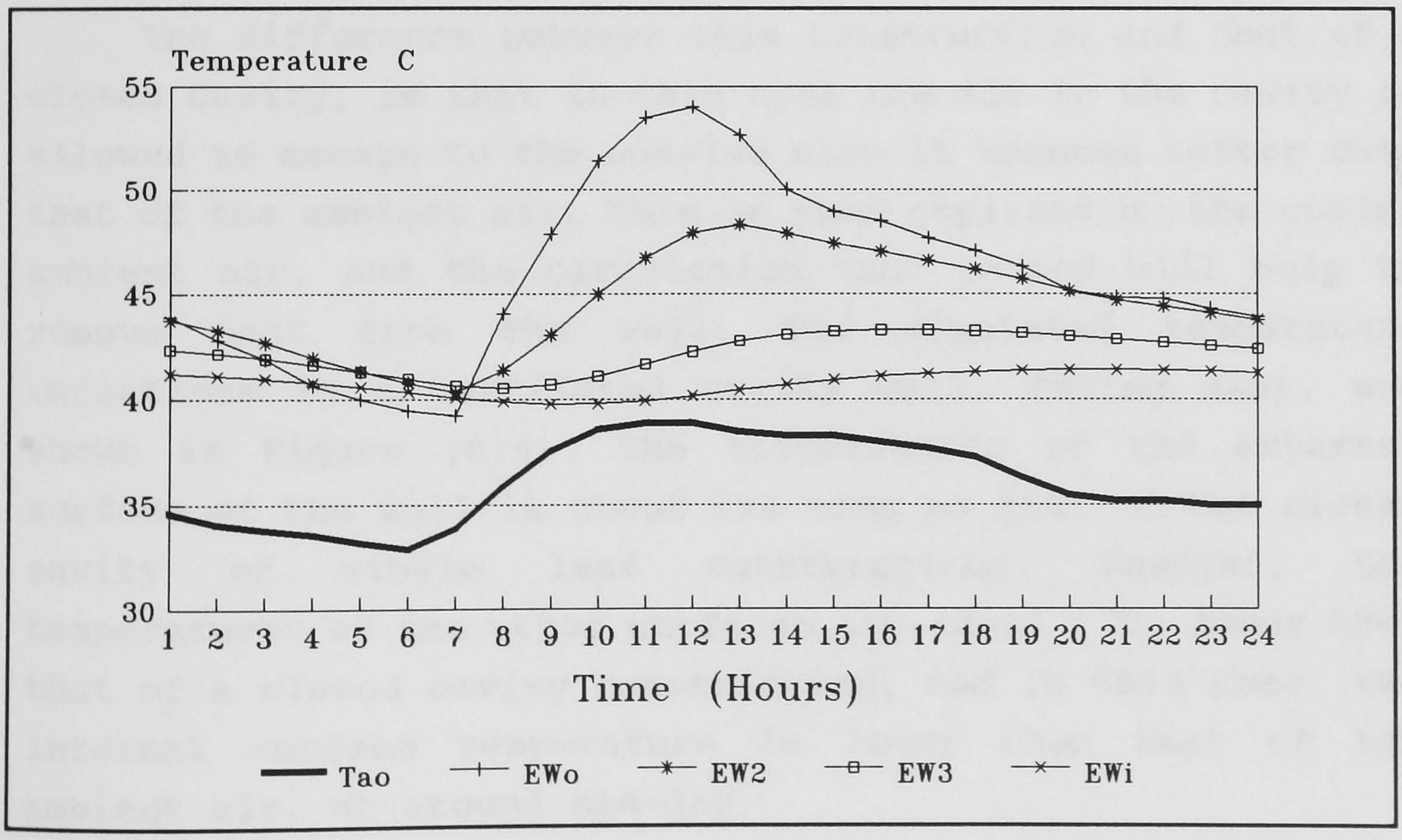

Figure 6.5: The temperature variations, in a **closed cavity** concrete block wall, facing east, through a 24-hour period, using the weather data for Muscat on 17-6-1988.

this with Figure (6.4), we see that the external surface temperatures are pretty much the same. However the temperature difference between **EW2**, representing the outer surface of the cavity in the cavity wall construction, and **EW3**, representing the inner surface of the cavity, is larger in the cavity wall construction than in the single leaf construction. This is especially at around mid-day. This means that the cavity has impeded the heat flow through the wall. This has the effect of stabilizing the temperature of the internal surface of the wall, and making it a couple of degrees lower than that of a single leaf construction. The internal surface temperature, however, is still higher than that of the ambient air.

6.4.3 Ventilated cavity concrete block walls

The difference between this construction and that of a closed cavity, is that in this case the air in the cavity is allowed to escape to the outside when it becomes hotter than that of the ambient air. This is then replaced by the cooler ambient air, and the circulation thus caused will help to remove heat from the wall. The simulated temperature variations in a ventilated cavity wall, facing east, are shown in Figure (6.6). The temperatures of the external surface of the wall is about the same as that of the closed cavity or single leaf constructions. However, the temperatures of the other surfaces are about 2 °C, lower than that of a closed cavity construction, and in this case, the internal surface temperature is lower than that of the ambient air, at around mid-day.

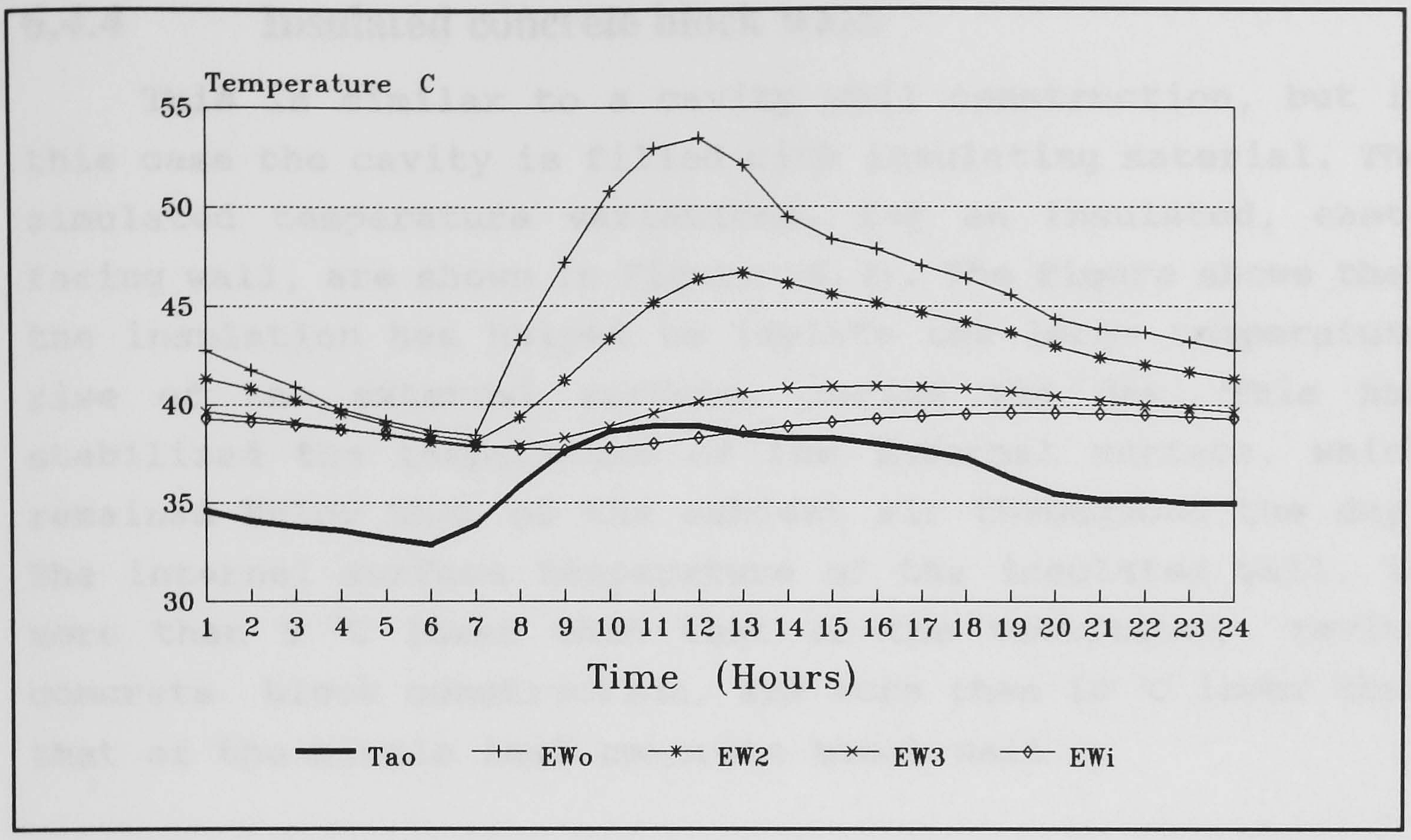

Figure 6.6: The temperature variations, in a **ventilated cavity** concrete block wall, facing east, through a 24-hour period, using the weather data for Muscat on 17-6-1988.

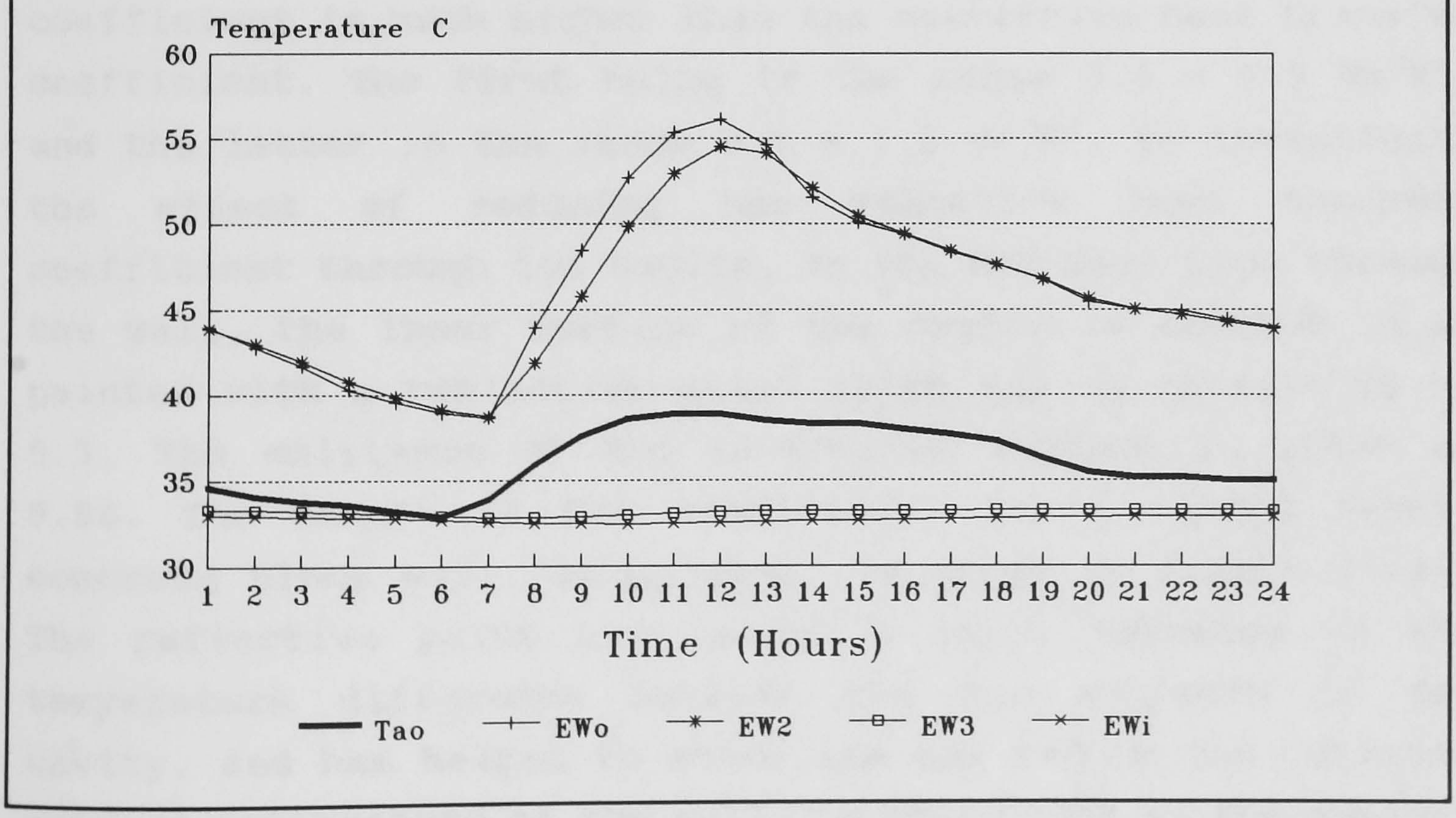

Figure 6.7: The temperature variations, in an **insulated cavity** concrete block wall, facing east, through a 24-hour period, using the weather data for Muscat on 17-6-1988.

6.4.4 Insulated concrete block walls

This is similar to a cavity wall construction, but in this case the cavity is filled with insulating material. The simulated temperature variations, for an insulated, east-facing wall, are shown in Figure (6.7). The Figure shows that the insulation has helped to isolate the large temperature rise of the external surface, during the day. This has stabilized the temperature of the internal surface, which remained below that of the ambient air throughout the day. The internal surface temperature of the insulated wall, is more than 5 °C lower than that of the ventilated cavity concrete block construction, and more than 10 °C lower than that of the single leaf concrete block wall.

6.4.5 The effect of reducing the radiative heat transfer through the cavity

In the analysis of the closed and ventilated cavity wall construction, it was noticed that the radiative heat transfer coefficient is much higher than the convective heat transfer coefficient. The first being in the range 5.0 - 5.5 $Wm^{-2}K^{-1}$, and the latter in the range 0.5 - 1.5 $Wm^{-2}K^{-1}$. To investigate the effect of reducing the radiative heat transfer coefficient through the cavity, on the net heat flow through the wall, the inner surface of the cavity is assumed to be painted with a reflective paint which has an emissivity of 0.3. The emittance of the un-treated surface is taken as 0.86. The result of the simulation, for a closed cavity concrete block wall facing east, is shown in Figure (6.8). The reflective paint has caused a large increase in the temperature difference between the two surfaces of the cavity, and has helped to stabilize and reduce the internal surface temperature of the wall, to below that of the ambient air at around mid-day. A similar improvement is achieved in the ventilated cavity construction, see Figure (6.9), where

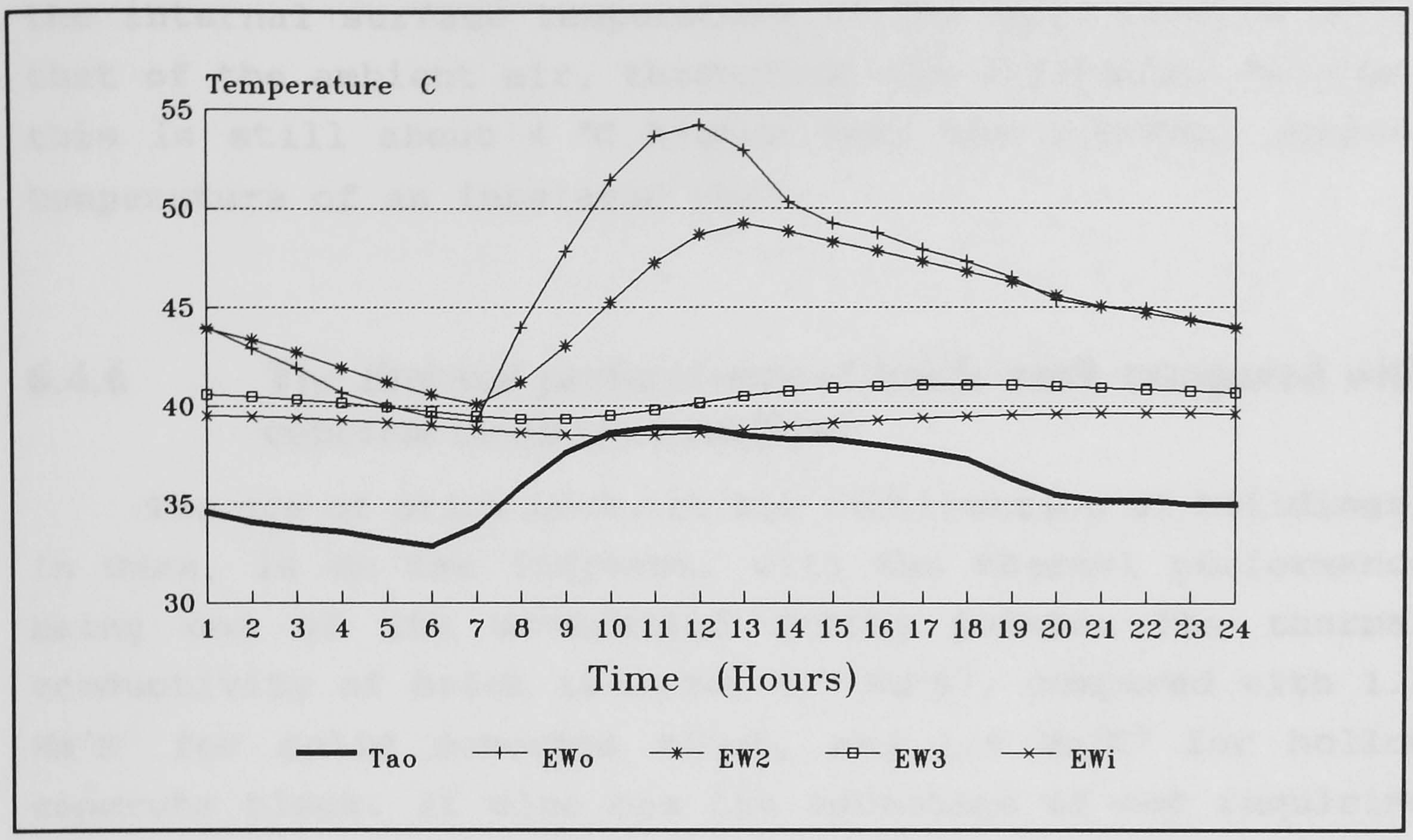

Figure 6.8: The temperature variations, in a **closed cavity** concrete block wall, facing east, through a 24-hour period, using the weather data of June. The emissivity of the inner leaf in the cavity is taken as 0.3.

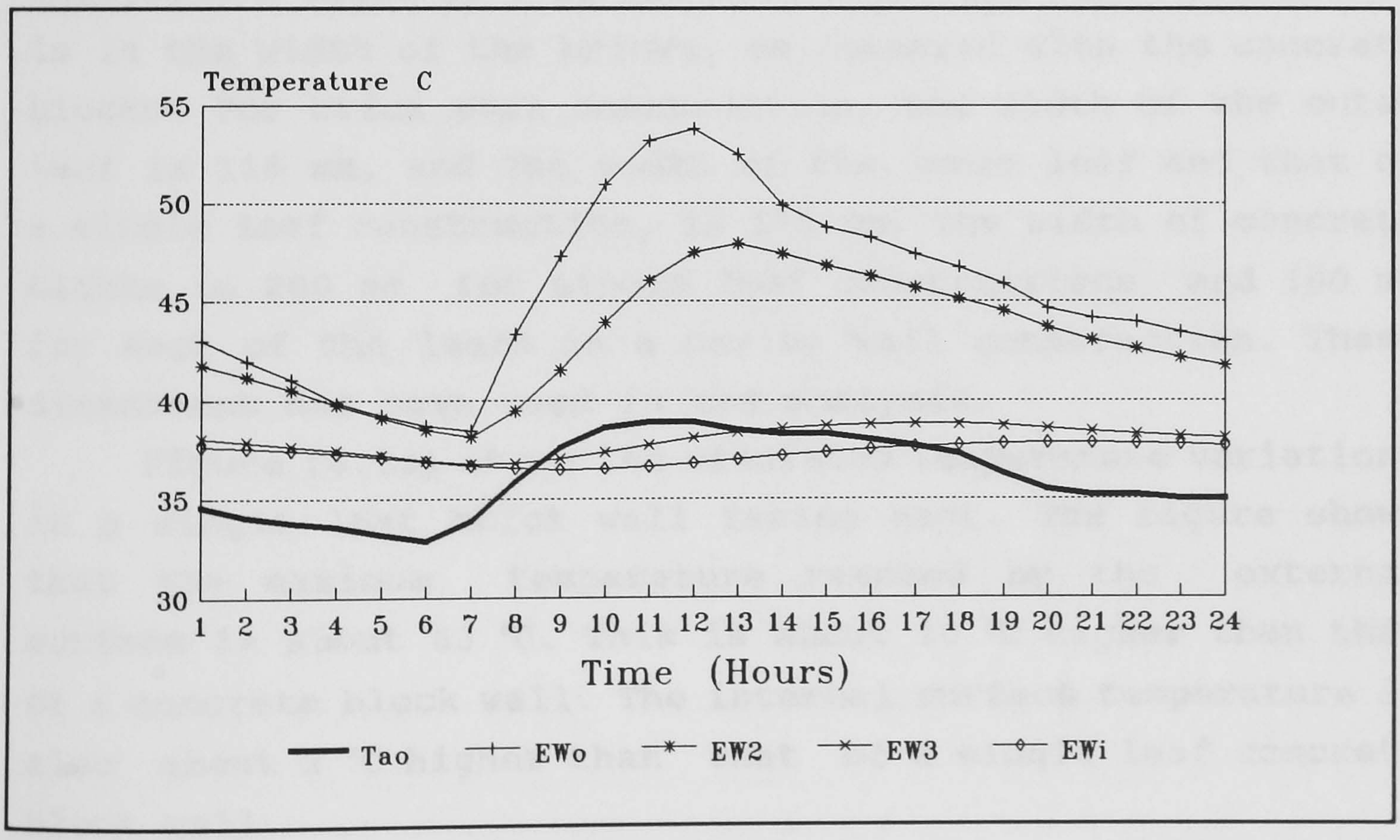

Figure 6.9: The temperature variations, in a **ventilated cavity** concrete block wall, facing east, through a 24-hour period, using the weather data of June. The emissivity of the inner leaf in the cavity is taken as 0.3.

the internal surface temperature of the wall remains below that of the ambient air, throughout the afternoon. However, this is still about 4 °C higher than the internal surface temperature of an insulated wall.

6.4.6 The thermal performance of brick work compared with concrete block constructions

The use of brick work for the construction of buildings, in Oman, is on the increase, with the thermal performance being one of its advertised strong points. The thermal conductivity of brick is about 0.7 $Wm^{-1}K^{-1}$, compared with 1.1 $Wm^{-1}K^{-1}$ for solid concrete block, and 1.0 $Wm^{-1}K^{-1}$ for hollow concrete block. It also has the advantage of not requiring external treatment, i.e. plastering and painting (the economics of this is discussed later in Chapter 8). But as mentioned earlier, bricks have a much higher absorptivity to solar radiation than white painted surfaces, and for this analysis, a value of 0.65 has been used. The other difference is in the width of the bricks, as compared with the concrete blocks. For brick work construction, the width of the outer leaf is 115 mm, and the width of the inner leaf and that of a single leaf construction, is 175 mm. The width of concrete blocks is 200 mm for single leaf constructions, and 100 mm for each of the leafs in a cavity wall construction. These dimensions has been used in the analysis.

Figure (6.10) shows the simulated temperature variations in a single leaf brick wall facing east. The figure shows that the maximum temperature reached by the external surface is about 63 °C. This is about 10 °C higher than that of a concrete block wall. The internal surface temperature is also about 2 °C higher than that of a single leaf concrete block wall.

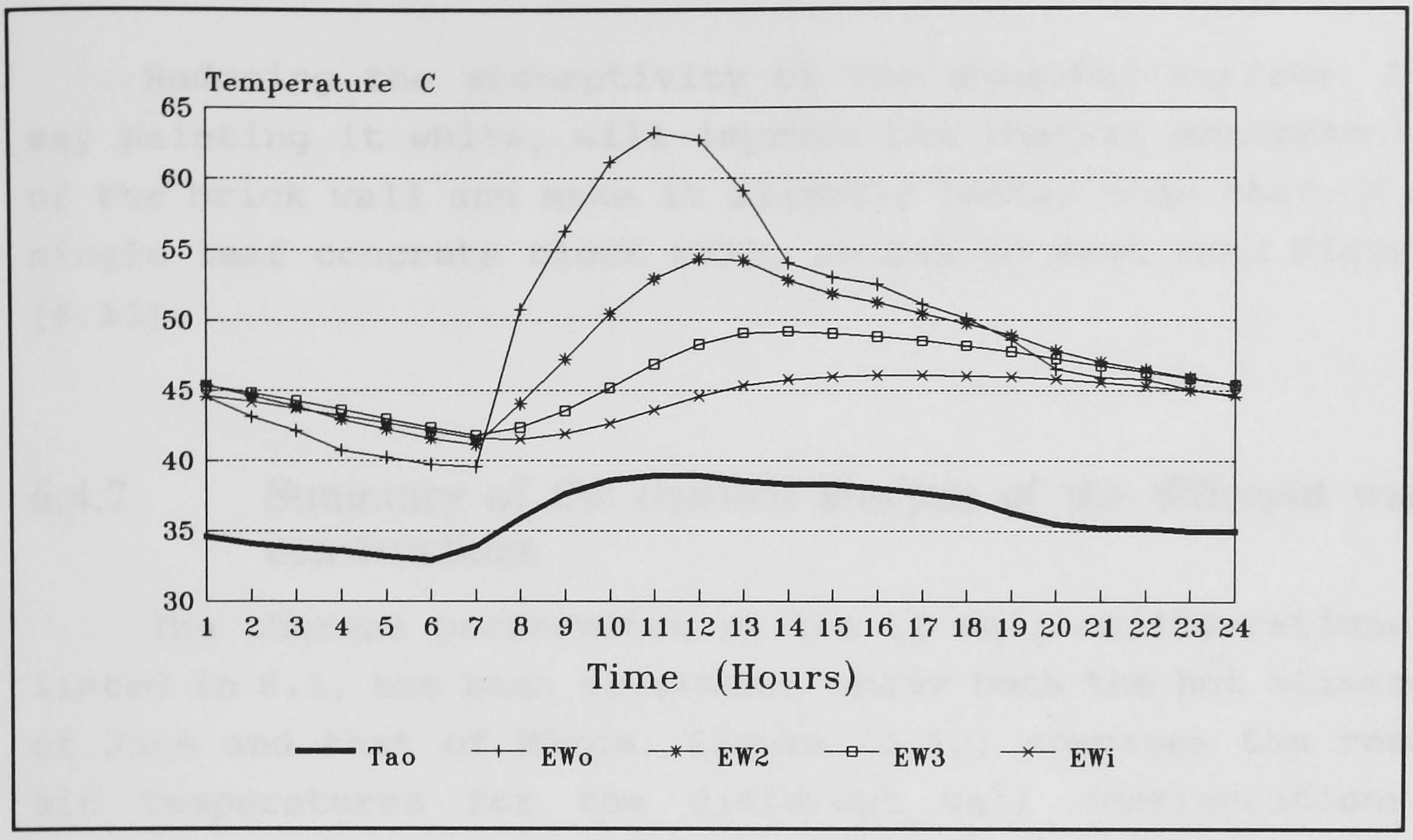

Figure 6.10: The temperature variations in a single leaf brick wall facing east, the external surface of which has an absorpattivity of 0.65.

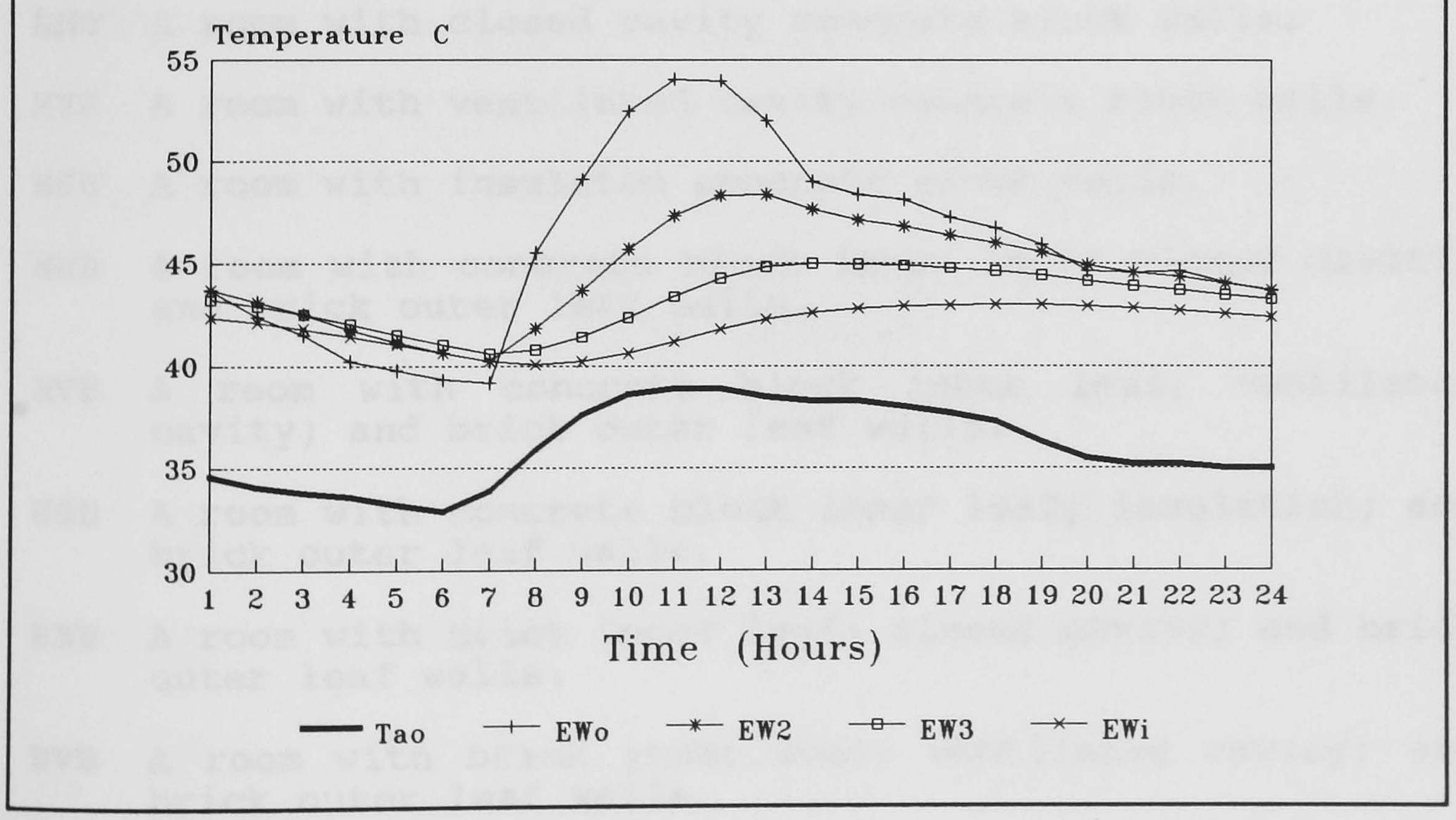

Figure 6.11: The temperature variations in a single leaf brick wall facing east, the external surface of which has an absorpattivity of 0.36.

Reducing the absorptivity of the external surface, by say painting it white, will improve the thermal performance of the brick wall and make it slightly better than that of a single leaf concrete block wall, as can be seen from Figure (6.11).

6.4.7 Summary of the thermal analysis of the different wall constructions

The thermal performance of the 11 wall configurations, listed in 6.1, has been simulated, under both the hot climate of June and that of March. Figure (6.12) compares the room air temperatures for the different wall configurations, simulated under the weather data of June. The abbreviations used in the figure has the following meanings:

Tao The ambient air temperature.

H A room with single leaf concrete block walls.

HNH A room with closed cavity concrete block walls.

HVH A room with ventilated cavity concrete block walls.

HSH A room with insulated concrete block walls.

HNB A room with concrete block inner leaf; closed cavity; and brick outer leaf walls.

HVB A room with concrete block inner leaf; ventilated cavity; and brick outer leaf walls.

HSB A room with concrete block inner leaf; insulation; and brick outer leaf walls.

BNB A room with brick inner leaf; closed cavity; and brick outer leaf walls.

BVB A room with brick inner leaf; ventilated cavity; and brick outer leaf walls.

BSB A room with brick inner leaf; insulation; and brick outer leaf walls.

B A room with single leaf brick walls.

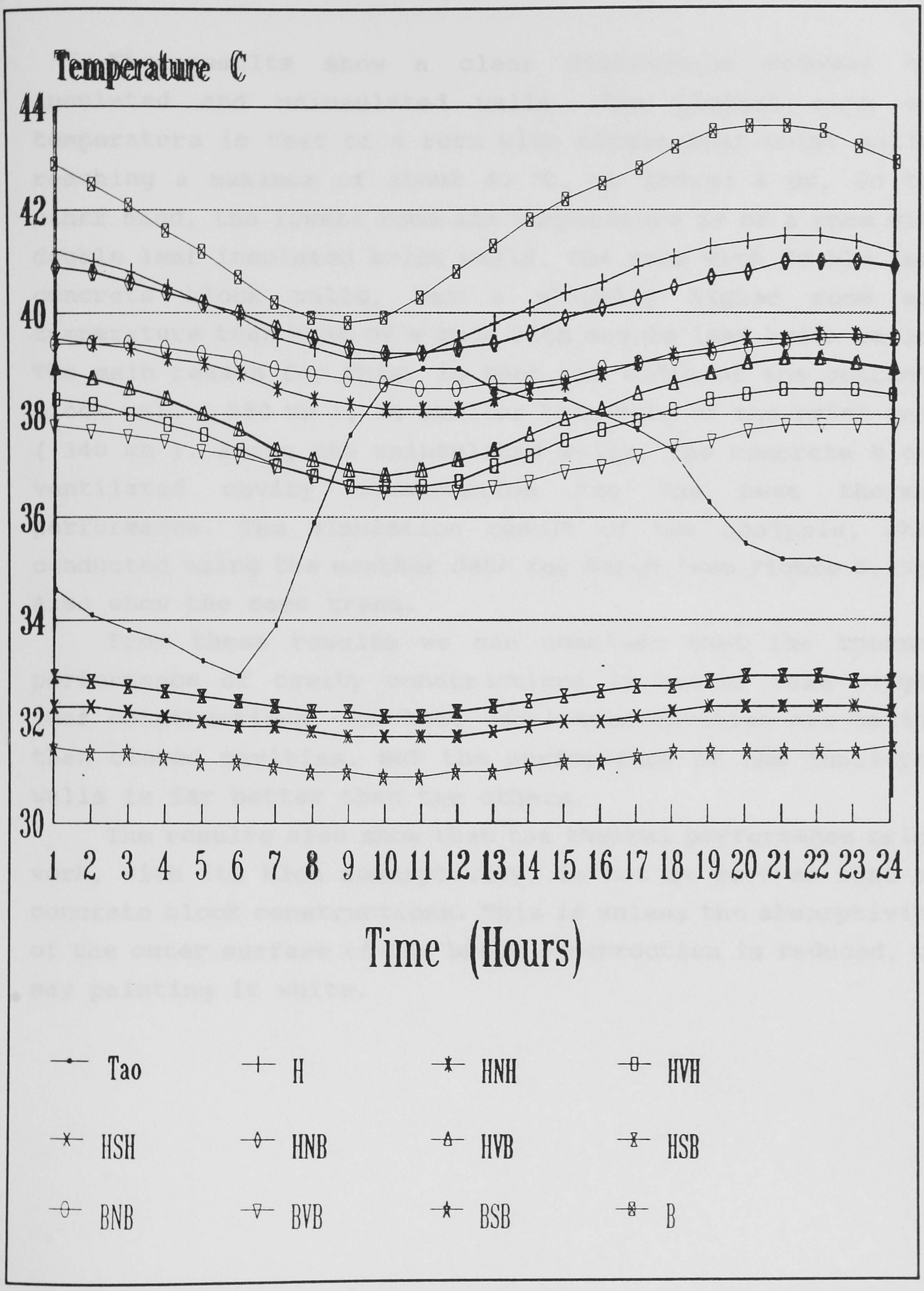

Figure 6.12: A comparison of the effectiveness of the different wall construction, in maintaining a low room air temperature, when simulated using the weather data for Muscat on 17-6-88.

The results show a clear distinction between the insulated and uninsulated walls. The highest room air temperature is that of a room with single leaf brick walls, reaching a maximum of about 43 °C, at around 8 pm. On the other hand, the lowest room air temperature is of a room with double leaf insulated brick walls. The room with double leaf concrete block walls, has a slightly higher room air temperature than that of a room with double leaf brick walls. The main reason for this, is that the width of the concrete block wall (250 mm), is smaller than that of the brick wall (340 mm). Among the uninsulated walls, the concrete block ventilated cavity construction has the best thermal performance. The simulation result of the analysis, when conducted using the weather data for March (see Figure 6.13), also show the same trend.

From these results we can conclude that the thermal performance of cavity constructions is better than single leaf constructions, and that ventilated cavities are better than closed cavities. But the performance of the insulated walls is far better than the others.

The results also show that the thermal performance brick work, with its high absorptivity, is not as good as that of concrete block constructions. This is unless the absorptivity of the outer surface of the brick construction is reduced, by say painting it white.

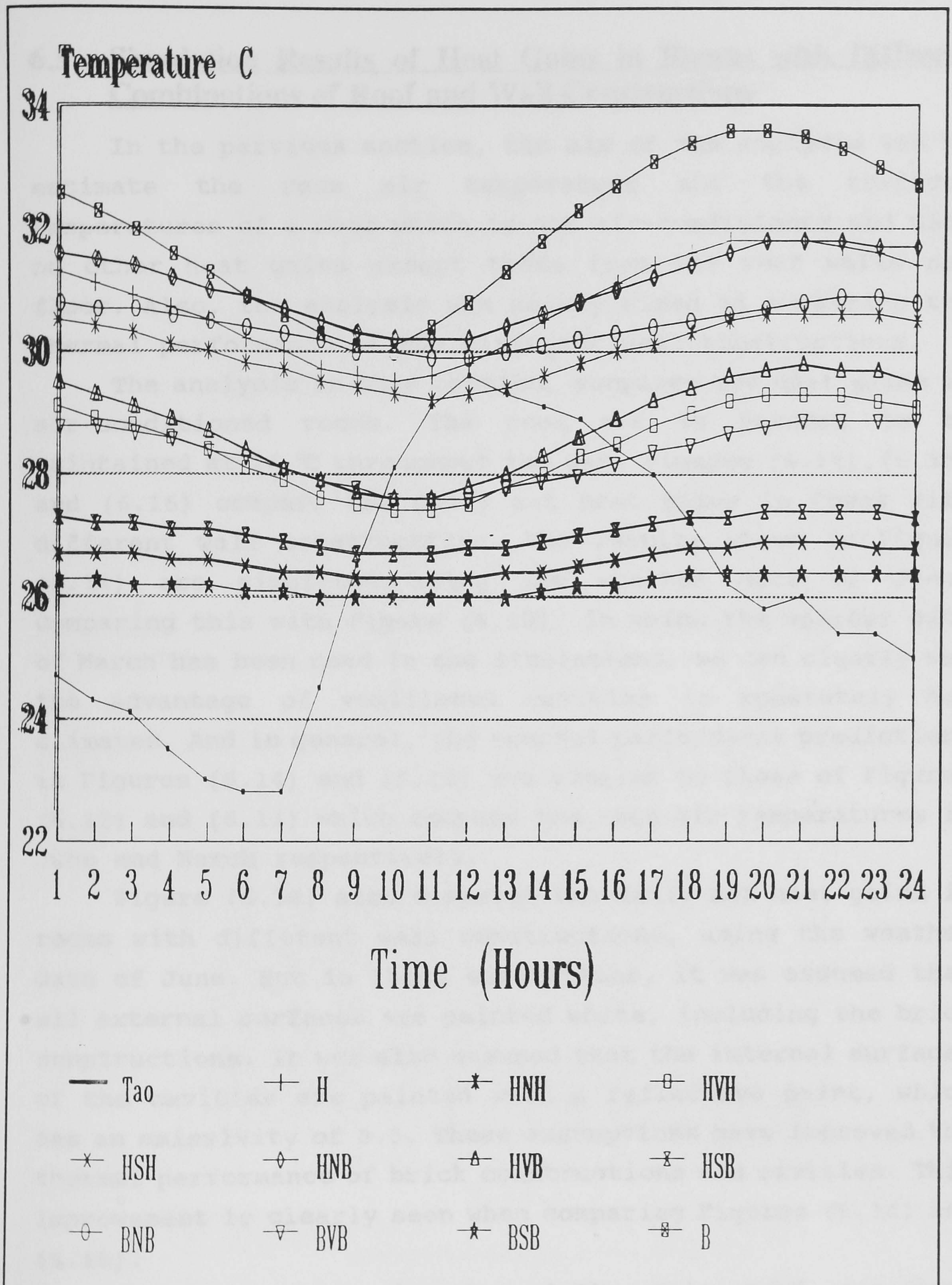

Figure 6.13: A comparison of the effectiveness of the different wall construction, in maintaining a low room air temperature, when simulated using the weather data for Muscat on 21-3-88.

6.5 Simulation Results of Heat Gains in Rooms with Different Combinations of Roof and Wall Constructions

In the pervious section, the aim of the analysis was to estimate the room air temperature and the surfaces temperatures of a room which is not air-conditioned and with no other heat gains except those from the roof walls and floor. Also, the analysis was mainly aimed at comparing the thermal performance of the different wall constructions.

The analysis in this section, compares the heat gains in air-conditioned rooms. The room air is assumed to be maintained at 26 °C throughout the day. Figures (6.14),(6.15) and (6.16) compare the daily net heat gains in rooms with different wall constructions. The results shown in Figure (6.14) are simulated using the weather data of June. Comparing this with Figure (6.15), in which the weather data of March has been used in the simulations, we can clearly see the advantage of ventilated cavities in moderately hot climates. And in general, the thermal performance predictions in Figures (6.14) and (6.15) are similar to those of Figures (6.12) and (6.13) which compare the room air temperatures in June and March respectively.

Figure (6.16) also compares the daily net heat gains in rooms with different wall constructions, using the weather data of June. But in these simulations, it was assumed that all external surfaces are painted white, including the brick constructions. It was also assumed that the internal surfaces of the cavities are painted with a reflective paint, which has an emissivity of 0.3. These assumptions have improved the thermal performance of brick constructions and cavities. This improvement is clearly seen when comparing Figures (6.14) and (6.16).

The hourly heat gains through the walls, roof, and floor of rooms with different wall constructions, are shown in Figures (6.17) - (6.20). Besides comparing the heat gains through the building elements of the rooms, the figures, for

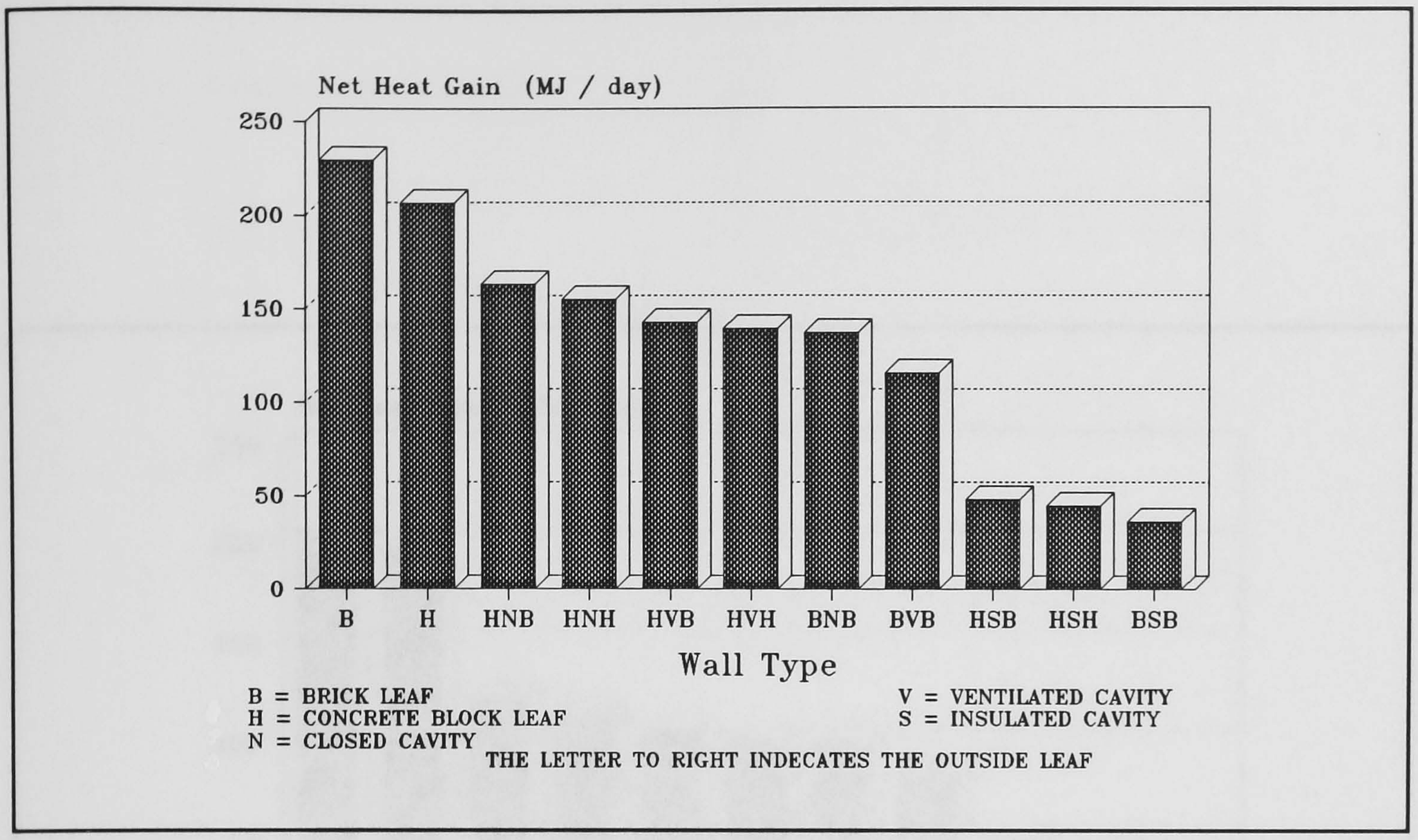

Figure 6.14: A comparison of the net daily heat gains for rooms with different wall constructions, simulated with the weather data of **June.**

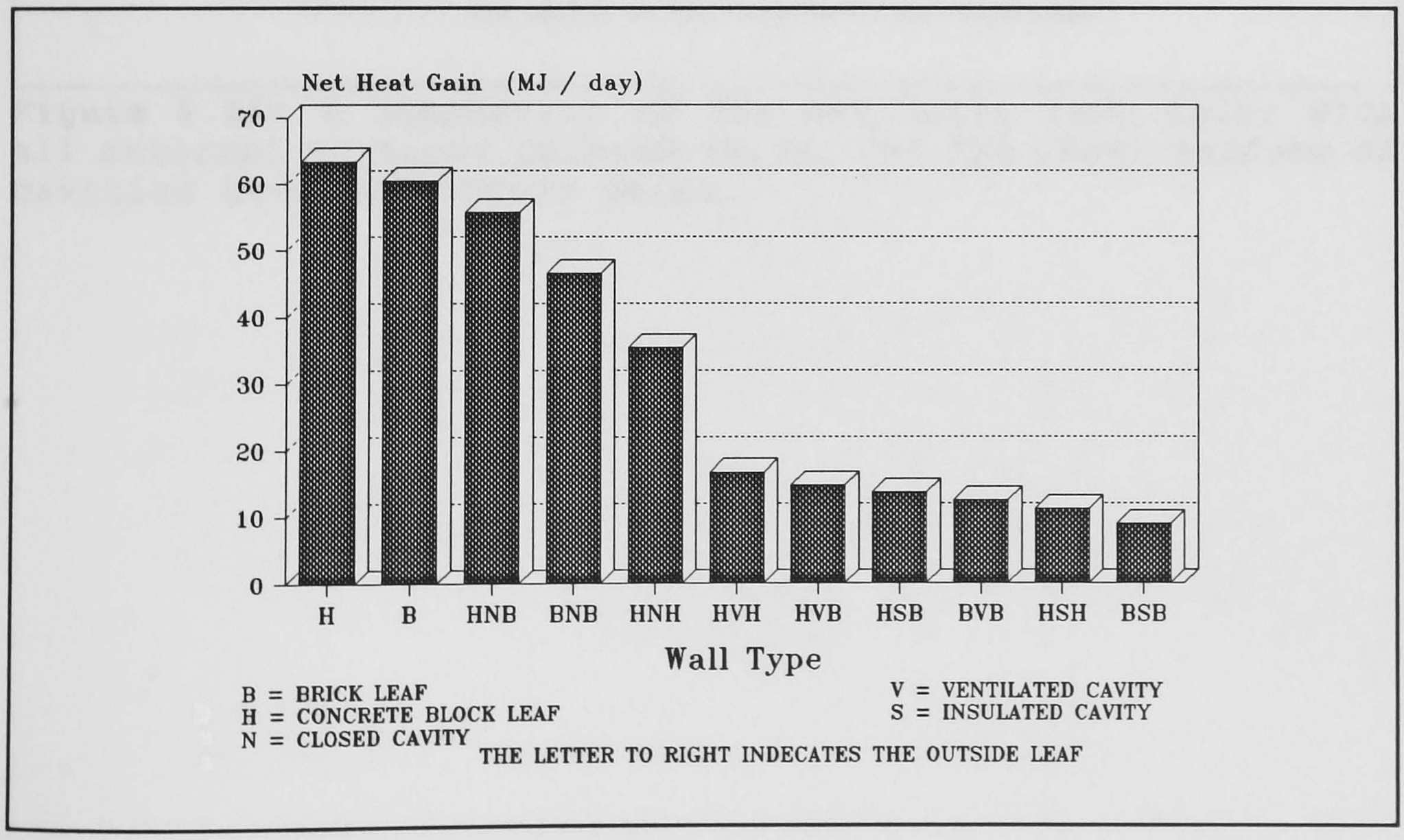

Figure 6.15: A comparison of the net daily heat gains for rooms with different wall constructions, simulated with the weather data of **March.**

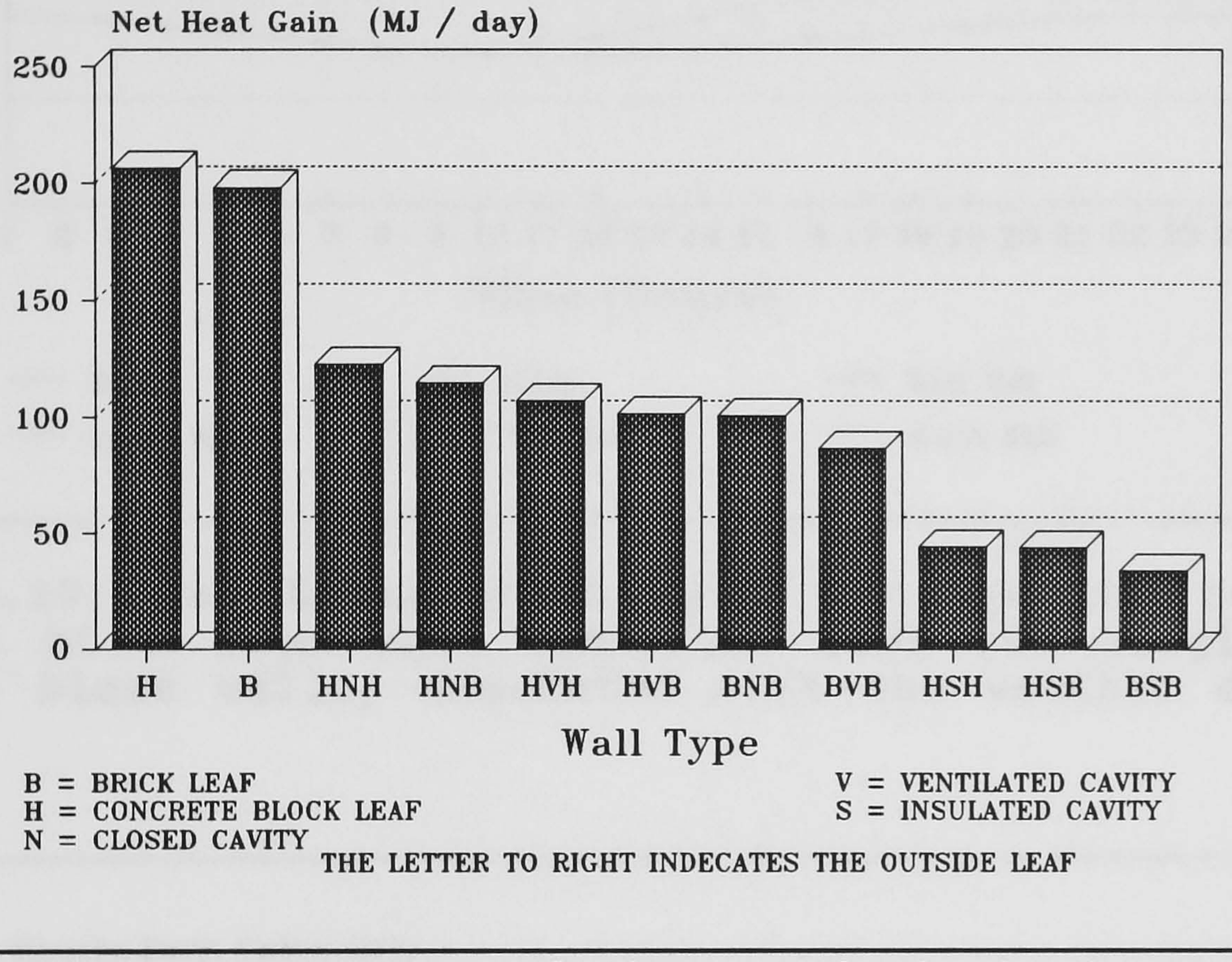

Figure 6.16: A comparison of the net daily heat gains with all external surfaces painted white, and the inner surface of cavities have reflective paint.

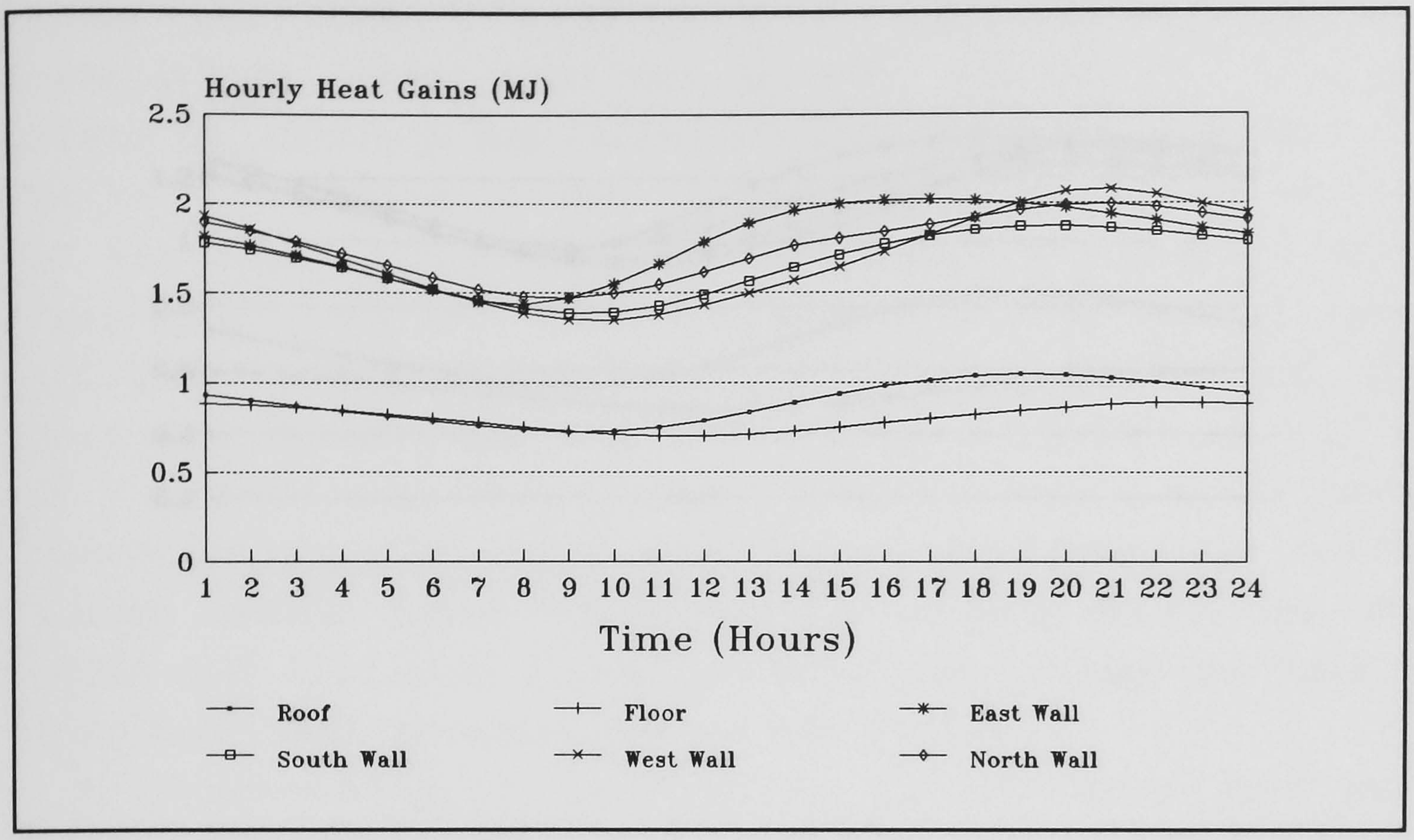

Figure 6.17: The hourly heat gains through the building elements of a room with insulated roof and **single leaf concrete block** walls, simulated with the weather data of June.

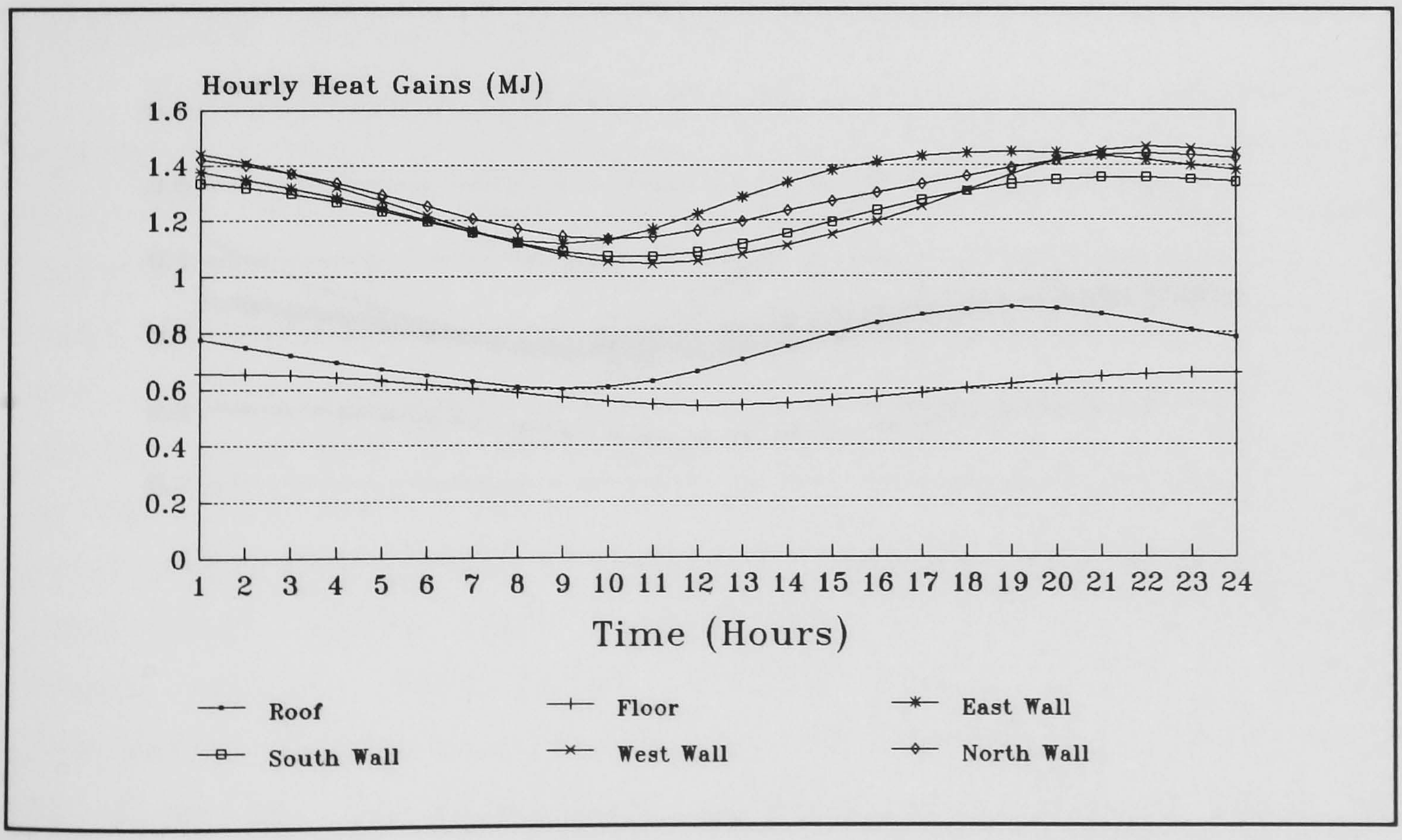

Figure 6.18: The hourly heat gains through the building elements of a room with insulated roof and **closed cavity concrete block** walls, simulated with the weather data of June.

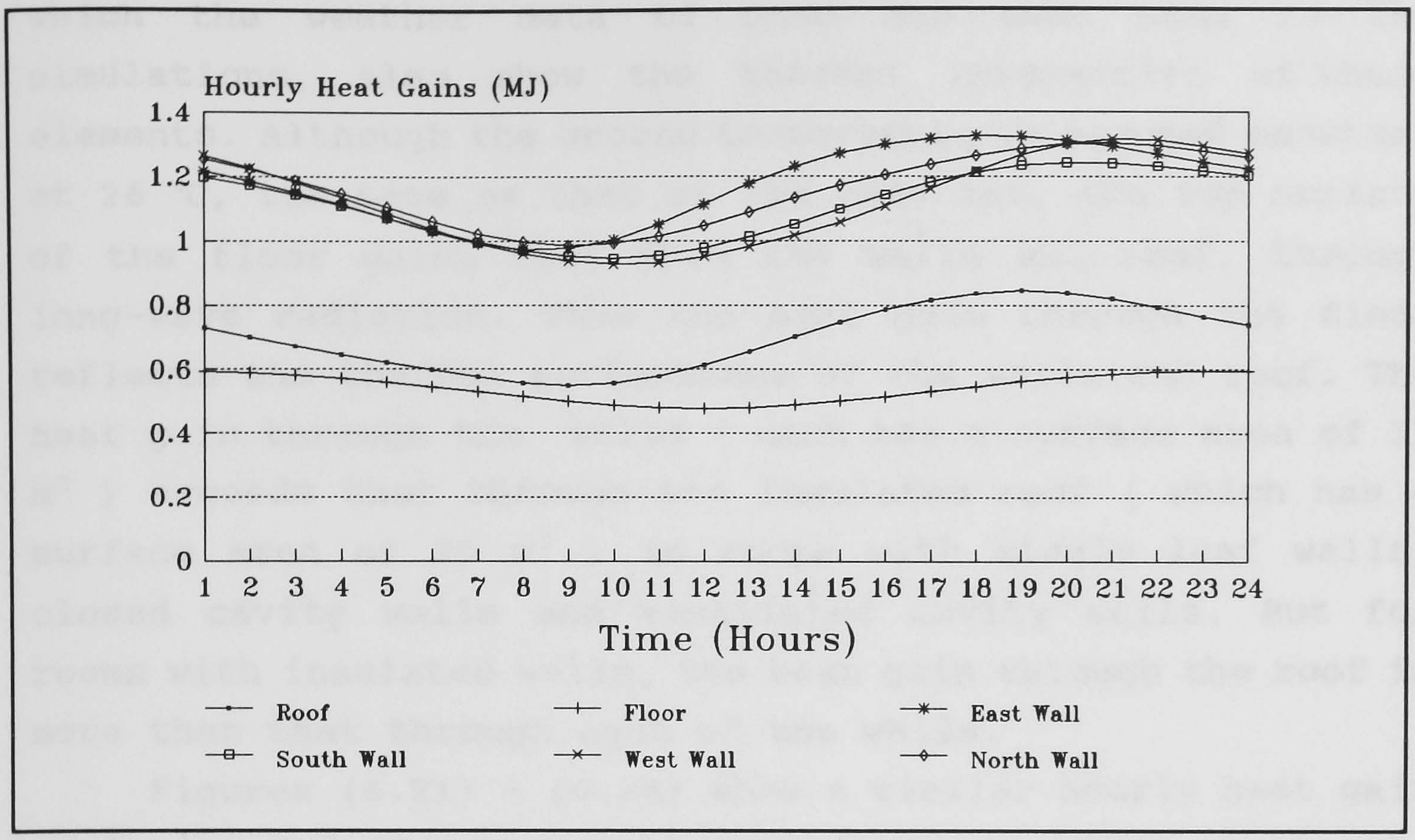

Figure 6.19: The hourly heat gains through the building elements of a room with insulated roof and **ventilated cavity concrete block** walls, simulated with the weather data of June.

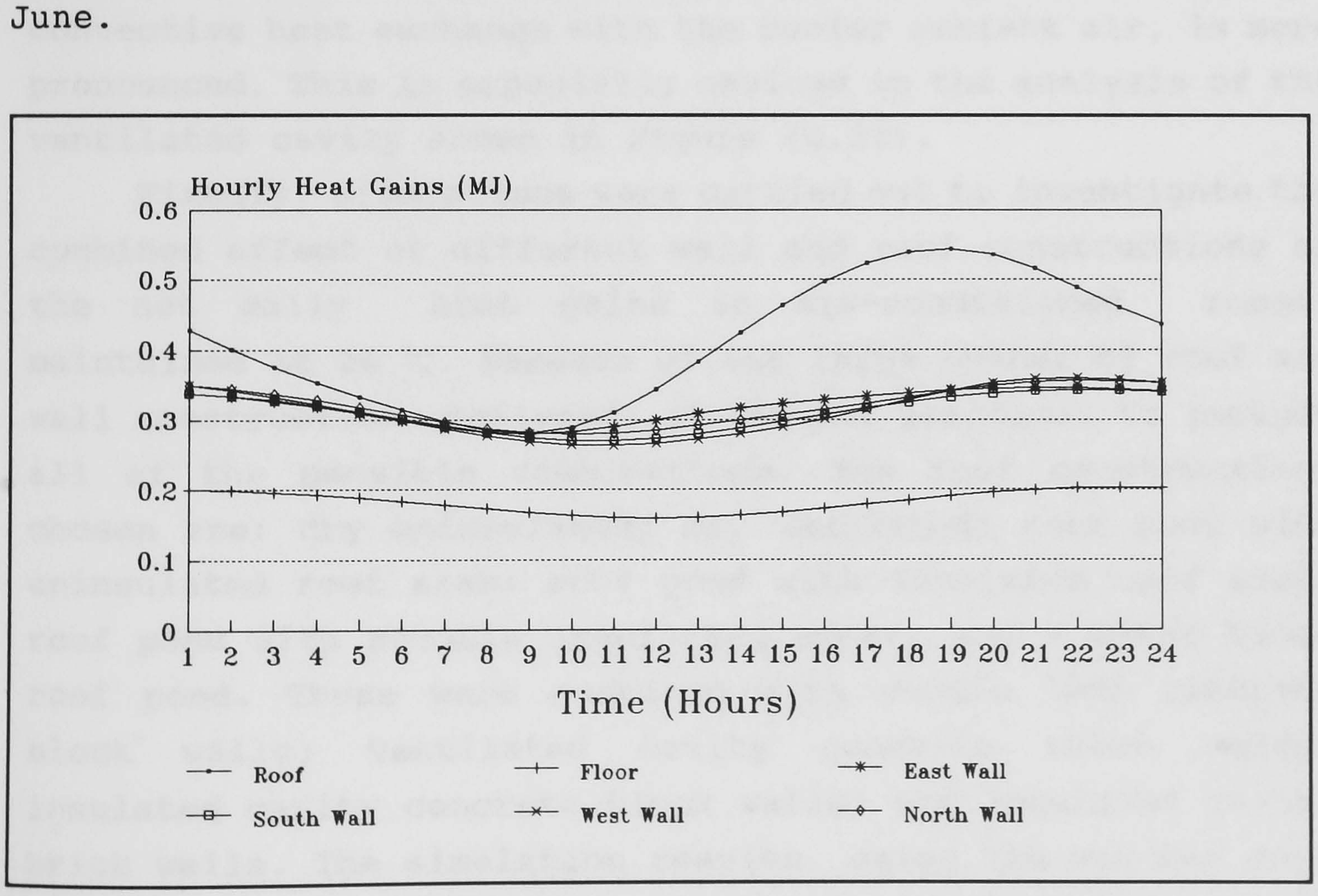

Figure 6.20: The hourly heat gains through the building elements of a room with insulated roof and **insulated cavity concrete block** walls, simulated with the weather data of June.

which the weather data of June has been used in the simulations, also show the thermal interaction of these elements. Although the ground temperature is assumed constant at 26 °C, the same as that of the room air, the top surface of the floor gains heat from the walls and roof, through long-wave radiation. Thus the heat gain through the floor reflects the thermal performance of the walls and roof. The heat gain through the walls (each has a surface area of 15 m^{-2}) exceeds that through the insulated roof (which has a surface area of 25 m^{-2}) in rooms with single leaf walls, closed cavity walls and ventilated cavity walls. But for rooms with insulated walls, the heat gain through the roof is more than that through each of the walls.

Figures (6.21) - (6.24) show a similar hourly heat gain analysis, for the four wall constructions above, using the weather data of March. In these figures, the effect "night cooling", due to the radiative heat exchange with the sky and convective heat exchange with the cooler ambient air, is more pronounced. This is especially obvious in the analysis of the ventilated cavity shown in Figure (6.23).

Finally, simulations were carried out to investigate the combined effect of different wall and roof constructions on the net daily heat gains in air-conditioned rooms, maintained at 26 °C. Because of the large number of roof and wall constructions analyzed, it was not practical to include all of the possible combinations. The roof constructions chosen are: dry uninsulated; dry insulated; roof pond with uninsulated roof slab; roof pond with insulated roof slab; roof pond with movable insulating cover; and a Water Diode roof pond. These were combined with single leaf concrete block walls; ventilated cavity concrete block walls; insulated cavity concrete block walls; and insulated cavity brick walls. The simulation results, using the weather data of June, are shown in Figure (6.25). The results show the big advantage of wall insulation in reducing the heat gain into the room, during the very hot weather. Also the combination

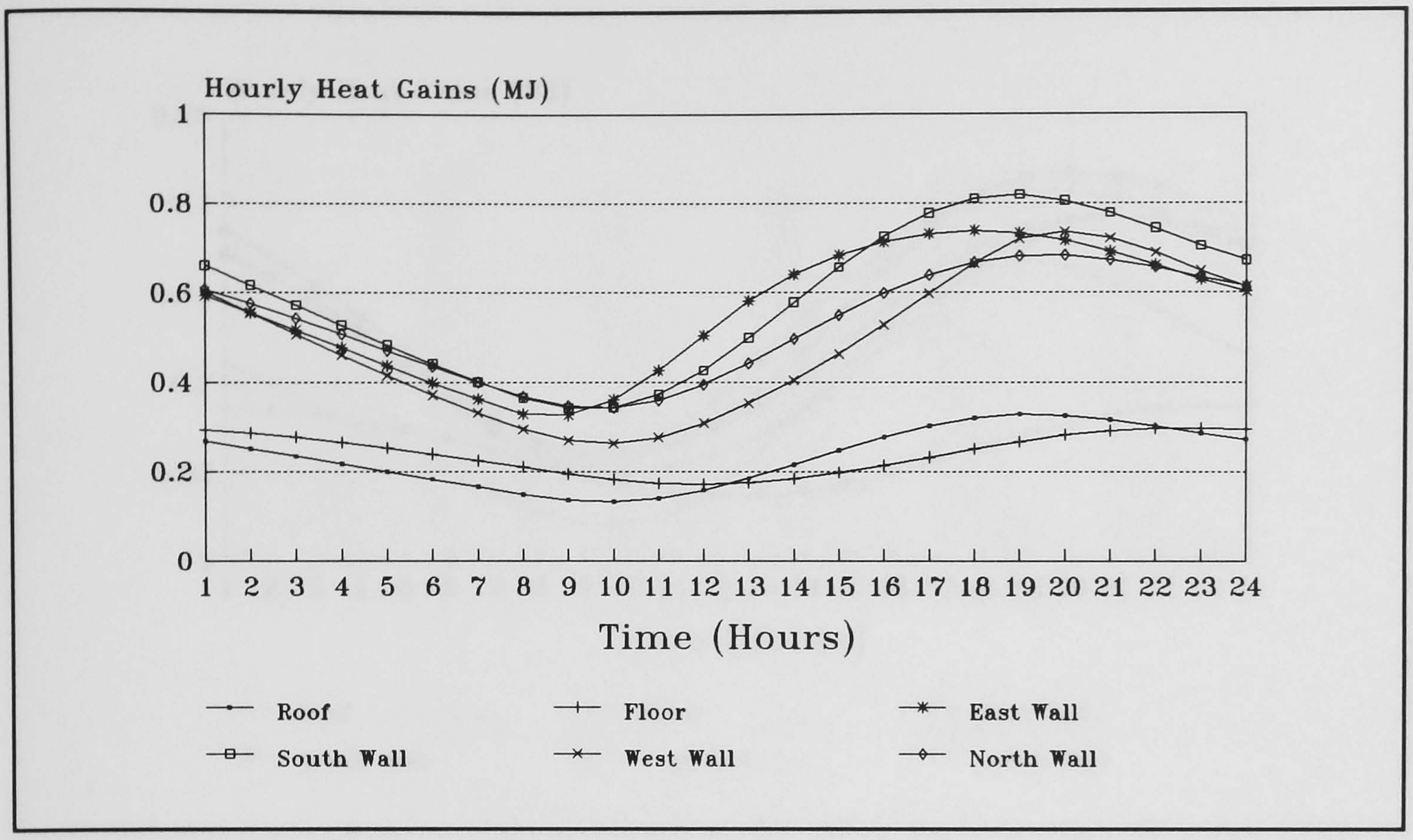

Figure 6.21: The hourly heat gains through the building elements of a room with insulated roof and **single leaf concrete block** walls, simulated with the weather data of March.

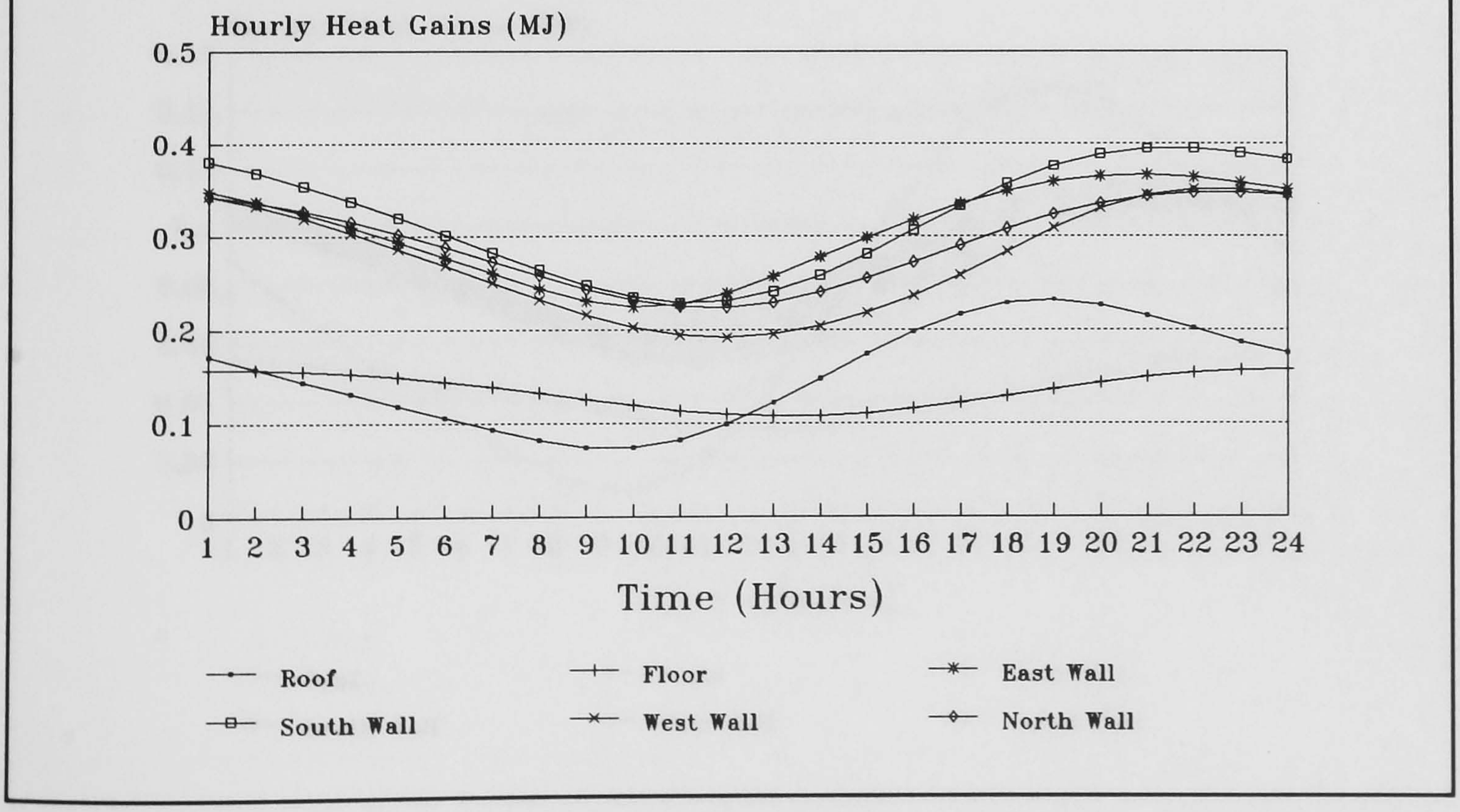

Figure 6.22: The hourly heat gains through the building elements of a room with insulated roof and **closed cavity concrete block** walls, simulated with the weather data of March.

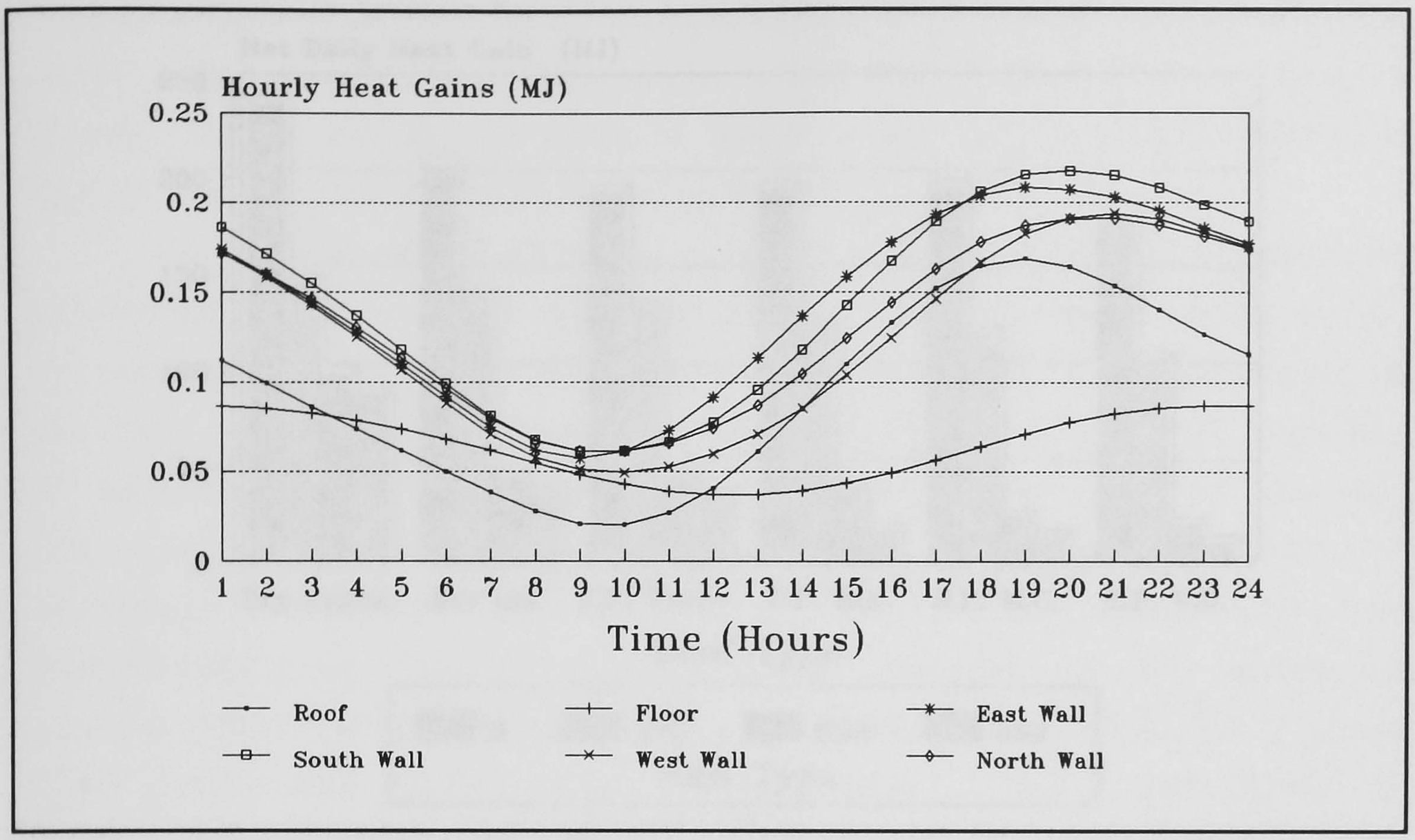

Figure 6.23: The hourly heat gains through the building elements of a room with insulated roof and **ventilated cavity concrete block** walls, simulated with the weather data of March.

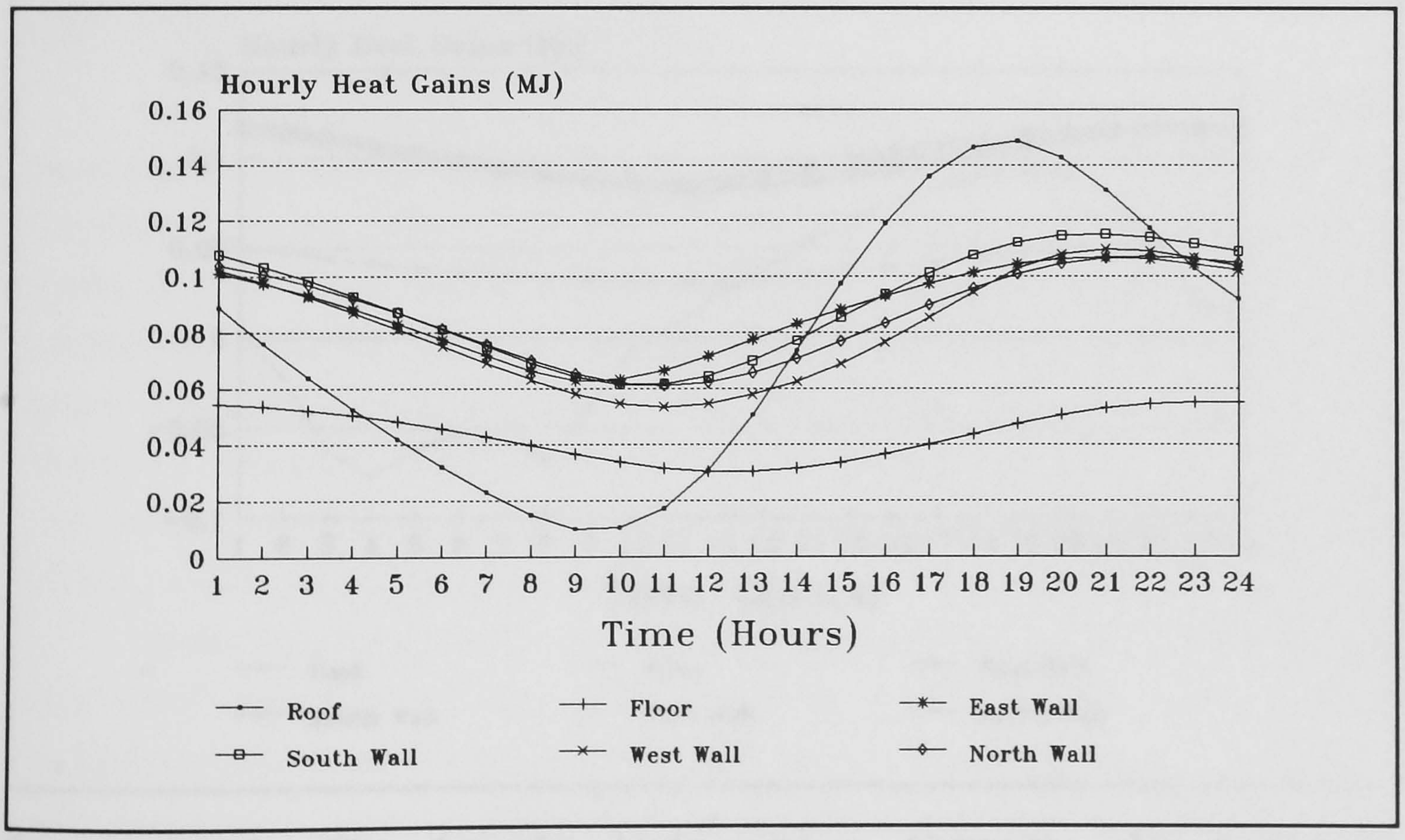

Figure 6.24: The hourly heat gains through the building elements of a room with insulated roof and **insulated cavity concrete block** walls, simulated with the weather data of March.

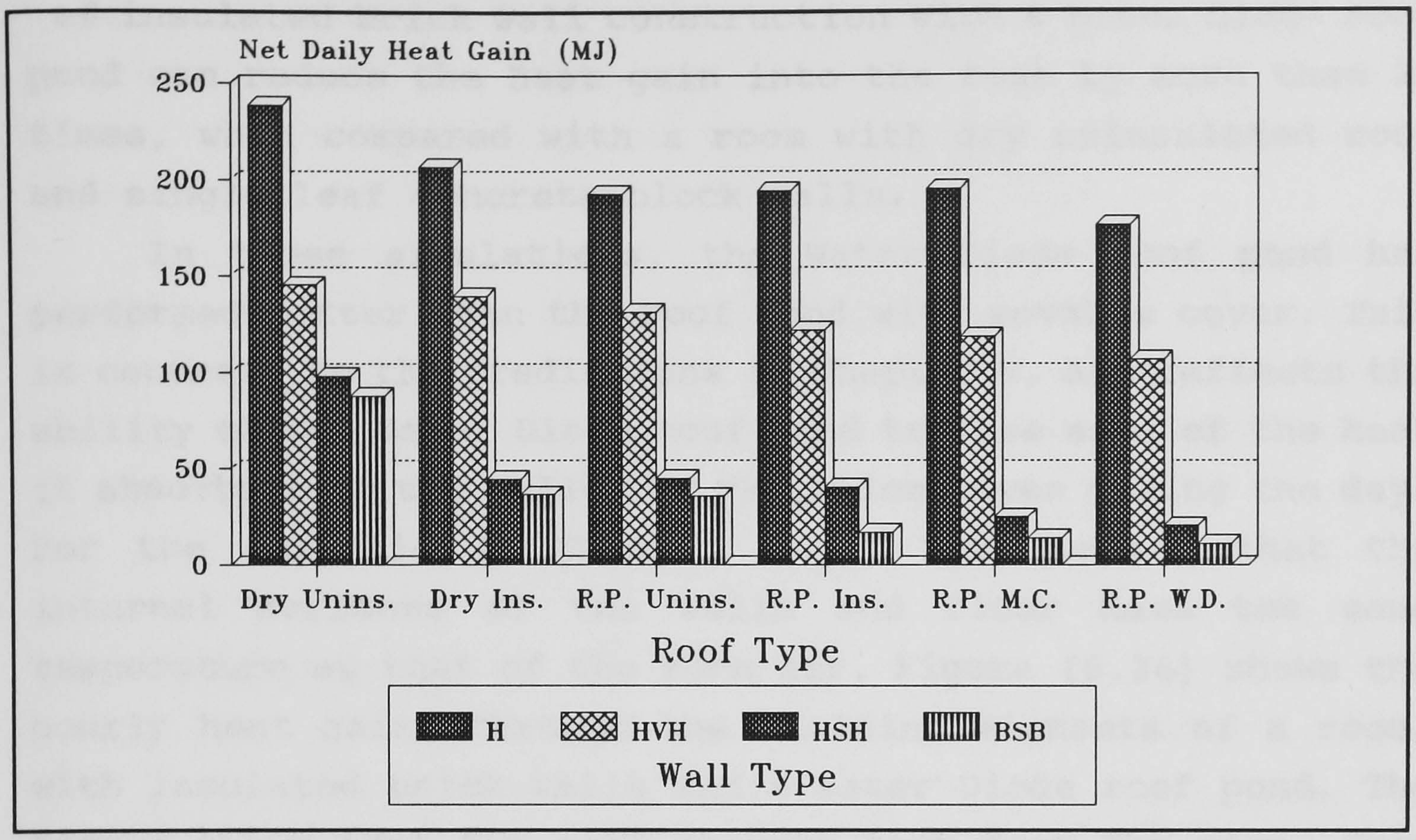

Figure 6.25: The daily net heat gains for combinations of different wall and roof constructions.

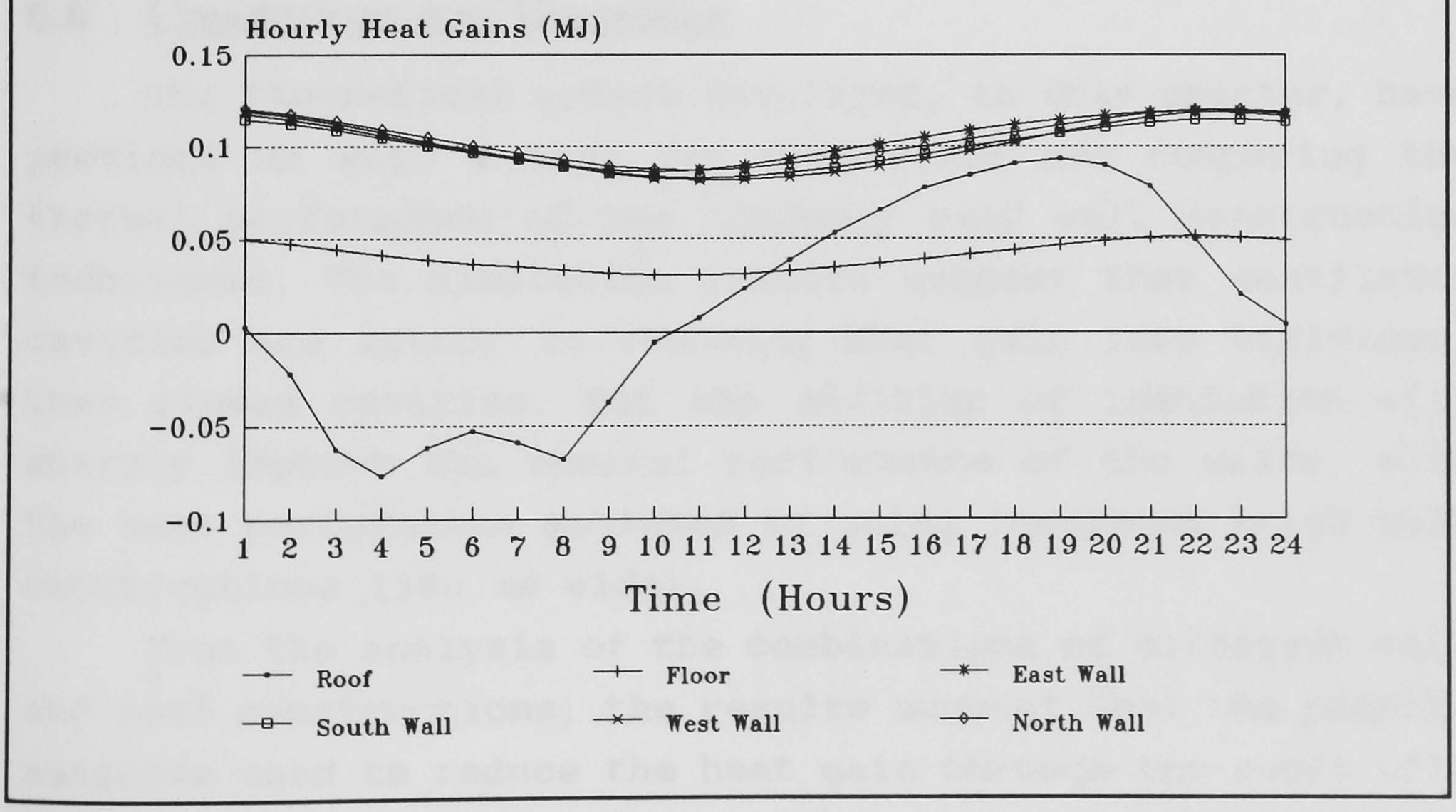

Figure 6.26: The hourly heat gains through the building elements of a room with insulated brick walls and a **Water Diode** roof pond, simulated using the weather data of June.

of insulated brick wall construction with a Water Diode roof pond can reduce the heat gain into the room by more than 25 times, when compared with a room with dry uninsulated roof and single leaf concrete block walls.

In these simulations, the Water Diode roof pond has performed better than the roof pond with movable cover. This is contrary to the predictions in Chapter 5, and reflects the ability of the Water Diode roof pond to lose some of the heat it absorbs from the walls, by radiation, even during the day. For the analysis in Chapter 5, it was assumed that the internal surfaces of the walls and floor have the same temperature as that of the room air. Figure (6.26) shows the hourly heat gains through the building elements of a room, with insulated brick walls and a Water Diode roof pond. The figure shows that the roof absorbs heat from the room, from mid-night until around 10 am.

6.6 Conclusions and Discussion

The theoretical models developed, in this chapter, have provided us with a tool for simulating and comparing the thermal performance of the commonly used wall construction techniques. The simulation results suggest that ventilated cavities are better in reducing heat gain into buildings, than closed cavities. But the addition of insulation will sharply improve the thermal performance of the walls, with the best performance achieved by using insulated brick wall constructions (340 mm wide).

From the analysis of the combinations of different wall and roof constructions, the results suggest that the passive measures used to reduce the heat gain through the roofs will not have a large effect on reducing the heat gains in rooms with uninsulated walls. On the other hand, combining wall insulation, with passive roof cooling techniques can sharply

reduce the cooling load of air-conditioned rooms. The Water Diode roof pond is found to be the most effective passive roof cooling technique, of those analyzed, and can remove heat from the room even in a very hot weather.

But mathematical models are built on many assumptions, and thus need to be validated, by experimental means, to have some assurance that their results are within reasonable bounds. The empirical validation of these models is discussed in the next chapter.

6.7 References

1. J.A. Duffie and W.A. Beckman, Solar Engineering Of Thermal Processes, John Wiley, New York, 1980.

2. M.P. Utrillas, J.A. Martine-Lozano and A.J. Casanovas, Evaluation Of Models For Estimating Solar Irradiation On Vertical Surfaces At Valencia - Spain, *Solar Energy*, Vol. 47, No. 3, pp 223 - 229, 1991.

3. M.A. Abdelrahman and M.A. Elhadidy, Comparison Of Calculated And Measured Values Of Total Radiation On Tilted Surfaces In Dhahran - Saudi Arabia, *Solar Energy*, Vol. 37, No. 3, pp 239 - 243, 1986.

4. D.T. Reindl, W.A. Beckman and J.A.Duffie, Diffuse Fraction Correlations, *Solar Energy*, Vol. 45, No.1, pp 1 - 7 , 1991.

5. T. Grandrille, G.P. Hammond and C. Melo, An Intermediate-level Model Of External Convection For Building Energy Simulation, *Energy and Buildings*, **12**, (1988), pp 53 - 66.

6. F.P. Incropera and D.P. Dewitt, Fundamentals Of Heat And Mass Transfer, 2nd edition, John Wiley, New York, 1985.

7. W.M. Rohsenow, J.P. Harnett and E.N. Ganic, Handbook Of Heat Transfer Fundamentals, 2nd edition, McGraw Hill, 1985.

8. C. Melo, Improved Convection Heat Transfer And Air Infiltration Models For Building Thermal Simulation, Ph.D. Thesis, Cranfield Institute Of Technology, Bedford, U.K., 1985.

Chapter (7)

Empirical Validation Of The Mathematical Models

Chapter (7)

Empirical Validation Of The Mathematical Models

7.1 Introduction

The mathematical models developed in chapters (4), (5) and (6), contained many assumptions. These assumptions were necessary in order to simplify the complex problems of heat and mass transfer, and to make the computer models developed practical in size and complexity. Although the correlations used in the analysis were chosen carefully, to be the most suitable for solving a given problem, each of them is based also on a set of assumptions and has its own limitations. Additionally, there are uncertainties with regard to the accuracy of the values of the physical properties of the materials used. Consequently, experimental work was conducted to check that the results obtained using the mathematical models were in agreement with the measured data.

Conversely, the experimental work also has its own uncertainties. The accuracy of the equipment; the un-representativeness of the samples; and the accuracy of the methods used, are but some of the problems encountered in experimental validation.

But in the field of building thermal simulation, which depends largely on the weather data, the inaccuracy in predicting the weather dominates all of the other parameters encountered. Thus the tools developed in this field, are not solely aimed at producing exact results, but they give us means of comparing different constructions and designs in order to improve the thermal environment and minimise the cost to the inhabitants. Thus the validation of the physical, mathematical model is also important.

7.2 The Validation Procedure

It was considered more appropriate to carry out the validation work in Oman, since the research work is aimed at improving the thermal design of buildings in hot arid climates. And due to the time and financial constraints, it was decided to use existing buildings, with different wall and roof constructions, rather than constructing special test rooms. However, test cells were constructed to validate the roof pond and the Water Diode roof pond models.

For validating the wall construction models, new houses, built by the Ministry of Housing in the Sultanate of Oman to accommodate low income families, were chosen. These were part of three groups of houses constructed in three towns in the interior of Oman, namely Nizwa, Bahla and Jabreen. These three groups of houses had double leaf external wall constructions, a feature rarely found in houses in Oman. The external wall constructions of the houses in Nizwa were made of bricks with insulated cavities. Those of the houses in Bahla, were made of concrete blocks, with insulated cavities, and those of the houses in Jabreen were made of double leaf bricks with closed, un-insulated cavities. The roofs in all of these houses have an insulation layer 50 mm thick. A room with single leaf concrete block walls and an un-insulated roof was also included in the testing.

The field work consisted of taking hourly recordings of the external and internal surfaces temperatures of a room in each of the houses. Due to the lack of essential equipment, the only weather data recorded was the ambient air temperature. For this reason, the validation work was divided into two parts. The first part consisted of using the measured external surface temperatures as input data for the computer models and compare the predicted and actual internal and room air temperatures. The second part of the validation consisted of using the monthly averaged weather data as

inputs to the models and comparing the actual and predicted external surface temperatures.

The room chosen in each of the houses is the one with most external surfaces. Care was taken to minimise the infiltration into the room. The effect of the heat gain and loss through the windows was minimised by boarding them up.

The surface temperatures were taken using thermocouple wires, fixed at the centre of the surface. The thermocouples were then covered by a small piece of polystyrene, 1 cm^2 and 0.5 cm thick. The pieces of polystyrene are fixed to the surfaces using a reflective adhesive tape - see Figure (7.1). This method of surface temperature recording, reduced the effects of direct solar gain by the thermocouple, and also minimised the instantaneous effect of the wind on the hourly temperature measurements. But because the immediate vicinity of the thermocouples is covered from the solar gain and convective and radiative heat transfer, the recorded temperatures will include some time-lag and a reduction in the amplitude of the temperature swings.

7.3 Using The Measured External Surfaces Temperatures To Predict The Temperatures Of The Internal Surfaces.

7.3.1 Single leaf concrete block wall construction

To check the validity of the model used to simulate the temperature variations in a room with single leaf concrete block walls, and un-insulated roof slab, external and internal surface temperatures were measured for an actual room. The room, which had an orientation 15° to the east of south, was located in the village of Al-Ghafat, and is part of the gate house shown in Figure (7.2). The room had the dimensions 4m x 4m x 3m, and had two windows, one on the north wall and the other was on the east wall. The south wall

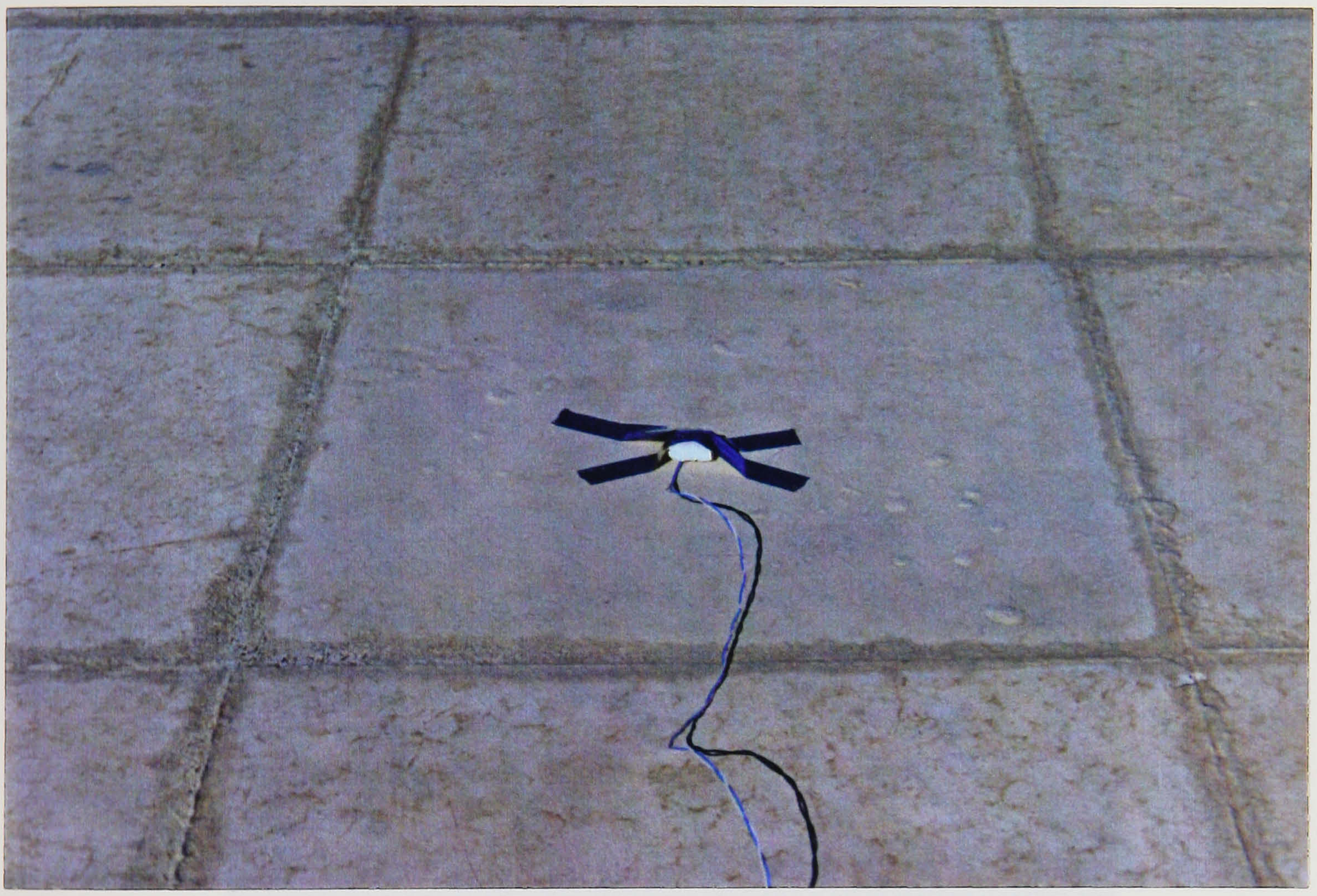

Figure 7.1: The method used to record the surface temperatures.

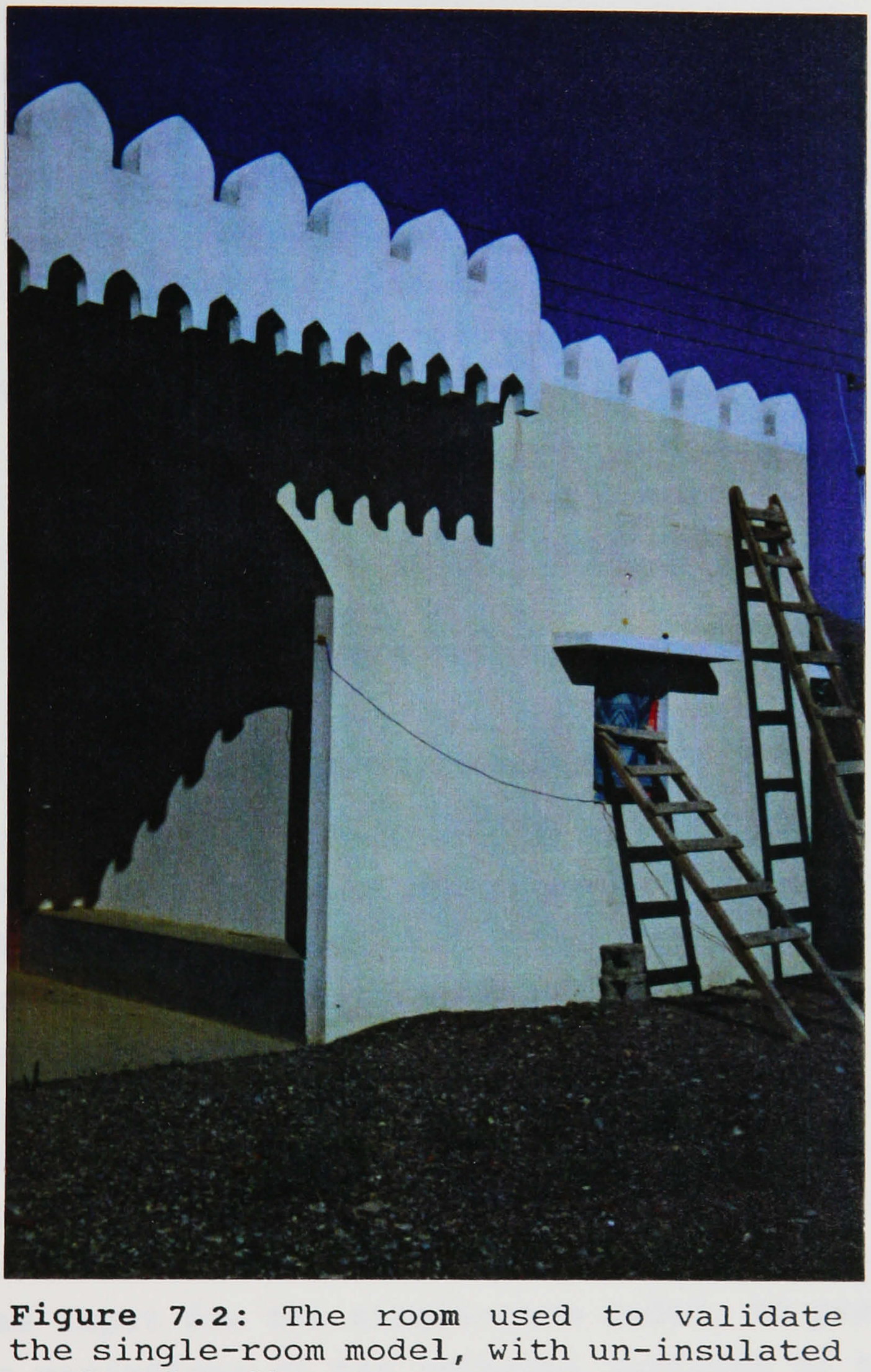

Figure 7.2: The room used to validate the single-room model, with un-insulated roof and walls.

of the room was shaded, and the west wall had an additional layer of stone, 100 mm thick. The external surfaces of the room were painted white, except the western wall which had an unpainted stone-facing.

The measurements were taken for four days, in the period 4-10-90 to 8-10-90. Figure (7.3) shows the recorded external surfaces temperatures. These temperatures were then used as input to the model, to predict the temperature variations of the internal surfaces of the room. Figure (7.4) compares the actual and predicted temperatures of the internal surfaces. The predicted temperature variations in Figure (7.4), show a good agreement with the recorded data, except for the slight dampening of the temperature swings. The inaccuracy of the recorded external surface temperatures, used as input to the model, is the most likely explanation for this dampening.

7.3.2 Closed cavity brick wall construction

The group of houses, built by the Ministry of Housing in Jabreen, had insulated roofs and closed cavity brick walls. The room chosen, see Figure (7.5), had three exposed walls, the western wall being an internal wall. The dimensions of the room were: 5m x 5m x 2.75m.

The surface temperature measurements of the floor, walls, roof and ambient were recorded at hourly intervals in the period 5-11-90 to 9-11-90. Figure (7.6) shows the recorded external surface temperatures. These temperatures were used as input for the single-room model, to predict the temperature variations of the internal surfaces of the room. Figure (7.7) shows a comparison between the actual and predicted temperatures of the internal surfaces. There is a good agreement between the predicted and recorded temperatures. The slight dampening of the predicted temperature swings is again evident. But the results confirm

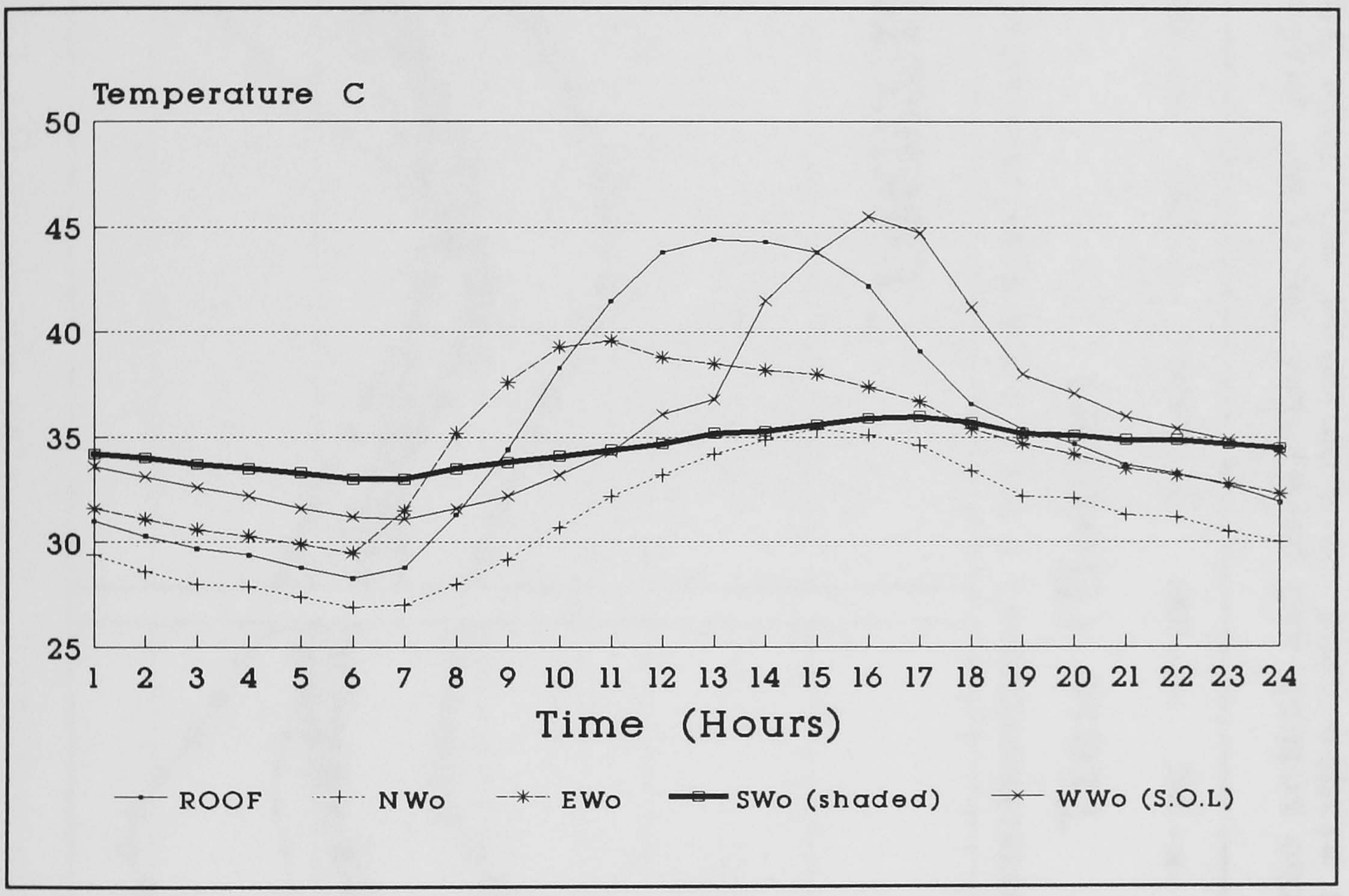

Figure 7.3: The recorded external surfaces temperatures for the room with un-insulated roof and single-leaf concrete block walls.

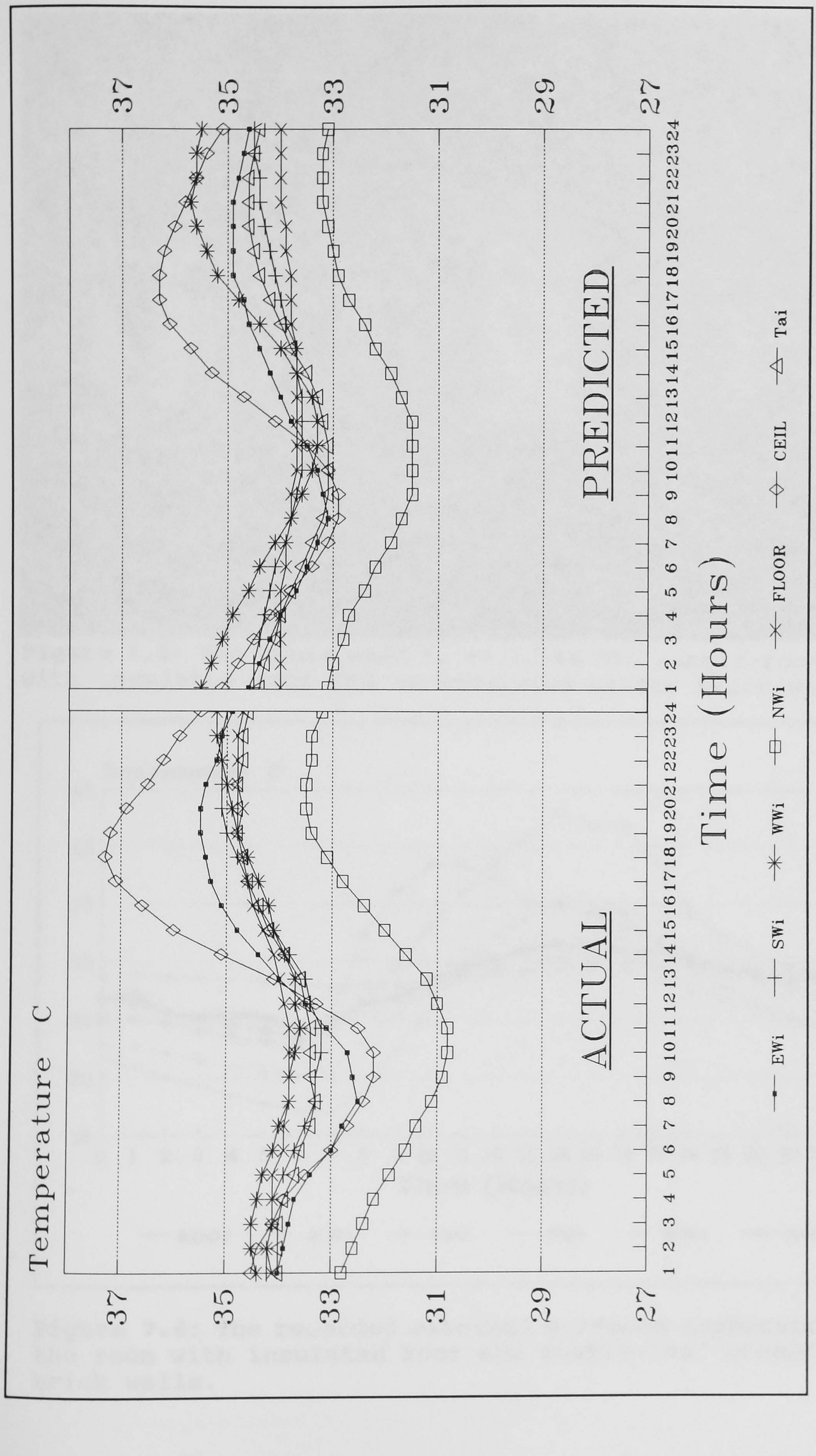

Figure 7.4: A comparison between the actual and predicted internal surfaces temperatures for a room with un-insulated concrete block walls, un-insulated roof and single-leaf

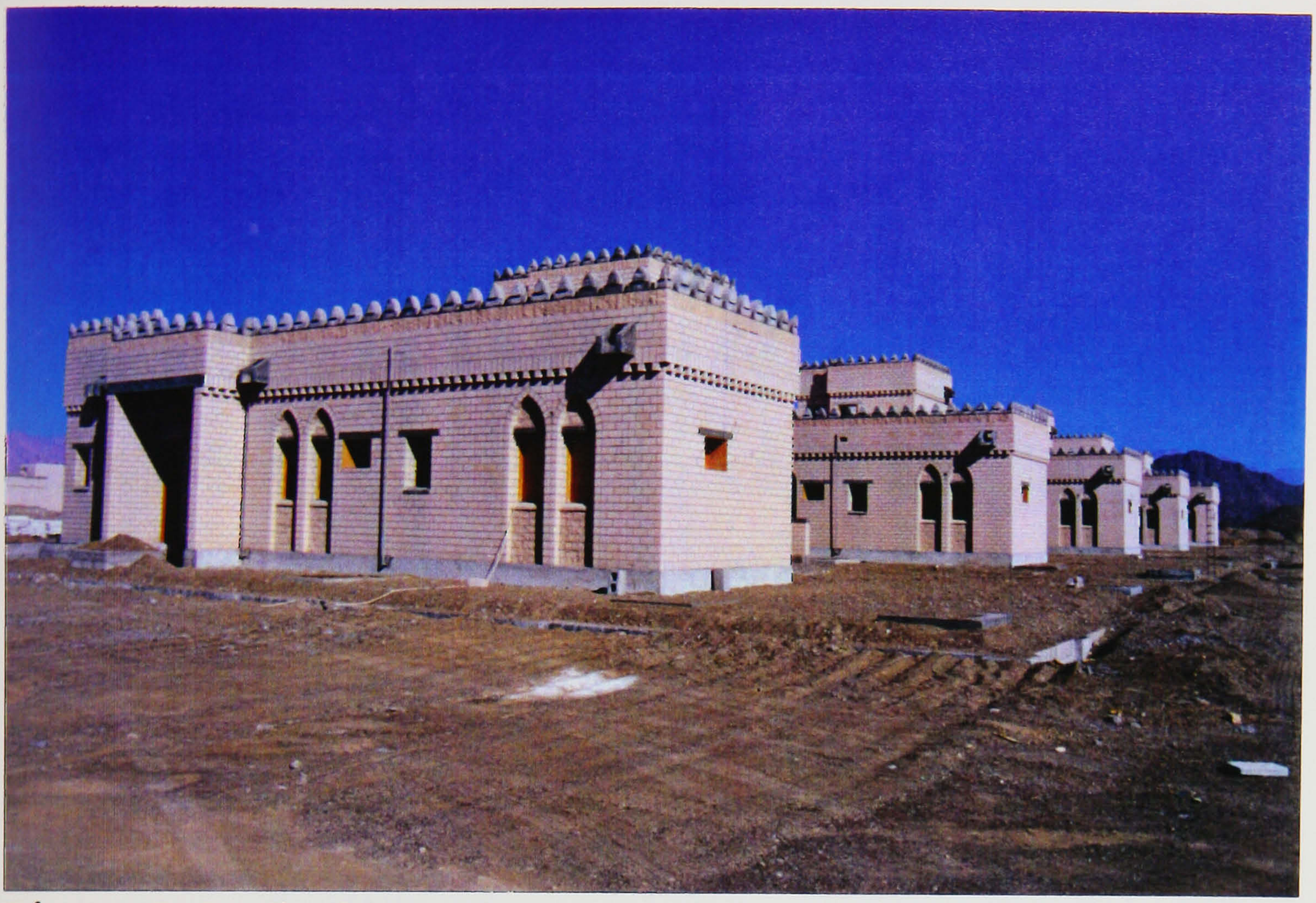

Figure 7.5: The house used to validate the single-room model, with insulated roof and un-insulated cavity brick walls.

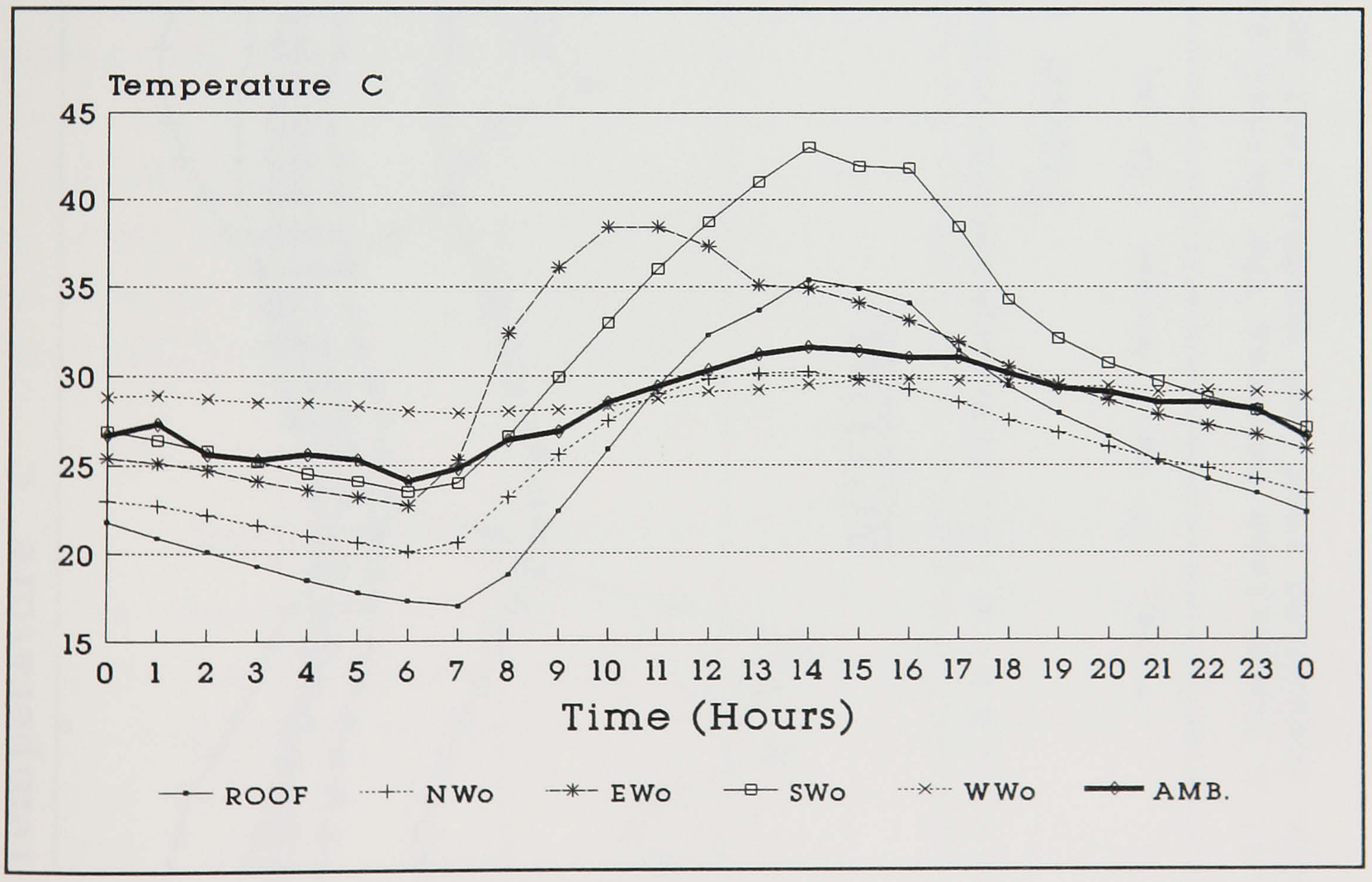

Figure 7.6: The recorded external surfaces temperatures for the room with insulated roof and double-leaf closed cavity brick walls.

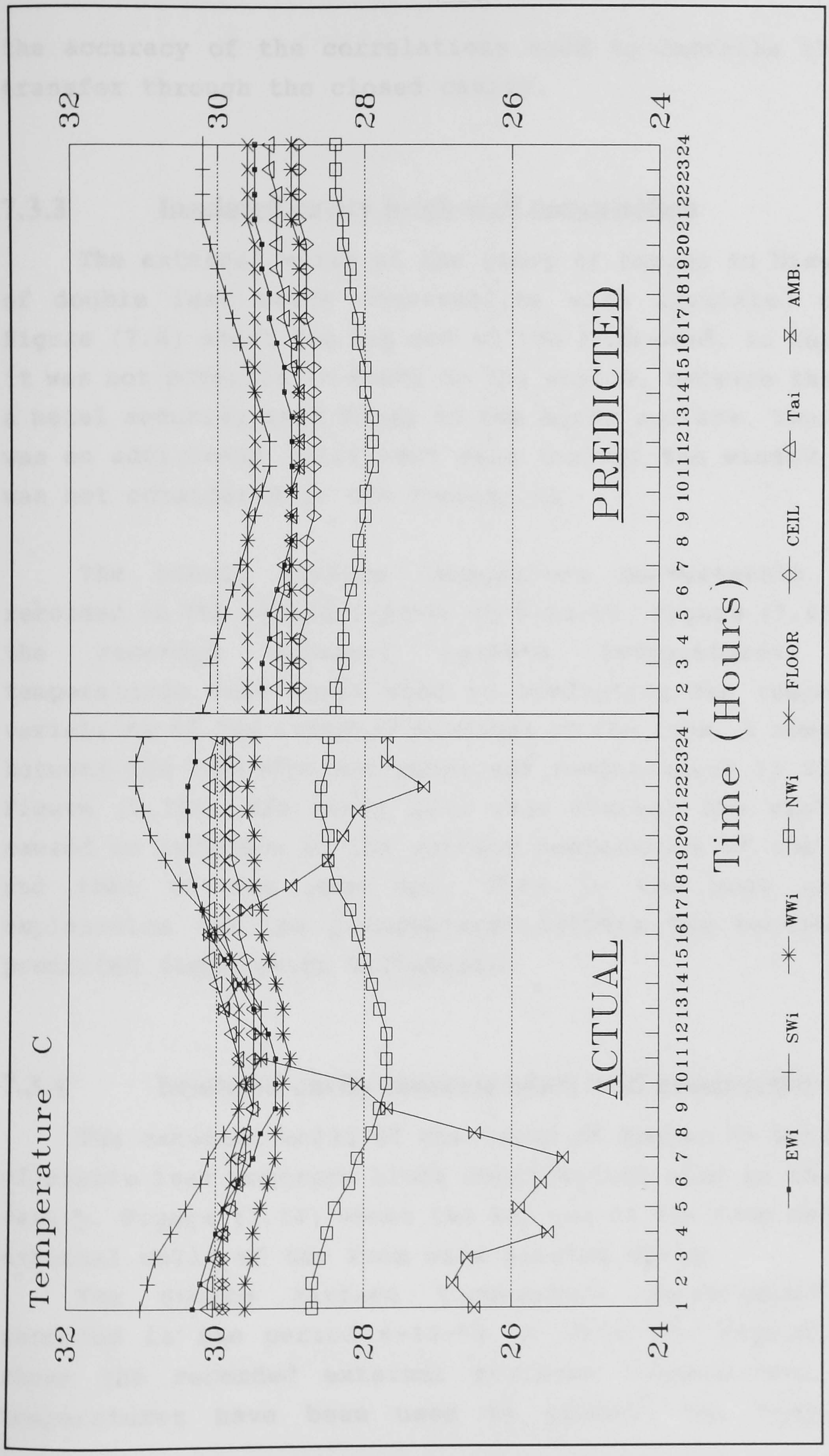

Figure 7.7: A comparison between the actual and predicted internal surfaces temperatures for a room with insulated cavity brick walls. un-insulated roof and double leaf

the accuracy of the correlations used to describe the heat transfer through the closed cavity.

7.3.3 Insulated cavity brick wall construction

The external walls of the group of houses in Nizwa were of double leaf brick construction with insulated cavity. Figure (7.8) shows the lay out of the room used. In this case it was not possible to board up the window, because there was a metal security grid fixed to the outer surface. Thus there was an additional solar heat gain through the window, which was not considered in the simulation.

The hourly surface temperature measurements were recorded in the period 1-12-90 to 5-12-90. Figure (7.9) shows the recorded external surface temperatures. These temperatures were again used in predicting the temperature variations of the internal surfaces of the room. A comparison between the recorded and predicted temperatures is shown in Figure (7.10). The solar heat gain through the window had caused an increase in the surface temperature of the floor, and that of the room air. This is the most probable explanation for the disagreement between the recorded and predicted temperature variations.

7.3.4 Insulated cavity concrete block wall construction

The external walls of the group of houses in Bahla were of double leaf concrete block construction with an insulated cavity. Figure (7.11) shows the lay out of the room used. The external walls of the room were painted white.

The hourly surface temperature measurements were recorded in the period 6-12-90 to 10-12-90. Figure (7.12) shows the recorded external surfaces temperatures. These temperatures have been used to predict the temperature

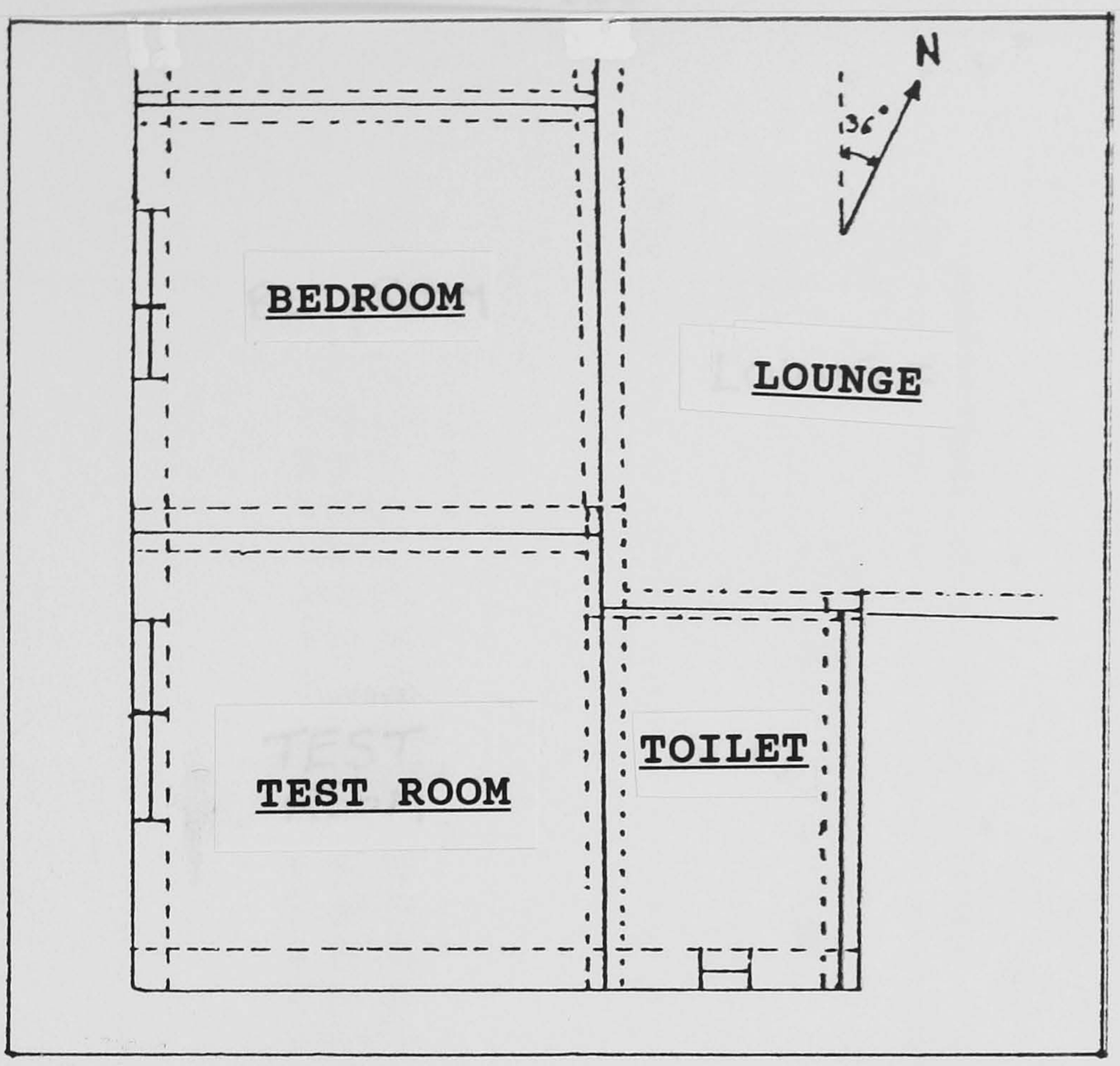

Figure 7.8: The lay out of the room used to validate the single-room model, with insulated roof and double-leaf insulated cavity brick walls.

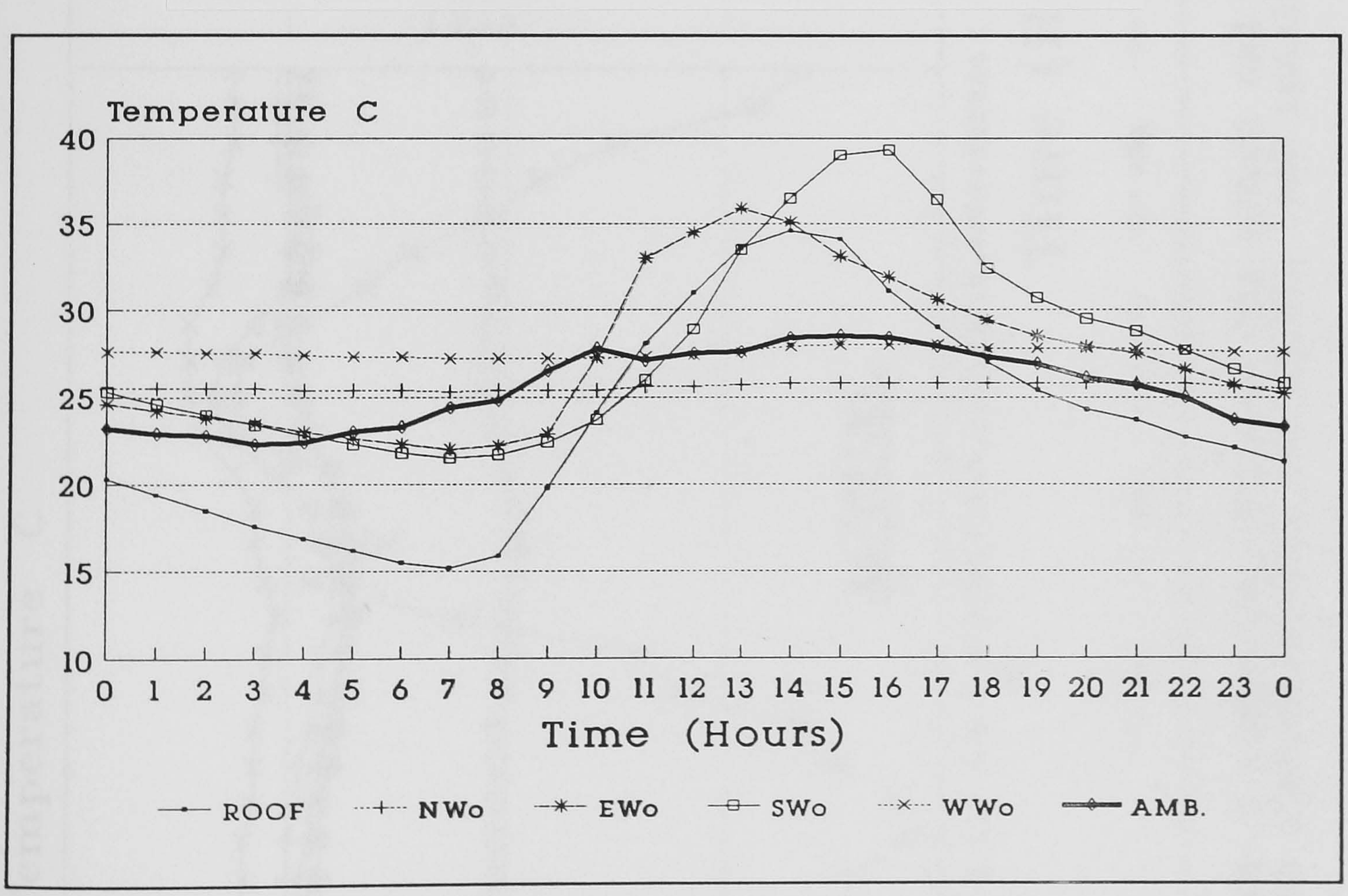

Figure 7.9: The recorded external surfaces temperatures for the room with insulated roof and double-leaf insulated brick walls.

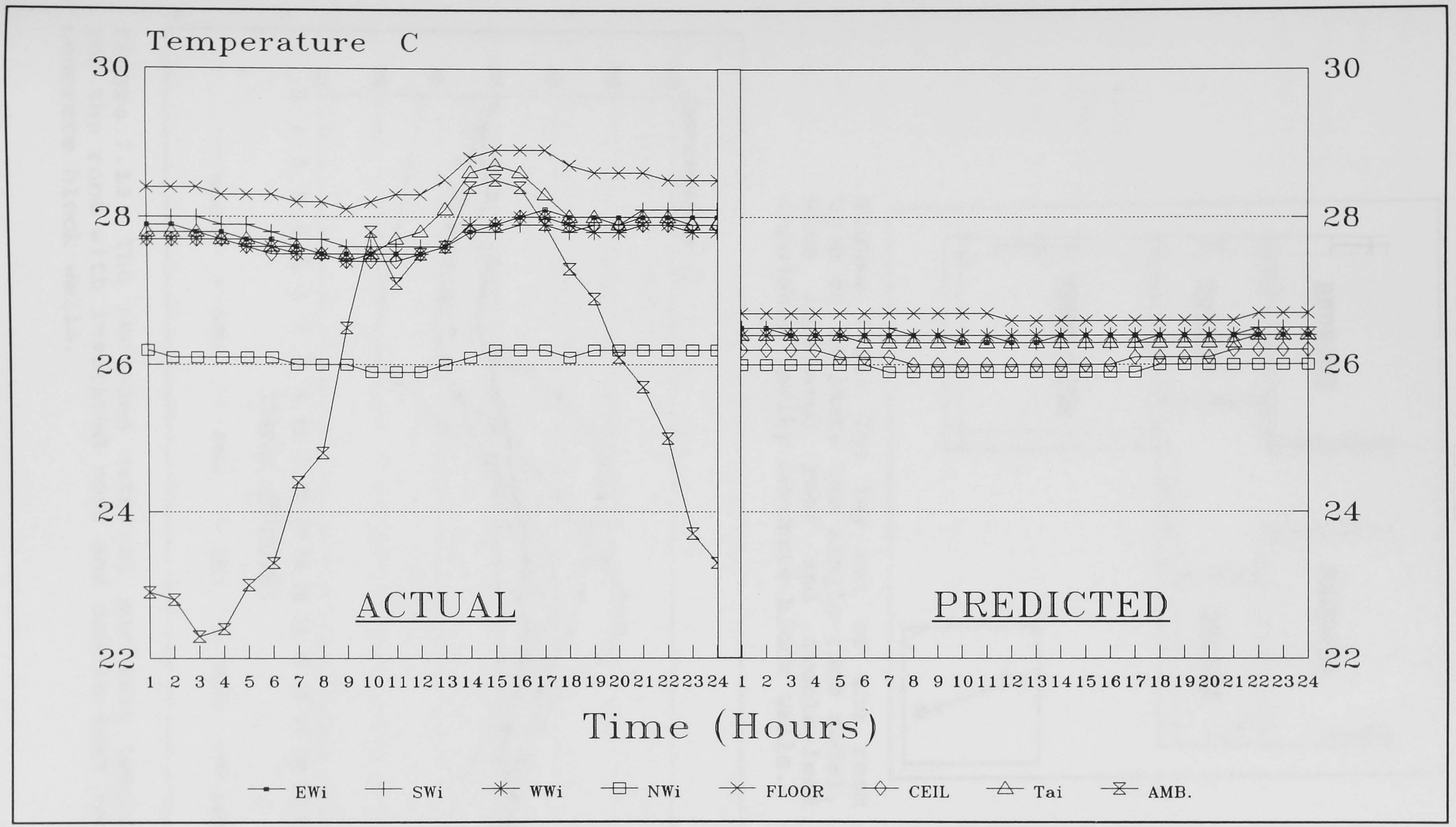

Figure 7.10: A comparison between the actual and predicted internal surfaces temperatures for a room with insulated roof and double leaf insulated brick walls.

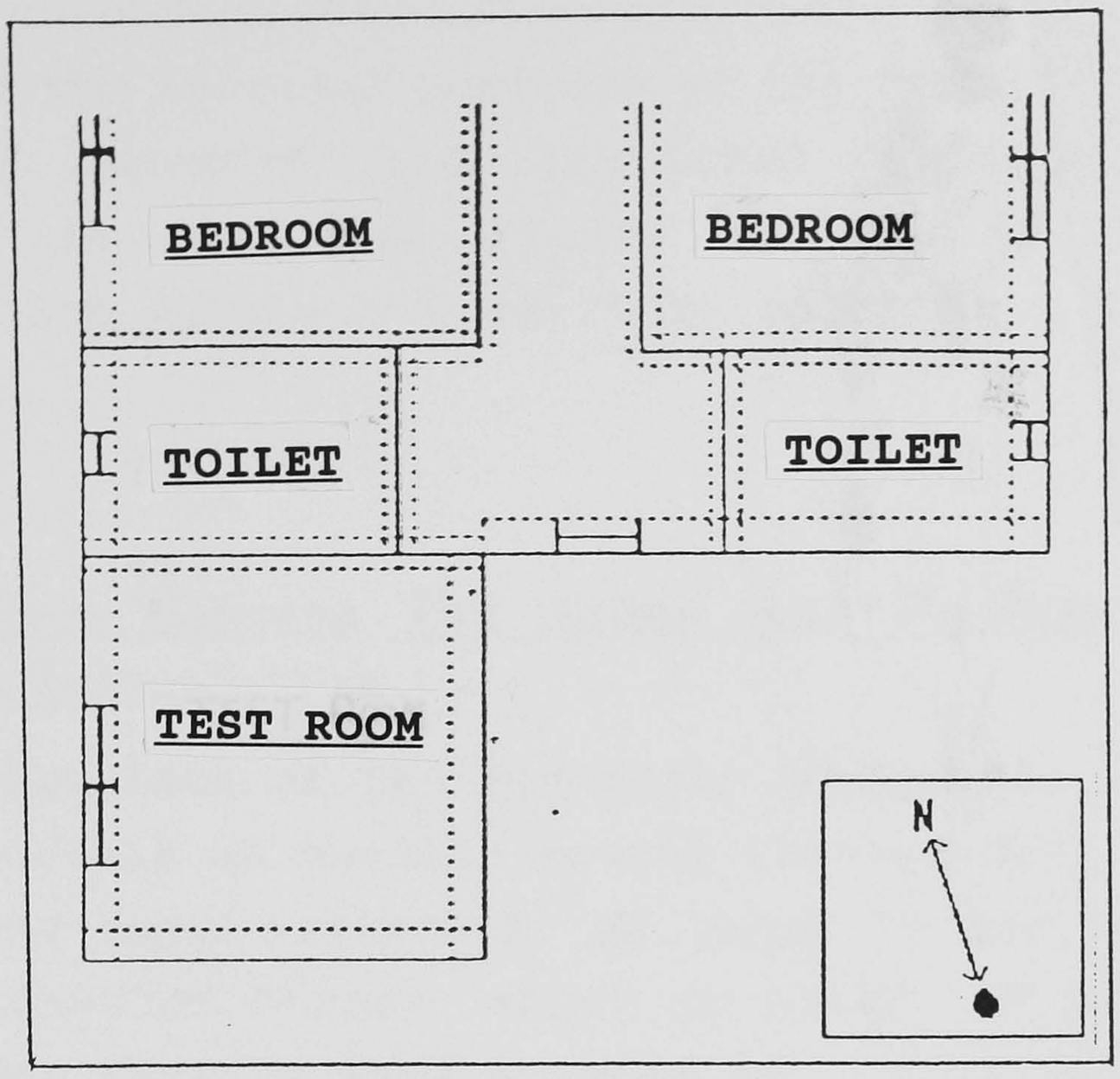

Figure 7.11: The lay out of the room used to validate the single-room model, with insulated roof and double-leaf insulated cavity concrete block walls.

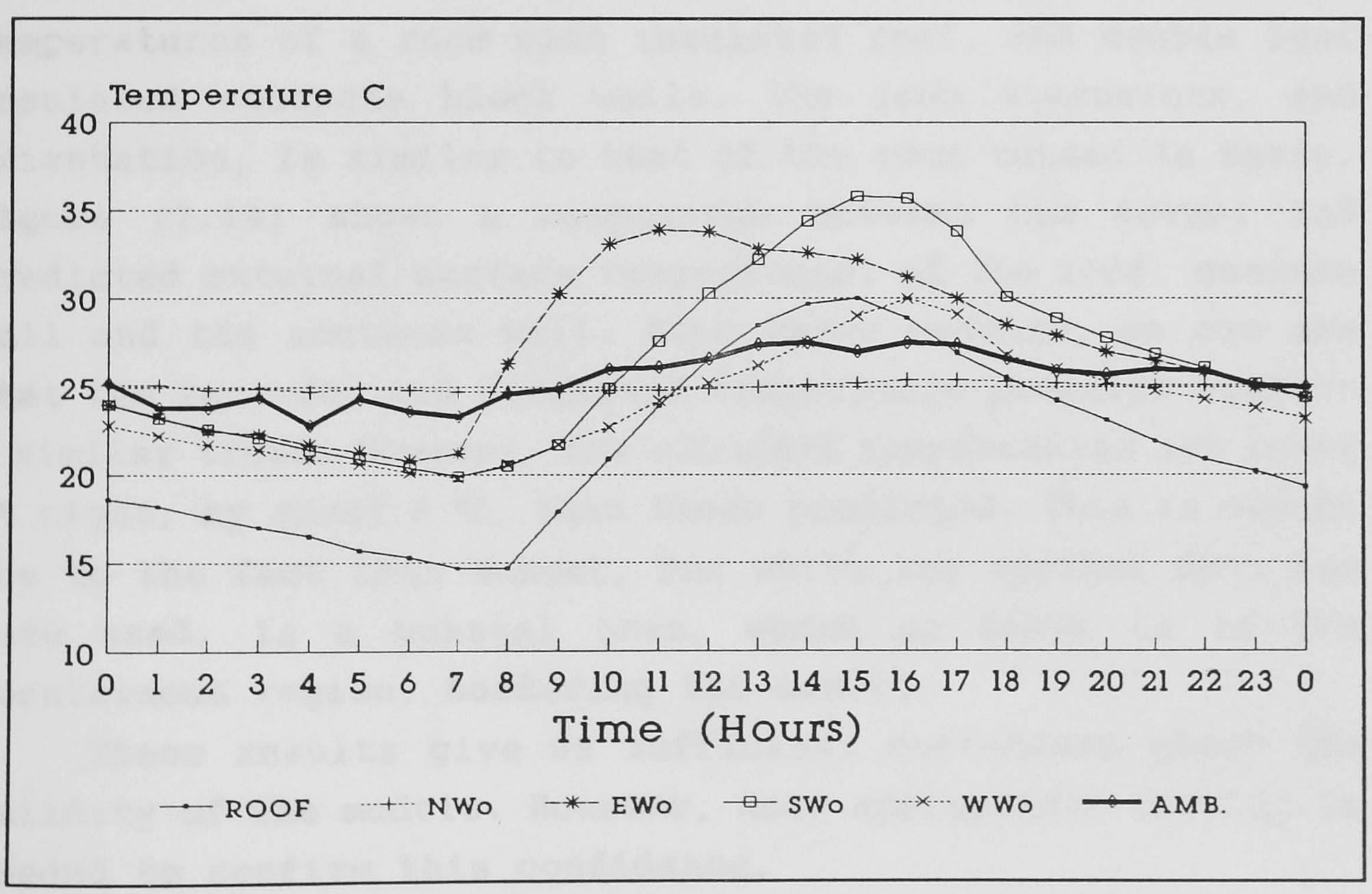

Figure 7.12: The recorded external surfaces temperatures for the room with insulated roof and double-leaf insulated concrete block walls.

variations of the internal surfaces of the room. A comparison between the recorded and predicted internal surface temperatures is shown in Figure (7.13). The predicted temperatures are within 1 ℃ of those recorded.

7.4 Comparison Between The Actual And Predicted External Surfaces Temperatures

Due to the lack of the necessary equipment, it was not possible to obtain an on-site hourly weather data. The only hourly weather data available, as input to the models, is that of the town of Muscat, which is about 150 km from the test location. Thus to have an idea of the validity of the models in predicting the external surface temperatures, the monthly averaged weather data, for the month of December at Muscat, has been used to predict the external surfaces temperatures of a room with insulated roof, and double leaf insulated concrete block walls. The room dimensions, and orientation, is similar to that of the room tested in Bahla. Figure (7.14) shows a comparison between the actual and predicted external surface temperatures of the roof, eastern wall and the southern wall. From these results, we can see that the recorded and predicted temperature profiles exhibit a similar trend. However, the recorded temperatures are lower at night, by about 5 ℃, than those predicted. This is may be due to the fact that Muscat, for which the weather data has been used, is a coastal town, where as Bahla is in the mountainous region, bordering the desert.

These results give us sufficient confidence about the validity of the models. However, more appropriate testing is needed to confirm this confidence.

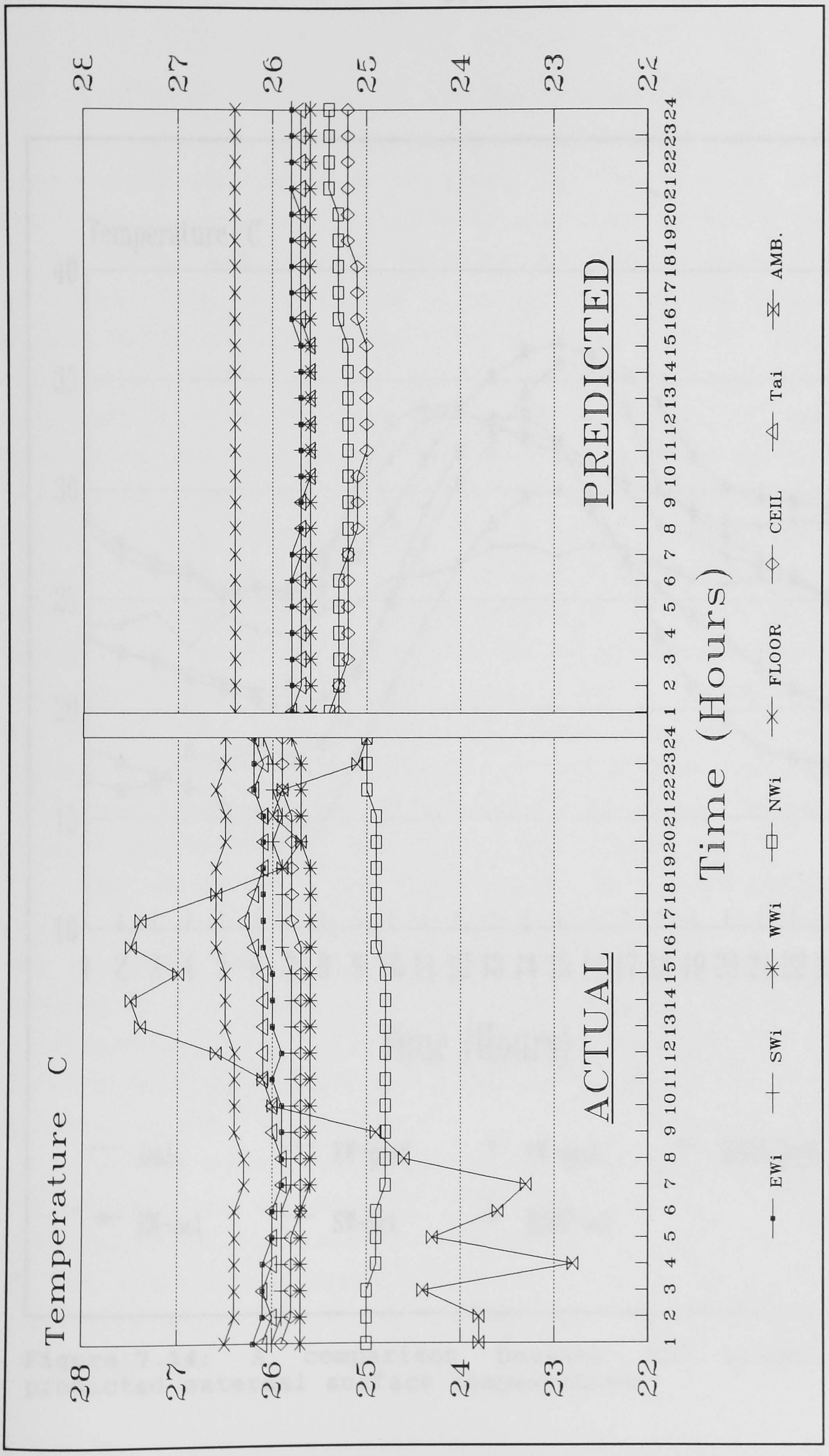

Figure 7.13: A comparison between the actual and predicted internal surfaces temperatures for a room with insulated roof and double leaf insulated concrete block walls.

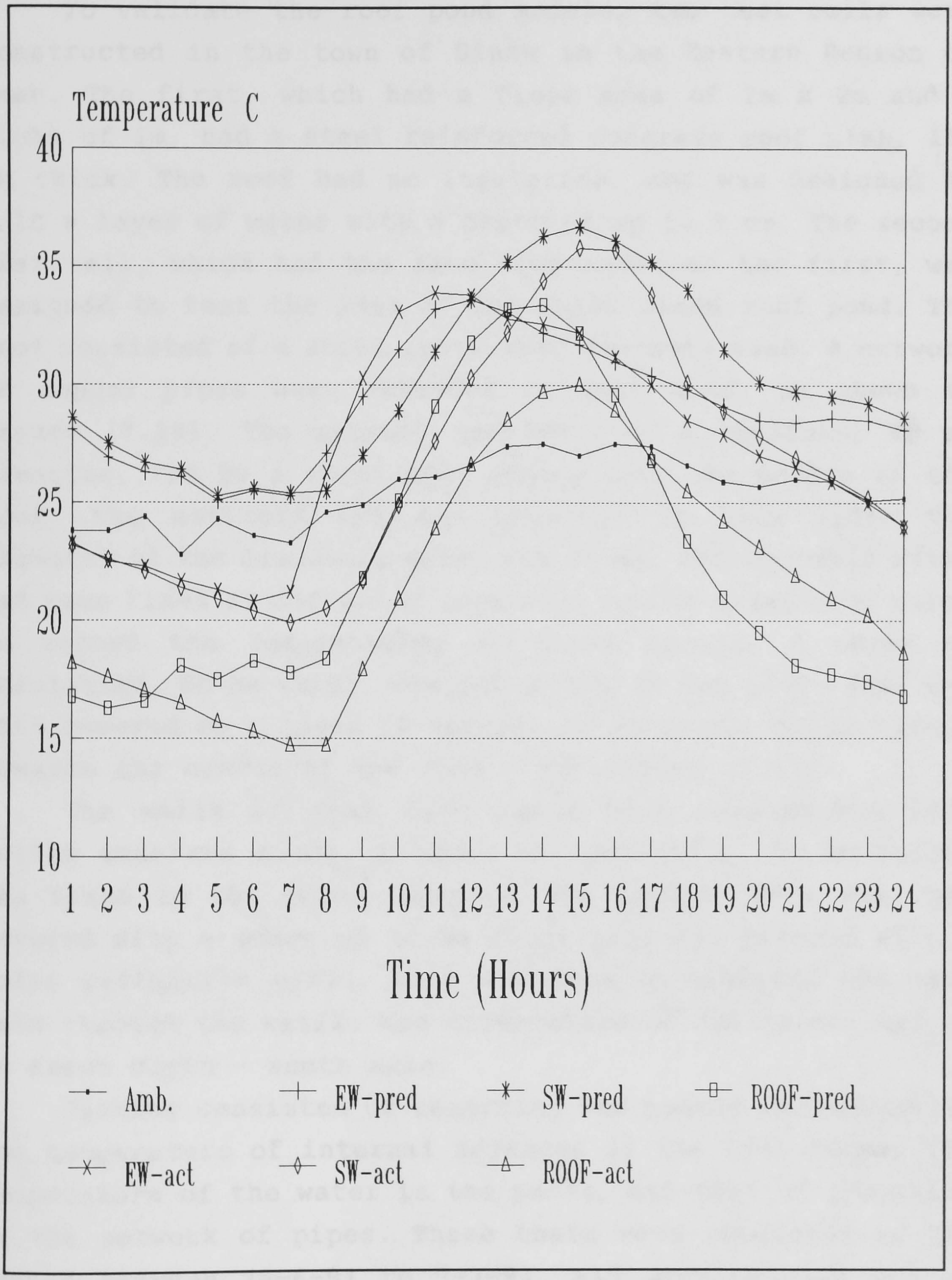

Figure 7.14: A comparison between the actual and predicted external surface temperatures.

7.5 Empirical Validation Of The Roof Pond Models

To validate the roof pond models, two test cells were constructed in the town of Sinaw in the Eastern Region of Oman. The first, which had a floor area of 2m x 2m and a hight of 1m, had a steel reinforced concrete roof slab, 150 mm thick. The roof had no insulation, and was designed to hold a layer of water with a depth of up to 5 cm. The second test cell, which had the same dimensions as the first, was designed to test the idea of the Water Diode roof pond. The roof consisted of a steel reinforced concrete slab. A network of copper pipes were embedded in this slab, as shown in Figure (7.15). The network consisted of a manifold, 50 mm diameter, fed by a short pipe coming from the centre of the roof. The manifold fed six branches on each side. The diameter of the branching pipes was 25 mm. Thermocouple wires had been fixed at different locations in the network of pipes to record the temperatures at these points. A layer of insulation, 50 mm thick, was put on top of the slab. This was then covered by a layer of screed, 40 mm thick, which sloped towards the centre of the roof - see Figure (7.16).

The walls of both test cells were constructed from hollow concrete block. A layer of insulation, 50 mm thick, was fixed to the outer layer of the blocks. This was then covered with a sheet of 12 mm thick plywood, painted with a solar reflective paint. This was done to minimise the heat gain through the walls. The orientation of the cells, was on an exact north - south axis.

Testing consisted of recording the hourly variations in the temperature of internal surfaces of the test rooms, the temperature of the water in the ponds, and that of the water in the network of pipes. These tests were conducted in the period between 26-6-91 to 7-7-91, and were carried out in three stages:

Figure 7.15: The lay out of the network of copper pipes impeded in the slab of the Water Diode roof pond.

Figure 7.16: The Water Diode roof pond under construction.

Stage 1: The temperatures were recorded with **dry** roofs. This was done to compare the thermal performance of the insulated roof slab, with that which had no insulation.

Stage 2: Water was then added to the roofs, but with pipes in the in the Water Diode roof pond plugged to prevent the water from entering the network of pipes. This was done to compare the thermal performance of the roof pond with insulated roof slab, with that which had no insulation.

Stage 3: The pipes were then unplugged, to allow the water to circulate naturally in the pipes. This was done to test the performance of the Water Diode roof pond.

The duration of each stage was about three days. This was thought sufficient to achieve stability for each of the conditions stated. Figure (7.17) shows the recorded ceiling temperature profiles in the two cells. As expected, the roof insulation in the dry roofs test had minimised the temperature fluctuations of the ceiling and reduced the temperature of the ceiling by about 5 °C. However, from the mathematical modelling results it was expected that the roof pond with insulated roof slab would perform better than that with no insulation. The test results, in Figure (7.17), show otherwise. The most likely explanation for this, is that the heat gain from the edges of the roof, assumed negligible in the model, had caused the rise in the actual temperature. The presence of the insulation layer had minimised the heat loss from the roof slab to the water above. On the other hand, the heat gain from the edges of the roof was quickly absorbed by the water in the roof pond with no roof insulation.

The effect of the edges on the roof temperature of the test cells, is especially strong, due to the small surface area of the roofs (4 m^{-2}). This effect was enhanced by the steel reinforcement and the network of copper pipes embedded

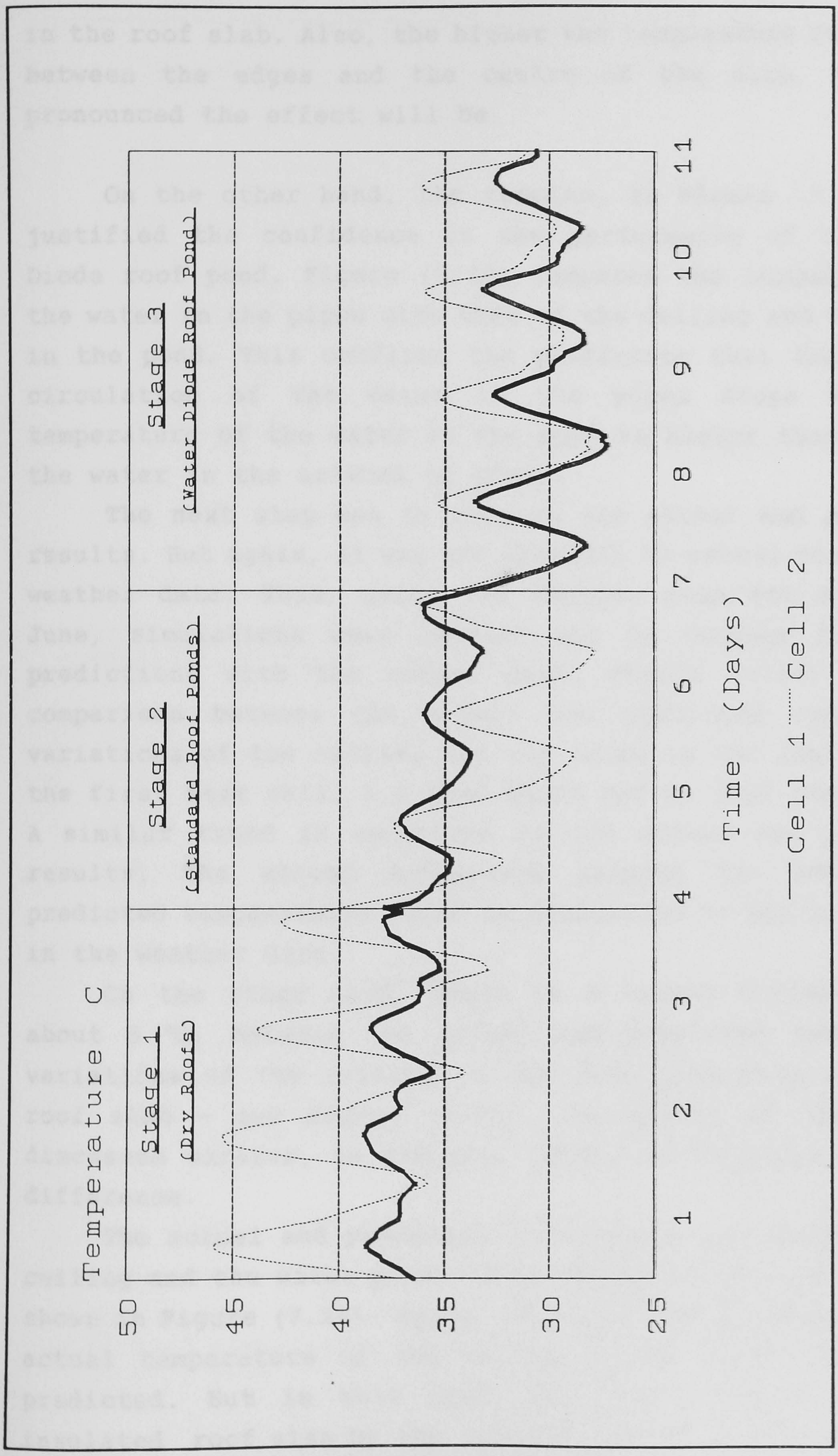

Figure 7.17: The recorded ceiling temperature profiles for the two test cells at the different stages.

in the roof slab. Also, the higher the temperature difference between the edges and the centre of the slab, the more pronounced the effect will be.

On the other hand, the results, in Figure (7.17), had justified the confidence in the performance of the Water Diode roof pond. Figure (7.18) compares the temperature of the water in the pipes with that of the ceiling and the water in the pond. This confirms the prediction that the natural circulation of the water in the pipes stops when the temperature of the water in the pond is higher than that of the water in the network of pipes.

The next step was to compare the actual and predicted results. But again, it was not possible to record the on-site weather data. Thus, using the weather data for Muscat on June, simulations were carried out to compare the model predictions with the actual data. Figure (7.19) shows a comparison between the actual and predicted temperature variations of the ceiling and the water in the roof pond of the first test cell, i.e that which had no roof insulation. A similar trend is exhibited by the actual and predicted results. The slight difference between the actual and predicted temperatures could be attributed to the difference in the weather data.

On the other hand, there is a marked difference, of about 5 ℃, between the actual and predicted temperature variations of the ceiling in the roof pond with insulated roof slab - see Figure (7.20). The effect of the edges, discussed earlier, is the most likely explanation for this difference.

The actual and predicted temperature variations of the ceiling and the water pond, in the Water Diode roof pond, is shown in Figure (7.21). Again, the edge effect had caused the actual temperature of the ceiling to be higher than that predicted. But in this case, the heat removed form the insulated roof slab by the natural water circulation in the

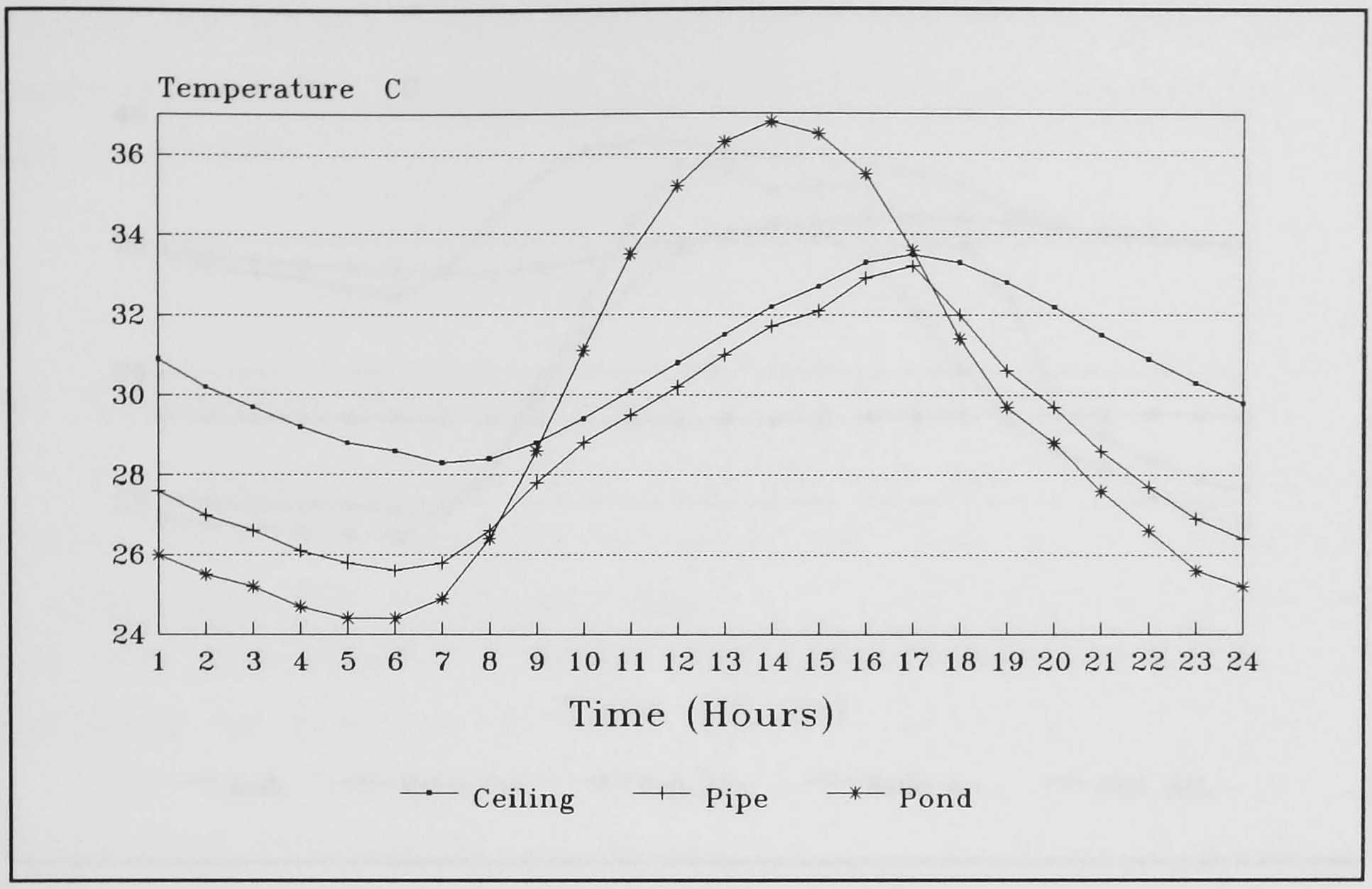

Figure 7.18: The temperature of the water in the pipes as compared with that of the ceiling and the water pond.

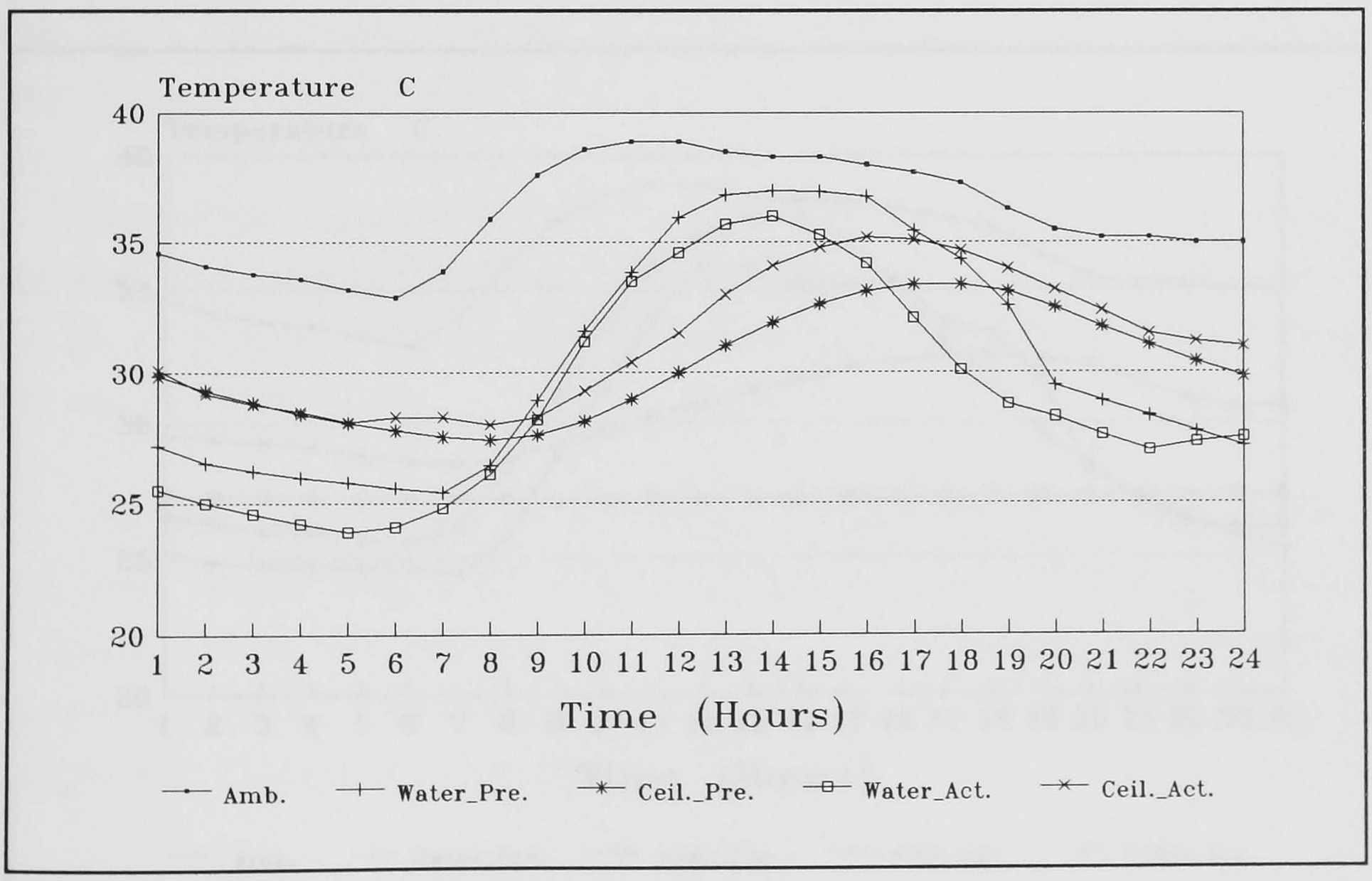

Figure 7.19: A comparison between the actual and predicted temperature variations of the water and ceiling in a roof pond.

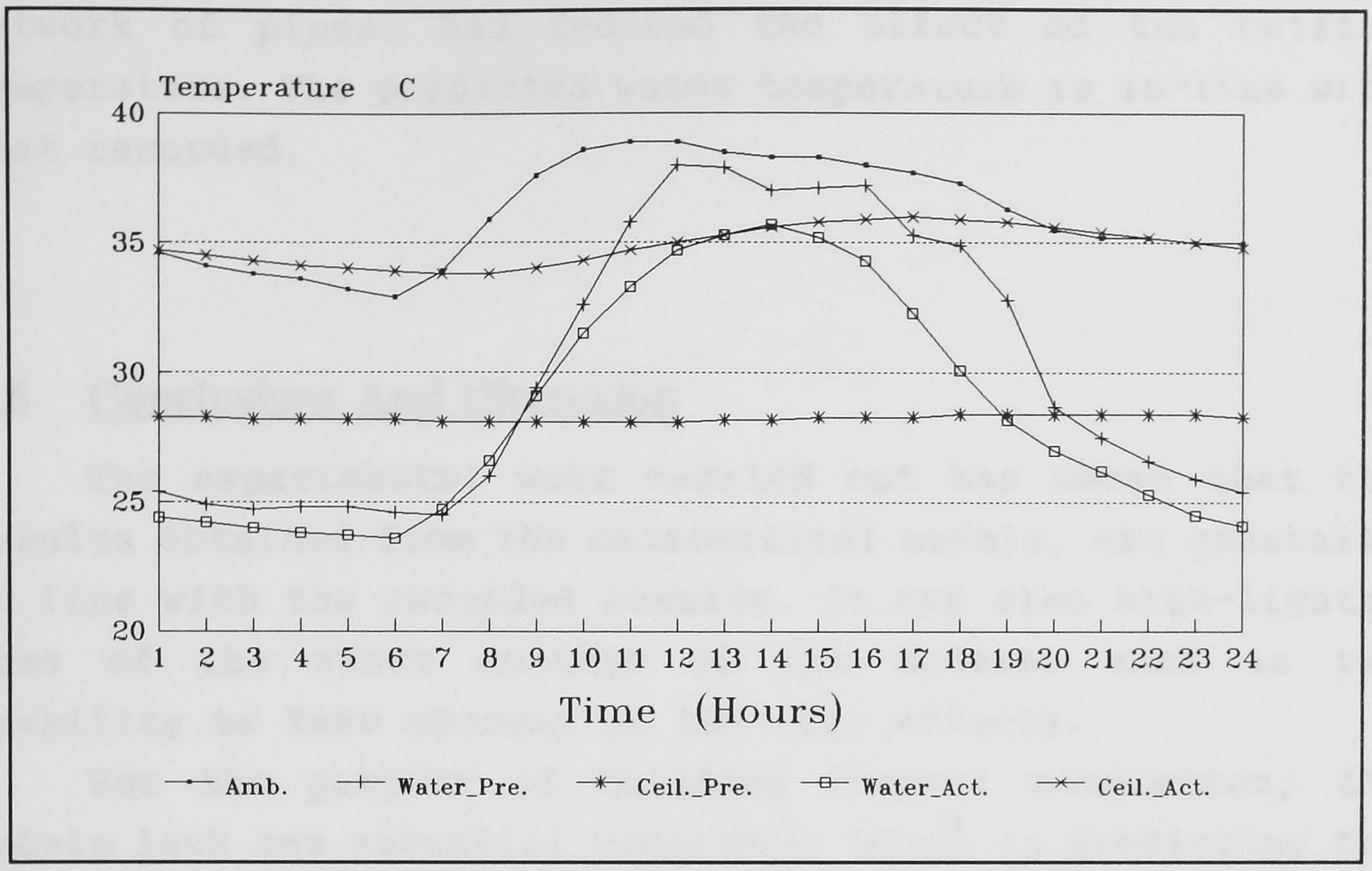

Figure 7.20: A comparison between the actual and predicted temperature variations of the water and ceiling in a roof pond with insulated roof slab.

Figure 7.21: A comparison between the actual and predicted temperature variations of the water and ceiling in a Water Diode roof pond.

network of pipes, had reduced the effect on the ceiling temperature. The predicted water temperature is in-line with that recorded.

7.6 Conclusions And Discussion

The experimental work carried out has shown that the results obtained from the mathematical models, are generally in line with the recorded results. It has also high-lighted some of the short comings of the models, such as the inability to take account of the edge effects.

For the purpose of building thermal simulation, the models lack one essential component, which is predicting the heat transfer through the windows. But on the other hand, these models were developed primarily to compare the thermal performance of different wall and roof constructions, and were not developed as a building thermal simulation tool. They seem to work well for the purpose they were developed for.

However, a more accurate validation procedure is need to improve the confidence in their validity. This involves the use of the appropriate weather data and thermal properties of the materials used.

Generally, there is an urgent need for the gathering of good and valid weather data, covering the different regions in Oman. This is essential for any research work aimed at improving the thermal environment of buildings in the different climatic regions.

Chapter （8）

Economic Analysis of Commonly Used Wall and Roof Constructions

Chapter (8)

Economic Analysis of Commonly Used Wall and Roof Constructions

8.1 Introduction

The analysis in this chapter is aimed at evaluating the cost benefit of concrete block and brick wall constructions with and without insulation. The cost benefit of roof insulation and double glazing are also evaluated. This analysis is carried out using the weather data for Muscat, Oman.

It is now widely acknowledged that considerations of the U-values or steady-state parameters alone, cannot indicate the compared performance of different constructions in dynamic situations. Similarly, design-day dynamic analysis is not sufficient to evaluate accurately the economic benefit of construction features, such as the addition of insulation to the roof and walls, or the use of double glazing and reflective glazing. For such an evaluation to be realistic, a period of a whole year, or a **cooling** or **heating** season, is needed.

Beside the thermal design, there are other factors affecting the energy consumption in a building. These include, the occupation pattern, the required internal conditions, and the heat gains and losses through, ventilation, infiltration, lighting, equipment, and the occupants.

8.2 Method of Analysis

The building thermal analysis system, **TAS**, was used to estimate the energy consumption of a building, with different commonly used wall and roof constructions, and for different occupation patterns. The lay-out of the single-story building is shown in Figure (8.1). Although the building is designed as a residential building, it has also been assumed to be used as a government office building, or a commercial office building. The difference between the later two, is in the occupation patterns expected, due to the different working hours.

Simulations were carried out for the hottest day of the year, and for a cooling season (from the 15th of April to the 15th of October). The **Hottest Day** simulations, were used mainly to estimate the required capacity of the cooling plant. The **Cooling Season** simulations, were used to estimate the summer cooling load.

8.2.1 The building elements evaluated

Nine different combinations of roof and external walls constructions were used. The external wall constructions are shown in Figure (8.2), and the two roof constructions evaluated are shown in Figure (8.3). The base case, ***Case 0***, is taken as the commonly used construction technique of single leaf hollow concrete block external walls and un-insulated, steel reinforced concrete roof slab. ***Case 1***, is used to investigate the economic benefit of roof insulation, with the same external wall construction as that of ***Case 0***. ***Cases 2 - 8*** also have insulated roofs. These are used to investigate the economic benefit of the different external wall constructions shown in Figure (8.2).

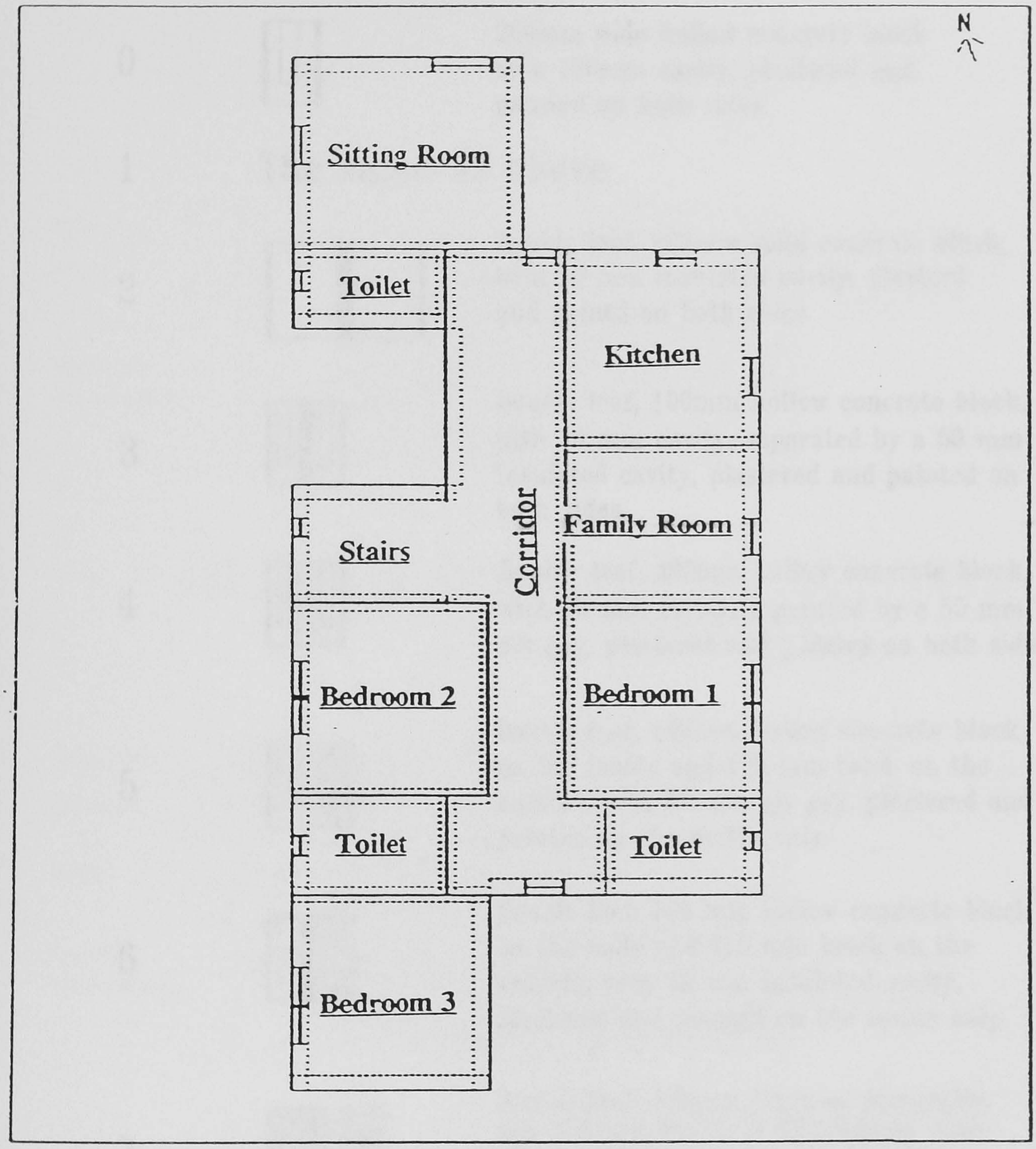

Figure 8.1: The lay out of the building used in the economic analysis simulations.

Case No.	Wall Construction	
0		200mm wide hollow concrete block with 100mm cavity, plastered and painted on both sides
1	The same as above	
2	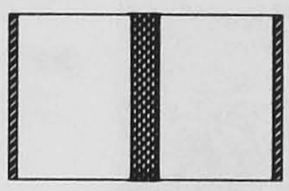	Double leaf, 200mm solid concrete block, with 50 mm insulated cavity, plasterd and paintd on both sides
3		Double leaf, 100mm hollow concrete block, with 50 mm cavity, separated by a 50 mm insulated cavity, plastered and painted on both sides.
4	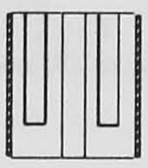	Double leaf, 100mm hollow concrete block, with 50 mm cavity, separated by a 50 mm air gap, plastered and painted on both sides
5	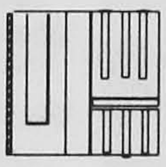	Double leaf, 100mm hollow concrete block on the inside and 115 mm brick on the outside, with 50 mm air gap, plastered and painted on the inside only.
6	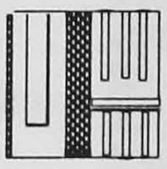	Double leaf, 100 mm hollow concrete block on the iside and 115 mm brick on the outside, with 50 mm insulated cavity, plastered and painted on the inside only.
7	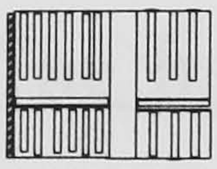	Double leaf, 175mm brick on the inside, and 115 mm brick on the outside, with 50 mm air gap, plastered and painted on the inside only.
8	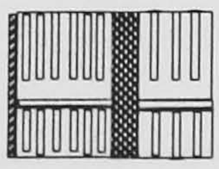	Double leaf, 175mm brick on the inside, and 115 mm brick on the outside, with 50 mm insulated cavity, plastered and painted on the inside only.

Figure 8.2: The different wall constructions evaluated in the analysis.

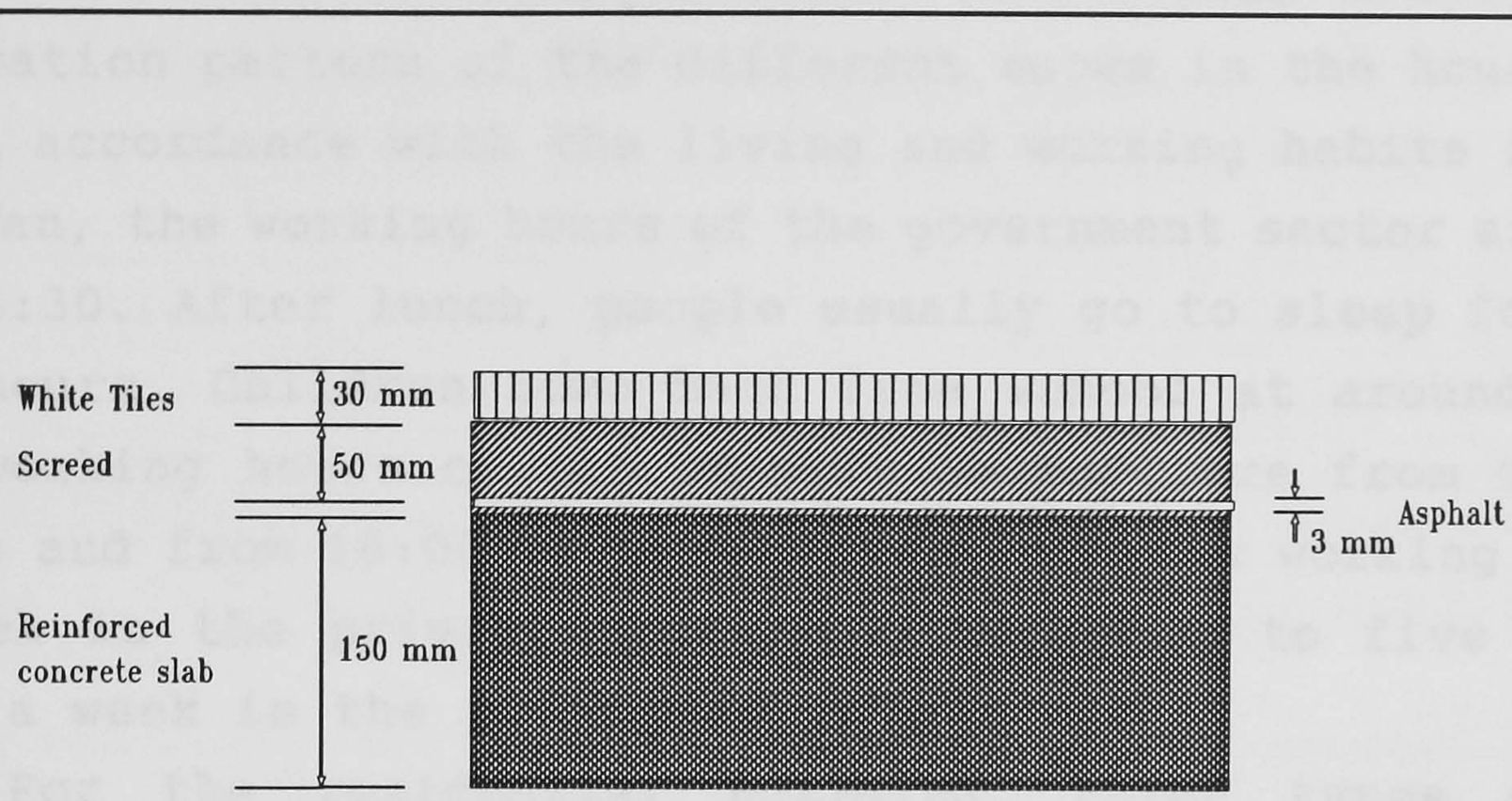

(a) The Un-insulated Roof Construction

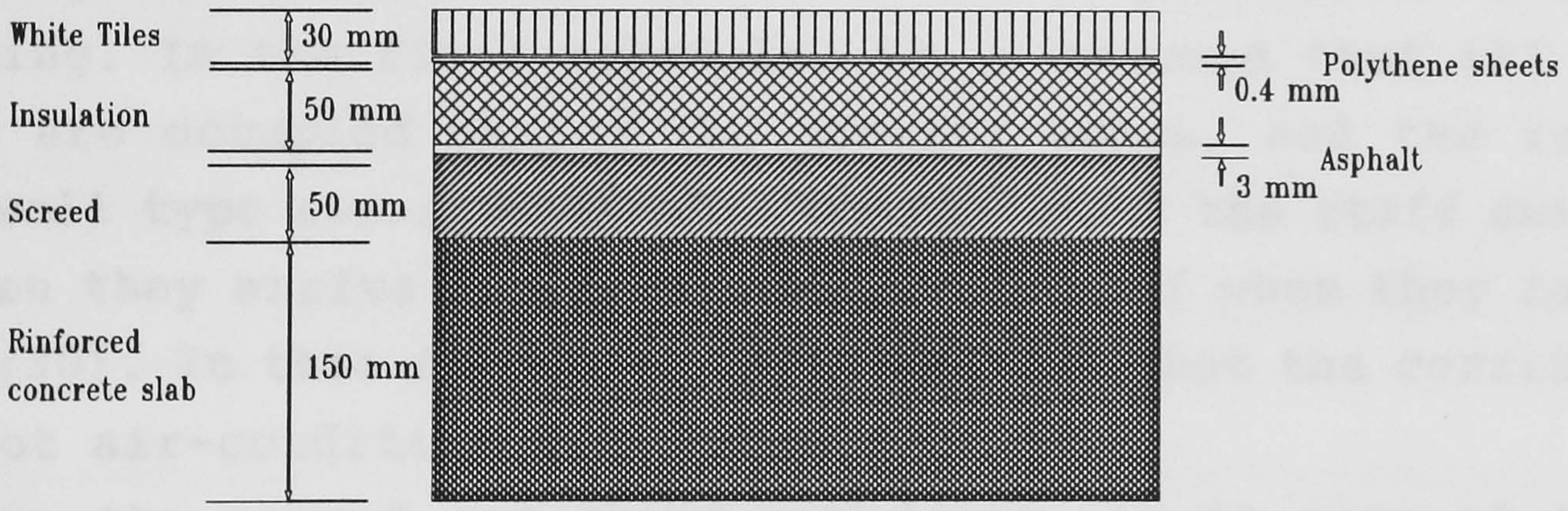

(b) The Insulated roof construction

Figure 8.3: The un-insulated and insulated roof constructions.

8.2.2 The air-conditioning schedules

The air-conditioning schedule is designed to reflect the occupation pattern of the different rooms in the house. This is in accordance with the living and working habits in Oman. In Oman, the working hours of the government sector are 07:30 to 14:30. After lunch, people usually go to sleep for about two hours. Children come back from school at around 13:00. The working hours of the private sector, are from 08:30 to 13:00 and from 16:00 to 19:00. There are six working days in a week in the private sector, as compared to five working days a week in the government sector.

For the residential building, three types of air-conditioning schedules were simulated; **Low Consumption**, **Medium Consumption**, and **High Consumption**. These are shown in Tables (8.1), (8.2) and (8.3) respectively.

Three schedules have also been simulated, when the building is assumed to be used as a government office building. In the first schedule, it is assumed that all the rooms are occupied during the working hours, and the rooms have wall type air-conditioning units, which the staff switch on when they arrive (@ 07:30), and switch off when they leave (@ 14:30). In this schedule, it is assumed that the corridors are not air-conditioned.

In the second and third schedules, it is assumed that all the building is air-conditioned, including the corridors. For the second schedule, the air-conditioning system is switched on at 06:00 and switched off after cleaning at 17:00. The building is not air-conditioned during the weekends. For the third schedule, it is assumed that the air-conditioning system works continuously throughout the day, including the weekends.

Two air-conditioning schedules have been simulated, for when the building is assumed to be used as a commercial office building. The first assumes that the rooms (but not

	Time periods during which the air-conditioning plant is "on"					
Room Type	**Week Day**			**Week End**		
Sitting	19-21			10-13	15-18	20-22
Family	11-16	19-22		11-16	19-22	
Bed1(Child)	14-16	20-06		14-16	20-06	
Bed.2	15-17	22-05		15-17	22-05	
Bed3(Mast.)	15-17	22-05		15-17	22-05	

Table 8.1: The Residential **Low Consumption** air-conditioning Schedule.

	Time periods during which the air-conditioning plant is "on"					
Room Type	**Week Day**			**Week End**		
Sitting	14-16	19-21		10-13	15-18	20-22
Family	08-23			09-24		
Bed1(Child)	14-16	20-06		14-16	20-08	
Bed.2	15-17	22-06		13-17	23-08	
Bed3(Mast.)	15-17	22-06		13-17	23-08	

Table 8.2: The Residential **Medium consumption** air-conditioning Schedule.

	Time periods during which the air-conditioning plant is "on"					
Room Type	**Week Day**			**Week End**		
Sitting	09-16	19-23		09-24		
Family	06-24			07-24		
Bed1(Child)	12-17	19-07		01-24		
Bed.2	13-17	20-07		01-24		
Bed3(Mast.)	14-17	21-07		12-17	22-09	

Table 8.3: The Residential **High Consumption** air-conditioning Schedule.

the corridors), are air-conditioned during the working hours, i.e. six days a week, from 08:00 to 13:00 and from 16:00 to 19:00. In the second, it is assumed that the whole building is air-conditioned, six days a week, from 07:00 to 19:00.

8.2.3 The internal conditions

In all the simulations carried out, it was assumed that the internal air, in the air-conditioned spaces, is maintained at 24 °C during occupation periods. The building is assumed to have an infiltration rate of 0.5 air changes per hour (ACH). The ventilation rate, during occupation periods, is set at 0.5 ACH, in a residential building, and 1.0 ACH in offices. The other heat gains accounted for are :

Lighting :	10 Wm^{-2} in residential rooms (night time only)
	15 Wm^{-2} in offices.
Occupants:	6.5 Wm^{-2} in residential rooms
	15 Wm^{-2} in offices.
Equipment:	5 Wm^{-2} in the residential sitting room (from TV)
	8 Wm^{-2} in all the offices.

8.3 Simulations Results

The results of the simulation carried out are summarised in Tables (8.4) - (8.11). From these results, we can see that the maximum cooling load, for the building as a whole, occurs at around 16:00. This is especially evident from the results in Table (8.9), where the cooling plant works continuously throughout the day. The different roof and external walls constructions, do not seem to have a large impact on shifting the period of the maximum cooling load.

Case No.	Peak Load Kw	Time Hours	Design Day Load Kwh	Summer Load Kwh	Resultant Temps. °C
0 R1	15.78	16	171.1	21923	29 - 32
1 R1	13.97	16	161.7	20987	28 - 30
2 R1	11.57	16	131.5	20625	27 - 29
3 R1	12.63	16	145.2	20657	27 - 29
4 R1	13.43	16	155.7	20716	28 - 30
5 R1	13.95	16	162.1	21655	28 - 31
6 R1	12.87	16	148.1	21033	28 - 30
7 R1	14.11	16	163.4	21815	28 - 30
8 R1	12.78	16	146.0	21089	27 - 29

Table 8.4: The simulation results for the **Low Consumption** Residential Building (Air-Conditioning Schedule R1).

Case No.	Peak Load Kw	Time Hours	Design Day Load Kwh	Summer Load Kwh	Resultant Temps. °C
0 R2	20.18	16	221.9	30711	28 - 31
1 R2	17.94	16	208.3	28964	28 - 30
2 R2	15.11	16	173.0	27505	27 - 29
3 R2	16.05	16	185.4	27530	27 - 29
4 R2	17.13	16	199.3	28190	28 - 30
5 R2	17.66	16	205.8	29162	28 - 31
6 R2	16.28	16	188.2	27910	28 - 30
7 R2	17.81	16	206.8	29250	28 - 30
8 R2	16.22	16	186.4	27950	27 - 28

Table 8.5: The simulation results for the **Medium Consumption** Residential Building (Air-Conditioning Schedule R2).

Case No.	Peak Load Kw	Time Hours	Design Day Load Kwh	Summer Load Kwh	Resultant Temps. °C
0 R3	17.74	17	299.4	41159	28 - 30
1 R3	15.09	17	270.1	36916	28 - 29
2 R3	12.54	17	221.7	33674	27 - 28
3 R3	13.05	17	232.3	33654	27 - 28
4 R3	14.14	17	254.0	35257	28 - 29
5 R3	14.56	17	262.1	36492	27 - 29
6 R3	13.21	17	235.6	34126	27 - 28
7 R3	14.64	18	263.6	36553	28 - 29
8 R3	13.21	17	234.6	34197	27 - 28

Table 8.6: The simulation results for the **High Consumption** Residential Building (Air-Conditioning Schedule R3).

Case No.	Peak Load Kw	Time Hours	Design Day Load Kwh	Summer Load Kwh	Resultant Temps. °C
0 G1	25.64	15	195.2	19336	29 - 32
1 G1	24.47	8	184.9	19358	28 - 30
2 G1	20.94	8	161.6	19875	28
3 G1	22.79	8	171.0	19762	28 - 29
4 G1	24.20	8	179.1	19530	28 - 29
5 G1	25.07	8	184.0	19941	29 - 30
6 G1	23.23	8	173.2	19936	28 - 29
7 G1	25.18	8	185.0	20312	29 - 30
8 G1	22.81	8	171.6	20042	28 - 29

Table 8.7: The simulation results for the **Low Consumption** Government office Building (Air-Conditioning Schedule G1).

Case No.	Peak Load Kw	Time Hours	Design Day Load Kwh	Summer Load Kwh	Resultant Temps. °C
0 G2	35.96	7	402.7	41344	28 - 32
1 G2	34.84	7	360.3	39307	28 - 30
2 G2	29.67	7	312.2	37580	28 - 29
3 G2	28.71	7	301.3	37415	28 - 29
4 G2	33.39	7	339.6	38299	28 - 29
5 G2	34.66	7	347.9	39196	28 - 29
6 G2	31.01	7	321.2	37638	28 - 29
7 G2	34.68	7	348.5	39518	28 - 29
8 G2	30.79	7	321.3	37815	28 - 29

Table 8.8: The simulation results for the **Medium Consumption** Government office Building (Air-Conditioning Schedule G2).

Case No.	Peak Load Kw	Time Hours	Design Day Load Kwh	Summer Load Kwh	Resultant Temps. °C
0 G3	35.64	16	675.0	98182	26 - 30
1 G3	28.81	16	587.9	88870	26 - 28
2 G3	23.97	16	492.5	79068	26 - 27
3 G3	23.77	16	490.2	78878	26 - 27
4 G3	26.02	16	541.4	83905	26 - 28
5 G3	26.53	16	553.8	85747	26 - 29
6 G3	24.27	16	501.2	79612	26 - 28
7 G3	26.28	16	550.3	85561	26 - 29
8 G3	24.30	16	500.8	79701	26 - 27

Table 8.9: The simulation results for the **High Consumption** Government office Building (Air-Conditioning Schedule G3).

Case No.	Peak Load Kw	Time Hours	Design Day Load Kwh	Summer Load Kwh	Resultant Temps. °C
0 C1	30.57	16	234.0	25133	29 - 32
1 C1	26.61	16	214.8	24420	29 - 31
2 C1	23.37	16	184.0	24149	28 - 30
3 C1	23.49	16	193.8	24103	28 - 30
4 C1	24.93	16	204.9	24191	28 - 30
5 C1	25.68	9	210.6	24844	28 - 30
6 C1	23.87	9	196.3	24373	28 - 30
7 C1	25.84	9	210.5	25039	28 - 30
8 C1	23.66	16	194.6	24444	28 - 30

Table 8.10: The simulation results for the **Low Consumption** Commercial office Building (Air-Conditioning Schedule C1).

Case No.	Peak Load Kw	Time Hours	Design Day Load Kwh	Summer Load Kwh	Resultant Temps. °C
0 C2	36.11	16	442.5	54699	28 - 31
1 C2	32.77	8	383.2	49847	28 - 30
2 C2	27.72	8	321.9	45587	27 - 28
3 C2	27.05	8	314.9	45421	27 - 28
4 C2	31.44	8	354.5	47594	28 - 29
5 C2	32.50	8	363.7	48813	27 - 29
6 C2	29.11	8	330.5	45881	27 - 28
7 C2	32.67	8	362.7	48916	27 - 29
8 C2	29.00	8	330.5	45995	27 - 28

Table 8.11: The simulation results for the **Medium Consumption** Commercial office Building (Air-Conditioning Schedule C2).

The value of the **peak load** depends on the number of rooms cooled at a certain time. Thus if the building, or part of the building is not used in the afternoon, especially at around 16:00, then the peak load will be reduced. This is the reason for the higher peak load values of the **Medium Consumption** residential building, as compared with those of the **Low Consumption** residential building. Obviously, if the cooling plant works for long periods, then the peak load will be reduced, but the total energy consumption will be increased. Thus the peak load values of the **High Consumption** residential building (Table 8.6), are lower than those of the **Medium consumption** residential building (Table 8.5).

Generally, the addition of roof and wall insulation seems to work well in reducing both the Design Day load and the Cooling Season load. This is except for the **Low Consumption** Government office building (Table 8.7). The reason for this, is that a building with un-insulated roof and walls, can take better advantage of the beneficial ambient conditions at night, especially during the early and late parts of the cooling season. Thus "coolness" will be stored in the structure of the building, reducing the cooling load during the morning. By the time the load becomes high, in the afternoon, the staff would have left the building.

The high thermal mass of the external walls, in **Case 2**, has generally helped to reduce both the Design Day load, and the Cooling Season load. On the other hand, a building with an outer brick surface (assumed to have an absorptivity of 0.65 as compared with 0.36 for a white painted concrete block) and no insulation (**Case 5**), seems to have a higher cooling load than **Case 4**, despite the lower thermal conductivity of brick (0.7 $Wm^{-2}K^{-1}$ as compared with 1.0 $Wm^{-2}K^{-1}$ for hollow concrete block).

It is quite common to find the air-conditioning system, in the centrally air-conditioned Government office buildings in Oman, functioning throughout the full 24 hours of the day and continuously throughout the year. From the results in

Tables (8.8) and (8.9), this strategy seems to double the energy consumption of the buildings analyzed. Thus half of the energy consumed is wasted, since the buildings are unoccupied from around 15:00 to 07:00 the next morning. This shows, the need for better energy management in such buildings, and the potential impact on energy demand from sensible use of this resource.

Finally, although the upper limit of the internal air temperature of air-conditioned parts of the building is set at 24 °C, the resultant temperature in the rooms generally varies between 28 and 30 °C and reaches as high as 32 °C in a building with no roof insulation.

8.4 Economic Analysis Of The Different Cases Considered

The energy saving measures considered earlier in this chapter, require an initial investment. Sometimes this initial investment is offset by the savings due to the reduced cooling plant capacity. On the other hand, the benefit may not be sufficient to encourage the building owners to invest in these energy saving measures. This is especially since electricity in most of the Gulf States is subsidised by more than 60%.

Because of the high subsides, and without regulations, the economic incentive for the individuals to invest in improving the thermal design of their buildings is not attractive enough. Thus to have a valid analysis, we must consider the benefit, of improving the thermal design of buildings, to the nation as a whole. And if the government is willing to carry on with the high subsidies of electricity, then equally it might be viable economically for them to subsidies the cost of improving the thermal efficiency of buildings. This is a question that will be looked at in more detail, later on in the chapter.

From the results in section 8.3, we can estimate the percentage savings in cooling plant capacity, and energy consumption, of the different construction types with the different air-conditioning schedules. These are summarised in Figures (8.4) - (8.11). From these figures, we can see that all of the construction types would yield a saving in cooling plant capacity when compared with the base case (**Case 0**). Generally, the highest saving is achieved by **Case 2** where the external walls have a relatively high thermal mass. The savings in the energy consumed is very much dependent on the air-conditioning schedule. The higher the consumption, the higher is the percentage saving achieved. Generally, **Case 2** again seems to give the best saving in energy consumption. For the air-conditioning schedule **G1**, virtually all of the cases yield an increase in the energy consumption when compared with the base case. The reason for this has been discussed earlier. However, the thermal comfort analysis check - see Appendix B - suggests that the base case (**Case 0**), with the air-conditioning schedule **G1**, will not meet the thermal comfort criterion. This would mean that the occupants will try to reduce the room-air temperature, and thus increase the energy consumption of the building.

A Net Present Cost analysis was used to compare the life-cycle costs of the different constructions, with the various air-conditioning schedules. The following assumptions has been used in the analysis:

- The life-cycle of the building is 60 years.
- The concrete block external surfaces (but not the brick external surfaces) require painting once every five years, at a cost of 1.7 R.O. / m^2 [1] - R.O. is the Omani currency of Rials, 1 R.O. = $ 2.6. The total cost of painting is 492 R.O.
- The average electricity production and transmission cost is 0.036 R.O. / kwh [2]

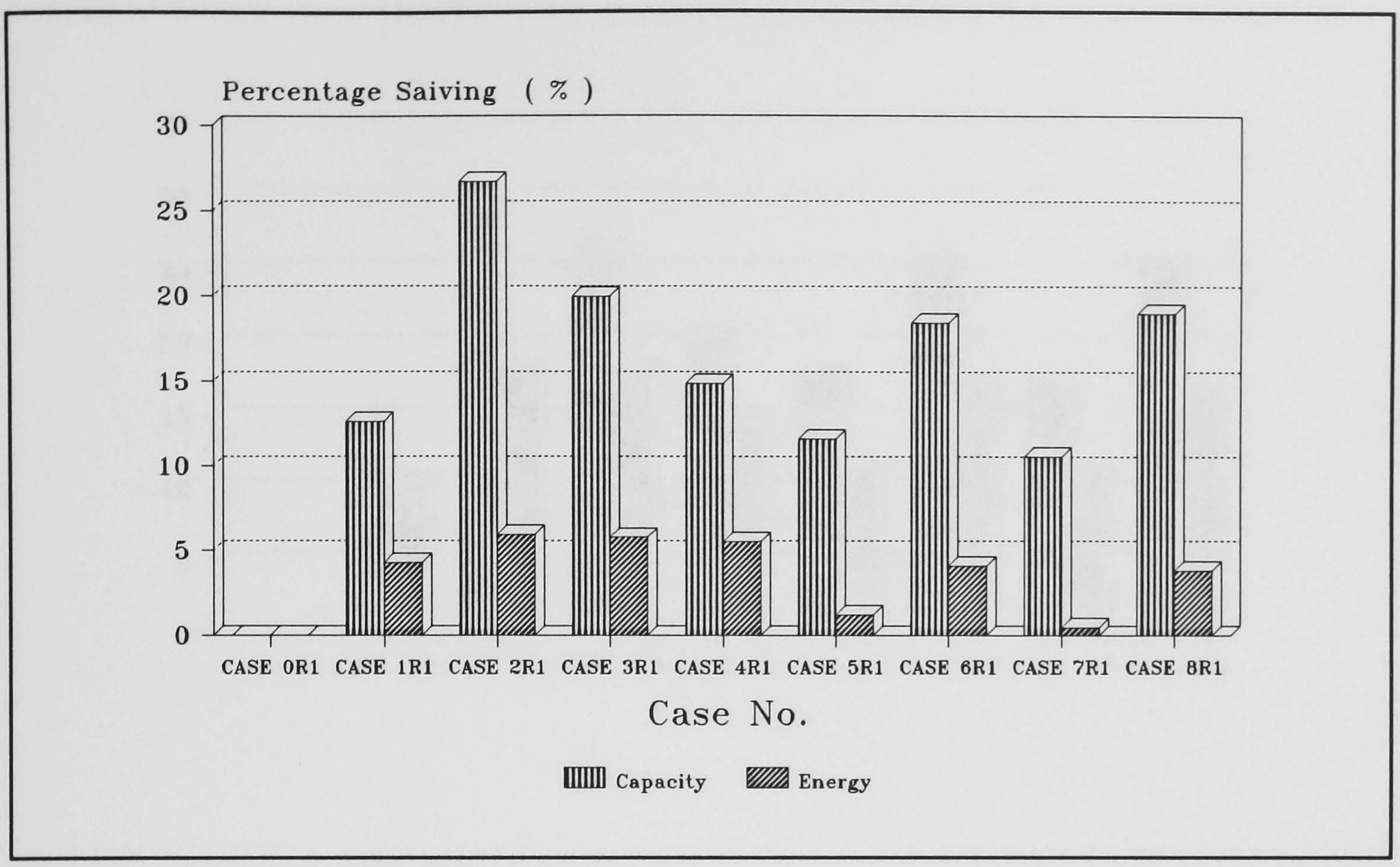

Figure 8.4: The percentage savings in installed capacity and energy consumption for a residential building with the **Low Consumption** air-conditioning schedule (R1).

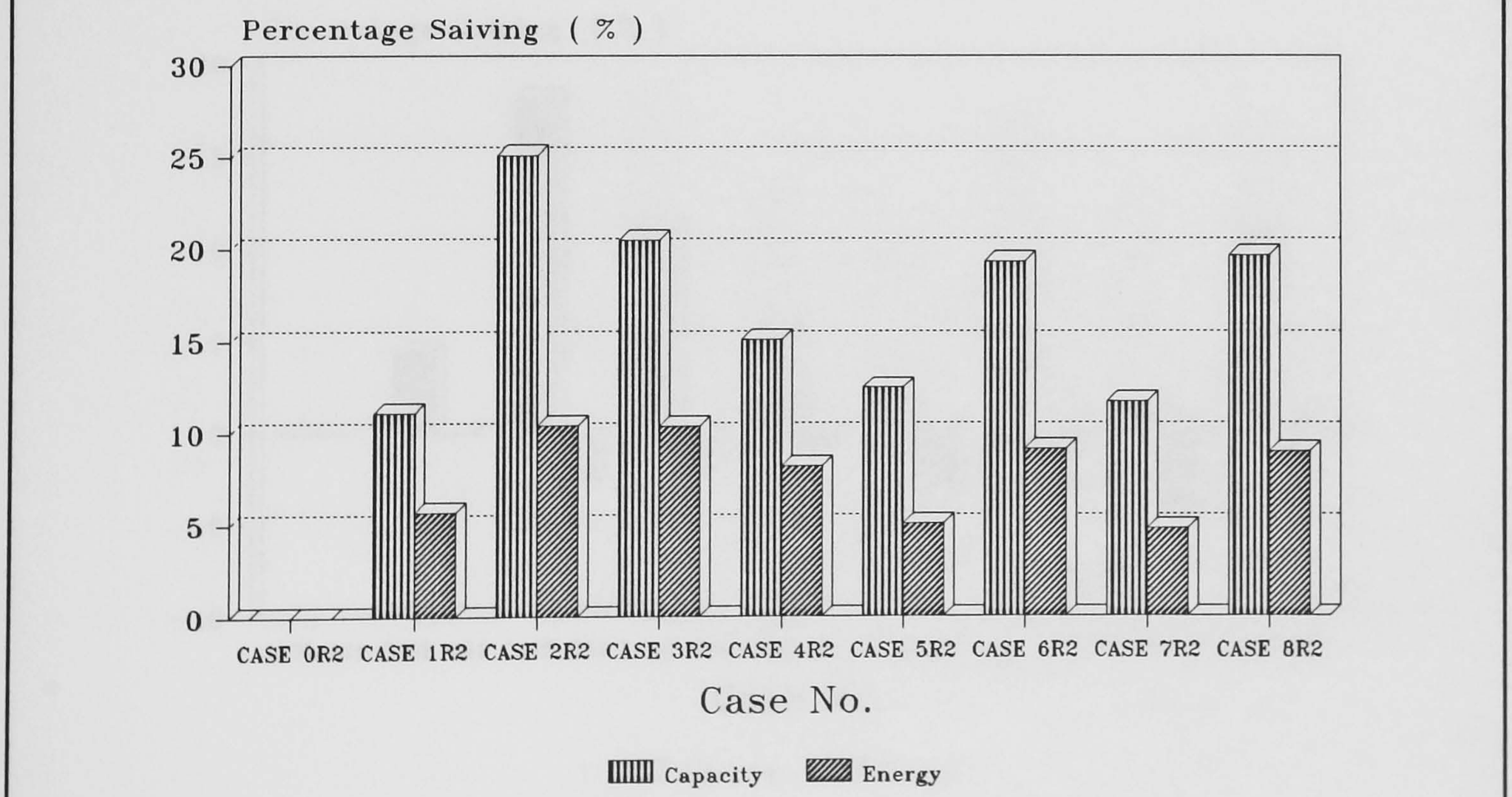

Figure 8.5: The percentage savings in installed capacity and energy consumption for a residential building with the **Medium Consumption** air-conditioning schedule (R2).

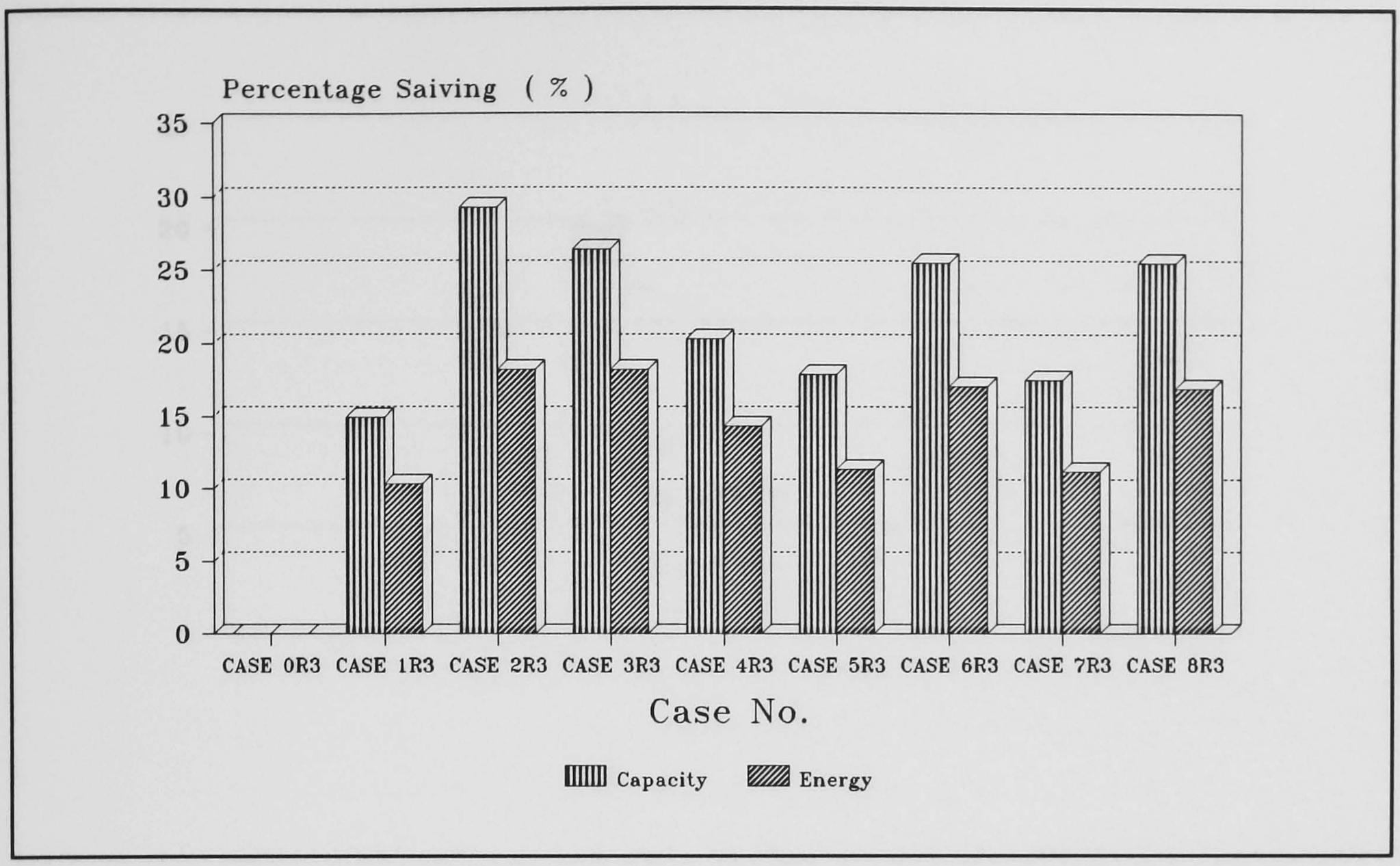

Figure 8.6: The percentage savings in installed capacity and energy consumption for a residential building with the **High Consumption** air-conditioning schedule (R3).

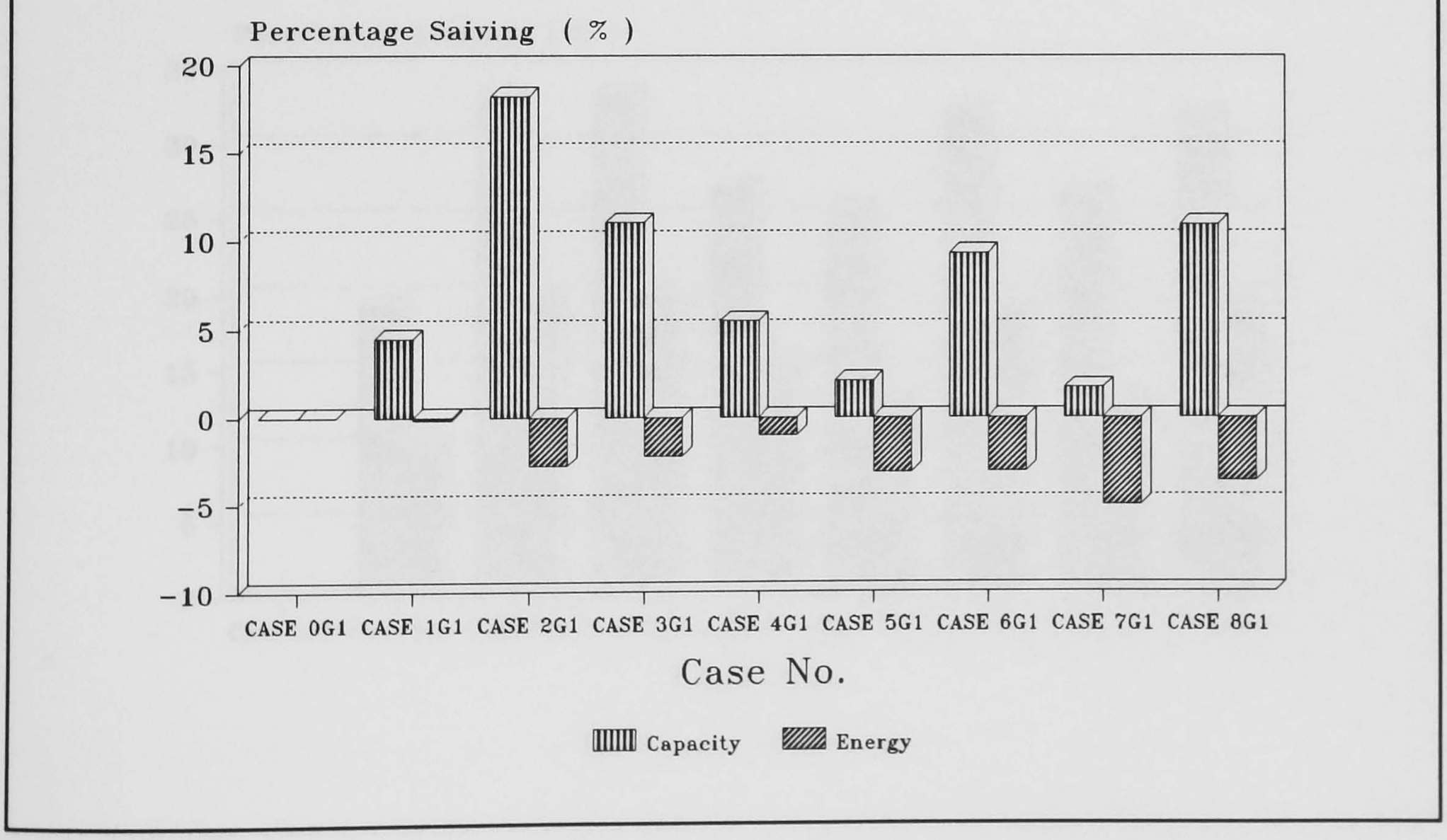

Figure 8.7: The percentage savings in installed capacity and energy consumption for a Government office building with the **Low Consumption** air-conditioning schedule (G1).

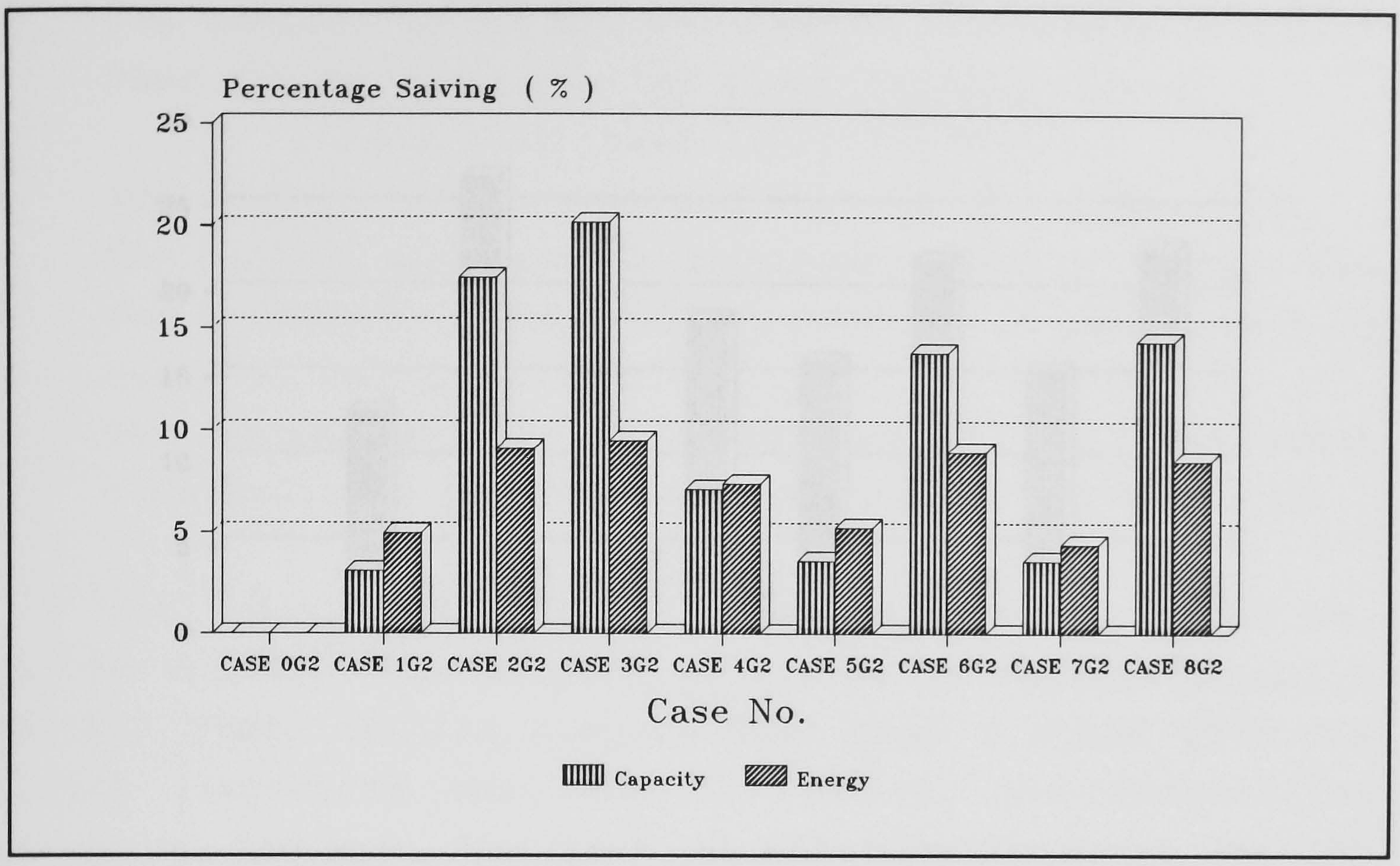

Figure 8.8: The percentage savings in installed capacity and energy consumption for a Government office building with the **Medium Consumption** air-conditioning schedule (G2).

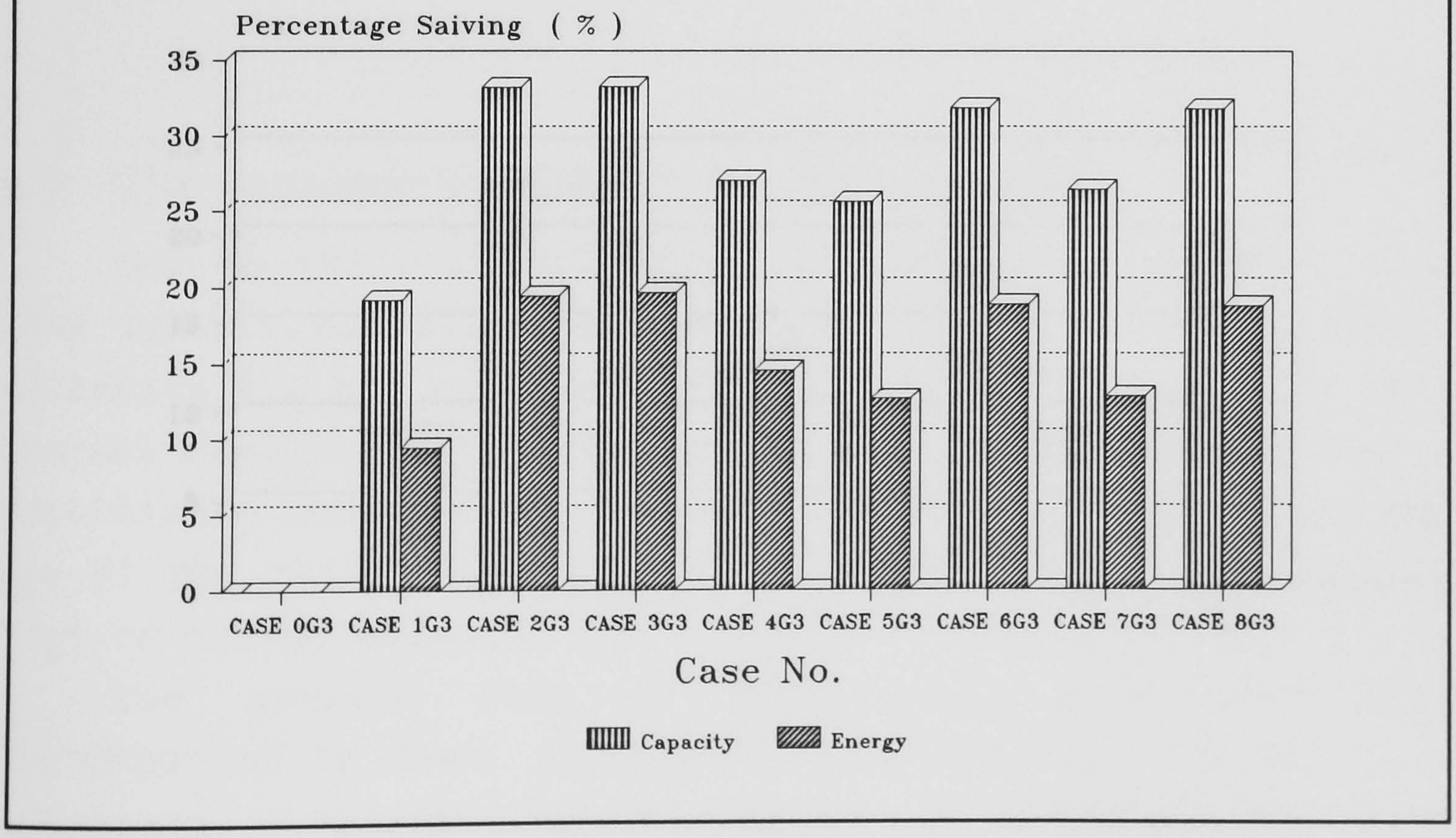

Figure 8.9: The percentage savings in installed capacity and energy consumption for a Government office building with the **High Consumption** air-conditioning schedule (G3).

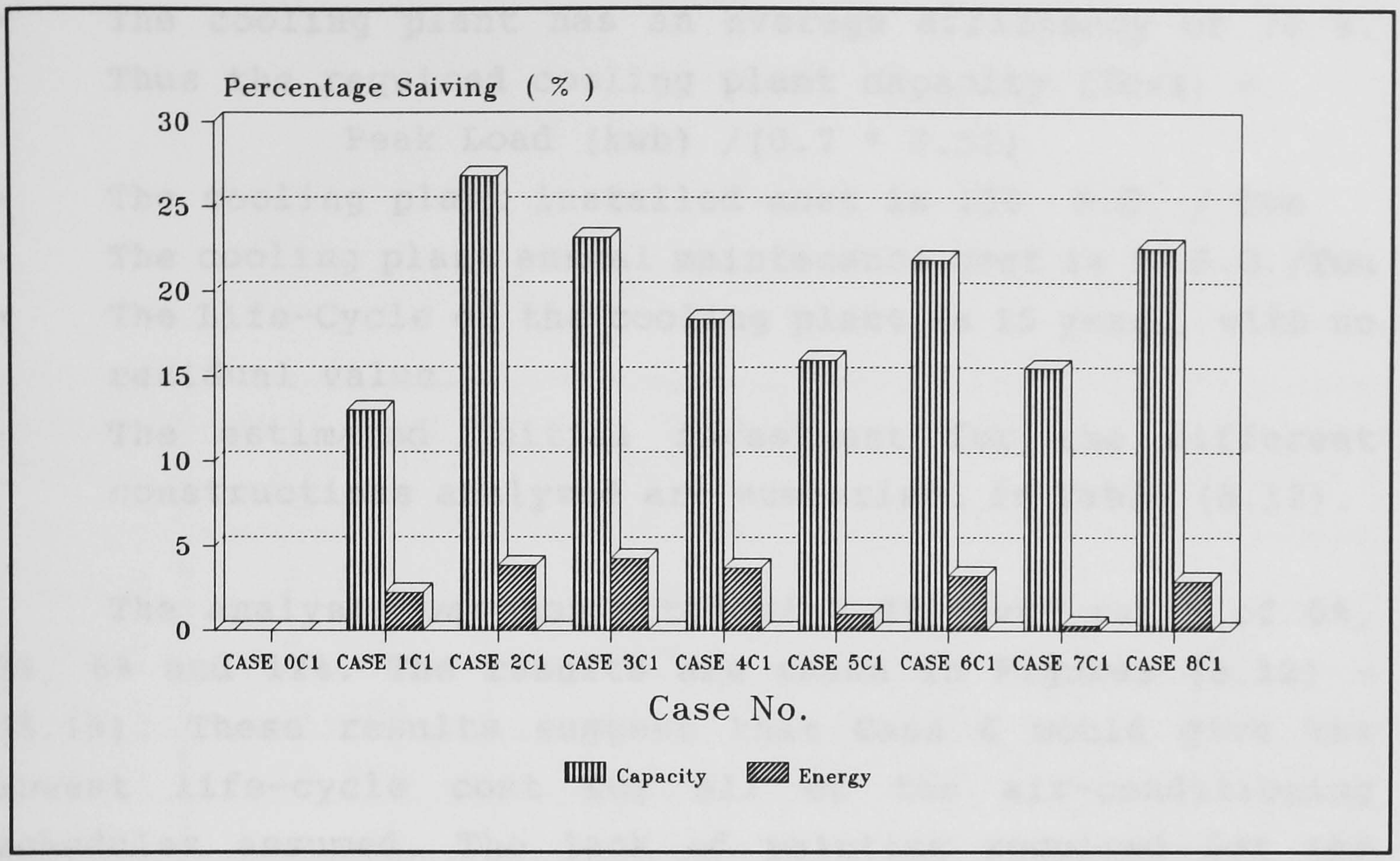

Figure 8.10: The percentage savings in installed capacity and energy consumption for a Commercial office building with the **Low Consumption** air-conditioning schedule (C 1).

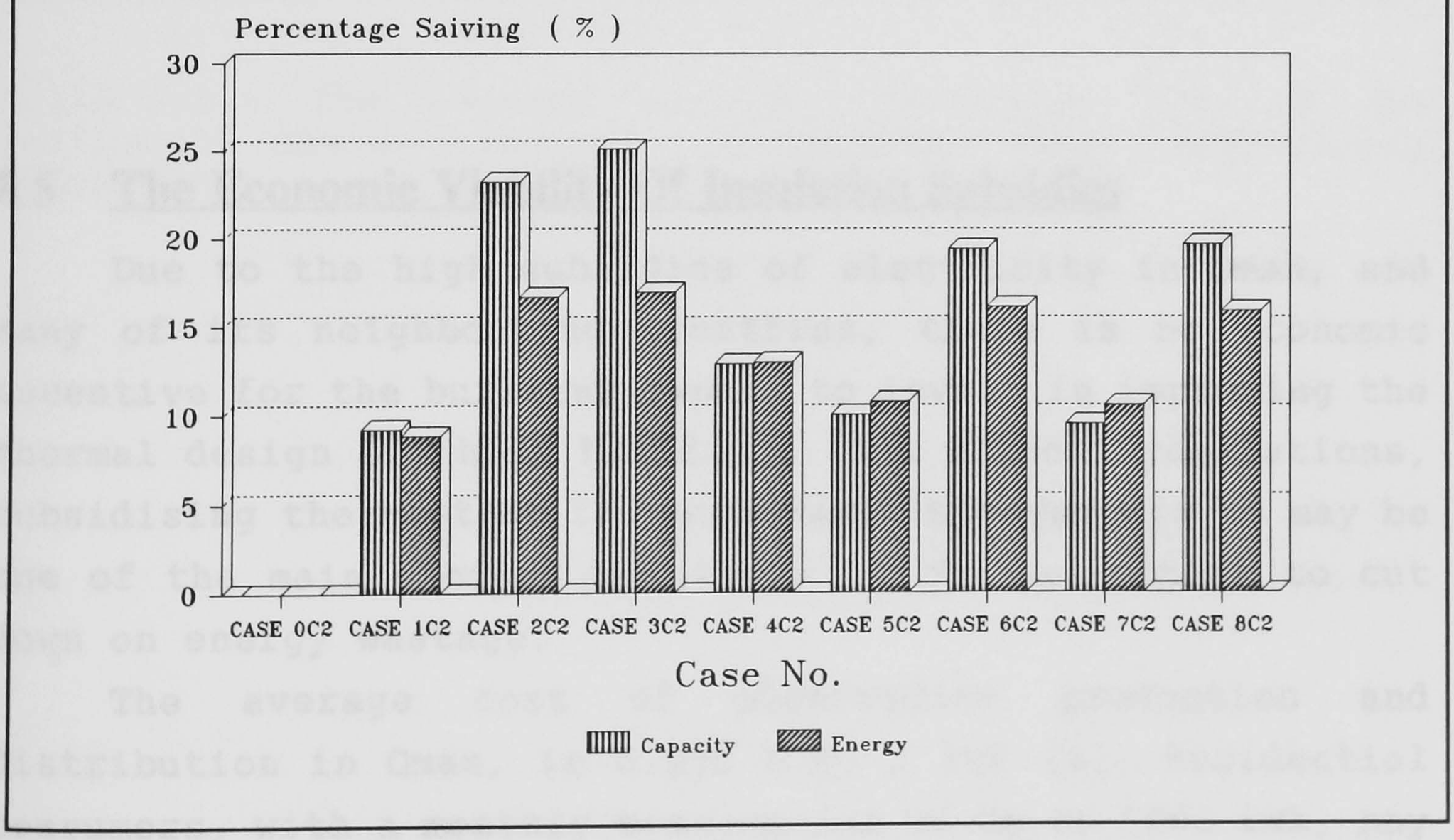

Figure 8.11: The percentage savings in installed capacity and energy consumption for a Commercial office building with the **Medium Consumption** air-conditioning schedule (C2).

- The cooling plant has an average efficiency of 70 %. Thus the required cooling plant capacity (Tons) = Peak Load (kwh) /(0.7 * 3.51)
- The cooling plant installed cost is 150 R.O. / Ton
- The cooling plant annual maintenance cost is 10 R.O./Ton
- The Life-Cycle of the cooling plant is 15 years, with no residual value.
- The estimated initial investment for the different constructions analyzed are summarised in Table (8.12).

The analysis was conducted with discount rates of 0%, 3%, 6% and 12%. The results are shown in Figures (8.12) - (8.19). These results suggest that **Case 6** would give the lowest life-cycle cost for all of the air-conditioning schedules assumed. The lack of painting required for the brick surface is the main reason for **Case 6** having a lower life-cycle cost than **Cases 2** and **3**, which consistently give high savings in energy consumption and cooling plant capacity.

8.5 The Economic Viability Of Insulation Subsidies

Due to the high subsidies of electricity in Oman, and many of its neighbouring countries, there is no economic incentive for the building owners to invest in improving the thermal design of their buildings. And without regulations, subsidising the cost of the necessary improvements is may be one of the main choices available to the government to cut down on energy wastage.

The average cost of electricity production and distribution in Oman, is 0.036 R.O. / kwh [2]. Residential consumers, with a monthly consumption of up to 1000 kwh, pay only 0.010 R.O./ kwh, and those with a monthly consumption of more than 1000 kwh pay 0.015 R.O. / kwh. Thus the government

House Type	Wall Cost per m^{-2} (R.O.)	Total Cost Of Walls (R.O.)	Cost Of Roof Ins. (R.O.)	Total Cost Difference (R.O.)
Case 0	8.700	2516	-	-
Case 1	8.700	2516	689	689
Case 2	14.300	4136	689	2309
Case 3	12.700	3673	689	1846
Case 4	11.200	3239	689	1412
Case 5	12.500	3615	689	1788
Case 6	14.000	4049	689	2222
Case 7	18.500	5351	689	3524
Case 8	20.000	5784	689	3957

Table 8.12: The assumed initial investment cost of the different cases analyzed. (**Source: Oman Engineering Consultancy**).

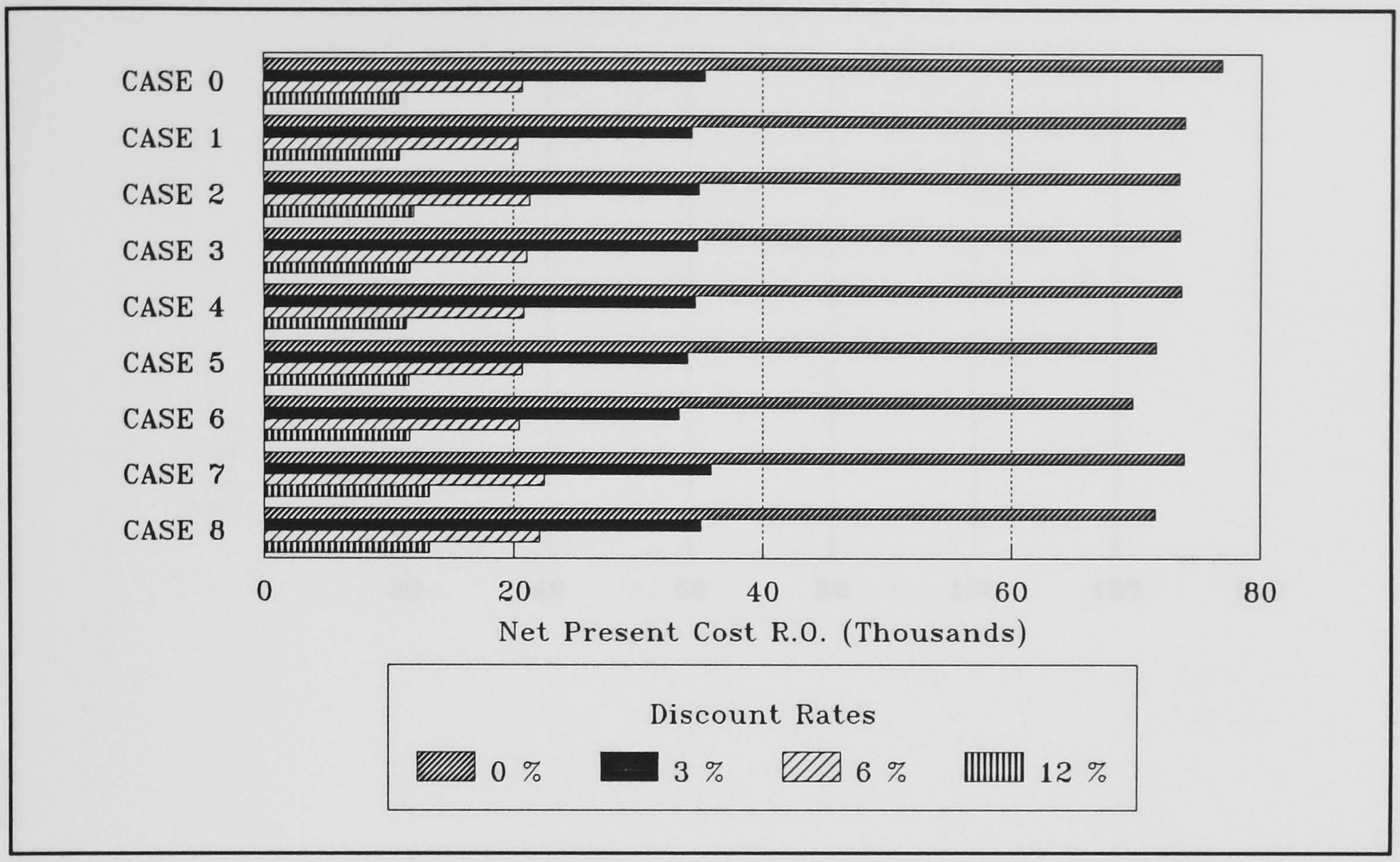

Figure 8.12: The Net Present Cost comparison of the different construction, for a residential building with air-conditioning schedule **R1.**

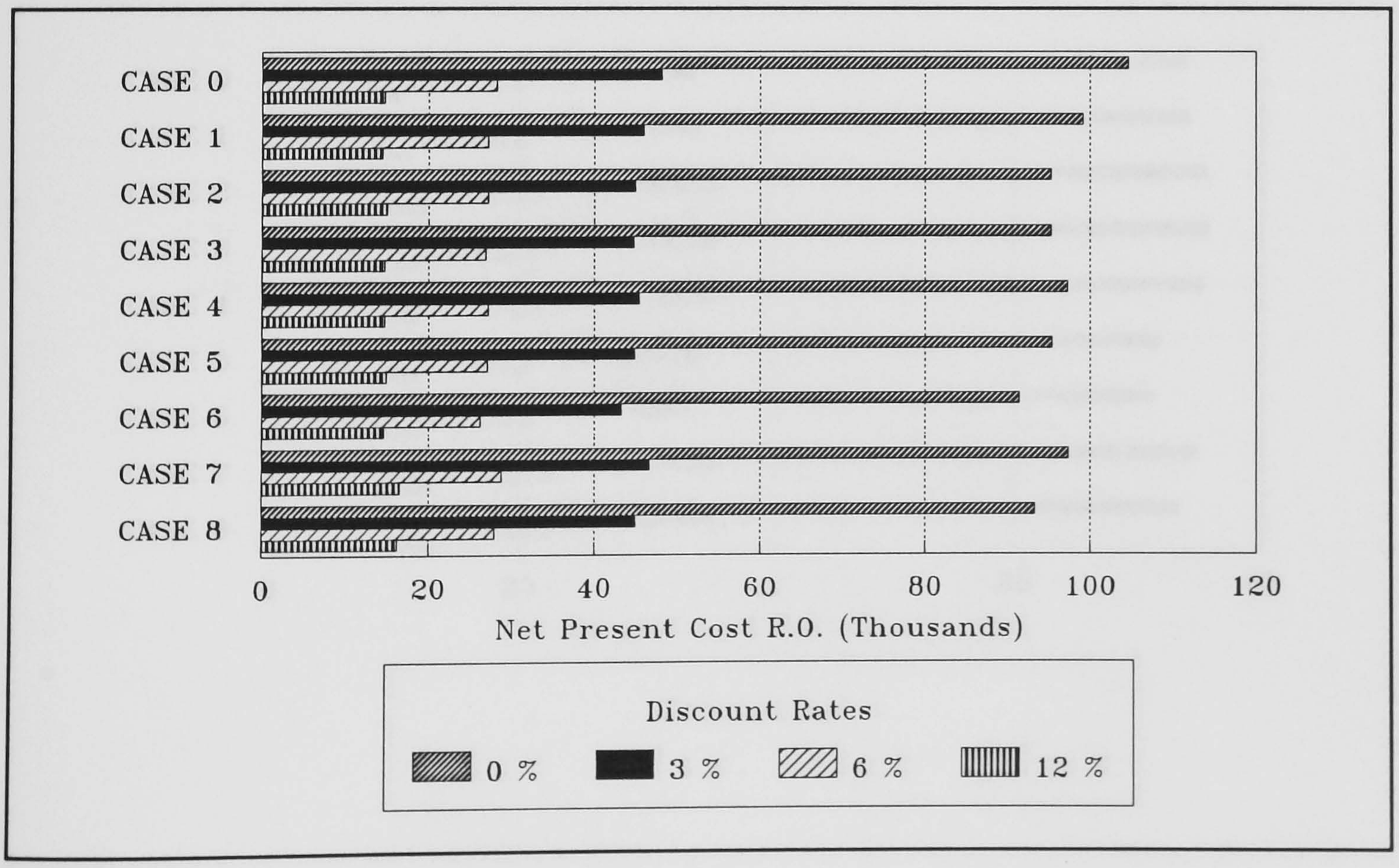

Figure 8.13: The Net Present Cost comparison of the different construction, for a residential building with air-conditioning schedule **R2.**

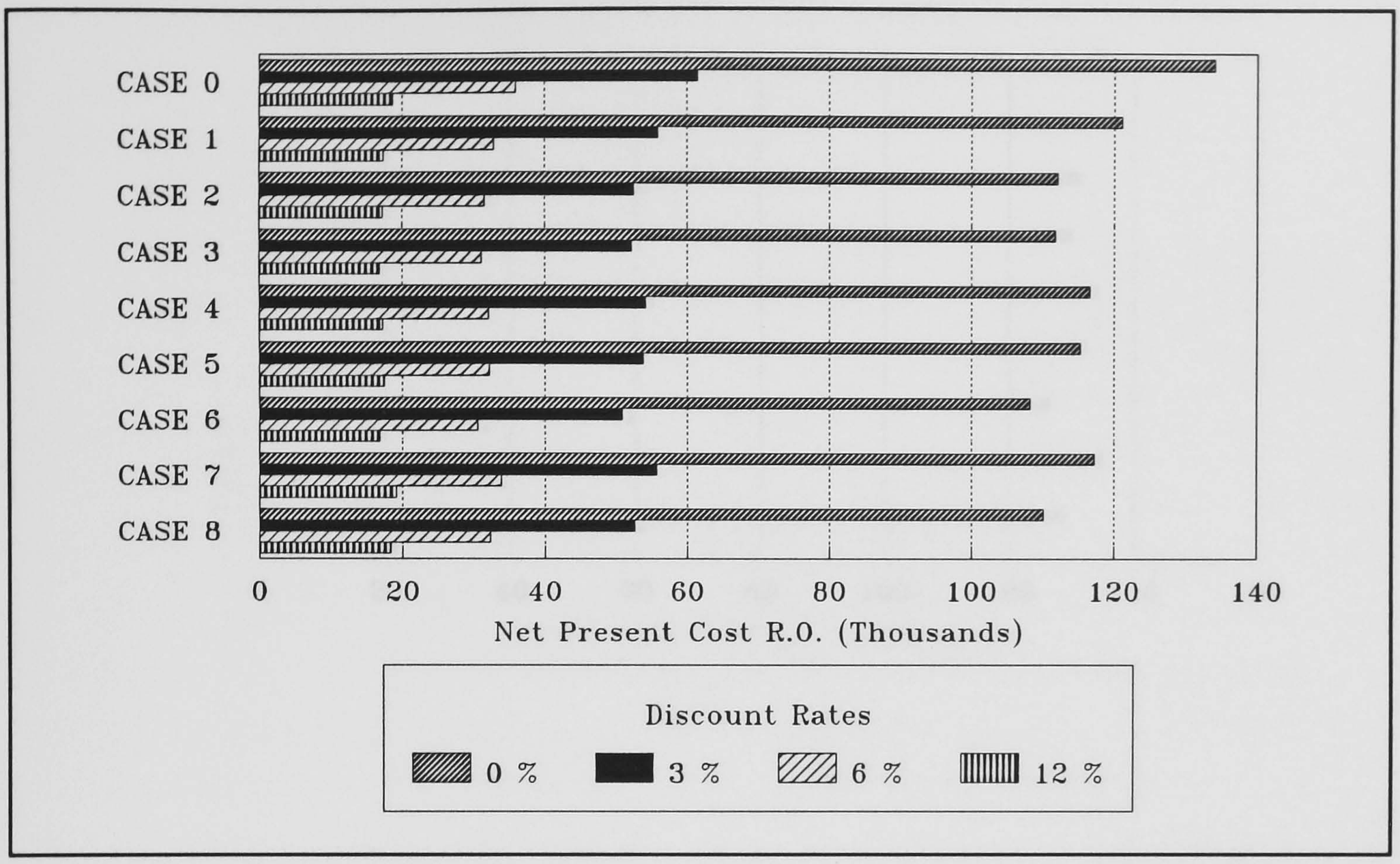

Figure 8.14: The Net Present Cost comparison of the different construction, for a residential building with air-conditioning schedule **R3.**

Figure 8.15: The Net Present Cost comparison of the different construction, for a Government office building with air-conditioning schedule **G1.**

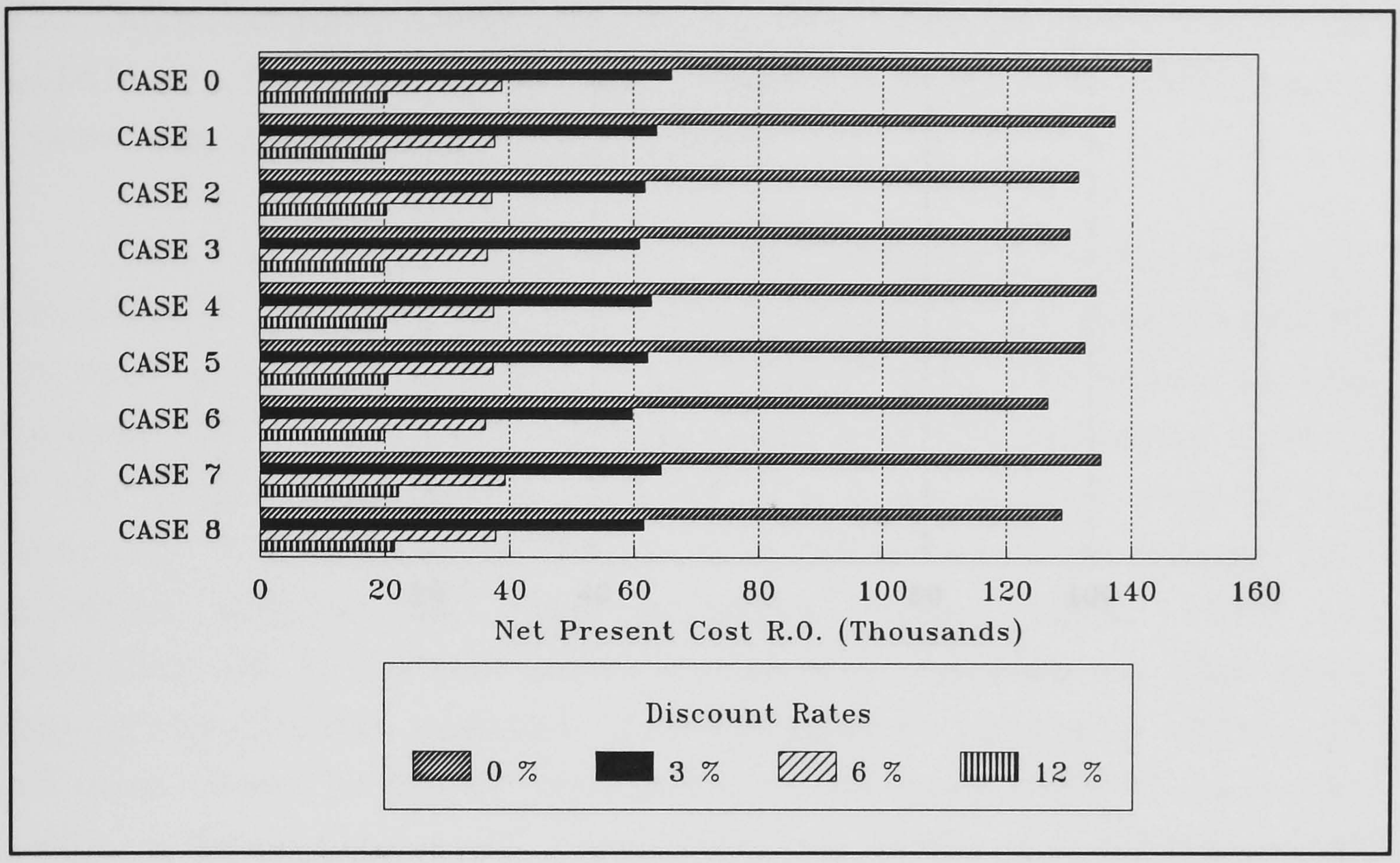

Figure 8.16: The Net Present Cost comparison of the different construction, for a Government office building with air-conditioning schedule **G2.**

Figure 8.17: The Net Present Cost comparison of the different construction, for a Government office building with air-conditioning schedule **G3.**

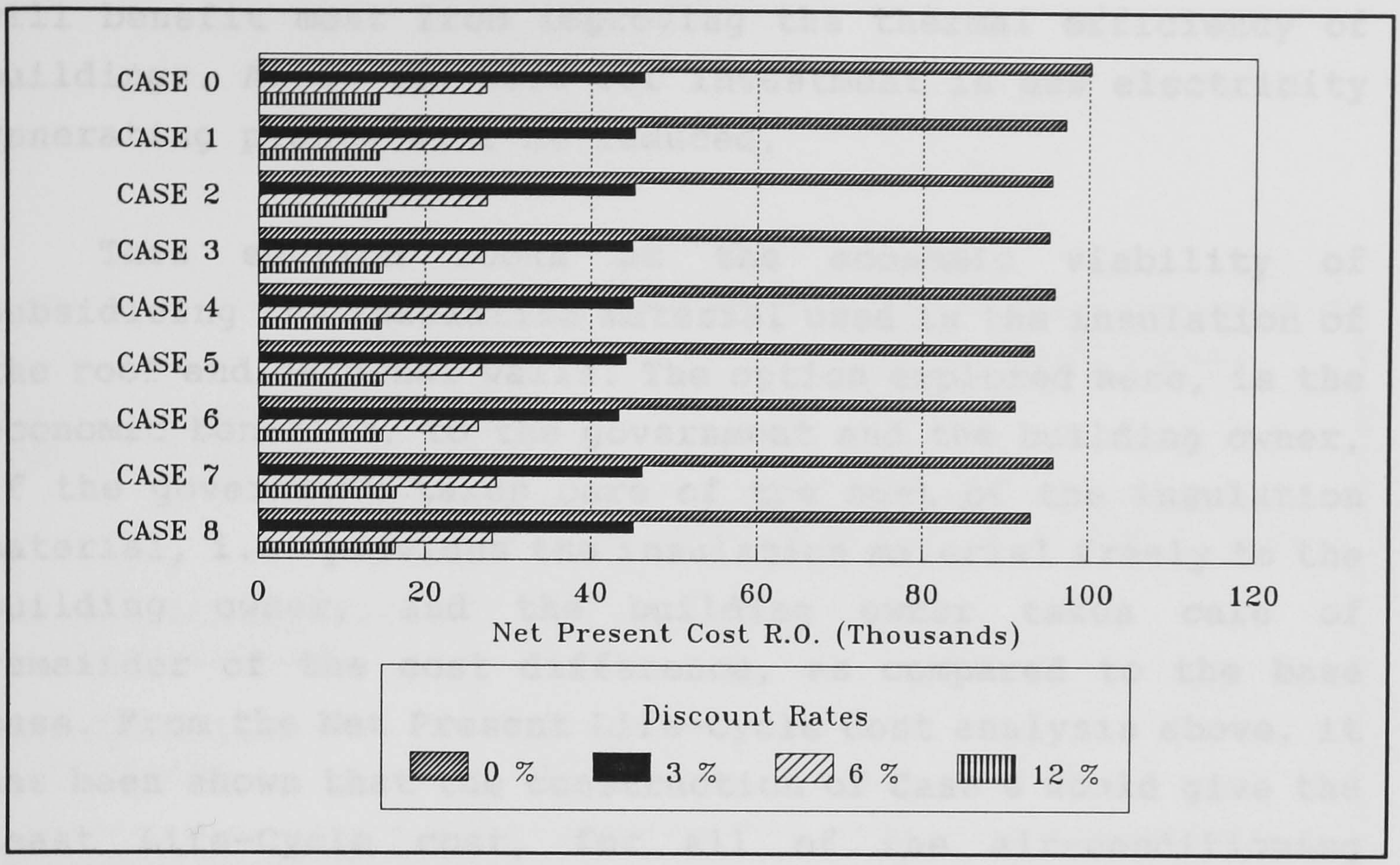

Figure 8.18: The Net Present Cost comparison of the different construction, for a Commercial office building with air-conditioning schedule **C1.**

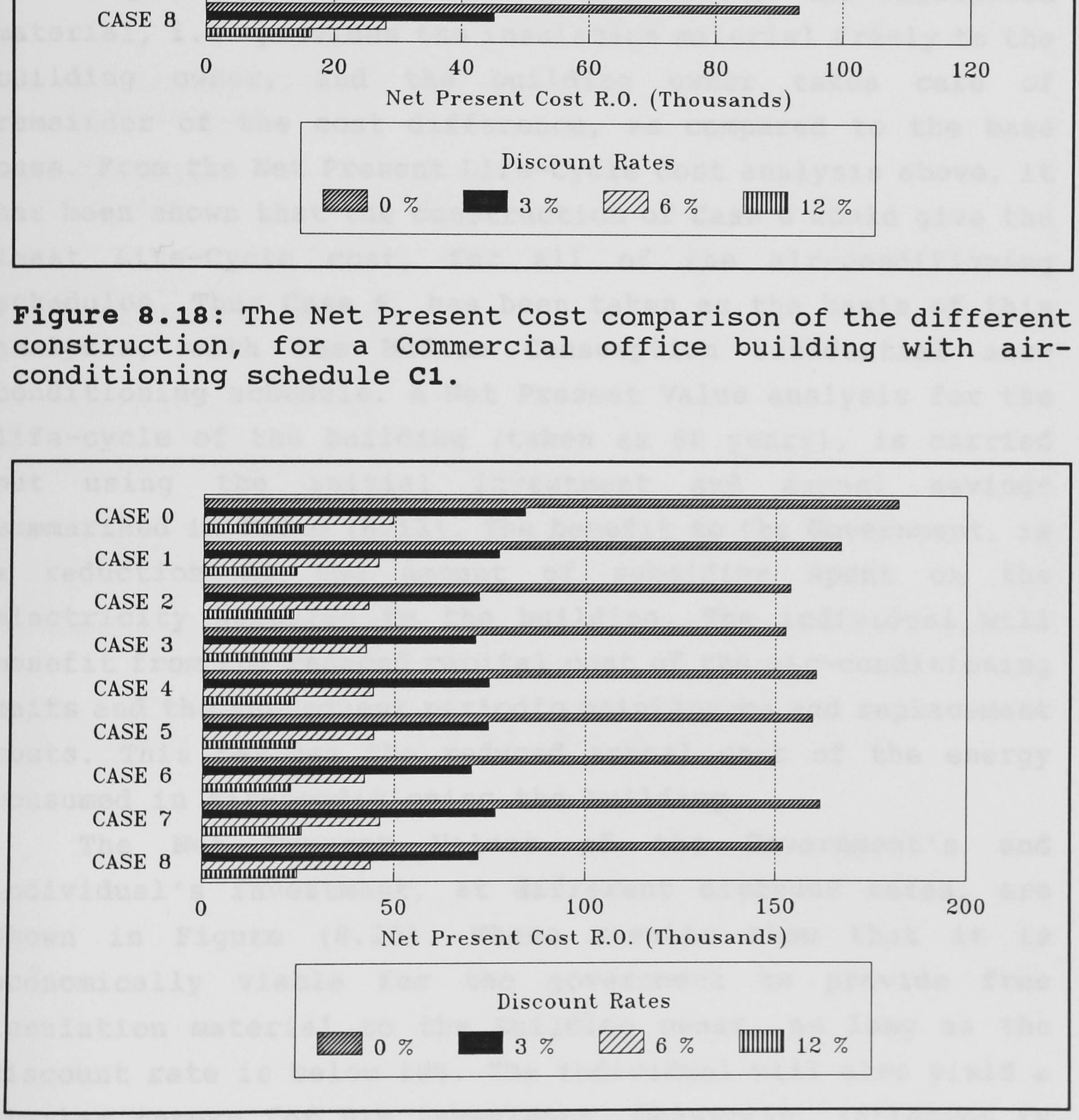

Figure 8.19: The Net Present Cost comparison of the different construction, for a Commercial office building with air-conditioning schedule **C2.**

will benefit most from improving the thermal efficiency of buildings. Also, the need for investment in new electricity generating plants will be reduced.

This section looks at the economic viability of subsidising the insulation material used in the insulation of the roof and external walls. The option explored here, is the economic benefits, to the government and the building owner, if the government takes care of the cost of the insulation material, i.e. provides the insulation material freely to the building owner, and the building owner takes care of remainder of the cost difference, as compared to the base case. From the Net Present Life-Cycle Cost analysis above, it has been shown that the construction of **Case 6** would give the least Life-Cycle cost, for all of the air-conditioning schedules. Thus **Case 6**, has been taken as the basis of this analysis, with the **Medium Consumption** residential air-conditioning schedule. A Net Present Value analysis for the life-cycle of the building (taken as 60 years), is carried out using the initial investment and annual savings summarised in Table (8.13). The benefit to the Government, is a reduction in the amount of subsidies spent on the electricity supplied to the building. The individual will benefit from the reduced capital cost of the air-conditioning units and the subsequent periodic maintenance and replacement costs. This besides the reduced annual cost of the energy consumed in air-conditioning the building.

The Net Present Values of the Government's and individual's investment, at different discount rates, are shown in Figure (8.20). These results show that it is economically viable for the government to provide free insulation material to the building owner, as long as the discount rate is below 10%. The individual will also yield a similar return for his investment. Generally, inflation in Oman has been very low during the past six years. Thus an appropriate discount rate should be in the range 3% - 5%.

	Government	Individual
Initial Investment (Omani Rials):		
Roof	2 x 237 = 474	0.9 x 237 = 214
Walls	1.5 x 290 = 435	3.8 x 290 = 1102
Saving in Cooling plant Capacity	_____	222.2
Net Initial Investment	909	1093.8
Annual saving in Energy Consumption (Omani Rials)	78.5	56.025
Annual saving in Cooling plant Maintenance (R.O.)	_____	14.800
Savings in Cooling Plant Replacement (every 15 years)	_____	222.2

Table 8.13: The initial investments and savings used in the Net Present Value analysis of insulation subsidies.

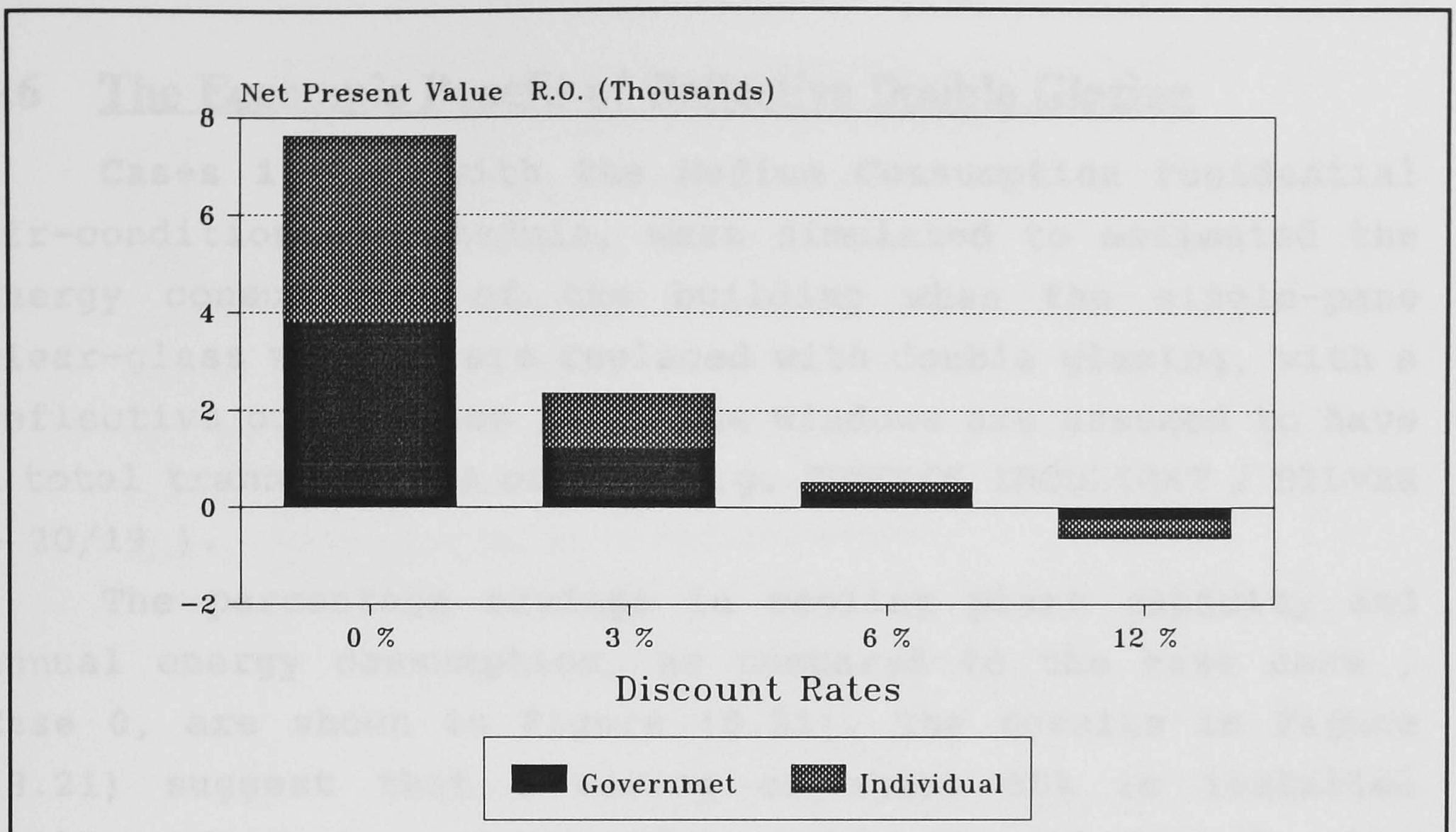

Figure 8.20: The Net Present Value of the Government's and Building Owner's investment, at different discount rates.

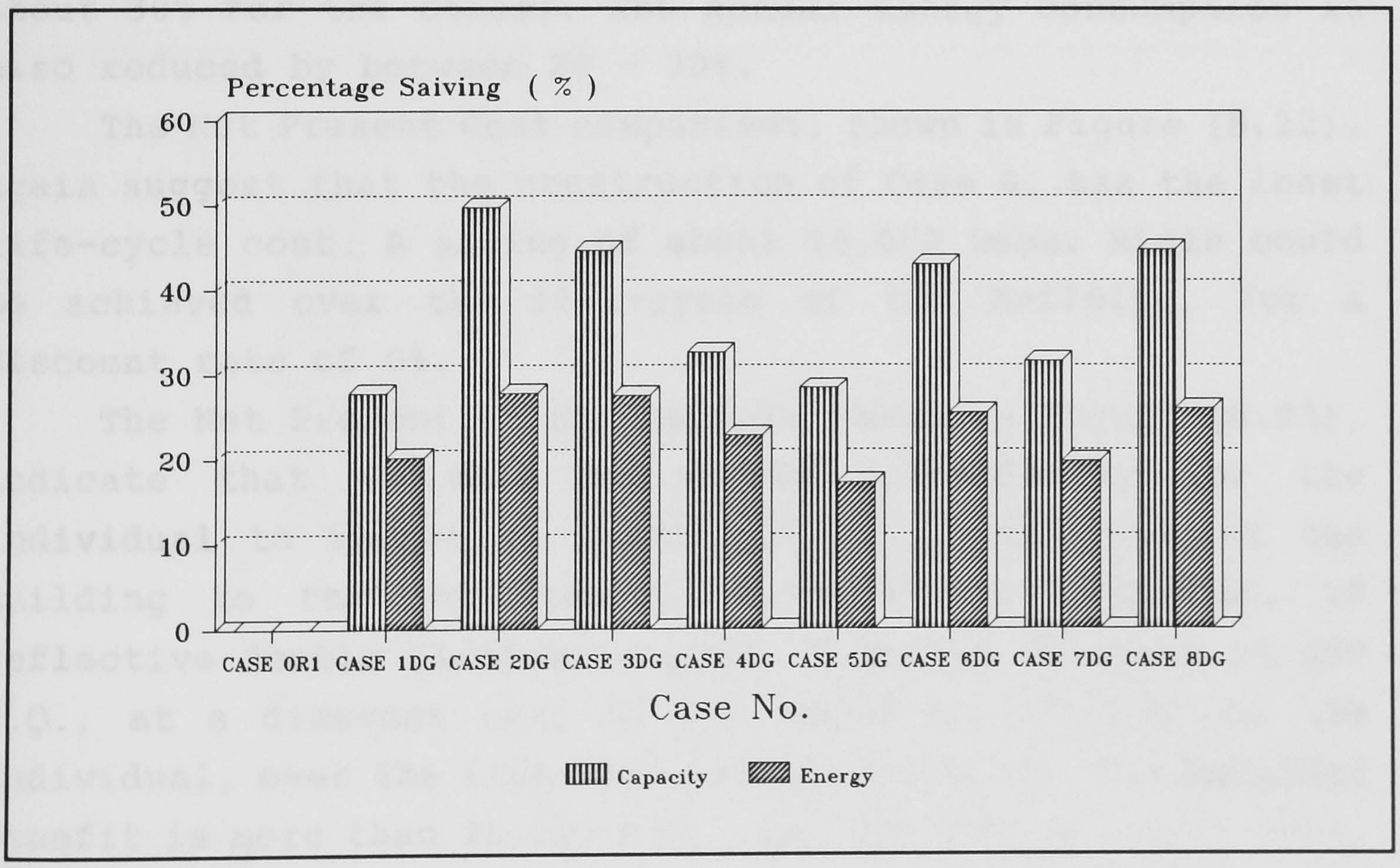

Figure 8.21: The percentage savings in installed capacity and energy consumption for a building with air-conditioning schedule (**R2**), and fitted with **Reflective Double Glazing.**

8.6 The Economic Benefit of Reflective Double Glazing

Cases 1 - 8, with the **Medium Consumption** residential air-conditioning schedule, were simulated to estimated the energy consumption of the building when the single-pane clear-glass windows are replaced with double glazing, with a reflective outer glass pane. The windows are assumed to have a total transmittance of 0.2 (e.g. SUNCOOL INSULIGHT / SILVER - 20/19).

The percentage savings in cooling plant capacity and annual energy consumption, as compared to the base case , **Case 0**, are shown in Figure (8.21). The results in Figure (8.21) suggest that a saving of about 50% in installed cooling plant capacity could be achieved with **Case 2**, when reflective double glazing is used. Generally a saving, in installed cooling plant capacity, of more than 40% is achieved in buildings with insulated roof and walls, and about 30% for the others. The annual energy consumption is also reduced by between 20 - 30%.

The Net Present Cost comparison, shown in Figure (8.22), again suggest that the construction of **Case 6**, has the least life-cycle cost. A saving of about 25,000 Omani Rials could be achieved over the life-cycle of the building, for a discount rate of 0%.

The Net Present Value analysis shown in Figure (8.23), indicate that it will be viable economically for the individual to invest in improving the construction of the building to that of **Case 6**, ***without any subsidies***, if reflective double glazing is used. A saving of about 10,000 R.O., at a discount rate of 0%, could be achieved by the individual, over the life-cycle of the building. The ***National*** benefit is more than 20,000 R.O., for the same discount rate, because of savings in the financial subsidy for electricity consumption.

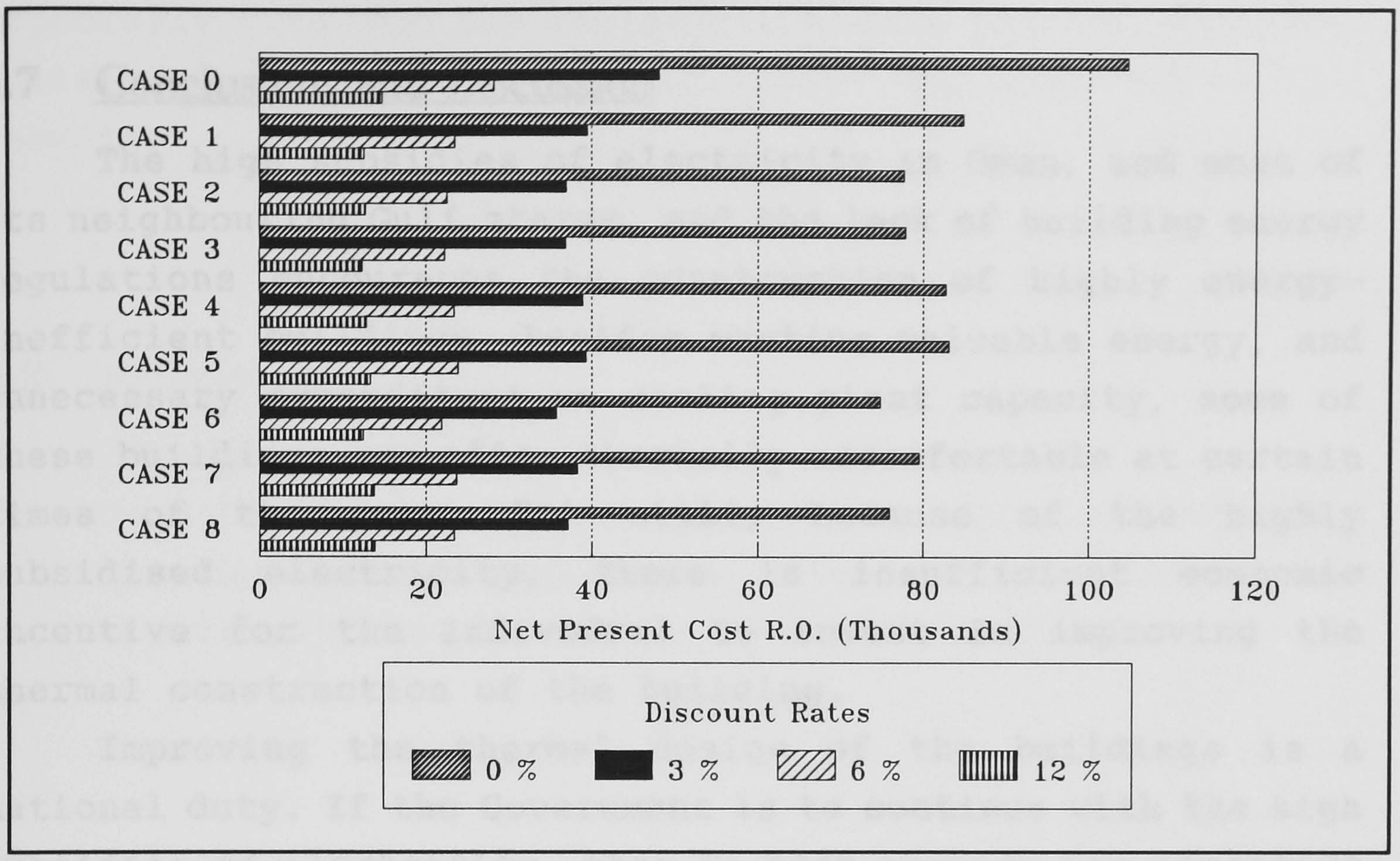

Figure 8.22: The Net Present Cost comparison of the different constructions, for a building with air-conditioning schedule (**R2**), and fitted with **Reflective Double Glazing.**

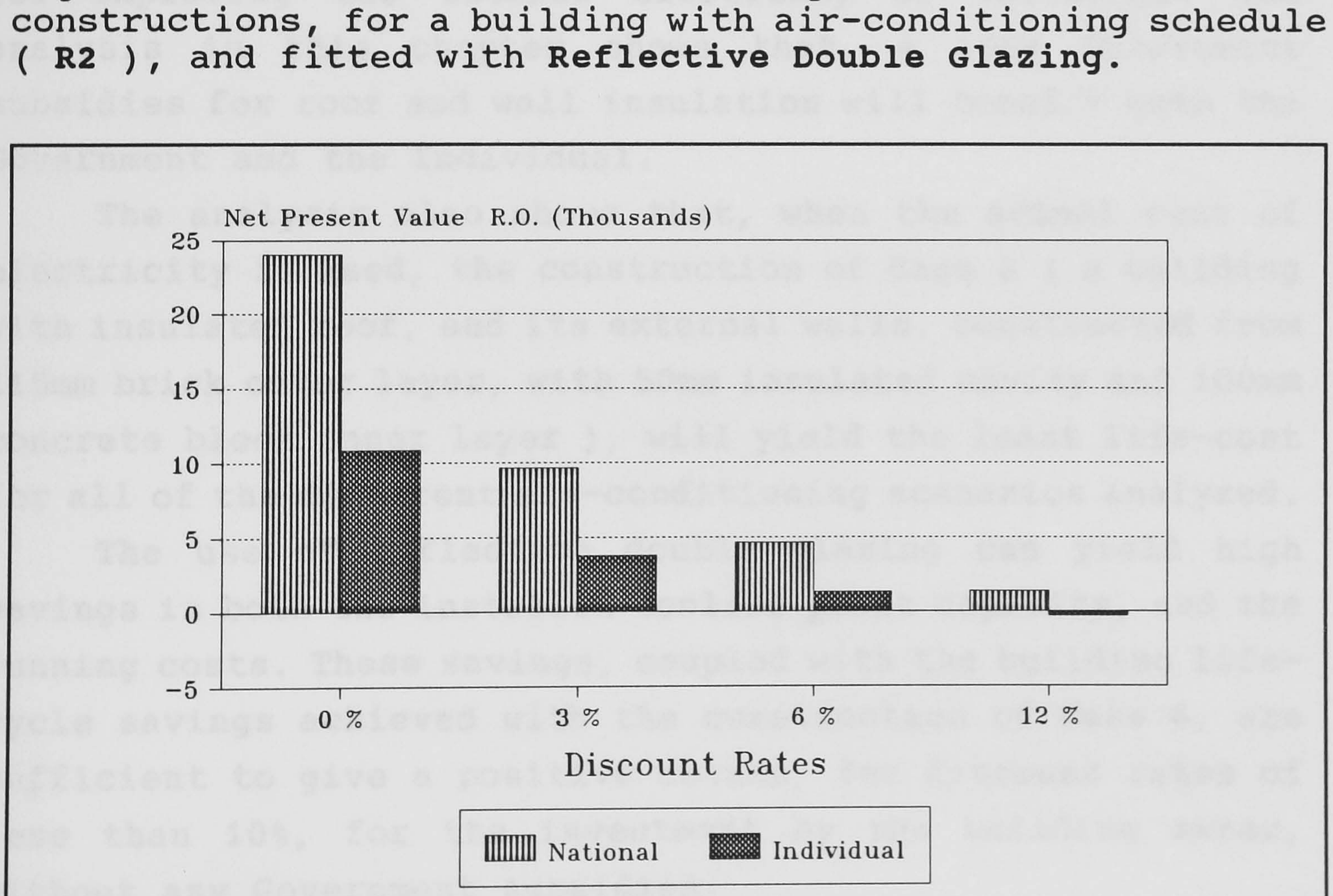

Figure 8.23: The life-cycle National and individual's benefit in improving the building envelope to **Case 6**, and using **Reflective Double Glazing**, For air-conditioning schedule (**R2**)

8.7 Conclusions and Discussion

The high subsidies of electricity in Oman, and most of its neighbouring Gulf states, and the lack of building energy regulations encourages the construction of highly energy-inefficient buildings. Besides wasting valuable energy, and unnecessary expenditure on cooling plant capacity, some of these buildings are often thermally uncomfortable at certain times of the year. But still, because of the highly subsidised electricity, there is insufficient economic incentive for the individual to invest in improving the thermal construction of the building.

Improving the thermal design of the buildings is a national duty. If the Government is to continue with the high subsidies of electricity, then it must provide the incentive for improving the thermal efficiency of buildings. The analysis in this chapter shows that, a 100% Government subsidies for roof and wall insulation will benefit both the Government and the Individual.

The analysis also shows that, when the actual cost of electricity is used, the construction of **Case 6** (a building with insulated roof, and its external walls, constructed from 115mm brick outer layer, with 50mm insulated cavity and 100mm concrete block inner layer), will yield the least life-cost for all of the different air-conditioning scenarios analyzed.

The use of reflective double glazing can yield high savings in both the installed cooling plant capacity, and the running costs. These savings, coupled with the building life-cycle savings achieved with the construction of **Case 6**, are sufficient to give a positive return, for discount rates of less than 10%, for the investment by the building owner, without any Government subsidies.

But it must be mentioned, that the variations in the shape and orientation of the building may give different results than those obtained in this chapter. This is

especially true for the reflective double glazing analysis. Variations in the construction costs may also affect the results.

8.8 References

1. Oman Engineering Consultancy, Ruwi, Sultanate of Oman.
2. The General Directorate of Electricity, Ministry of Electricity and Water, Sultanate of Oman.

Chapter (9)

Conclusions and Recommendations

Chapter (9)

Conclusions and Recommendations

9.1 Summary

The electrical energy consumed for the air-conditioning of buildings in Oman, accounts for about 70% of the national annual electrical-energy consumption in the country. This is accompanied by very high summer peak-loads, which have almost doubled during the past five years. This high rate of increase is set to continue as new areas are connected to the electricity grid, and to account for the high rate of population growth and the increasing use of electricity by the individuals.

The thoughtless adoption of the highly energy-inefficient concrete block buildings; the abandonment of the energy-thrift principals of the vernacular architecture and the consequent use of poorly controlled air-conditioning systems, has fuelled this rapid growth in energy consumption. The review of the vernacular architecture in Oman has shown that building forms, and town planning in general, relate specifically to the provision of thermal comfort by taking due regards of the regional topographies and climates. The vernacular buildings in the Coastal region utilised the sea breezes, and used low-density construction materials, such as palm fronds, for achieving thermal comfort. In the Mountainous and Desert regions, vernacular settlements relied on the effect of vegetation to modify the micro-climate, and utilised the daily occurring phenomena of slope ⇄ valley breezes. This was accompanied by the use of the most appropriate building form, orientation and construction materials.

In general, the vernacular architecture, in the different regions in Oman, has demonstrated various solutions for achieving thermal comfort by ***Natural*** means. The challenge for modern town planners and building designers, is to once again adopt these energy-thrift architectural principals. This does not preclude the use of modern martials, or new ideas, and even where mechanical air-conditioning is still considered desirable, the energy consumption rates could be drastically reduced.

The design of energy-efficient buildings, taking due regard of the local climatic conditions, should be a primary aim of any building designer. Because in most cases, this should be a relatively low-cost exercise. It will lead to savings in the capital and operating costs of the air-conditioning plants that may need to be installed. Hybrid systems, such as direct and in-direct evaporative air coolers, are financially more viable than vapour compression units in **hot-arid** climates. But although such systems are available in the market, some effort is needed to reduce their noise and improve their appearance. Also better marketing is needed to encourage the wide-spread use of such units. But it must be stressed that such units will not work satisfactorily in humid climates, such as the coastal regions of Oman.

Active, solar-powered, air-cooling units are generally as yet not financially viable. More local research and pilot projects are needed in this field and the field of solar energy in general.

Mathematical models were developed in this work to compare the thermal performance of some of the passive cooling techniques suitable for a climate like that of Oman. The roof analysis, indicate that shading a dry un-insulated roof can help in reducing the heat gain through the roof in a very hot climate. But it will also reduce the beneficial long-wave radiative heat exchange with the sky, and in

clement climates, shading will increase the net daily **heat gain** through the roof. Conversely, shading of roof ponds will be beneficial in both the very hot and temperate climates. This is mainly because the surface temperature of the water is relatively low, and thus the heat loss by radiation to the sky is less significant.

Insulation will reduce the heat gain through the roof by more than 50% in both a very hot and temperate climates. The roof models also indicate that a roof pond on an insulated roof slab will work better in reducing the heat gain through the roof in a very hot climate, but will be less beneficial in clement climates, as compared to a roof pond on an un-insulated roof slab.

It was clear from the literature survey that roof ponds are among the best passive natural cooling techniques for buildings in hot arid climates. Different types of roof ponds have been analyzed in this work. These include; roof ponds on un-insulated roof slabs, with and without shading; roof ponds on insulated roof slabs, with and without shading; roof ponds with movable insulating covers, covered during the day and uncovered at night; and the Water Diode roof pond initiated in this work. The result of this analysis indicate that, for an inside air temperature maintained at 26 °C, the roof pond with movable insulating cover is the best way of minimising the heat gain through the roof. This method was found to be capable of removing heat from the room, even in the very hot climate of Muscat in mid-June. On the other hand, the single-room model, which takes account of the heat gains through the walls and floor as well as that from the roof, suggested that the Water Diode roof pond works better than the roof pond with movable cover. It also has the advantage of eliminating the need for the daily operation of covering and uncovering the roof pond.

The idea of an insulated roof slab, cooled by forced ventilation, through air-channels in the slab, when the ambient temperature is cooler than that of the slab, has also been investigated. Such a technique was found to help in reducing the heat gain through the roof, and can remove heat from a room maintained at 26 ºC in clement climates, where the temperature of the ambient air at night becomes lower than 26 ºC. The roof cooled at night, works as a "coolth" store, absorbing heat from the room during the day.

Mathematical models have also been developed to investigate the thermal performance of different wall constructions. These include; single-leaf concrete block and brick walls; closed cavity and naturally ventilated cavity wall constructions; and insulated cavity double-leaf wall constructions. The results suggest that naturally ventilated cavities are better in reducing the heat gain through the wall than closed cavities. But the addition of insulation will sharply improve the thermal performance of the walls, with the best performance achieved by using insulated double-leaf brick wall constructions.

The results have also demonstrated that the thermal performance of bricks, which have a thermal conductivity of 0.7 $Wm^{-2}K^{-1}$ and an absorptivity of 0.65, is worse than that of white painted concrete block, which has a conductivity of 1.0 $Wm^{-1}K^{-1}$ and an absorptivity of 0.36. Thus, considerations of the thermal conductivity alone, cannot indicate the compared performances for real, dynamic climatic conditions.

From the analysis of the combinations of different wall and roof constructions, the results suggest that passive measures used to reduce the heat gain through the roofs, will not have a large effect on reducing the heat gains in rooms with un-insulated walls. Conversely, combining wall insulation with passive roof cooling techniques, can sharply reduce the cooling load of air-conditioned rooms. The Water

Diode roof pond was found to be the most effective passive roof cooling technique, of those analyzed, and can remove heat from a room maintained at 26 ℃, in a very hot climate.

But unconventional measures will not be adopted easily in the construction market. Pilot projects are needed to evaluate and demonstrate the benefits of these techniques. Meanwhile, we need to find the most appropriate of the conventional techniques, that will yield savings to the individual and the nation as a whole. For this reason, the economic analysis conducted, focused only on those techniques commonly used in modern-day constructions.

The high subsidies of electricity in Oman, and most of its neighbouring Gulf States, make it economically unattractive for the individuals to invest in improving the thermal efficiency of their buildings. But having said that, it was found, for the building analyzed, that the investment by the individual in insulating the roof, constructing the external walls from 115mm brick outer layer, with 50mm insulated cavity, and 100mm concrete block inner leaf, and using reflective double glazing, will give a positive return over the life-cycle of the building, for discount rates of less than 10%.

The economic Viability analysis of subsidising roof and wall insulation suggest that, a 100% government subsidies of insulation will yield long-term benefits for both the individual and the government. In the situations where there is a lack of regulations, such incentives will give a big boost for the individual to invest in the additional improvements.

9.2 Recommendations

To curb the high rate of increase in electric energy consumption in Oman, the thermal efficiency of buildings must be improved. The following steps are recommended :

- To promote the general awareness of the benefits, both nationally and at the individual level, of improving the thermal efficiency of buildings.

- Town planning should take into account the energy consumption in general, and in particular, the energy consumption for the air-conditioning of buildings. Designing the lay-out of building plots should take into consideration the daily and seasonal sun paths, the daily and seasonal wind-flow patterns, the presence of near by micro-climate modifiers such as a large area of vegetation and water mass, and the local topography. Generally for Oman, a south facing orientation is the best in terms of reducing solar summer heat gains. But the optimum orientation should also take account of the other factors mentioned above. Lessons should be drawn from the vernacular architecture of the locality, where the experience of thousands of years of natural cooling has been accumulated.

- There is an urgent need for Energy Building Regulations, to put a stop to the wide-spread construction of highly energy-inefficient buildings, which is encouraged by the massive subsidies of electricity. To start with, the regulations should be easy to understand and implement. These should be accompanied by seminars and workshops to familiarise the local planners and building designers with the passive building design techniques. The latter task could be undertaken by the university in Oman.

- In conventional building design, roof insulation is essential. External walls constructed from 115mm brick outer layer, with 50mm insulated cavity, and 100mm concrete block inner-leaf, were found to be the most economic over the life-cycle of the building.

- Reflective double glazing should be used for windows.

- It is economically viable for the government to give a 100% subsidies to the insulation material used in the roof and external walls. The additional construction costs should be met by the building owner. Such incentives could be used during an interim period before the introduction of regulations.

- There is a need for better energy management in centrally air-conditioned buildings, both in the government and private sectors.

- Local research is needed in the fields of passive and active solar air-conditioning, and thermal storage for air-conditioning.

- Pilot projects should be used to evaluate and demonstrate the benefits of natural cooling techniques for buildings.

Appendix A

Table A1: The weather data used as input for the simulation programs (Muscat 17-6-1988).

TIME HOURS	T_{ao} ^{o}C	V_{ao} m/s	RH %	$Qsol_1$ W/m^2	$Qsol_2$ W/m^2	$Qsol_r$ W/m^2
1	34.6	2.1	46	0	0	0
2	34.1	2.6	49	0	0	0
3	33.8	4.1	51	0	0	0
4	33.6	4.1	52	0	0	0
5	33.2	4.1	53	0	0	0
6	32.9	3.6	54	0	0	0
7	33.9	4.1	51	49.8	28.9	134.5
8	35.9	4.6	47	121.6	140.2	359.8
9	37.6	4.1	42	189.0	273.2	610.8
10	38.6	4.1	40	246.8	397.8	857.9
11	38.9	4.1	40	290.9	499.8	1067.0
12	38.9	4.6	40	318.6	567.0	1208.0
13	38.5	5.1	42	328.0	590.5	1257.0
14	38.3	5.1	43	318.6	567.0	1208.0
15	38.3	4.6	42	290.9	499.8	1067.0
16	38	4.6	42	246.8	397.8	857.9
17	37.7	3.7	42	189.0	273.2	610.8
18	37.3	3.1	43	121.6	140.2	389.8
19	36.3	2.6	46	49.8	28.9	134.5
20	35.5	1	49	0	0	0
21	35.2	0.5	48	0	0	0
22	35.2	1	47	0	0	0
23	35	1	46	0	0	0
24	35	2.6	44	0	0	0

-**T_{ao}** is the ambeint air temperature.
-**V_{ao}** is the wind speed.
-**RH** is the relative humidity of ambeint air.
-**$Qsol_1$** is the solar energy absorped by the water layer.
-**$Qsol_2$** is the solar energy absorped by the wet roof.
-**$Qsol_r$** is the solar radiation falling on a horizontal surface.

Table A2: The weather data used as input for the simulation programs (Muscat 21-3-1988).

TIME HOURS	T_{ao} ^{o}C	V_{ao} m/s	RH %	$Qsol_1$ W/m^2	$Qsol_2$ W/m^2	$Qsol_r$ W/m^2
1	28.6	2.1	32	0	0	0
2	29.4	4.1	23	0	0	0
3	28.0	3.6	31	0	0	0
4	28.7	3.1	28	0	0	0
5	28.5	5.1	28	0	0	0
6	27.3	3.1	34	0	0	0
7	25.4	3.1	43	5.7	48.5	81.1
8	26.0	1.0	52	12.7	152.1	179.7
9	28.7	0	48	18.5	257.2	280.8
10	31.5	0.5	28	22.6	344.7	368.8
11	31.7	3.1	30	25.0	402.8	428.7
12	32.4	3.6	24	25.8	423.3	449.9
13	33.0	4.6	24	25.0	402.8	428.7
14	33.5	5.1	22	22.6	344.7	368.8
15	33.0	5.1	29	18.5	257.2	280.8
16	32.5	5.1	32	12.7	152.1	179.7
17	33.0	4.1	21	12.7	48.5	81.1
18	29.5	4.6	53	5.7	0	0
19	27.2	4.1	67	0	0	0
20	26.0	2.1	76	0	0	0
21	26.4	0	72	0	0	0
22	25.2	0	78	0	0	0
23	25.0	1.0	77	0	0	0
24	25.7	1.5	66	0	0	0

-**T_{ao}** is the ambeint air temperature.
-**V_{ao}** is the wind speed.
-**RH** is the relative humidity of ambeint air.
-**$Qsol_1$** is the solar energy absorped by the water layer.
-**$Qsol_2$** is the solar energy absorped by the wet roof.
-**$Qsol_r$** is the solar radiation falling on a horizontal surface.

Table A3: The values of the properties of materials used in the simmulations :

	AIR	WATER	CONCRETE	SCREED	INSULATION
K (W/m^{2}K)	.0267	0.62	1.73	1.28	0.033
ρ (Kg/m^3)	1.145	1000	2700	2100	25
Cp (J/KgK)	1007	4178	880	1000	1200
μ (Ns/m^2)	187x10^{-7}	700x10^{-6}			
Pr	0.707	7.02			
ϵ		0.9	0.9	0.9	

The thickness of the roof slab was taken as 0.15m

and the roof area was chosen as 5 x 5m.

The Nodal Equations For The Dry Uninsulated Roof Analysis

Node 1 :

$$T_1^{t+1} = T_1^t + \frac{2 . \Delta t}{\rho_c . Cp_c . l} \{ Qsol_r - Qrad_{net} + h_o . (T_{ao}^{t+1} - T_1^{t+1}) + \frac{K_c}{l} . (T_2^{t+1} - T_1^{t+1}) \}$$

Node 2 :

$$T_2^{t+1} = T_2^t + \frac{K_c . \Delta t}{\rho_c . Cp_c . l^2} \{ T_1^{t+1} - 2 . T_2^{t+1} + T_3^{t+1} \}$$

Node 3 :

$$T_3^{t+1} = T_3^t + \frac{K_c . \Delta t}{\rho_c . Cp_c . l^2} \{ T_2^{t+1} - 2 . T_3^{t+1} + T_4^{t+1} \}$$

Node 4 :

$$T_4^{t+1} = T_4^t + \frac{2 . \Delta t}{\rho_c . Cp_c . l} \left\{ h_i . (T_{ai} - T_4^{t+1}) + \frac{K_c}{l} . (T_3^{t+1} - T_4^{t+1}) \right\}$$

The Nodal Equations For The Dry Insulated Roof Analysis

The nodal equations assumed are :

Node 1 :

$$T_1^{t+1} = T_1^t + \frac{2.\Delta t}{\rho_{c1}.Cp_{c1}.l_{c1}}\{ Qsol_r - Qrad_{net} + h_o.(T_{ao}^{t+1} - T_1^{t+1}) + \frac{K_{c1}}{l_{c1}}.(T_2^{t+1} - T_1^{t+1})\}$$

Node 2 :

$$T_2^{t+1}=T_2^t+\frac{\Delta t}{\left(\frac{\rho_{c1}+\rho_s}{2}\right).\left(\frac{Cp_{c1}+Cp_s}{2}\right).\left(\frac{l_{c1}+l_s}{2}\right)^2}\left\{K_{c1}.T_1^{t+1}-2\left(\frac{K_{c1}+K_s}{2}\right)T_2^{t+1}+K_s.T_3^{t+1}\right\}$$

Node 3 :

$$T_3^{t+1}=T_3^t+\frac{\Delta t}{\left(\frac{\rho_{c2}+\rho_s}{2}\right).\left(\frac{Cp_{c2}+Cp_s}{2}\right).\left(\frac{l_{c2}+l_s}{2}\right)^2}\left\{K_s.T_2^{t+1}-2\left(\frac{K_{c2}+K_s}{2}\right)T_3^{t+1}+K_{c2}.T_4^{t+1}\right\}$$

Node 4 :

$$T_4^{t+1} = T_4^t + \frac{K_{c2}.\Delta t}{\rho_{c2}.Cp_{c2}.l_{c2}^2}\{ T_3^{t+1} - 2.T_4^{t+1} + T_5^{t+1} \}$$

Node 5 :

$$T_5^{t+1} = T_5^t + \frac{2.\Delta t}{\rho_{c2}.Cp_{c2}.l_{c2}}.\left\{ h_i.(T_{ai} - T_5^{t+1}) + \frac{K_{c2}}{l_{c2}}.(T_4^{t+1} - T_5^{t+1}) \right\}$$

The Nodal Equations For The Roof Pond Analysis

Node 1 :

$$T_1^{t+1} = T_1^t + \frac{2.\Delta t}{\rho_w.Cp_w.d}\left\{Qsol_1 - Qrad_{net} - Qevap + h_o.(T_{ao}^{t+1} - T_1^{t+1}) + h_1.(T_2^{t+1} - T_1^{t+1})\right.$$

Node 2 :

$$T_2^{t+1} = T_2^t + \frac{2.\Delta t}{\rho_c.Cp_c.l_c^2}\left\{\frac{l_c}{K_c}[Qsol_2 + h_1.(T_1^{t+1} - T_2^{t+1})] + (T_3^{t+1} - T_2^{t+1})\right\}$$

Node 3 :

$$T_3^{t+1} = T_3^t + \frac{K_c.\Delta t}{\rho_c.Cp_c.l^2}\left\{T_2^{t+1} - 2.T_3^{t+1} + T_4^{t+1}\right\}$$

Node 4 :

$$T_4^{t+1} = T_4^t + \frac{K_c.\Delta t}{\rho_c.Cp_c.l^2}\left\{T_3^{t+1} - 2.T_4^{t+1} + T_5^{t+1}\right\}$$

Node 5 :

$$T_5^{t+1} = T_5^t + \frac{2.\Delta t}{\rho_c.Cp_c.l}\left\{h_i.(T_{ai} - T_5^{t+1}) + \frac{K_c}{l}.(T_3^{t+1} - T_5^{t+1})\right\}$$

The Nodal Equations For The Roof Pond With Insulated Roof Slab

Node 1 :

$$T_1^{t+1}=T_1^t+\frac{2.\Delta t}{\rho_w.Cp_w.d}\{Qsol_1-Qrad_{net}-Qevap+h_o.(T_{ao}^{t+1}-T_1^{t+1})+h_1.(T_2^{t+1}-T_1^{t+1})$$

Node 2 :

$$T_2^{t+1}=T_2^t+\frac{2.\Delta t}{\rho_{c1}.Cp_{c1}.l_{c1}}\left\{Qsol_2+h_1.(T_1^{t+1}-T_2^{t+1})+\frac{K_{c1}}{l_{c1}}(T_3^{t+1}-T_2^{t+1})\right\}$$

Node 3 :

$$T_3^{t+1}=T_3^t+\frac{\Delta t}{\left(\frac{\rho_{c1}+\rho_s}{2}\right).\left(\frac{Cp_{c1}+Cp_s}{2}\right).\left(\frac{l_{c1}+l_s}{2}\right)^2}\left\{K_{c1}.T_2^{t+1}-2\left(\frac{K_{c1}+K_s}{2}\right)T_3^{t+1}+K_s.T_4^{t+1}\right\}$$

Node 4 :

$$T_4^{t+1}=T_4^t+\frac{\Delta t}{\left(\frac{\rho_{c2}+\rho_s}{2}\right).\left(\frac{Cp_{c2}+Cp_s}{2}\right).\left(\frac{l_{c2}+l_s}{2}\right)^2}\left\{K_s.T_3^{t+1}-2\left(\frac{K_{c2}+K_s}{2}\right)T_4^{t+1}+K_{c2}.T_5^{t+1}\right\}$$

Node 5 :

$$T_5^{t+1}=T_5^t+\frac{K_{c2}.\Delta t}{\rho_{c2}.Cp_{c2}.l_{c2}^2}\left\{T_4^{t+1}-2.T_5^{t+1}+T_6^{t+1}\right\}$$

Node 6 :

$$T_6^{t+1}=T_6^t+\frac{2.\Delta t}{\rho_{c2}.Cp_{c2}.l_{c2}}.\left\{h_i.(T_{ai}-T_6^{t+1})+\frac{K_{c2}}{l_{c2}}.(T_5^{t+1}-T_6^{t+1})\right\}$$

The Nodal Equations For The Roof With Air Channels

Node 1 :

$$T_1^{t+1} = T_1^t + \frac{2\,\Delta t}{\rho_{c1}\, Cp_{c1}\, l}\{ Qsol_r - Qrad_{net} + h_o(T_{ao}^{t+1} - T_1^{t+1}) + \frac{K_{c1}}{l}(T_2^{t+1} - T_1^{t+1}) + \frac{K_{c1}}{l}(T_4^{t+1} - T_1^{t+1})\}$$

Node 2 :

$$T_2^{t+1} = T_2^t + \frac{2\,\Delta t}{\rho_{c1}\, Cp_{c1}\, l}\{ Qsol_r - Qrad_{net} + h_o(T_{ao}^{t+1} - T_2^{t+1}) + \frac{K_{c1}}{2l}(T_1^{t+1} - T_2^{t+1}) + \frac{K_{c1}}{2l}(T_3^{t+1} - T_2^{t+1}) + \frac{K_{c1}}{l}(T_5^{t+1} - T_2^{t+1})\}$$

Node 3 :

$$T_3^{t+1} = T_3^t + \frac{2\,\Delta t}{\rho_{c1}\, Cp_{c1}\, l}\{ Qsol_r - Qrad_{net} + h_o(T_{ao}^{t+1} - T_3^{t+1}) + \frac{K_{c1}}{l}(T_2^{t+1} - T_3^{t+1}) + \frac{K_{c1}}{l}(T_6^{t+1} - T_3^{t+1})\}$$

Node 4 :

$$T_4^{t+1} = T_4^t + \frac{\Delta t}{\left(\frac{\rho_{c1}+\rho_s}{2}\right)\left(\frac{Cp_{c1}+Cp_s}{2}\right) l^2}\{ K_{c1}(T_1^{t+1} - T_4^{t+1}) + 2\left(\frac{K_{c1}+K_s}{2}\right)(T_5^{t+1} - T_4^{t+1}) + K_s(T_7^{t+1} - T_4^{t+1})\}$$

Node 5 :

$$T_5^{t+1} = T_5^t + \frac{\Delta t}{\left(\frac{\rho_{c1}+\rho_s}{2}\right)\left(\frac{Cp_{c1}+Cp_s}{2}\right) l^2}\{ K_{c1}(T_2^{t+1} - T_5^{t+1}) + \left(\frac{K_{c1}+K_s}{2}\right)(T_4^{t+1} - 2\,T_5^{t+1} + T_6^{t+1}) + K_s(T_8^{t+1} - T_5^{t+1})\}$$

Node 6 :

$$T_6^{t+1} = T_6^t + \frac{\Delta t}{\left(\frac{\rho_{c1}+\rho_s}{2}\right)\left(\frac{Cp_{c1}+Cp_s}{2}\right) l^2} \{ K_{c1} (T_3^{t+1} - T_6^{t+1}) + 2\left(\frac{K_{c1}+K_s}{2}\right) (T_5^{t+1} - T_6^{t+1}) + K_s (T_9^{t+1} - T_6^{t+1}) \}$$

Node 7 :

$$T_7^{t+1} = T_7^t + \frac{\Delta t}{\left(\frac{\rho_{c2}+\rho_s}{2}\right)\left(\frac{Cp_{c2}+Cp_s}{2}\right) l^2} \{ K_s (T_4^{t+1} - T_7^{t+1}) + 2\left(\frac{K_{c2}+K_s}{2}\right) (T_8^{t+1} - T_7^{t+1}) + K_{c2} (T_{10}^{t+1} - T_7^{t+1}) \}$$

Node 8 :

$$T_8^{t+1} = T_8^t + \frac{\Delta t}{\left(\frac{\rho_{c2}+\rho_s}{2}\right)\left(\frac{Cp_{c2}+Cp_s}{2}\right) l^2} \{ K_s (T_5^{t+1} - T_8^{t+1}) + \left(\frac{K_{c2}+K_s}{2}\right) (T_7^{t+1} - 2\,T_8^{t+1} + T_9^{t+1}) + K_{c2} (T_{11}^{t+1} - T_8^{t+1}) \}$$

Node 9 :

$$T_9^{t+1} = T_9^t + \frac{\Delta t}{\left(\frac{\rho_{c2}+\rho_s}{2}\right)\left(\frac{Cp_{c2}+Cp_s}{2}\right) l^2} \{ K_s (T_6^{t+1} - T_9^{t+1}) + 2\left(\frac{K_{c2}+K_s}{2}\right) (T_8^{t+1} - T_9^{t+1}) + K_{c2} (T_{12}^{t+1} - T_9^{t+1}) \}$$

Node 10 :

$$T_{10}^{t+1} = T_{10}^t + \frac{2\,\Delta t}{\rho_{c2}\, Cp_{c2}\, l} \{ h_{ch} (T_{13}^{t+1} - T_{10}^{t+1}) + \frac{K_{c2}}{l} (T_{11}^{t+1} - T_{10}^{t+1}) + \frac{K_{c2}}{l} (T_7^{t+1} - T_{10}^{t+1}) \}$$

Node 11 :

$$T_{11}^{t+1} = T_{11}^{t} + \frac{2\,\Delta t}{\rho_{c2}\, Cp_{c2}\, l}\left\{ h_{ch}\left(T_{13}^{t+1} - \frac{2}{3} \cdot T_{11}^{t+1} \right) + \frac{K_{c2}}{3l}\left(T_{10}^{t+1} - T_{11}^{t+1} \right) \right.$$

$$\left. + \frac{2\,K_{c2}}{3l}\left(T_{12}^{t+1} - T_{11}^{t+1} \right) + \frac{2\,K_{c2}}{3l}\left(T_{8}^{t+1} - T_{11}^{t+1} \right) + \frac{K_{c2}}{3l}\left(T_{14}^{t+1} - T_{11}^{t+1} \right) \right\}$$

Node 12 :

$$T_{12}^{t+1} = T_{12}^{t} + \frac{\Delta t \,.\, K_{c2}}{\rho_{c2}\, Cp_{c2}\, l^{2}}\left\{ 2\left(T_{11}^{t+1} - T_{12}^{t+1} \right) \right.$$

$$\left. + \left(T_{9}^{t+1} - T_{12}^{t+1} \right) + \left(T_{15}^{t+1} - T_{12}^{t+1} \right) \right\}$$

Node 13 :

$$T_{10}^{t+1} = T_{10}^{t} + \frac{2\,\Delta t}{\rho_{c2}\, Cp_{c2}\, l}\left\{ h_{ch}\left(T_{13}^{t+1} - T_{14}^{t+1} \right) + \frac{K_{c2}}{l}\left(T_{15}^{t+1} - T_{14}^{t+1} \right) \right.$$

$$\left. + \frac{K_{c2}}{2l}\left(T_{11}^{t+1} - T_{14}^{t+1} \right) + \frac{K_{c2}}{2l}\left(T_{17}^{t+1} - T_{14}^{t+1} \right) \right\}$$

Node 14 :

$$T_{15}^{t+1} = T_{15}^{t} + \frac{\Delta t \,.\, K_{c2}}{\rho_{c2}\, Cp_{c2}\, l^{2}}\left\{ 2\left(T_{14}^{t+1} - T_{15}^{t+1} \right) \right.$$

$$\left. + \left(T_{12}^{t+1} - T_{15}^{t+1} \right) + \left(T_{18}^{t+1} - T_{15}^{t+1} \right) \right\}$$

Node 15 :

$$T_{16}^{t+1} = T_{16}^{t} + \frac{2\,\Delta t}{\rho_{c2}\, Cp_{c2}\, l}\left\{ h_{ch}\left(T_{13}^{t+1} - T_{16}^{t+1} \right) \right.$$

$$\left. + \frac{K_{c2}}{l}\left(T_{17}^{t+1} - T_{16}^{t+1} \right) + \frac{K_{c2}}{l}\left(T_{19}^{t+1} - T_{16}^{t+1} \right) \right\}$$

Node 16 :

$$T_{17}^{t+1} = T_{17}^{t} + \frac{2\,\Delta t}{\rho_{c2}\,Cp_{c2}\,l}\left\{ h_{ch}\left(T_{13}^{t+1} - \frac{2}{3}\,.\,T_{17}^{t+1}\right) + \frac{K_{c2}}{3l}\left(T_{16}^{t+1} - T_{17}^{t+1}\right)\right.$$

$$\left. + \frac{2\,K_{c2}}{3l}\left(T_{18}^{t+1} - T_{17}^{t+1}\right) + \frac{2\,K_{c2}}{3l}\left(T_{20}^{t+1} - T_{17}^{t+1}\right) + \frac{K_{c2}}{3l}\left(T_{14}^{t+1} - T_{17}^{t+1}\right)\right\}$$

Node 17 :

$$T_{18}^{t+1} = T_{18}^{t} + \frac{\Delta t\,.\,K_{c2}}{\rho_{c2}\,Cp_{c2}\,l^{2}}\left\{ 2\left(T_{17}^{t+1} - T_{18}^{t+1}\right)\right.$$

$$\left. + \left(T_{15}^{t+1} - T_{18}^{t+1}\right) + \left(T_{21}^{t+1} - T_{18}^{t+1}\right)\right\}$$

Node 18 :

$$T_{19}^{t+1} = T_{19}^{t} + \frac{2\,\Delta t}{\rho_{c2}\,Cp_{c2}\,l}\left\{ h_{i}\left(T_{ai}^{t+1} - T_{19}^{t+1}\right)\right.$$

$$\left. + \frac{K_{c2}}{l}\left(T_{20}^{t+1} - T_{19}^{t+1}\right) + \frac{K_{c2}}{l}\left(T_{16}^{t+1} - T_{19}^{t+1}\right)\right\}$$

Node 19 :

$$T_{20}^{t+1} = T_{20}^{t} + \frac{2\,\Delta t}{\rho_{c2}\,Cp_{c2}\,l}\left\{ h_{i}\left(T_{ai}^{t+1} - T_{20}^{t+1}\right) + \frac{K_{c2}}{l}\left(T_{17}^{t+1} - T_{20}^{t+1}\right)\right.$$

$$\left. + \frac{K_{c2}}{2l}\left(T_{19}^{t+1} - T_{20}^{t+1}\right) + \frac{K_{c2}}{2l}\left(T_{21}^{t+1} - T_{20}^{t+1}\right)\right\}$$

Node 20 :

$$T_{21}^{t+1} = T_{21}^{t} + \frac{2\,\Delta t}{\rho_{c2}\,Cp_{c2}\,l}\left\{ h_{i}\left(T_{ai}^{t+1} - T_{21}^{t+1}\right)\right.$$

$$\left. + \frac{K_{c2}}{l}\left(T_{20}^{t+1} - T_{21}^{t+1}\right) + \frac{K_{c2}}{l}\left(T_{18}^{t+1} - T_{21}^{t+1}\right)\right\}$$

The temperature of the air inside the channels is taken as the lower between the ambeint air and the average temperature of the channel surfaces:

$$T_{ac} = Min\left(T_{ao} \, , \; T_{ch_{av}}\right)$$

$$T_{ch_{av}} = \frac{\left(T_{10} + 2\,T_{11} + 2\,T_{13} + T_{15} + 2\,T_{16}\right)}{8}$$

Appendix B

Thermal Comfort Analysis

A simple check was carried out to insure that thermal comfort conditions will be satisfied in the building used in the economical analysis in chapter 8. The analysis consists of estimating the resultant temperature for a person sitting near a corner in one of the rooms. The base case, **Case 0**, is compared with cases 1, 2, 3 and 6, for the air-conditioning schedule **G1**.

The internal surface temperatures in the room, on day 165 at 2 pm, are shown in Table (B1).

Table B1 : The internal surface temperatures, on day 165 at 2 pm (Muscat88 weather file).

	Case 0	**Case 1**	**Case 2**	**Case 3**	**Case 6**
Floor	33.7	32.9	31.9	32.2	32.3
Ceiling	45.2	35.9	34.2	34.8	35.1
North Wall	34.3	33.3	31.9	32.5	32.7
East Wall	35.8	35.1	32.5	34.1	34.5
South Wall	35.4	34.7	32.5	34.1	34.4
West Wall	35.6	34.9	32.6	32.4	32.7
Window	43.4	43.1	42.9	42.9	42.9

The Mean Radiant Temperature (MRT) at a certain point in the room is estimated from :

$$MRT = \sum_{i=1}^{i} (F_{si} \cdot T_i^4)^{\frac{1}{4}}$$

Where F_{si} is the view factor of surface i

and T_i is the temperature of surface i (K).

The view factors are worked out using Figure (B1), and summarised in Table (B2).

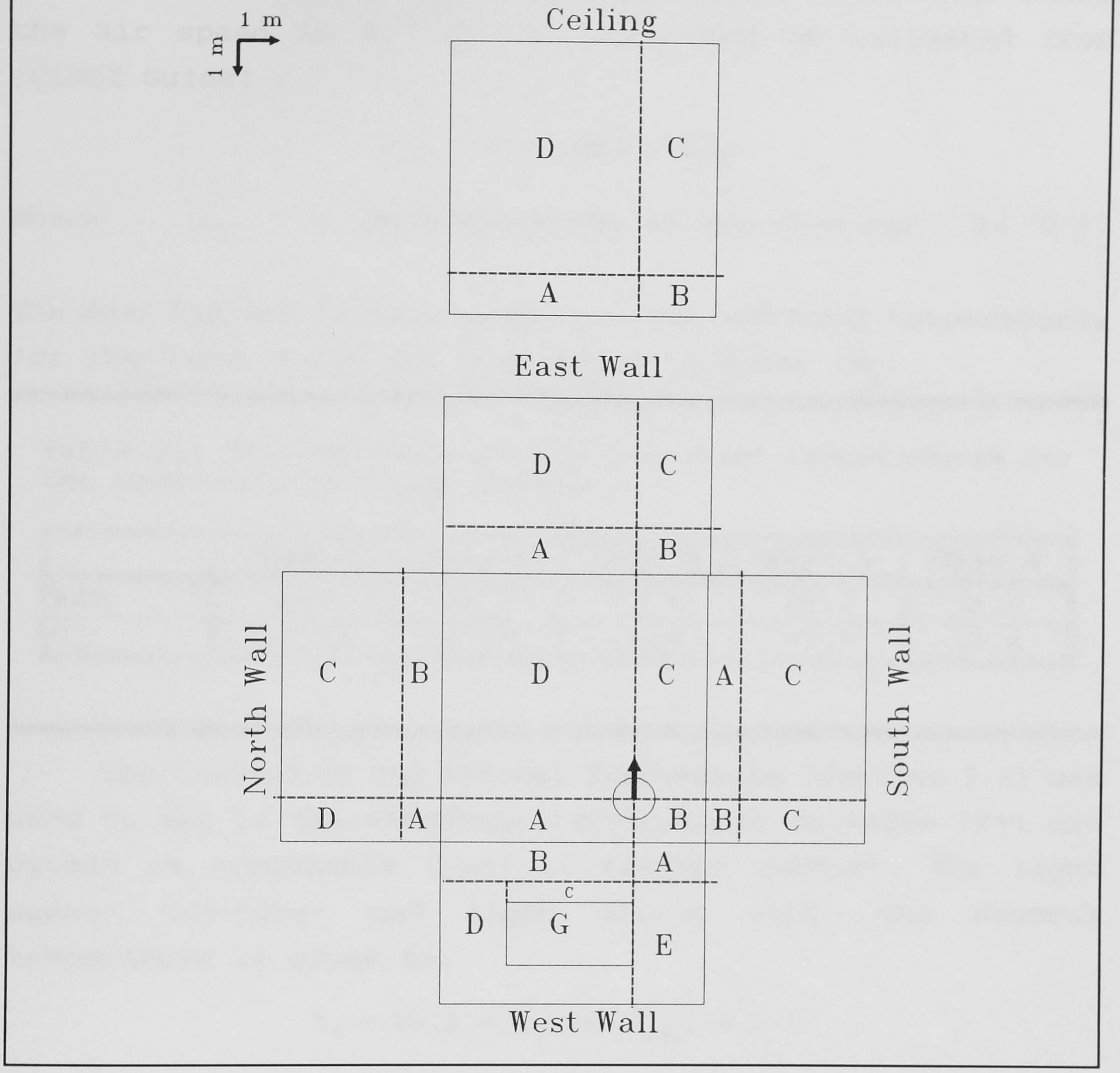

Figure B1: The relative position of the person to the internal surfaces of the room.

Table B2: The view factors between the person and the internal surfaces.

$F_{P\text{-}NW}$	$F_{P\text{-}SW}$	$F_{P\text{-}EW}$	$F_{P\text{-}WW}$	$F_{P\text{-}C}$	$F_{P\text{-}F}$	$F_{P\text{-}G}$
0.07	0.12	0.065	0.208	0.167	0.34	0.03

The resultant temperature for indoor conditions where the air speed is 0.1 ms^{-1} or less, can be estimated from [CIBSE Guide] :

$$T_{res} = 0.5\ (MRT + T_{ai})$$

Where T_{ai} is the temperature of the room air (24 °C).

The Mean Radiant Temperatures, and the resultant temperatures for the cases above are summarised in Table (B3).

Table B3: The Mean Radiant and resultant temperatures for the construction cases analyzed.

	Case 0	**Case 1**	**Case 2**	**Case 3**	**Case 6**
MRT	36.7	34.5	32.8	33.3	33.6
T_{res}	30.4	29.25	28.4	28.7	28.8

The Concept of the **Neutral Temperature** (section 3.2) was used to see if the resultant temperatures in Table (B3) are within an acceptable level of thermal comfort. For light summer clothing, and light office work, the Neutral temperature is given as:

$$T_n = 10.2 + 0.534\,(T_{amb}) \pm 2.5$$

Where T_{amb} is the mean monthly out-door temperature (°C). For Muscat, the mean monthly out-door temperature in June is 36.1 °C. The Neutral temperature for the month of June is thus:

$$T_n = 10.2 + 0.534\,(31.6) \pm 2.5 \quad = 29.5 \pm 2.5$$

So if the resultant temperature exceeds 29.5 °C, the occupants might feel uncomfortably warm, and will tend to reduce the room air temperature. This will lead to an increased energy consumption, and thus an increased life-cycle cost. The 29.5 °C target, has only been exceeded by **Case 0**.